INVESTIGATING SETD1A AS A NOVEL EPIGENETIC REGULATOR OF PARP INHIBITION

by

Ellie Louise Sweatman

A thesis submitted to the University of Birmingham for the degree of

DOCTOR OF PHILOSOPHY

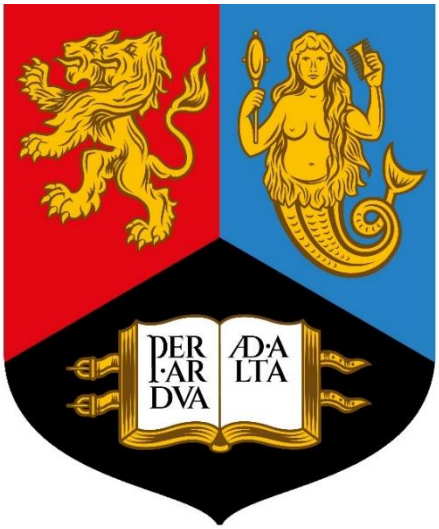

UNIVERSITY OF BIRMINGHAM

Department of Cancer and Genomic Sciences

College of Medical and Dental Sciences

University of Birmingham

September 2024

ABSTRACT

Poly (ADP-ribose) polymerase (PARP) inhibitors (PARPi) have transformed the treatment of BRCA1-deficient tumours and further evidence suggests their efficacy also extends to deficiencies in other genetic factors associated with homologous recombination (HR), including ATM. However, the clinical success of these compounds is hampered by resistance, as well as a lack of good biomarkers to determine which patients are likely to benefit from PARPi treatment. Recent findings identified the lysine methyltransferase SETD1A as a novel factor conferring PARPi resistance in BRCA1-deficient cells by restoring HR. In this thesis I build upon these previous findings to ask if SETD1A contributes to PARPi resistance in ATM-deficient cells and determine the mechanisms responsible.

Clonogenic survival and immunofluorescent DNA repair assays revealed SETD1A knockdown reduced olaparib sensitivity in ATM-deficient cells through partial restoration of HR, driven by abrogation of H3K4 methylation. On the other hand, Cas9-mediated gene editing of SETD1A increased PARPi sensitivity in the absence of ATM, which was attributed to depletion of residual SETD1A protein expression and increased p53 expression. Based on its role as a H3K4 methyltransferase, we performed RNA-sequencing analysis revealing SETD1A-dependent transcription of the crossover junction endonuclease EME1 correlated with olaparib sensitivity. Accordingly, loss of EME1 phenocopied loss of SETD1A, inducing PARPi resistance and restoring HR in BRCA1 or ATM-deficient cells.

In conclusion, loss of SETD1A or EME1 may underlie PARPi resistance in the clinic and their expression or activity could offer potential new biomarkers to predict patient response and improve outcomes following PARPi treatment.

ACKNOWLEDGEMENTS

I would firstly like to express my deepest appreciation to my supervisor Dr Martin Higgs for accepting me into Team Higgs and providing me with unwavering support and encouragement throughout these four years. Without your guidance and expertise this thesis would not have been possible. I would also like to extend my sincere thanks to Clare Davies, Tatjana Stankovic, Marco Saponaro and other members of the Birmingham Centre for Genome Biology (BCGB) for their invaluable discussions and feedback.

I am grateful to our collaborators Simon Boulton for providing iCas9 cells and lentiviruses, and to Graham Dellaire for providing plasmids for the CRISPR-based HR assays. Thanks, should also go to Cancer Research UK whose financial support made this research possible.

I express my gratitude to all my colleagues in the Higgs lab past and present for their technical and moral support. Special thanks go to Sofia, Lucy, Amalia, Alice, and Olga for your friendship and for sharing in all the highs and lows of this PhD.

I would not have undertaken this journey without the support of my friends and family, especially my parents who have encouraged and motivated to be the person I am today. They may not fully understand my job, but they always ask me how my cells are doing. To my fiancé and life-long proof-reading partner Harry, thank you for always believing in me and for cooking me dinner every night during my long thesis writing days.

Lastly, I would be remiss in not mentioning Taylor swift, whose music has kept me company through many long tissue culture and microscope sessions.

TABLE OF CONTENTS

LIST OF FIGURES

LIST OF TABLES

LIST OF ABBREVIATIONS

18s rRNA	18S ribosomal RNA
53BP1	Tumour protein 53-binding protein 1
A	Ampere (unit of electric current)
AA	Amino acid
ABCB1	ATP binding cassette subfamily B member 1
Ac	Acetylation
ACAD10	Acyl-CoA dehydrogenase family member 10
ACTMAP	Actin maturation protease
ADAM10	ADAM metallopeptidase domain 10
ADP	Adenosine diphosphate
ALKBH2	Alpha-ketoglutarate-dependent dioxygenase AlkB homolog 2
ALKBH3	Alpha-ketoglutarate-dependent dioxygenase AlkB homolog 3
Alt-EJ	Alternative-end joining
Amx	Almondex
ANOVA	Analysis of variance
APE1	Apurinic/apyrimidinic endodeoxyribonuclease 1
APLF	Aprataxin and PNKP like factor
ARID1A	AT-rich interaction domain 1A
ARL6IP6	ADP ribosylation factor like GTPase 6 interacting protein 6
ART	ADP-ribosyl transferase
ASH2L	Ash 2-like histone methyltransferase complex subunit
A-T	Ataxia-telangiectasia
ATCC	American Type Culture Collection
ATM	Ataxia telangiectasia mutated
ATR	Ataxia telangiectasia mutated - and rad3-related
ATRi	ATR inhibitor
ATRIP	ATR-interacting protein
ATRX	ATRX chromatin remodeler
Bak	BCL2 antagonist/killer
BARD1	BRCA1-associated ring domain protein 1
Bax	BCL2 associated X protein
BER	Base excision repair
BIR	Break induced replication
BLM	Bloom helicase
BOD1	Biorientation defect 1
BOD1L	Biorientation defect 1-like
bp	Base pairs
BRAF	V-Raf murine sarcoma viral oncogene homolog B
BRCA1	Breast cancer susceptibility protein 1
BRCA2	Breast cancer susceptibility protein 2
BRCT	BRCA1 C-terminal domain
BRIP1	BRCA1 interacting helicase 1
BSA	Bovine serum albumin

C12orf66	Chromosome 12 open reading frame 66
C19orf54	Chromosome 19 open reading frame 54
C22orf54	Chromosome 22 open reading frame 54
Cas9	CRISPR associated protein 9
CBX4	Chromobox 4
CD180	CD180 antigen
CDC25	Cell division cycle 25
CDC25A	Cell division cycle 25A
CDC25C	Cell division cycle 25B
CDC7	Cell division cycle 7
CDK	Cyclin-dependent kinase
CDK12	Cyclin-dependent kinase 12
CDK2	Cyclin-dependent kinase 2
cDNA	Complementary DNA
CENPF	Centromere protein F
CETN2	Centrin 2
CF	Chromatin fractionation
CFP1	CXXC zinc finger protein 1
CFS	common fragile sites
CH507-42P11.6	Uncharacterized CH507-42P11.6
CHAC1	ChaC glutathione specific gamma-glutamylcyclotransferase 1
CHAMP1	Chromosome alignment maintaining phosphoprotein 1
CHD2	Chromodomain helicase DNA-binding protein 2
CHD4	Chromodomain helicase DNA-binding protein 4
ChIP	Chromatin immunoprecipitation
Chk1	Checkpoint protein 1
Chk2	Checkpoint protein 2
CIN	Chromosomal instability
CNS	Central nervous system
COMPASS	Complex proteins associated with Set1
CPM	Counts per million
Cq	Quantification cycle
CREB	CAMP responsive element binding protein 1
CRISPR	Clustered, regularly interspaced, short palindromic repeats
CST	CTC1-STN1-TEN1
C-terminus	Carboxyl terminus
CtIP	CtBP-interacting protein
CXXC	CXXC zinc finger domain
DAPI	4', 6-diamidino-2-phenylindole
DARS	Aspartyl-tRNA synthetase 1
DARS1	Aspartyl-tRNA synthetase 1
DCX	Doublecortin
DDR	DNA damage response
DEG	Differentially expressed gene
dHJ	Double Holliday junction

D-loop	Displacement-loop
DLX5	Distal-less homeobox 5
DMEM	Dulbecco’s modified Eagle’s medium
DMSO	Dimethyl sulfoxide
DNA	Deoxyribonucleic acid
DNA2	DNA replication helicase/nuclease 2
DNA-PK	DNA-dependent protein kinase
DNA-PKcs	DNA-dependent protein kinase catalytic subunit
DNase	Deoxyribonuclease
Dox	Doxycycline
DPC	DNA-protein crosslink
DPY30	Dpy-30 histone methyltransferase complex regulatory subunit
DSB	Double-strand break
dsDNA	Double-stranded DNA
DTT	Dithiothreitol
E2F	E2F transcription factor
E2F1	E2F transcription factor 1
ECL	Enhanced chemiluminescence
EDTA	Ethylene-diamine-tetra-acetic acid
EHMT1	Euchromatic histone-lysine N-methyltransferase 1
EHMT2	Euchromatic histone-lysine N-methyltransferase 2
EME1	Essential meiotic structure-specific endonuclease 1
EME2	Essential meiotic structure-specific endonuclease subunit 2
EMT	Epithelial-mesenchymal transition
ERCC1	Excision repair cross-complementing group 1
ERCC6	Excision repair cross-complementation group 6
ERCC8	Excision repair cross-complementation group 8
ESC	Embryonic stem cell
EXO1	Exonuclease 1
EZH2	Enhancer of zeste homolog 2
FA	Fanconi anaemia
FANC	Fanconi anaemia complementation group
FANCA	Fanconi anaemia complementation group A
FANCB	Fanconi anaemia complementation group B
FANCC	Fanconi anaemia complementation group C
FANCD1	Fanconi anaemia complementation group D1
FANCD2	Fanconi anaemia complementation group D2
FANCDN	Fanconi anaemia complementation group DN
FANCE	Fanconi anaemia complementation group E
FANCF	Fanconi anaemia complementation group F
FANCG	Fanconi anaemia complementation group G
FANCJ	Fanconi anaemia complementation group J
FANCL	Fanconi anaemia complementation group L
FANCM	Fanconi anaemia complementation group M
FANCS	Fanconi anaemia complementation group S
FAT	FRAP-ATM-TRRAP domain

FATC	FRAP-ATM-TRRAP C-terminal domain
FCS	Foetal calf serum
FDA	U.S. Food and Drug Administration
FEN1	Flap structure-specific endonuclease 1
FL	Full-length
FLOS	Functional location on SETD1A domain
FLP	Flippase
FOXM1	Forkhead box M1
FRT	Flippase recognition target
g	g-force (unit of acceleration)
G1	Cell cycle growth phase 1
G2	Cell cycle growth phase 2
GAPDH	Glyceraldehyde 3-phosphate dehydrogenase
GEN1	GEN1 Holliday junction 5' flap endonuclease
GEO	Gene expression omnibus
GFP	Green fluorescent protein
GG-NER	Global genome nucleotide excision repair
gRNA	Guide RNA
GUSB	Glucuronidase beta
Gy	Gray (ionising radiation unit)
H1	Histone H1
H2	Histone H2
H2A	Histone H2A
H2AK13	Histone H2A lysine 13
H2AK15	Histone H2A lysine 15
H2AX	Histone H2A variant X
H2B	Histone H2B
H3	Histone H2
H3B	Histone H3B
H3K27	Histone H3 lysine 27
H3K4	Histone H3 lysine 4
H3K9	Histone H3 lysine 9
H3R2	Histone H3 arginine 2
H4K16	Histone 4 lysine 16
H4K20	Histone H3 lysine 20
HCF1	Host cell factor 1
HCl	Hydrochloric acid
HD	Helical domain
HDAC1	Histone deacetylase 1
HDAC2	Histone deacetylase 1
HEAT	Huntingtin, elongation factor 3, protein phosphatase 2A, TOR1 domain
HELQ	Helicase POLQ-like
HER2	Human epidermal growth factor receptor 2
HF	High fidelity
HGSOC	High grade serious ovarian cancer

HIF1α	Hypoxia inducible factor 1 subunit Alpha
HJ	Holliday junction
HMG	High mobility group
HPF1	Histone PARylation factor 1
HPRT	Hypoxanthine phosphoribosyl transferase
HPV	Human papilloma virus
HR	Homologous recombination
HRP	Horseradish peroxidase
HSC	Haemopoietic stem cell
HSD17B7	Hydroxysteroid 17-beta dehydrogenase 7
HSPC	Haematopoietic stem and progenitor cell
HU	Hydroxyurea
IC50	Half-maximal inhibitory concentration
iCas9	Inducible CRISPR associated protein 9
ICL	Inter-strand crosslink
IGEPAL	Octyl phenoxy poly(ethyleneoxy)ethanol
IgG	Immunoglobulin G
IGV	Integrated genome viewer
INDELS	Insertions/deletions
IP	Immunoprecipitation
IR	Ionising radiation
IRF2BPL	Interferon regulatory factor 2 binding protein like
ITGAM	Integrin subunit alpha M
JMJD2A/B	Jumonji D2A/2B demethylase
K4A	Lysine 4 to Alanine mutation
KAP1	KRAB-associated protein 1
Kb	Kilobases
KCl	Potassium chloride
KDa	Kilodaltons
KDM	Lysine demethylase
KDM1A	Lysine demethylase 1A
KDM1B	Lysine demethylase 1B
KDM5A	Lysine demethylase 5A
KDM5B	Lysine demethylase 5B
KDM5C	Lysine demethylase 5C
KDM5D	Lysine demethylase 5D
KICS2	KICSTOR subunit 2
KICSTOR	KPTN, ITFG2, C12orf66, and SZT2
KMT	Lysine methyltransferase
KMT2A	Lysine methyltransferase 2A
KMT2B	Lysine methyltransferase 2B
KMT2C	Lysine methyltransferase 2C
KMT2D	Lysine methyltransferase 2D
KMT2F	Lysine methyltransferase 2F
KMT2G	Lysine methyltransferase 2G
KMT5A	Lysine methyltransferase 5A

KMT5B	Lysine methyltransferase 5B
KMT5C	Lysine methyltransferase 5C
KMT7	Lysine methyltransferase 7
Ku 80	ATP-dependent DNA helicase II, 80 kDA subunit
Ku70	ATP-dependent DNA helicase II, 70 kDA subunit
LIG1	DNA ligase 1
LIG3	DNA ligase 3
LIG4	DNA ligase 4
LINC00319	Long intergenic non-protein coding RNA 319
LMNA	Lamin A/C
LoF	Loss of function
LP-BER	Long patch-base excision repair
LSD1	Lysine specific demethylase 1A
Lys	Lysine
M	Mole (unit of concentration)
M (phase)	Cell cycle mitotic phase
MAR	Mono (ADP-ribose)
MBT	Malignant brain tumour domain
mCRPC	Metastatic castration-resistant prostate cancer
MDC1	Mediator of DNA damage checkpoint protein 1
MDR1	Multidrug resistance protein 1
me	Methylation
me0	Unmethylated
me1	Mono-methylation
me2	Di-methylation
me3	Tri-methylation
METABRIC	Molecular Taxonomy of Breast Cancer International Consortium
$MgCl_2$	Magnesium chloride
MGMT	O-6-methylguanine-DNA methyltransferase
MiDAS	Mitotic DNA synthesis
MLH1	MutL homolog 1
MLL	Mixed-lineage leukaemia
MLL1	Mixed lineage leukaemia protein 1
MLL2	Mixed lineage leukaemia protein 2
MLL3	Mixed lineage leukaemia protein 3
MLL4	Mixed lineage leukaemia protein 4
MMC	Mitomycin C
MMR	Mismatch repair
MRE11	Meiotic recombination 11 homologue
MRN	MRE11-Rad50-Nbs1
mRNA	Messenger ribonucleic acid
MSH	Beta-melanocyte stimulating hormone
MSH2	MutS homolog 2
MSH6	MutS homolog 6
mTOR	Mammalian target of rapamycin
mTORC1	Mammalian target of rapamycin complex 1

MTT	3-(4, 5-dimethylthiazolyl-2)-2, 5-diphenyltetrazolium bromide assay
MUS81	MUS81 structure-specific endonuclease subunit
MYC	MYC proto-oncogene, BHLH transcription factor
MYND	Myeloid, Nervy and DEAF-1
NaCl	Sodium chloride
NAD	Nicotinamide adenine dinucleotide
NBS1	Nijmegen breakage syndrome 1
NCBI	National Centre for Biotechnology Information
NEDD8	Neural precursor cell expressed, developmentally down-regulated 8 ubiquitin like modifier
NER	Nucleotide excision repair
NHEJ	Non-homologous end joining
NKD2	NKD inhibitor of WNT signalling pathway 2
NLRX1	NLR family member X1
NLS	Nuclear localisation signal
NOTCH1	Notch receptor 1
NP-40	Ethoxylated nonylphenol
NSCLC	Non-small cell lung cancer
N-SET	N-terminal to the SET domain
nt	Nucleotide
NTC	Non targeting/transfected control
N-terminus	Amino terminus
NURF	Nucleosome-remodelling factor subunit BPTF
OF	Okazaki fragment
OMA1	OMA1 zinc metallopeptidase
P	Phosphorylation
p53	Tumour protein 53
PAAF1	Proteasomal ATPase associated factor 1
PAGE	Polyacrylamide gel electrophoresis
PALB2	Partner and localizer of BRCA2
PAR	Poly (ADP-ribose)
PARG	Poly (ADP-ribose) glycohydrolase
PARP	Poly (ADP-ribose) polymerase
PARPi	Poly (ADP-ribose) polymerase inhibitor
PAXX	Paralog of XRCC4 and XLF
PBS	Phosphate-buffered saline
P-CHK1	Phosphorylated checkpoint protein 1
PCNA	Proliferating cell nuclear antigen
PCR	Polymerase chain reaction
P-CREB	Phosphorylated CAMP responsive element binding protein 1
PDAC	Pancreatic ductal adenocarcinoma
PDX	Patient-derived xenograft
PEX10	Peroxisomal biogenesis factor 10
PEX12	Peroxisomal biogenesis factor 12
PFA	Paraformaldehyde
PHD	Plant homeodomain

PI	Propidium iodide
PI3K	Phosphatidyl inositol 3 kinase
PIKK	Phosphatidyl inositol 3 kinase like kinase
PIN1	Peptidylprolyl cis/trans isomerase, NIMA-interacting 1
PIPES	Piperazinediethanesulfonic acid
P-KAP1	Phosphorylated KRAB-associated protein 1
P-NBS1	Phosphorylated Nijmegen breakage syndrome 1
Polμ	Polymerase μ
POLE4	DNA polymerase epsilon 4 accessory subunit
Polλ	Polymerase λ
PRIMPOL	Primase and DNA directed polymerase
PRMT5	Protein arginine methyltransferase 5
PRMT6	Protein arginine methyltransferase 6
P-RPA	Phosphorylated replication protein A
PTGR2	Prostaglandin reductase 2
PTIP	PAX interacting protein 1
PTM	Post-translational modification
PWWP	Proline-tryptophan-tryptophan-proline motif
qPCR	Quantitative polymerase chain reaction
RAD18	RAD18 E3 ubiquitin protein ligase
RAD23B	RAD23 homolog B
RAD50	RAD50 double-strand break repair protein
RAD51	RAD51 recombinase
RAD51C	RAD51 paralog C
RAD51D	RAD51 paralog D
RAD52	RAD50 homolog double-strand break repair protein
RAD6	Ubiquitin-conjugating enzyme E2B
RAD9B	RAD9 checkpoint clamp component B
RADX	RPA-related and RAD51-agonist, X-chromosome
RAP80	Receptor-associated protein 80
RBBP2	Retinoblastoma-binding protein 2 (KDM5A)
RBBP5	Retinoblastoma-binding protein 5
RBM15	RNA binding motif protein 15
RECQL1	RecQ-like helicase 1
RECQL4	RecQ like Helicase 4
RECQL5	RecQ-like helicase 5
REV1	REV1 DNA directed polymerase
REV7	REV7 homologue
RF	Replication fork
RFP	Red fluorescent protein
RIF1	Rap1-interacting factor 1
RNA	Ribonucleic acid
RNase	Ribonuclease
RNase H2	Ribonuclease H2
RNF168	Ring finger protein 168
RNF20	Ring finger protein 20

RNF8	Ring finger protein 8
rNTP	Ribonucleotide triphosphate
ROS	Reactive oxygen species
RPA	Replication protein A
rpm	Revolutions per minute
RRM	RNA recognition motif
rRNA	Ribosomal RNA
RT-qPCR	Real-time quantitative polymerase chain reaction
RUVB1	RuvB like AAA ATPase 1
S (phase)	Cell cycle synthesis phase
SD	Standard deviation
SDS	Sodium dodecyl sulphate
SDSA	Synthesis-dependent strand annealing
SDS-PAGE	Sodium dodecyl-sulphate polyacrylamide gel electrophoresis
SEM	Standard error of the mean
Ser	Serine
SET	Su(var)3-9, Enhancer-of-zeste and Trithorax
SETD1A	SET domain-containing protein 1A
SETD1B	SET domain-containing protein 1B
sgRNA	Single-guide RNA
SHLD1	Shieldin subunit 1 (C20orf196)
SHLD2	Shieldin subunit 2 (FAM35A)
SHLD3	Shieldin subunit 3 (CTC-534A2.2)
shRNA	Short hairpin RNA
siRNA	Small interfering RNA
SIRT1	Sirtuin 1
SIRT2	Sirtuin 2
SLX1	Structure-specific endonuclease subunit SLX1
SLX4	Structure-specific endonuclease subunit SLX4
SMARCAL1	SWI/SNF-related matrix-associated actin-dependent regulator of chromatin subfamily A-like protein 1
SMX	SMX trinuclease (SLX1-SLX4, MUS81-EME1, and XPF-ERCC)
SMYD	SET and MYND domain
SMYD1	SET and MYND domain containing 1
SMYD2	SET and MYND domain containing 2
SMYD3	SET and MYND domain containing 3
SP-BER	Short patch-base excision repair
SPRTN	Spartan
SSA	Single-strand annealing
SSB	Single-strand break
ssDNA	Single-strand DNA
STX1B	Syntaxin 1B
SUMO	Small ubiquitin-like modifier
TAF3	TATA-box binding protein associated factor 3
TBS-T	Tris-buffered saline with Tween 20
TCGA	The Cancer Genome Atlas

TC-NER	Transcription coupled nucleotide excision repair
TFIIH	Transcription factor II H
THRAP3	Thyroid hormone receptor associated protein 3
TIP60	Tat Interacting Protein, 60kDa (Lysine acetyltransferase 5)
TLS	Translesion synthesis
TM2D3	TM2 domain containing 3
TMEM143	Transmembrane protein 143
TOP1	Topoisomerase 1
TOP3	Topoisomerase 3
TP53	Tumour protein P53
TRC	Transcription-replication conflict
TRF2	Telomeric repeat binding factor 2
Tris	Tris(hydroxymethyl)aminomethane
TRMT1L	TRNA methyltransferase 1 like
TSS	Transcription start site
TWIST2	Twist family BHLH transcription factor 2
Ub	Ubiquitination
UBC13	Ubiquitin-conjugating enzyme E2 13
UDR	Ubiquitylation-dependent recruitment motif
UNG	Uracil-DNA glycosylase
USP1	Ubiquitin specific peptidase 1
UV	Ultraviolet
V	Volt (unit of electric potential)
V(D)J	Variable–diversity–joining rearrangement
v/v	Volume per volume (concentration)
w/v	Weight per volume (concentration)
WDR5	WD repeat domain 5
WDR82	WD repeat domain 82
WGR	Tryptophane (W), glycine (G), arginine (R) motif
WT	Wild-type
XLF	XRCC4-like factor
XPC	Xeroderma pigmentosum complementation group C
XPF	Xeroderma pigmentosum complementation group F
XPG	Xeroderma pigmentosum complementation group G
XRCC1	X-ray repair cross-complementing 1
XRCC4	X-ray repair cross-complementing 4
XRCC5	X-ray repair cross complementing 5
XRCC6	X-ray repair cross complementing 6
ZFP41	Zinc finger protein 41 homolog
Zn	Zinc
γH2AX	Phosphorylated (gamma)-histone H2AX

1. CHAPTER 1: INTRODUCTION

1.1 DNA damage

Cells are exposed to between 1,000 and 1,000,000 lesions per day as a result of DNA damage arising from a variety of sources (Alhmoud *et al.*, 2020) (**Fig. 1.1**). Endogenous DNA damaging agents are intrinsic to the cell, arising naturally from physiological processes. The most frequent sources of this type of DNA damage are spontaneous replication errors, resulting in the misincorporation of nucleotide bases into the DNA and reactive oxygen species (ROS), produced as by-products of cellular oxidative respiration (De Bont and van Larebeke, 2004).

In contrast, exogenous damage occurs from external sources to the body. Key sources of exogenous damage include: ultraviolet (UV) radiation, responsible for up to 1 x 10^5 lesions per cell per day (Hoeijmakers, 2001); ionising radiation (IR), which causes both single- and double-strand DNA breaks; as well as alkylating agents present within the diet, tobacco smoke and chemotherapeutic agents (Milligan *et al.*, 2000; Alberg *et al.*, 2007).

Regardless of the source of damage, these genotoxic agents disrupt covalent bonds between nucleotides causing structural changes in the DNA which prevent accurate replication of the genome. Consequently, DNA damage can alter nucleotide sequences to produce dysfunctional proteins that are detrimental to cellular physiology, resulting in a wide variety of human pathologies, including neurological defects, immunodeficiencies and increased cancer susceptibility (Ma *et al.*, 2017).

1.2 DNA damage repair

To avoid the cytological consequences of DNA damage cells are equipped with multiple, distinct but complementary repair mechanisms, to deal with the wide range of specific DNA lesions that threaten genomic integrity. Collectively these repair pathways make up the DNA damage response (DDR), which senses, signals, and initiates DNA damage repair (Lord and Ashworth, 2012) (**Fig. 1.1**).

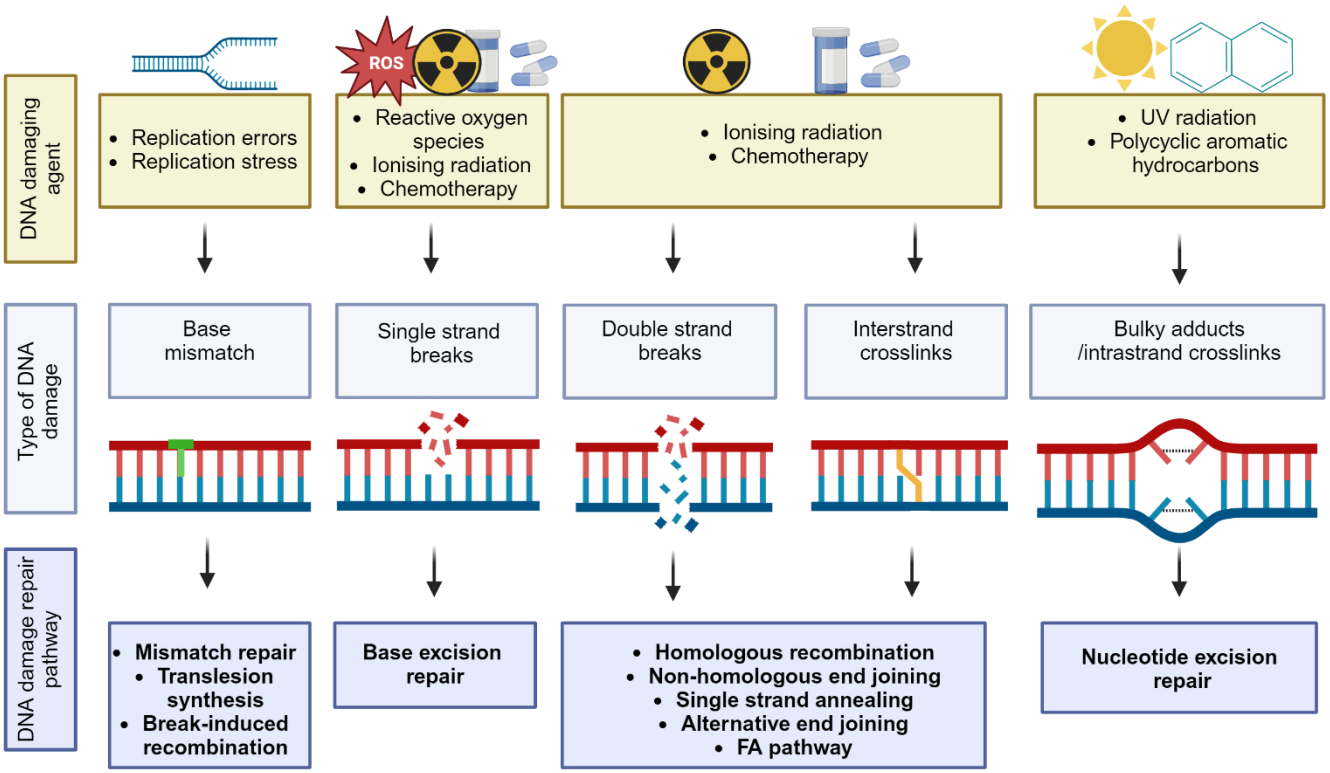

Figure 1.1- Types of DNA damage and DNA damage repair pathways.

DNA damage results from a wide variety of sources including ionising radiation, reactive oxygen species and chemotherapeutic agents. These agents can cause different types of lesions on the DNA which are repaired by multiple, lesion-specific DNA repair mechanisms. Figure created with BioRender.com.

1.2.1 DNA repair pathway activation

The DDR begins with recognition of DNA damage and activation of the appropriate repair pathways. This occurs through cellular signalling cascades mediated by the apical DDR signalling kinases: Ataxia telangiectasia mutated (ATM), Ataxia telangiectasia and Rad3 related (ATR) and DNA-dependent protein kinase catalytic subunit (DNA-PKcs) (Lanz, Dibitetto and Smolka, 2019).

Appropriate and timely recruitment of these DDR kinases to sites of DNA damage is modulated by specific co-factors. Generally, ATR is recruited to replication protein A (RPA)-associated single-strand DNA (ssDNA) via interaction with ATR-interacting protein (ATRIP) (Shigechi *et al.*, 2012), whilst ATM and DNA-PKcs associate with double-strand breaks (DSBs) via the MRE11-RAD50-NBS1 (MRN) complex (Zhou and Paull, 2013) and Ku70/Ku80 (Gottlieb and Jackson, 1993), respectively.

A key event in the initiation of the DDR is phosphorylation of the histone H2 variant H2A.X at serine 139 (γH2AX). Phosphorylation of H2AX can be performed by ATM or DNA-PKcs in a functionally redundant manner (Stiff *et al.*, 2004). This marks the genomic lesion and leads to the recruitment of mediator of DNA damage checkpoint protein 1 (MDC1) to the DSB. MDC1 then acts as a docking site to recruit the MRN complex to the site of damage (Reginato and Cejka, 2020). In turn, MRN recruitment promotes further deposition and activation of ATM via autophosphorylation at serine 1981, leading to dissociation from its dimeric form to its active monomeric form. The active ATM monomer further promotes downstream phosphorylation and interaction with ATM partners including MDC1, RNF8, RNF168, BRCA1 and 53BP1 to alert cells to the presence of DSBs and alter chromatin structure in the vicinity of the break. ATM is also responsible for the phosphorylation of KAP1 (KRAB associated protein

1) and CREB (Cyclic AMP response element binding protein), modulating heterochromatic DSB repair and transcriptional regulation of DDR proteins in response to DNA damage (White *et al.*, 2012; Shi *et al.*, 2004)

DNA-PKcs also undergoes autophosphorylation, facilitating the recruitment of downstream repair proteins such as Artemis and allowing for complex disassembly to complete DSB repair (Gottlieb and Jackson, 1993). Furthermore, dissociation of DNA-PKcs from DSBs by autophosphorylation can promote DNA end-resection (Zhou and Paull, 2013).

On the other hand, ATR is primarily activated in response to replication stress and the presence of RPA-bound ssDNA (Adams *et al.*, 2006). Whilst kinase substrate analysis revealed that ATR phosphorylates many of the same targets as ATM (Matsuoka *et al.*, 2007), ATR has unique targets associated with replication fork repair. For example, ATR has been shown to phosphorylate FANCI promoting FANCD2 ubiquitination, a key step in the Fanconi anaemia pathway (described below) (Ishiai *et al.*, 2008).

Activation of the apical DDR kinases in response to DNA damage also stimulates the phosphorylation of the downstream checkpoint kinases, CHK1 and CHK2. These kinases further mediate regulation of cyclin-dependent kinases (CDKs) to activate the DNA damage checkpoint, preventing cell-cycle progression, allowing the cell time to undertake repair before replication continues (Awasthi, Foiani and Kumar, 2015). ATM is the principal kinase responsible for phosphorylating CHK2 at threonine 68, activating the G1/S cell cycle checkpoint (Matsuoka *et al.*, 2000). CHK2 subsequently phosphorylates CDC25A and CDC25C phosphatases, resulting in their inactivation to

remove the inhibitory phosphorylation of CDK2 (Falck *et al.*, 2001). On the other hand, ATR phosphorylates CHK1 at serine 317 and 345, activating the intra-S and G2/M checkpoints. Similarly to CHK2, CHK1 also mediates cell cycle arrest through inactivation of CDC25 phosphatases by promoting ubiquitination and subsequent proteasomal degradation (Ruiz *et al.*, 2016). Furthermore, cell cycle arrest is mediated by the p53 transcription factor, which is directly phosphorylated by all the DNA damage signalling kinases (Chao *et al.*, 2006).

There is significant crosstalk between all three of these DDR signalling kinases. For example, ATM also contributes to the intra-S and G2/M checkpoint as ATM-dependent end-resection generates the RPA-coated ssDNA required for ATR activation (Myers and Cortez, 2006). This is further supported by Adams *et al.* who showed ATM kinase activity was required for ATR recruitment to IR-induced DNA damage (Adams *et al.*, 2006). Additionally, many kinase substrates possess motifs that are sites for phosphorylation by multiple kinases, indicating significant crossover in function (Matsuoka *et al.*, 2007). Lasty, these kinases can function as phosphorylation targets for each other. For example, ATM-dependent phosphorylation of DNA-PKcs at threonine 4102, located within the FATC domain, regulates its role in DSB repair (Lu *et al.*, 2023). Conversely, loss of DNA-PKcs function results in hyperactivation of ATM, suggesting an inhibitory role for DNA-PKcs in ATM signalling (Finzel *et al.*, 2016).

The most common types of DNA damage are those affecting a single strand of the DNA double helix, including single-strand breaks (SSB) and chemical base modifications. As the focus of this thesis is double-strand break repair, these single strand repair pathways will be discussed briefly below.

1.2.1.1 Direct reversal repair

Some types of ssDNA damage caused by alkylation, oxidation and UV exposure can be repaired by direct reversal. During direct reversal the phosphodiester backbone of DNA remains intact, as DNA synthesis is not required for repair (Yi and He, 2013). O^6methylguanine lesions are removed by the O^6-methylguanine-DNA methyltransferase (MGMT) in a process that results in the ubiquitination of MGMT and subsequent degradation. Alternatively, alkylated DNA repair protein homologs ALKBH2 and ALKBH3 remove a number of modified bases including 1-methyladenine and 3-methylcytosine through oxidative demethylation, requiring ferrous iron and the conversion of α-ketoglutarate to succinate (Gutierrez and O'Connor, 2021).

1.2.1.2 Ribonucelotide excision repair

Ribonucleotide excision repair refers to the removal of mis-incorporated ribonucleotide triphosphates (rNTPs) into the DNA. This process is initiated by cleavage of the DNA-RNA junction by RNase H2 to produce a SSB. Polymerase δ performs strand displacement synthesis to create a flap structure containing the rNTP, which is subsequently removed by Flap endonuclease 1 (FEN1) or exonuclease 1 (EXO1). The SSB is then ligated by DNA ligases (Sparks *et al.*, 2012).

1.2.1.3 Nucleotide excision repair

Lesions that distort the DNA helix such as bulky adducts caused by UV radiation, chemotherapeutic agents and polyaromatic hydrocarbons are repaired by the nucleotide excision repair (NER) pathway (Schärer, 2013). NER is further categorised into global genomic NER (GG-NER), which is activated when the DNA helix becomes distorted, and transcription coupled NER (TC-NER), which occurs when lesions are

detected by blocked RNA polymerases. During GG-NER the distorted helix is recognised by the XPC/RAD23B/CETN2 complex, alternatively in TC-NER the blocked RNA polymerases recruits ERCC6, followed by ERCC8 to the damage site. Formation of these recognition complexes subsequently recruits TFIIH helicase to unwind the DNA helix. Next, XPG and XPF/ERCC1 are recruited to excise the nucleotides surrounding the DNA damage. The repair process is then completed by DNA polymerases and ligases which synthesise missing nucleotides and fill the gaps. DNA polymerase ε and ligase I act in replicating cells, whilst DNA polymerases δ and κ and DNA ligase IIIα, together with its cofactor XRCC1, predominate in non-replicating cells (Schärer, 2013; Ogi *et al.*, 2010). Deficiencies in this pathway are associated with a variety of human diseases, including xeroderma pigmentosum (Spivak, 2015).

1.2.1.4 Mismatch repair

Replication errors such as insertions, deletions and mis-incorporation of DNA bases by DNA polymerases are repaired by mismatch repair (MMR) (Jiricny, 2013). Firstly, MSH proteins recognise mismatched bases, binding to the DNA to form a sliding clamp (Chakraborty, Dinh and Alani, 2018). EXO1 excises the mismatched nucleotides producing ssDNA, which is subsequently bound by RPA to prevent further degradation. DNA is then synthesised and ligated by DNA polymerase δ and ligases (Bowen and Kolodner, 2017), with assistance from PCNA to finalise repair (Dieckman, 2021).

1.2.1.5 Fanconi anaemia pathway

The Fanconi anaemia (FA) pathway is a complex pathway involving twenty-two genes critical for the repair of interstrand cross-links (ICLs). Briefly the

FANCD2/FANCI heterodimer is localised to the damaged chromatin promoted via monoubiquitylation by the FA core complex (FANCA, FANCB, FANCC, FANCE, FANCF, FANCG, FANCL, and FANCM). Here FANCD2/FANCI interacts with FANCD1, FANCDN, FANCJ, FANCS and other DDR proteins to perform repair via homologous recombination (HR) (Kim and D'Andrea, 2012), described in further detail below. Following this, the FANCD2/FANCI complex is deubiquitylated by USP1 to complete repair (Kim and Kim, 2016).

1.2.1.6 DNA-protein cross-link repair

DNA-protein cross-links (DPCs) can be induced by chemotherapeutic agents and other exogenous sources, such as UV and IR. These lesions are repaired by three distinct processes. Firstly, covalent links between the DNA and protein are hydrolysed by tyrosyl DNA-phosphodiesterases (Debéthune *et al.*, 2002; Ledesma *et al.*, 2009). Next, the MRN complex excises the cross-linked DNA fragment (Sacho and Maizels, 2011) and lastly, the spartan (SPRTN)/weak suppressor of SMT3 protein 1 (Wss1) protease family degrades the protein (Stingele *et al.*, 2014).

1.2.1.7 Translesion synthesis

Translesion synthesis (TLS) is a DNA damage tolerance pathway that allows DNA replication to bypass DNA damage. During this process DNA polymerases are replaced by translesion polymerases such as, REV1, DNA polymerase nu, kappa and iota, which can synthesise DNA using template strands containing DNA damage (Prakash, Johnson and Prakash, 2005). This process is initiated by monoubiquitylation of PCNA at lysine 164 by the RAD6/RAD18 E2-E3 ubiquitin ligase complex (Hoege *et al.*, 2002). TLS can help to prevent fork reversal and degradation and contribute to ssDNA gap filling (Khatib, Nicolae and Moldovan, 2024).

1.2.1.8 Base excision repair

Finally, base excision repair (BER) is the major repair pathway for base lesions and SSBs induced by oxidative damage, ionising radiation and alkylating agents (Krokan and Bjørås, 2013). BER is initiated by DNA glycosylases, which recognise and remove damaged bases by cleaving the N-glycosidic bond between the base and deoxyribose to generate abasic sites. There are 11 known glycosylases which recognise specific base lesions (Jacobs and Schär, 2012). This abasic site is subsequently recognised by the APE1 endonuclease which hydrolyses the DNA backbone to form a SSB with 5′-deoxyribosephosphate and 3′-hydroxyl ends. PARP1 functions with APE1 to protect the SSB from nuclease degradation and recruit repair proteins through poly(ADP-ribosyl)ation (Woodhouse *et al.*, 2008). From here, BER can proceed by two pathways: short-patch BER (SP-BER) or long-patch BER (LP-BER). In SP-BER DNA polymerase β lyses the 5′-deoxyribosephosphate and incorporates the correct nucleotide, which is then sealed by DNA LIG3 and XRCC1. If the sugar group has been oxidised or reduced LP-BER is initiated. Instead, DNA polymerase δ is employed to synthesise a 2-8 nucleotide flap. PCNA displaces the damaged strand, which is then removed by FEN1. The resulting nick is then ligated by DNA LIG1 (Dianov and Hübscher, 2013).

1.2.2 Double-strand break repair

The most dangerous of all DNA lesions are double-strand breaks (DSBs). DSBs occur when the two complementary strands of the double helix are simultaneously broken in proximity. Common sources of DSBs include IR, unresolved replication stress, ROS, as well as programmed genome rearrangements, including V(D)J recombination and class switch recombination. Dividing mammalian cells are subject

to approximately 10 DSBs per day per cell (Martin *et al.*, 1985). Failure to repair these DSBs can promote tumorigenesis, through the inactivation of essential genes or promotion of inappropriate recombination events (Khanna and Jackson, 2001). To avoid the tumorigenic consequences of DSBs, mammalian cells have evolved two major complementary pathways for DSB repair; non homologous end joining (NHEJ) and homologous recombination (HR).

1.2.2.1 Non-homologous end joining

Non-homologous end joining (NHEJ) is the preferential pathway for DSB repair, accounting for > 90% of DSB repair. NHEJ directly ligates DNA ends and thus does not require a homologous DNA template for repair. Due to this, there is potential for chromosomal rearrangements and loss of genetic information if DNA ends require processing prior to ligation, as a result NHEJ is considered error-prone (Kakarougkas and Jeggo, 2014).

The first step in NHEJ is the formation of the Ku70/80 heterodimer. Ku70/80 binds both ends of the DNA break, providing protection from DNA end-resection and a scaffold for the loading of other NHEJ proteins. The C-terminal domain of Ku80 then recruits DNA-PKcs, forming the DNA-PK holoenzyme complex (Smith and Jackson, 1999). DNA-PK is phosphorylated at threonine 2609 by ATM in response to DNA damage (Lu *et al.*, 2023). If the DNA ends are compatible then the DNA-PK complex recruits X-ray repair cross-complementing protein 4 (XRCC4), XRCC4-like factor (XLF) and paralogue of XRCC4 and XLF (PAXX) to bring the two DNA ends together through a process called ‘synapsis’ (Ochi *et al.*, 2015). The recruitment of these factors is also aided by Aprataxin and PNK-like factor (APLF) (Grundy *et al.*, 2013). Alternatively, synapsis can also be mediated by DNA polymerase μ. Subsequently,

DNA polymerases λ and μ fill in the gaps at the site of the break. Finally, the blunt DNA ends are directly ligated by DNA LIG4, with the assistance of XRCC4 (Brouwer *et al.*, 2016). XLF and XRCC4 form a sleeve around the DNA to stabilise the DNA ends prior to ligation. However, if the ends are not compatible DNA-PKcs is auto-phosphorylated to activate Artemis-dependent DNA resection prior to ligation (Goodarzi *et al.*, 2006). The Artemis-DNA-PKcs complex cleaves DNA overhangs to create regions of homology that are subsequently ligated by XRCC4-DNA LIG4. It is estimated that 20-50% of IR-induced DSBs require Artemis mediated resection for their repair (Kurosawa *et al.*, 2008) (**Fig. 1.2**).

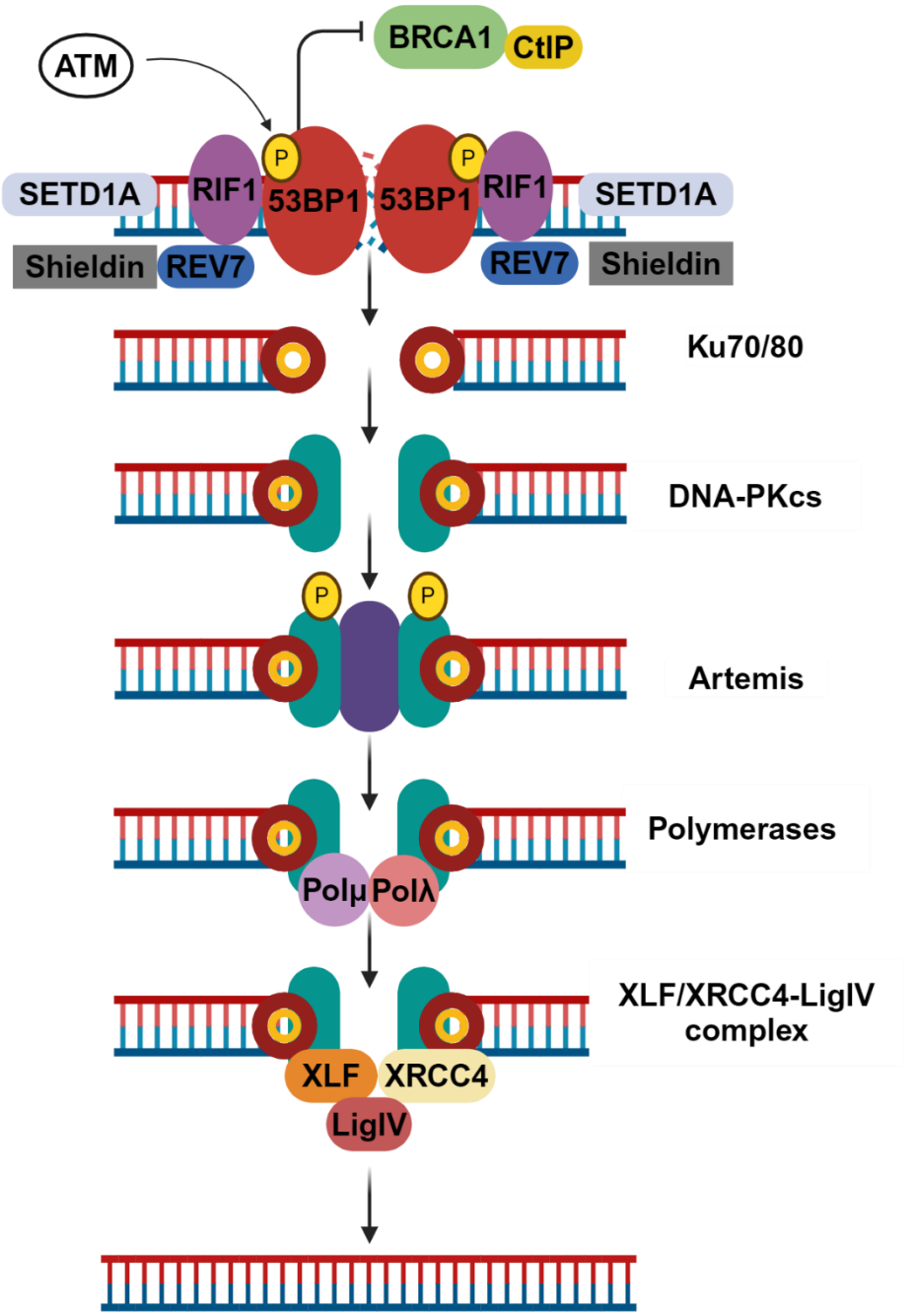

Figure 1.2- Non-homologous end joining.

During the repair of double strand breaks (DSBs) by non-homologous end joining (NHEJ), the Ku70/80 heterodimer binds the DSB recruiting DNA-PKcs. DNA-PKcs undergoes autophosphorylation recruiting the Artemis nuclease. Following limited resection, XRCC4 and DNA ligase IV ligate the DSB ends. Figure created with BioRender.com

1.2.2.2 Homologous recombination

The second pathway, accounting for ~10% of DSB repair, is homologous recombination (HR). HR is less error prone than NHEJ, due to the requirement for a homologous sister chromatid template to prime repair synthesis. Consequently, HR occurs following DNA replication during S phase (Heyer, Ehmsen and Liu, 2010).

DSB repair by HR is initiated by removal of Ku from DNA ends by extensive DNA resection generating ssDNA. Firstly, the endonuclease activity of MRE11 creates a DNA nick approximately 300 nucleotides away from the DSB. Subsequently, MRE11's exonuclease activity extends this nick back towards the DSB (Garcia *et al.*, 2011). This initial DNA resection is then extended by the exonuclease activity of CtIP, and further resection is performed by EXO1, with support from the nuclease DNA2 and the DNA helicase BLM (Nimonkar *et al.*, 2011). DNA resection generates ssDNA with 3' overhangs, which are subsequently bound by the ssDNA binding protein RPA complex. RPA stabilises the ssDNA and prevents the formation of secondary structures. RPA is then removed from the DNA and replaced by the RAD51 recombinase to form a RAD51-ssDNA nucleoprotein filament. BRCA1, along with PALB2, facilitates the recruitment of BRCA2 and RAD51 to the ssDNA, sustaining RPA displacement and facilitating RAD51 loading (Zhang *et al.*, 2009). The RAD51 nucleoprotein filament mediates the search for homologous sequences on the sister chromatid to provide a template for repair. BRCA1 and its binding partner BARD1, enhance RAD51 recombinase activity and help promote the pairing of homologous sequences (Zhao *et al.*, 2017). The RAD51 nucleoprotein filament binds to the complementary DNA forming a displacement-loop (D-loop). Following D-loop formation, DNA is synthesised across the break using the sister chromatid as a repair

template. The invading strand is then displaced, and HR is completed by synthesis-dependent strand annealing (SDSA), break induced replication (BIR) or double Holliday junction (dHJ) formation.

During SDSA the newly synthesised DNA binds to the opposite end of the DSB, preventing crossover formation. If the DSB is a result of a collapsed replication fork the break is resolved by BIR to form a new replication fork. Finally, dHJ can be dissolved by the BLM helicase and topoisomerase 3 to produce non-crossover products. Alternatively, they can be resolved by the SMX and GEN1 endonucleases, resolution in this manner can result in both non-crossover and crossover events, which can lead to chromosomal rearrangements (**Fig. 1.3**).

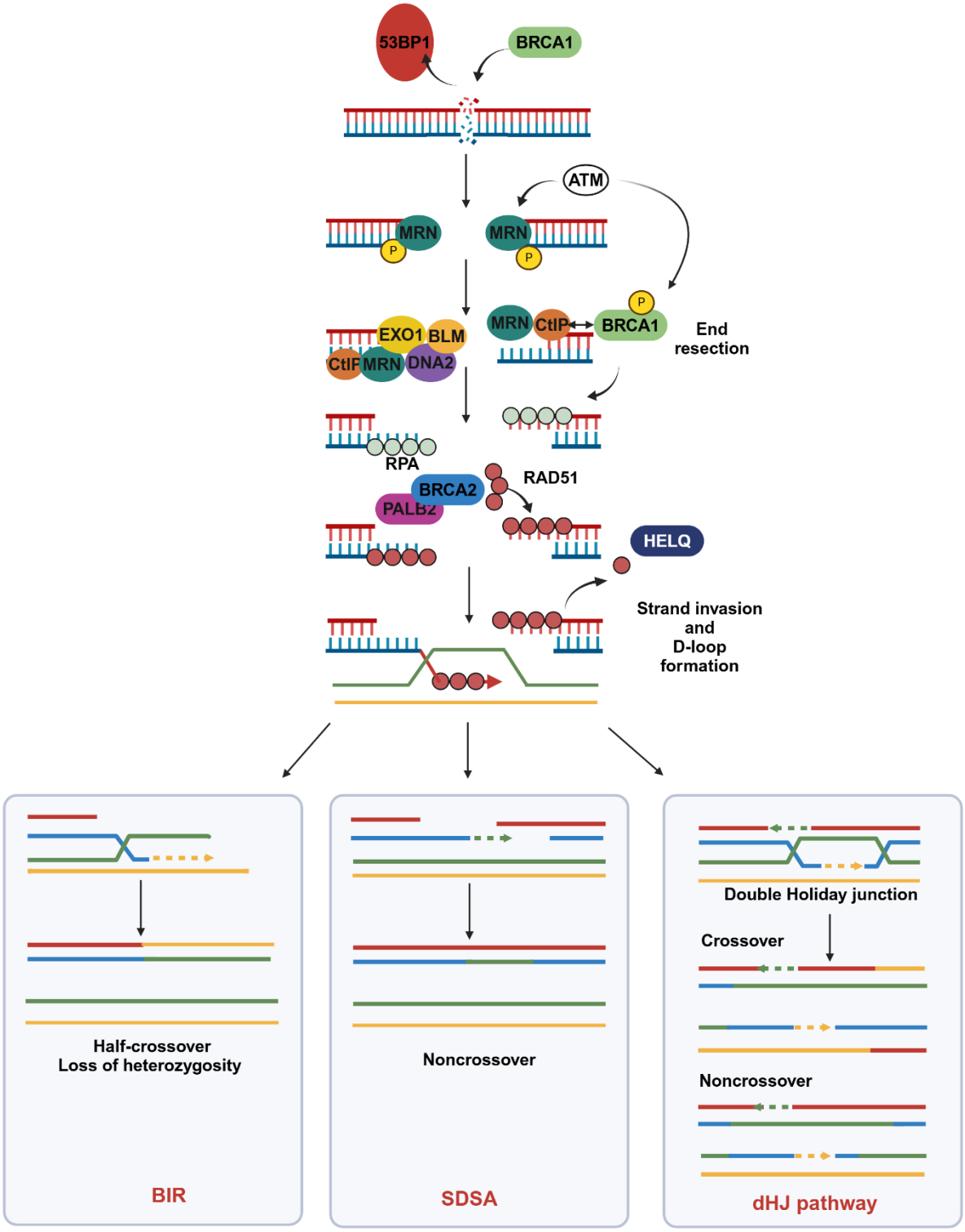
53BP1
BRCA1
ATM
MRN
P
MRN
P
EXO1
BLM
CtIP
MRN
DNA2
MRN
CtIP
P
BRCA1
End resection
RPA
BRCA2
PALB2
RAD51
HELQ
Strand invasion and D-loop formation
Half-crossover
Loss of heterozygosity
BIR
Noncrossover
SDSA
Double Holiday junction
Crossover
Noncrossover
dHJ pathway

Figure 1.3- Homologous recombination.

In S and G2, DSBs are repaired via homologous recombination (HR). The MRN complex is recruited to the DSB via ATM signalling. MRE11 begins DNA resection, which is extended by CtIP and EXO1, with support from the endonuclease DNA2 and the DNA helicase BLM. The resulting ssDNA is bound by RPA, which is subsequently removed and replaced by the RAD51 recombinase facilitated by the BRCA1-PALB2-BRCA2 complex to form a nucleoprotein filament. The RAD51 nucleoprotein filament mediates strand invasion into homologous sequences on the sister chromatid to from a D-loop. DNA is synthesised across the break using the sister chromatid as a repair template. The invading strand is then displaced, and HR is completed by break induced replication (BIR), synthesis-dependent strand annealing (SDSA), or double Holliday junction (dHJ) formation. Figure created with BioRender.com.

.

1.2.2.3 Alternative double-strand break repair pathways

In addition to the two classical DSB repair pathways, there are additional error-prone, mutagenic sub-pathways, including alternative-end joining (alt-EJ) and single-strand annealing (SSA). These backup-pathways can be activated when the canonical DSB repair pathways are disrupted. Both SSA and alt-EJ require extensive DNA resection at the DSB site to reveal regions of microhomology, which can cause extensive loss of genetic information (Simsek and Jasin, 2010).

During SSA DSBs are repaired by pairing tandem repeats. To initiate repair ssDNA is coated with RPA, which is subsequently replaced by RAD52 (Liang *et al.*, 2024). The ERCC1/XPF nuclease complex then eliminates DNA flaps, followed by ligation of gaps by DNA LIG 1 (Al-Minawi, Saleh-Gohari and Helleday, 2008).

Alternatively, during alt-EJ small regions of resected DNA containing homologous sequences can be joined. The switch from NHEJ to alt-EJ is initiated by PARP1 annealing at microhomologies to prevent Ku binding to the DSB. Next, non-homologous tails are removed by unknown nucleases, then DNA is synthesised to fill gaps by DNA polymerase θ (Mateos-Gomez *et al.*, 2015). The strands are then ligated by DNA LIG3 and XRCC1 (Della-Maria *et al.*, 2011).

1.2.3 Regulation of repair pathway choice

Due to the availability of multiple DSB repair pathways, cells have developed control mechanisms to ensure the most appropriate pathway is engaged according to the cellular context, including phosphorylation of repair proteins, cell cycle regulation, control of DNA end-resection, as well as epigenetic control mechanisms.

1.2.3.1 CDK activity

DSBs are initially primed for NHEJ and for this to be overridden the Ku70/80 complex must be displaced from the DSB ends. The key mechanism mediating Ku70/80 displacement and the main determinant of DSB repair pathway choice is DNA end-resection. DNA end-resection is tightly regulated throughout the cell cycle through cell cycle dependent kinase (CDK) activity. CDK activity is typically low during G1 and progressively increases during S/G2. During the S and G2 cell-cycle phases CDK-dependent phosphorylation of CtIP at threonine 847 and serine 327 promotes binding to BRCA1, stimulating DNA end-resection and HR (Anand *et al.*, 2016; Tomimatsu *et al.*, 2014). Consequently, mutations in threonine 847 disrupt the CDK target motif, resulting in defects in DNA end-resection (Huertas and Jackson, 2009). Furthermore, CDK1/2 dependent phosphorylation of RECQL4 promotes its interaction with MRE11 to drive HR. Conversely, in G1 phase of the cell cycle, when CDK activity is low, unphosphorylated RECQL4 is able to bind to Ku to promote NHEJ (Lu *et al.*, 2017).

CDK-mediated modifications can also counteract end-resection activity. For example, CDK2-mediated phosphorylation of CtIP at threonine 315 and serine 276 promotes its polyubiquitination and degradation through interactions with PIN1 (Steger *et al.*, 2013), preventing DNA end-resection to inhibit HR and promote repair by NHEJ.

1.2.3.2 Regulation of resection by 53BP1 and BRCA1

HR and NHEJ differ in their requirement for DNA end-resection to initiate repair, thus regulation of resection is key mechanism of DSB repair pathway choice. The antagonistic relationship between the HR protein BRCA1 and the NHEJ regulator 53BP1 is a major regulator of DNA end-resection. Highlighted by the fact BRCA1

mutated cells regain their ability to initiate HR directed DSB repair following loss of 53BP1 expression (Bunting *et al.*, 2010).

The CtIP nuclease controls DSB end-resection during S/G2 phase of the cell cycle to promote HR and prevent NHEJ (Huertas and Jackson, 2009). Thus, CtIP activity is a key determinant of DSB repair pathway choice. During G1, phosphorylation of 53BP1 by ATM rapidly localises it to DSBs to prevent access of end-resection nucleases, such as CtIP (Bunting *et al.*, 2010). Phosphorylation of CtIP also inhibits its recruitment to DSBs and subsequently blocks BRCA1 recruitment, preventing DNA end-resection occurring during G1 and promoting repair via NHEJ (Biehs *et al.*, 2017).

ATM-dependent 53BP1 phosphorylation also promotes recruitment of several downstream factors including, RIF1 and REV7, to the DSB to further limit DNA end-resection (Chapman *et al.*, 2013). RIF1 and REV7 subsequently recruit the distal 53BP1 effector complex shieldin, comprised of SHLD1, SHLD2 and SHLD3, possessing additional end-protection activities (Dev *et al.*, 2018; Noordermeer *et al.*, 2018; Sifri *et al.*, 2023; Susvirkar and Faesen, 2023). This recruitment is mediated by interaction between RIF1 HEAT-repeat domains and the eIF4E-like domain of SHLD3 (Sifri *et al.*, 2023). Additionally, SHLD2 converts ssDNA tails into blunt ends by CST-polymerase-α mediated fill-in synthesis, thus antagonising the interaction between ssDNA and BRCA1 (Mirman *et al.*, 2018). As such, depleting components of the shieldin complex promotes end-resection (Mirman *et al.*, 2022), offering another potential mechanism by which the 53BP1 pathway promotes NHEJ. However, recent studies have shown that 53BP1 promotes DNA end joining even in the absence of shieldin and CST, suggesting shieldin is not required for HR suppression (King *et al.*,

2024). These results highlight that 53BP1 promotes end joining independently of shieldin and this pathway can function through other downstream effectors in its absence. Instead, it has been shown that RIF1 recruits protein phosphatase 1 to DSBs preventing the accumulation of CtIP and limiting DNA end-resection prior to the action of Shieldin (Isobe *et al.*, 2021).

Upon progression into S phase, BRCA1 antagonises the end-protection activity of 53BP1 by promoting 53BP1 removal, allowing resection to occur. DNA end-resection suppresses NHEJ due to the lower affinity for the Ku70/80 heterodimer for ssDNA (Falzon, Fewell and Kuff, 1993). As previously described, CDK-mediated CtIP phosphorylation at threonine 847 and serine 327 is another key factor initiating end-resection (Huertas and Jackson, 2009). This can also be mediated through sumoylation of CtIP at lysine 896 by the E3 ligase CBX4. Subsequently, deletion of CBX4 impairs CtIP-mediated end-resection (Soria-Bretones *et al.*, 2017). More recently, the REV7 binding protein CHAMP1 has been shown to promote HR through recruitment of RPA and CtIP to DSBs to promote DNA end-resection. Furthermore, CHAMP1 depletion was able to restore sensitivity of 53BP1 depleted cells to PARP inhibitors, suggesting CHAMP1 counteracts the inhibitory effect of 53BP1 on HR (Fujita *et al.*, 2022).

1.2.3.3 Epigenetic control

Epigenetic histone modifications have also been shown to play a key role in regulating the recruitment of BRCA1 and 53BP1 to dictate DSB repair pathway choice. For example, histone phosphorylation plays a key role in the initiation of the DNA damage response. Upon DSB induction the ATM signalling kinase phosphorylates histone H2AX serving as a signal to recruit further DNA repair factors

to the chromatin. Following on from this, histone ubiquitination acts to recruit 53BP1 to damaged chromatin. Together with ubiquitin-conjugating enzyme E2 13 (UBC13), the E3 ubiquitin ligases RNF8 and RNF168 catalyse the formation of Lys63-linked ubiquitin chains on H2AK13 and H2AK15. 53BP1 binds to H2AK15 histone marks via the ubiquitylation-dependent recruitment (UDR) motif (Fradet-Turcotte *et al.*, 2013).

53BP1 also possesses a tandem Tudor domain which aides its recruitment to the DSB through binding to Histone 4 di-methylated at lysine 20 (H4K20me2). This process is highly regulated throughout the cell cycle. During G2 and M phases of the cell cycle H4K20me1 levels peak, catalysed by KMT5A. Further methylation is then carried out by KMT5B/C during G1 and S phase to produce H4K20me2 (Pesavento *et al.*, 2008). In the absence of DNA damage, the Jumonji D2A/2B (JMJD2A/B) demethylases, binds H4K20me2 with a higher affinity than 53BP1, however DSB induction promotes degradation of JMJD2A/B, allowing 53BP1 to bind to H4K20Me2. As H4K20me2 is only present on mature chromatin, this prevents 53BP1 binding to nascent DNA during S phase (Simonetta *et al.*, 2018). During S phase, H4K20me2 becomes diluted, meaning nascent chromatin significantly lacks methylation at H4K20 (H4K20me0) (Saredi *et al.*, 2016). The BRCA1-BARD1 complex preferentially binds to H4K20me0 at this time, ensuring that BRCA1 is recruited to damaged DNA during replication, allowing initiation of end-resection and promoting repair via HR (Nakamura *et al.*, 2019).

Histone acetylation also plays a role in mediating 53BP1 binding to H4K20me2. TIP60 mediated acetylation of H4K16 reduces the affinity of the 53BP1 Tudor domain for H4K20me, limiting 53BP1 recruitment to the chromatin (Tang *et al.*, 2013). H4K16 acetylation also relies on the methylation of RUVB1 directed by the arginine

methyltransferase, PRMT5 (Clarke *et al.*, 2017). H4K16 acetylation is subsequently removed by SIRT1 and 2, as well as the histone deacetylases HDAC1 and HDAC2. Transient H4K16 deacetylation occurs following DSB induction to facilitate 53BP1 recruitment to DSBs, favouring NHEJ (González-Bermúdez *et al.*, 2022).

Finally, Neddylation, a post-translation modification involving the conjugation of ubiquitin-like protein NEDD8 to target proteins, is required for the displacement of the Ku70/80 heterodimer from chromatin to allow DNA repair to occur (Brown *et al.*, 2015).

1.3 DNA damage and cancer

The DDR has an important role in preventing tumorigenesis. Defects in the DDR cause cells to accumulate unrepaired DNA damage, which increases the likelihood of mutations affecting oncogenes and tumour suppressor genes. The physiological importance of DDR mechanisms in preventing tumorigenesis is highlighted by the fact that a third of different cancer types harbour somatic mutations affecting DDR-related genes (Pon and Marra, 2015). Further analysis of somatic DDR gene alterations highlighted genes related to HR were the most frequently altered in 17.4% of cancer types (Knijnenburg *et al.*, 2018). To further support these findings Heeke *et al.* revealed up to 34% of tumours from a range of cancer types exhibited mutations in HR genes (Heeke *et al.*, 2018). Notably, mutations in the key HR genes *BRCA1* and *BRCA2* are associated with a 40-80% lifetime risk of breast cancer and 11-40% lifetime risk of epithelial ovarian cancer (King, Marks and Mandell, 2003). Mutations in other HR genes including, *PALB2, RAD51C, RAD51D, BARD1, BRIP1* and *MRE11* are also associated with hereditary breast and ovarian cancer. Furthermore, germline mutations in the DDR signalling genes *ATM* and *CHEK2* are observed in around 26%

and 41% of breast cancers, respectively (Toss *et al.*, 2021). *ATM* mutations are also observed in up to 20% of metastatic castrate-resistant prostate cancers (Robinson *et al.*, 2015). Mutations in *PALB2* and *RAD51C* are also commonly observed in prostate cancer, as well as pancreatic cancer (Nguyen *et al.*, 2020). Furthermore, mutations in the BLM helicase are frequently observed in stomach adenocarcinoma and endometrial cancer (Shi *et al.*, 2024), to name a few examples.

The large contribution of DDR defects to tumorigenesis led to the hypothesis that these defects could be exploited for anti-cancer therapies. Tumour cell death can be induced through inhibition of their remaining functional DNA repair capacities utilising DNA damaging agents through a concept called ‘synthetic lethality.’ This concept was first described in 1946 as an interaction occurring between two genes in which inactivation of each gene individually as no effect on cell viability, whilst simultaneous inactivation of the two genes together results in cell death (Dobzhansky, 1946). The most successful example of the synthetic lethal approach is the use of poly (ADP-ribose) polymerase (PARP) inhibitors to selectively kill HR-deficient tumours.

1.4 Poly (ADP-ribose) polymerases

Poly (adenosine diphosphate-ribose) (ADP) polymerases (PARP) are a family of enzymes consisting of 18 members, based on their homology to the founding member, PARP1(Amé, Spenlehauer and de Murcia, 2004). PARP1, PARP2, PARP5a and PARP5b possess intrinsic polymerase activity and are thus considered bona fide PARPs, whilst other members such as PARP3 only have mono (ADP-ribose) (MAR) transferase activity or are not enzymatically active.

PARP1, which is responsible for 85% of PARP activity in mammalian cells, consists of 1014 amino acids with three main functional domains. Namely, three N-terminal zinc finger domains, which are responsible for binding to damaged DNA, a BRCA1 carbon-terminus (BRCT) auto modification domain, and a C-terminal catalytic domain responsible for binding NAD^+ (Liu *et al.*, 2022) (**Fig. 1.4 A**). PARP2 shares 60% sequence homology with PARP1 within the catalytic domain and is capable for compensating for some of the activity of PARP1. This is highlighted by the fact that PARP1 knockout mice display a mild phenotype, whereas PARP1/PARP2 double knockout mice are embryonic lethal (Ménissier de Murcia *et al.*, 2003).

PARP enzymes catalyse a post-translational modification (PTM) called poly ADP-ribosylation (PARylation), in which negatively charged ADP-ribose groups from nicotinamide adenine dinucleotide (NAD+) donors are transferred onto the glutamate, aspartate, lysine and serine residues of target proteins (Leidecker *et al.*, 2016). Multiple ADP-ribose units are transferred sequentially to form homopolymer poly-ADP-ribose chains of 200-300 units (Langelier *et al.*, 2018).

Histone PARylation Factor 1 (HPF1) is a key cofactor and regulator of PARP1 and 2 activities, controlling the catalytic output of these enzymes and enabling increased amino acid specificity. HPF1 is required for modification of serine residues (Bonfiglio *et al.*, 2017) and increases the mono PARylation (MARylation) activity of PARP1 and 2. Furthermore, studies have shown that increased HPF1 levels decrease the length of PAR chains by inhibiting elongation (Langelier *et al.*, 2021).

Large proteomic screens have identified PARylation occurs on a wide variety of protein targets to regulate multiple cellular processes (Jungmichel *et al.*, 2013). Key targets for PARylation include DDR factors involved in SSB repair and BER, such as XRCC1, PCNA and LIG3. In addition to this PARP proteins influence other pathways such as NER, MMR and NHEJ as XPC, MSH2 and MSH6, as well as XRCC5 and XRCC6 have all been identified in PARylation screens. PARylation also effects proteins involved in RNA metabolic pathways. For example, the pre-mRNA splicing factor THRAP3 is PARylated in response to oxidative damage (Jungmichel *et al.*, 2013). Histone proteins including H1 and H2B are also PARylated at multiple sites following DNA damage, mediating the recruitment of chaperone proteins to remove histones at DNA lesions (Yang *et al.*, 2020a). PARP1 itself also undergoes autoPARylation, this process is critical for PARP1 regulation.

PARylation is a transient and reversible modification, and its turnover is mediated by poly (ADP-ribose) glycohydrolase (PARG) and ADP-ribosyl hydrolase 3 (ARH3). PARG cleaves 2',1''-O-glycosidic ribose-ribose bonds that link ADP-ribose monomers of PAR (**Fig. 1.4 B**), however, PARG is unable to remove the terminal MAR residues on proteins. ARH3, on the other hand, is responsible for removal of MAR groups on serine residues, but has significantly lower activity in PAR chain removal compared to PARG (Abplanalp *et al.*, 2017).

The formation of PAR chains by PARP1 facilitates cellular processes including gene transcription, cell death and DNA repair by driving local changes in chromatin structure and recruiting DNA repair effector proteins. In particular, the enzymatic activity of PARP1 has been implicated in the detection and repair of SSBs through the BER pathway (Wei and Yu, 2016).

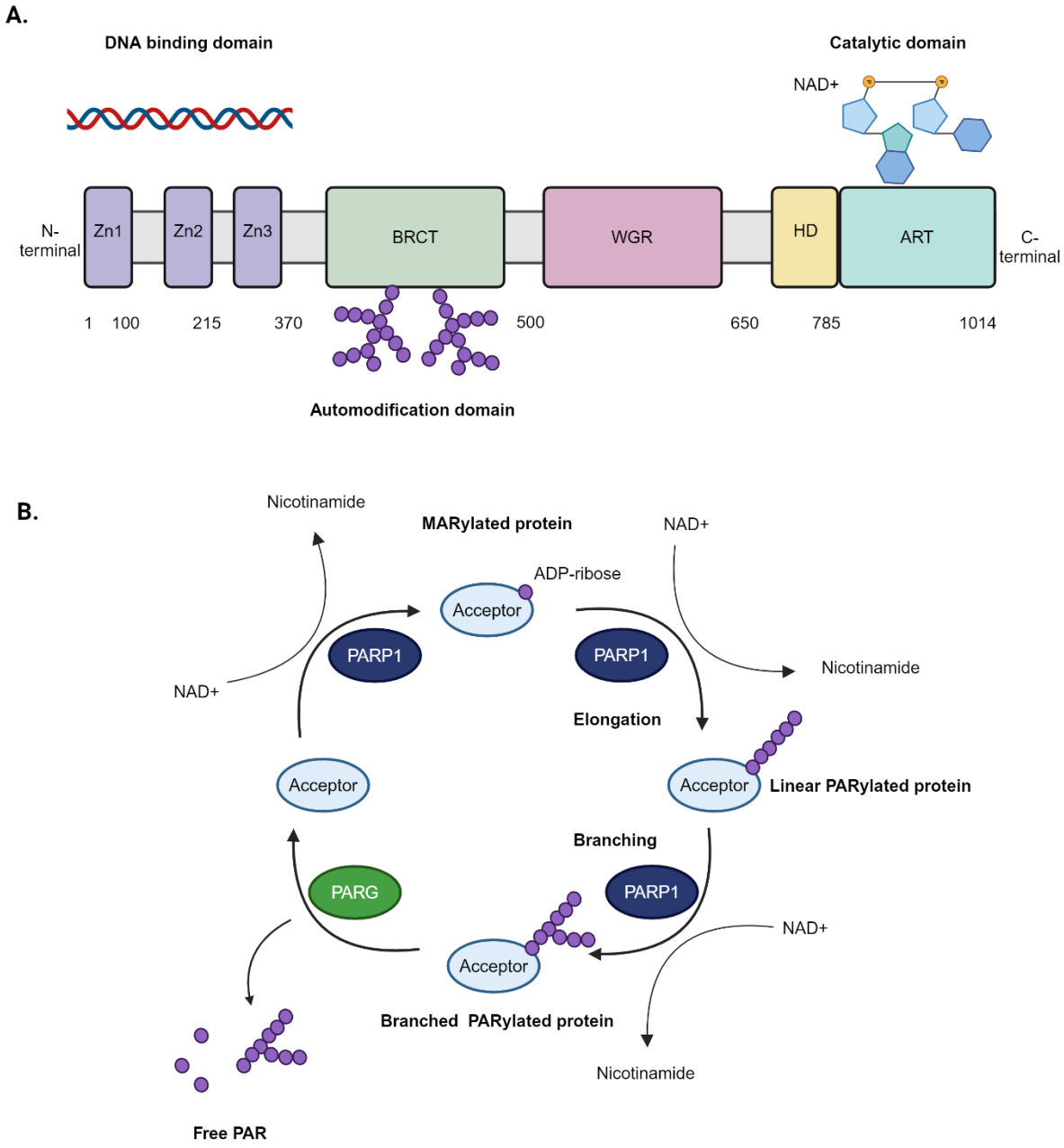

Figure 1.4- Structure of PARP1 and generation of poly (ADP-ribose).

(A.) *Structure of human PARP1 including three N-terminal zinc finger domains (Zn1-3) responsible for DNA binding, a BRCA1 C-terminal (BRCT) phosphopeptide binding motif within the auto modification domain, a WGR motif and a C-terminal catalytic domain containing the helical domain (HD) and ADP-ribosyl transferase (ART) subdomains. (B.) PARP1 forms mono ADP-ribose (MAR) and subsequently branched poly (ADP-ribose) (PAR) chains on acceptor proteins, using nicotinamide as a donor. PARG subsequently catalyses hydrolysis of PAR to free ADP-ribose units. Figure created with Biorender. Adapted from (Liu et al., 2022).*

1.4.1 Biological functions of PARPs

1.4.1.1 Single-strand break repair

PARP1 is a key enzyme facilitating the repair of SSBs induced by oxidative base damage, alkylation and abasic sites via the BER pathway. This is evidenced through hypersensitivity to alkylating agents and accumulation of BER intermediates upon PARP inhibition (Caldecott, 2020). PARP1 becomes activated upon binding to SSBs and abasic sites generated during BER via N-terminal zinc fingers (Schwarz *et al.*, 2024). PARP1 binding to DNA activates an allosteric signalling cascade where conformational changes within the catalytic domain leads to the release of an autoinhibitory interaction between the helical domain (HD) and the catalytic ADP-ribosyl transferase (ART) domain. This allows NAD+ to access the ART domain to drive PARylation. This process breaks down NAD+ to ADP and nicotinamide. ADP forms long, branching, negatively charged PAR chains on target proteins, as well as PARP1 itself (Campalans *et al.*, 2013). AutoPARylation activates PARP1, promoting subsequent PARylation of BER proteins, including APE1, XRCC1, polymerase beta and LIG3, driving their recruitment to the SSB (Schwarz *et al.*, 2024). Furthermore, the accumulation of PAR chains creates a spatial barrier around the site of DNA damage allowing for the recruitment of additional DNA repair proteins. PARylation also alters to electrostatic properties of target proteins, altering their binding affinity to further assist the recruitment of additional repair proteins. However, binding of PARP1 to chromatin is transient and PARP1 autoPARylation drives the dissociation of PARP1 from the DNA (Campalans *et al.*, 2013). Evidence suggests that PARP1 and PARP2 are redundant in BER and in the absence of PARP1, PARP2 can promote SSB repair (Ronson *et al.*, 2018).

1.4.1.2 Double-strand break repair

PARP1 interacts with and becomes activated by DSBs (Haince *et al.*, 2008), implicating this enzyme in DSB repair. A specific role for PARP1 in regulating NHEJ was suggested as PARP1 modifies key DSB repair proteins involved in this process, including DNA-PKcs (Ruscetti *et al.*, 1998) and Ku (Galande and Kohwi-Shigematsu, 1999). Furthermore, PARP1 recruits CHD2 to trigger chromatin remodelling and deposition of the histone variant H3.3 at DSBs, driving recruitment of the NHEJ factor XRCC4 (Luijsterburg *et al.*, 2016).

Despite this, however, PARP1-deficient mice display normal NHEJ activity (Yang *et al.*, 2004). Instead, PARP3 was shown as the main PARP functioning to promote classical NHEJ. Rulten *et al* showed that PARP3 facilitated NHEJ through promoting the accumulation of APLF followed by xRCC4-ligase IV at DSBs (Rulten *et al.*, 2011). PARP1 was instead required for alt-EJ, which is activated in the absence of functional NHEJ (Yang *et al.*, 2018). More recently, ADP-ribosylation of histone variant H3B at serine 10 and 28 by PARP/HPF1 was shown to be required for initiation of NHEJ, promoting the recruitment of Ku70/80 to DSBs (Brustel *et al.*, 2022).

PARP1 has also been implicated in the repair of DSBs through HR. For example, PARP1 physically interacts with MRE11 and NBS11 and this interaction is required for their recruitment to DNA (Haince *et al.*, 2008). Furthermore, PARP1 is required for the recruitment of BRCA1 to DSBs, as the BRCA1 binding partner, BARD1, binds PARylated targets (Li and Yu, 2013). On the other hand, PARylation of BRCA1 may function to limit HR by facilitating stabilisation of the BRCA1-RAP80 complex (Hu *et al.*, 2014), suggesting PARP1 has a regulatory role to limit HR levels in cells. To

further support this Caron *et al.* showed that loss of PARP1 results in hyper-resection of DSBs by MRE11, EXO1 and DNA2, due to decreased accumulation of the 53BP1 and RIF1 end-protection factors (Caron *et al.*, 2019).

1.4.1.3 Replication fork processing

PARP1 has also been implicated in replication fork (RF) protection by promoting fork reversal and preventing the formation of DSBs due to fork collapse. During RF reversal the two nascent strands are annealed to create a four-way chicken foot structure. Fork restart is mediated by the RECQ1 helicase, which subsequently reverses the four-way chicken structure into a three-way structure (Berti *et al.*, 2013). PARylated PARP1 binds to RECQ1 to inhibit its helicase activity, preventing restart at stalled RFs to allow time for DNA repair to occur.

In addition to this, PARP1 recruits MRE11 to enable restart at stalled forks (Haince *et al.*, 2008). PAR polymers co-localise with hydroxyurea induced RPA foci, indicating that PARP1 is activated at stalled RFs. Furthermore, PARP1 was required to reactivate stalled RFs by recruiting MRE11 to mediate DNA resection, subsequently allowing for RAD51 loading and recombination mediated repair to promote replication restart (Bryant *et al.*, 2009). Additionally, both PARP1 and 2 have been shown to be required to stabilise Rad51 nucleofilaments at damaged RFs by opposing the role of Fbh1 (Ronson *et al.*, 2018)

1.5 Poly (ADP-ribose) polymerase inhibitors

In 2005, two seminal studies identified that inhibition of PARP1 resulted in decreased survival of BRCA1/2-deficient cells compared to wild-type cells through synthetic lethality (Bryant *et al.*, 2005; Farmer *et al.*, 2005). Due to the selectivity of PARP

inhibition in only the mutant cells, poly (ADP) ribose polymerase inhibitors (PARPi) were subsequently developed as a tumour cell specific therapy for BRCA1/2-deficient patients. The first clinically approved PARPi, olaparib, entered clinics in 2015 as a monotherapy for the maintenance of platinum sensitive, BRCA1/2-mutated high grade serous ovarian cancer (HGSOC) (Kim *et al.*, 2015).

1.5.1 Molecular mechanisms of PARP inhibition

PARPi are designed to competitively inhibit binding of NAD+ molecules to the catalytically active site of PARP1. Binding of PARPi to the catalytic domain distorts PARP1 structure, preventing dissociation of PARP1 from damaged DNA. Although several theories of the mechanism underlying the anti-cancer action of PARPi have been proposed, a consensus on the precise mechanisms has yet to be reached (**Fig. 1.5**).

1.5.1.1 Catalytic inhibition

Due to the essential role of PARP1 in SSB repair, it was first hypothesised that inhibiting PARP1 activity resulted in the persistence of unrepaired SSBs. Unrepaired SSBs evolve into one-ended DSBs through increased fork collapse during DNA replication. DSBs subsequently require repair via the HR pathway, thus proficiency in HR is required for survival of PARP1-deficient cells. Failure of HR, such as in *BRCA1*- or *BRCA2*-mutated tumours, results in the accumulation of genome instability, eventually leading to cell death through mitotic catastrophe.

Despite this, researchers have shown that there is no increase in SSBs following PARPi treatment. For example, Gottipati *et* al. observed no difference in DNA breaks in BRCA2-deficient cells following PARPi, as measured by the alkaline comet assay,

suggesting no overall increase in SSBs (Gottipati *et al.*, 2010). To support this, there is no increase in the level of SSBs following PARPi treatment in cells depleted of the essential BER factor, XRCC1 (Ström *et al.*, 2011), suggesting increased PARPi sensitivity of these cells is via a mechanism independent of SSB repair. Furthermore, depletion of XRCC1 does not affect cell viability of BRCA-deficient ovarian cancer cell lines (Patel, Sarkaria and Kaufmann, 2011). This evidence suggests that the accumulation of SSBs may not be the only mechanism for PARPi induced cytotoxicity.

Alternatively, PARP1 has been shown to interact with the NHEJ factors Ku70/80 (Galande and Kohwi-Shigematsu, 1999) and DNA-PKc (Gagné *et al.*, 2008). This suggests that NHEJ could play a role in the cellular response to PARPi. PARPi treatment induces genomic instability, which is characterised by accumulation of chromosomal aberrations, including radial structures. Evidence suggests that the formation of aberrant chromosomes is mediated by NHEJ, as a DNA-PKc inhibitor alleviated the effects of PARPi on radial structure formation. In further support of this theory, PARP inhibition resulted in increased DNA-PKc phosphorylation and subsequent NHEJ and genomic instability in HR-deficient cells (Patel, Sarkaria and Kaufmann, 2011). This is supported by Mamar *et al.* who showed DNA-PKc signalling is significantly upregulated following a combination of ATRi and PARPi treatment in POLE4-deficient cells, indicative of elevated NHEJ activity (Mamar *et al.*, 2024).

1.5.1.2 PARP trapping

Evidence against the importance of catalytic inhibition in the cellular sensitivity to PARPi also comes from the fact that different PARPi show various levels of cytotoxicity, despite similar catalytic inhibition of PARP1 (**Table 1.1**). For example,

veliparib does not induce as significant cell killing in comparison to olaparib, despite a similar degree of catalytic inhibition of PARP1. Instead, it was show that olaparib has a greater degree of PARP trapping in comparison to veliparib (Diéras *et al.*, 2024). These findings suggest that PARPi block the ability of PARP1 to undergo autoPARylation, preventing the removal of PARP from the DNA. Trapping of PARP on the DNA creates a DPC, which prevents progression of the RF. During the S-phase of the cell cycle these stalled RFs collapse, resulting in DSB formation. In HR-deficient cells these DSBs are left unrepaired.

Different PARPi compounds vary in their PARP trapping ability; the PARPi talazoparib is the most effective PARP trapping agent, followed by niraparib, olaparib, rucaparib then veliparib (Murai *et al.*, 2012) (**Table 1.1**). For example, Talazoparib is 50 – 100 times more potent in PARP trapping ability in comparison to niraparib, olaparib and rucaparib (Valabrega *et al.*, 2021). The cytotoxicity of PARP inhibitors is directly correlated to PARP trapping ability but not catalytic inhibition, as such lower concentrations of Talazoparib can elicit antitumour cell response compared to other PARPi compounds (Shen *et al.*, 2013). Furthermore, cellular sensitivity to talazoparib can be reversed upon mutation of PARP1, reducing its ability to bind DNA, consequently reducing the PARP trapping effect of PARPi (Pettitt *et al.*, 2018). To further support the role of PARP trapping as a critical determinant of PARPi sensitivity, Saha *et al.* demonstrated that the DPC repair protein, SPRTN, is required for the repair of PARP-DNA complexes formed in response to PARPi. Consequently, SPRTN depleted cells are hypersensitive to PARP inhibition, specifically those with strong trapping potency such as talazoparib but not the weak PARP trapper veliparib (Saha *et al.*, 2021).

Table 1.1- PARP trapping potency of clinical PARP inhibitors.

Catalytic inhibition and PARP trapping potency of clinically approved PARP inhibitors. Catalytic inhibition was measured as half-maximal inhibitory concentration (IC_{50}) for PARP level inhibition in DT40 cells. PARP trapping potency was measured relative to olaparib. Table adapted from (Bruin et al., 2022).

PARP inhibitor	Catalytic inhibition (IC_{50}, nm)	PARP trapping potency
Talazoparib	4	100
Olaparib	6	1
Rucaparib	21	1
Niraparib	60	2
Veliparib	30	<0.02

1.5.1.3 Replication gaps

The modes of action described above highlight DSBs as the sensitising lesions induced by PARPi treatment. However, more recently, PARPi induced cytotoxicity has been attributed to the accumulation of ssDNA gaps. It has been shown that PARPi treatment causes excessive ssDNA gap accumulation behind RFs in BRCA1- or BRCA2-deficient cells, due to the role of PARP1 in Okazaki fragment (OF) processing (Cong *et al.*, 2021). Additionally, PARPi was shown to increase ssDNA gaps via PRIMPOL-mediated repriming of stalled forks, resulting in the formation of ssDNA gaps on the leading strand in BRCA-deficient cells (Simoneau, Xiong and Zou, 2021). Furthermore, increased PARPi sensitivity following loss of DNA polymerase epsilon subunit POLE4 was attributed to accumulation of ssDNA gaps. Subsequently, this PARPi sensitivity could not be rescued by restoring HR through loss of 53BP1 (Mamar *et al.*, 2024).

Alternatively, it has been proposed that PARPi can make ssDNA gaps more persistent due to PARP trapping without directly increasing the number of gaps present. These gaps persist into mitosis and are subsequently converted into DSBs during S phase. This leads to cytotoxicity in BRCA-deficient cells which cannot repair these gap-derived DSBs (Cong *et al.*, 2021). In further support of this mechanism, BRCA1-deficient cells are unable to protect ssDNA gaps from degradation by MRE11. Subsequently, MRE11 inhibition has been shown to restore gap filling in PARPi treated cells (Tirman *et al.*, 2021).

Although, different modes of action for PARPi have been proposed, it is likely that different models may work together linked by a common underlying mechanism or multiple mechanisms may act at once to contribute to PARPi-induced cell death. For example, defects in gap suppression can increase the chances of PARP trapping and generate more DSBs which cannot be repaired due to HR-defects in BRCA-deficient cells. Furthermore, it is likely that protection of RFs and ssDNA gaps by BRCA proteins are mechanistically linked. For example, in the absence of BRCA1/2 reversed forks and ssDNA gaps are both resected by MRE11.

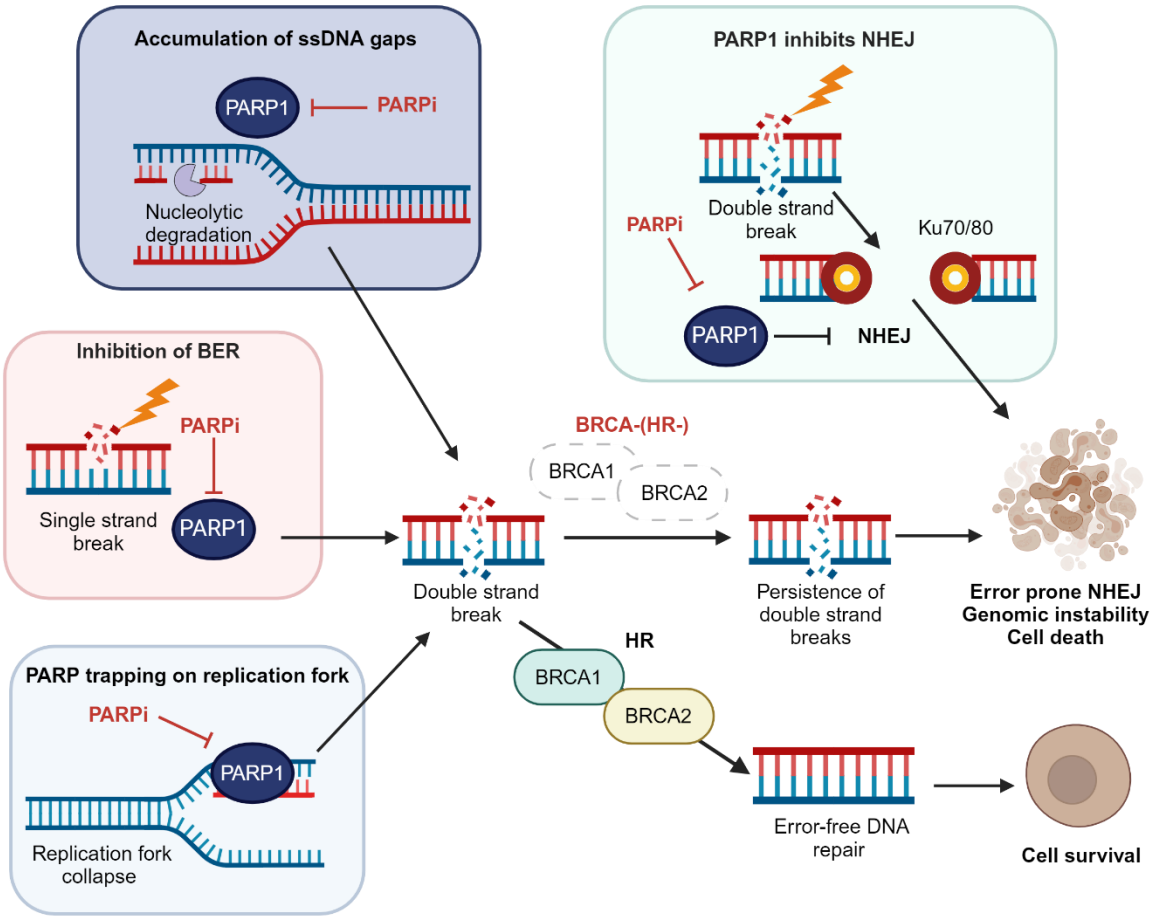

Figure 1.5- Poly (ADP-ribose) polymerase inhibitor mechanisms of action.

PARP inhibitor sensitivity can occur due to the accumulation of DSBs, which can arise from inhibition of PARP enzymatic activity leading to unrepaired single-strand DNA (ssDNA) breaks or PARP1 trapping and subsequent collision with an approaching replication fork. Alternatively, inhibition of PARP can result in the accumulation of post-replicative ssDNA gaps. Figure created with Biorender.

1.5.2 Clinical uses of PARP inhibitors

Following on from the original landmark studies demonstrating the utility of PARPi as an anti-cancer therapy, olaparib was the first PARPi to be granted clinical approval for the treatment of BRCA1/2 mutated metastatic ovarian cancer (Kim *et al.*, 2015). Olaparib is now approved in the use of breast (Robson *et al.*, 2017), ovarian (Moore *et al.*, 2018) and pancreatic cancer (Golan *et al.*, 2019). Additionally, three other PARP inhibitors: rucaparib, niraparib and talazoparib have gained approval in a range of clinical indications including ovarian, breast and peritoneal cancer. Furthermore, in a significant advancement in PARPi therapy olaparib and rucaparib gained approval for use in metastatic castration-resistant prostate cancer in 2020 (Abida *et al.*, 2020; de Bono *et al.*, 2020) (**Table 1.2**).

Next-generation PARPi are constantly in development to identify more specific inhibitors with reduced side effects. Current PARPi target both PARP1 and PARP2 enzymes and some of the side effects associated with PARPi treatments have been attributed to its effects on PARP2. AZD5305 is a novel highly selective PARP1 inhibitor, which is 500-fold more selective for PARP1 over PARP2 (Illuzzi *et al.*, 2022). AZD5305 has shown promising clinical activity and safety in patients with BRCA1/2-mutant advanced HER2-negative breast, ovarian, prostate and pancreatic cancer (Yap *et al.*, 2022).

More recently, thioparib, a novel PARPi has been shown to be more potent than olaparib and talazoparib due to its stronger ability for PARP trapping, as well as inhibition of multiple PARP enzymes, including PARP7. Due to the increased potency thioparib monotherapy can overcome mechanisms of PARPi resistance such as 53BP1 knockout in HR-deficient cells (Wang *et al.*, 2023) (**Table 1.2**).

Table 1.2- Clinical approvals for PARP inhibitors.

List of indications for clinically approved PARP inhibitors. Approvals obtained from FDA drug approval notifications (FDA, 2023).

PARP inhibitor	Clinical approval
Olaparib	• First-line maintenance treatment of BRCA-mutated advanced ovarian cancer • First-line maintenance treatment of advanced ovarian cancer with HR deficiency in combination with bevacizumab • Maintenance of BRCA-mutated recurrent ovarian cancer • Adjuvant treatment of germline BRCA mutated and HER2-negative high risk early breast cancer and metastatic breast cancer • First-line maintenance treatment of germline BRCA mutated metastatic pancreatic adenocarcinoma • Treatment of HR gene mutated metastatic castration resistant prostate cancer • Treatment of BRCA mutated metastatic castration resistant prostate cancer in combination with abiraterone and prednisone or prednisolone
Rucaparib	• Maintenance treatment of BRCA mutated recurrent ovarian cancer • Treatment of BRCA mutated metastatic castration resistant prostate cancer
Niraparib	• Maintenance treatment of advanced ovarian cancer after response to platinum-based chemotherapy • Maintenance treatment of BRCA mutated recurrent ovarian cancer after response to platinum-based chemotherapy • Treatment of BRCA mutated metastatic castration resistant prostate cancer in combination with abiraterone and prednisone or prednisolone
Talazoparib	• Treatment of BRCA mutated locally advanced or metastatic HER2 negative breast cancer • Treatment of HR gene mutated metastatic castration resistant prostate cancer in combination with enzalutamide
Veliparib	• Orphan drug status for non-small cell lung carcinoma • Clinical trials in a variety of cancer types including metastatic melanoma, non-small cell lung carcinoma and prostate cancer
AZD5305	• Clinical trials in breast, ovarian, pancreatic, and prostate cancer
Thioparib	• Pre-clinical development

1.5.3 PARP inhibitors beyond BRCA1

Following the landmark discovery of the specific killing of BRCA1- and BRCA2-deficient cells with PARPi (Bryant *et al.*, 2005; Farmer *et al.*, 2005), further studies revealed that many other proteins involved in HR display synthetic lethality with PARPi. These include other proteins crucial to the HR pathway such as MRE11, RAD51, PALB2, BARD1, BRIP1, ARID1A and RPA, components of the Fanconi

anaemia pathway, as well as the key DDR signalling proteins CHK1/2, ATM and ATR (Turner *et al.*, 2008; McCabe *et al.*, 2006). Therefore, alterations in other HR pathway genes could provide additional biomarkers of PARPi treatment. Next generation sequencing analysis of multiple tumour types revealed mutations in genes effecting the HR pathway are seen in >20 % of tumours, of which mutations in *BRCA1/2* genes were the most prevalent (~5%). However, a significant proportion were also observed in *ARID1A* (~4 %), *ATRX* (~ 2 %) and *ATM* genes (~2 %) (Tsantikidi *et al.*, 2023), indicating a significant number of patients could benefit from PARPi treatment beyond those with BRCA mutations.

1.5.3.1 ATM

Ataxia–telangiectasia mutated (ATM) is a serine threonine protein kinase belonging to the phosphatidyl inositol 3 kinase like (PIKK) family. ATM is a large 370 KDa protein consisting of 3056 amino acids. The C-terminus of ATM contains a kinase domain, with significant homology to that of the phosphatidyl inositol 3 kinase (PI3K), along with the FRAP-ATM-TRRAP (FAT) domain and FAT C-terminal (FATC) domain. The FAT domain is required for ATM dimerisation and contains an autophosphorylation site, whilst the FATC domain is required for protein interactions and full ATM activation. The N-terminus of ATM consists of alpha helical HEAT repeat motifs, which are required for interaction and recruitment of DNA repair proteins to sites of DNA damage (Ueno, Sudo and Hirasawa, 2022) (**Fig. 1.6**).

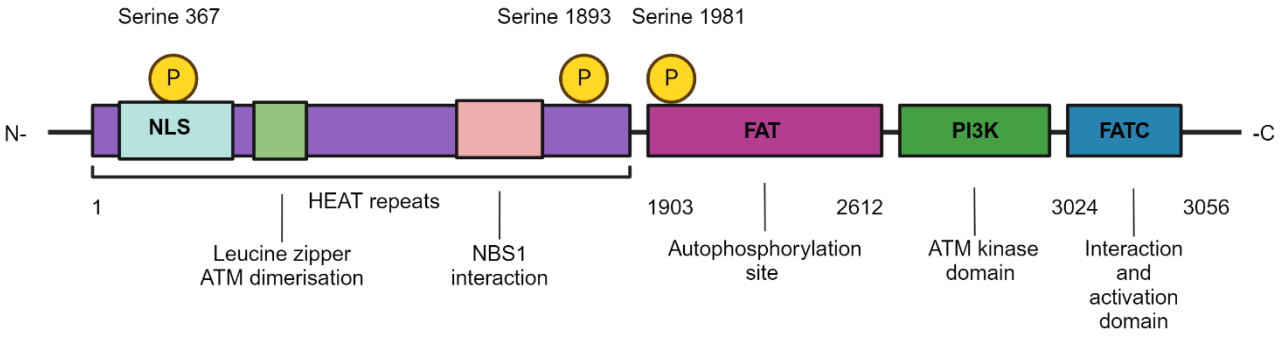

Figure 1.6- Domain structure of ATM.

Schematic of ATM domain structure and associated functions. ATM is a 3056 amino acid protein containing a NLS (nuclear localisation signal), leucine zipper for ATM dimerisation, NBS1 interaction domain, FRAP-ATM-TRRAP (FAT) domain (containing an autophosphorylation site), phosphatidyl inositol 3 kinase domain and a FAT C-terminal (FATC) domain (required for full ATM activation). P= phosphorylation site. Figure created with Biorender.

As described above, ATM plays a key role in the initiation of the cellular response to DSB repair through sensing and signalling DNA damage. ATM has a pro-HR role as it phosphorylates several downstream HR factors including BLM, BRCA1, NBS1, CtIP and MRE11, signalling their activation. As such, mutations in the *ATM* gene result in deficiencies in HR-mediated response to DNA damage.

Mutations in *ATM* are also associated with the development of a rare autosomal recessive disorder called Ataxia-Telangiectasia (A-T). A-T is a condition characterised by cerebellar ataxia, oculocutaneous telangiectasia and frequent pulmonary infections. A-T cells are also more sensitive to radiation and premature aging and patients with A-T are also predisposed to cancer development, particularly lymphoid and breast cancer. The higher risk of cancer susceptibility associated with A-T is directly due to the homozygous loss-of-function of the *ATM* gene (Taylor *et al.*, 2015). High rates of cancer are also reported in patients with heterozygous germline

variants of *ATM (*Thompson *et al.,* 2005*).* Studies have shown that *ATM* is mutated in 5% of all cancers, including 40% of mantle cell lymphomas, 20% of colorectal cancer and 10% of prostate and lung cancers (Gao *et al.*, 2013). Comparing the frequency of *ATM* mutations to *TP53* mutations, a gene frequently mutated in up to 50% all cancer types, highlights their significant contribution in cancer. For example, *ATM* mutations are observed at a similar rate to *TP53* mutations in prostate cancer (10%) (Gesztes *et al.*, 2022) and at much higher rates in mantle cell lymphoma (10%) (Eskelund *et al.*, 2017). Demonstrating *ATM* mutations are significant factors in the development of several different tumour types.

The first evidence that *ATM* mutated cancers could be candidates for PARPi therapy came from early studies indicating that ATM defective A-T cell lines displayed PARPi sensitivity (Bryant, 2006). Subsequent studies have revealed that ATM-deficient lymphoid (Weston *et al.*, 2010) and gastric (Kubota *et al.*, 2014) tumours exhibit PARPi sensitivity and depletion of ATM using shRNA in colorectal cancer cell lines induced sensitivity to olaparib treatment (Wang *et al.*, 2017a). Furthermore, deletion of ATM in mouse models of lung (Schmitt *et al.*, 2017) and pancreatic cancer (Perkhofer *et al.*, 2017) also conferred PARPi sensitivity.

In 2016, olaparib gained approval from the FDA for monotherapy treatment of *BRCA1/2*- or *ATM* gene-mutated metastatic castration-resistant prostate cancer (mCRPC) who had received prior taxane-based chemotherapy. This approval was given based on the positive results from the TOPARP-A phase II trial. In this trial 33% of patients showed homozygous deletions or deleterious mutations in DNA repair genes, including *ATM.* Of these DDR mutated patients, 88% showed a response to

olaparib treatment, including 4/5 patients harbouring *ATM* aberrations (Mateo *et al.*, 2015).

Despite the clinical approval and promising pre-clinical results, other studies have shown more variable sensitivity of ATM-deficient cells to PARP inhibition (Marshall *et al.*, 2019; Tung *et al.*, 2020; Rafiei *et al.*, 2020; Neeb *et al.*, 2021). For example, the TOPARP-B trial found only 7 out of 19 patients with ATM aberrations showed response to olaparib treatment (Mateo *et al.*, 2020). This study highlights that whilst some ATM mutated cancers respond to PARPi therapy, detection of ATM alterations alone might not be sufficient to identify sensitivity of tumours. Further investigations revealed that loss of ATM protein expression by immunohistochemical staining rather than mutation status, was associated with better outcomes following PARPi. This was because only a small number of patients with germline ATM mutations showed loss of ATM protein expression (Carreira *et al.*, 2021). Together these studies highlight that the synthetic lethality in ATM-deficient cells treated with PARPi depends on levels of ATM protein expression, as well as cellular background and molecular events co-occurring with ATM loss.

1.5.4 Resistance to PARP inhibitors

Despite the success that PARPi have demonstrated in the clinic, there is significant heterogeneity in response to PARPi therapy and a significant number of patients develop resistance. For example, approximately 40% of metastatic breast cancer patients harbouring germline BRCA1/2 mutations failed to respond to olaparib treatment (Robson *et al.*, 2017). Similarly, in a phase three trial investigating olaparib treatment in newly diagnosed advanced ovarian cancer, 39% of patients showed disease progression (Moore *et al.*, 2018). Similar observations have been achieved

with other PARPi. For example, 46.7% of ovarian cancer patients treated with niraparib also displayed disease progression (González-Martín *et al.*, 2019). These findings emphasise the need to further characterise novel PARPi resistance mechanisms alongside identifying strategies to overcome resistance. Multiple mechanisms of PARPi resistance have been described including, increased drug efflux, altered PARP expression, restoration of HR or replication fork protection, PARG loss and ssDNA gap suppression. Some of these mechanisms have been verified as bone fide PARPi resistance mechanisms in patients, whilst the clinical relevance of other remains to be determined (**Fig. 1.7**).

1.5.4.1 Increased drug efflux

Increased drug efflux from cells was one of the first identified mechanisms of PARPi resistance. Upregulation of the multidrug resistance protein (MDR1) encoded by ATP-binding cassette subfamily B member 1 *(ABCB1)* gene is associated with development of multidrug resistance due to its broad drug specificity. Increased MDR1 expression induces resistance by preventing the accumulation of PARPi drugs in cells. Upregulation of MDR1 resulting from *ABCB1* gene fusions and translocations have been observed in 8% of chemo-resistant ovarian cancer (Christie *et al.*, 2019). Resistance to olaparib caused by upregulation of *ABCB1* encoded efflux pumps can be overcome by addition of the p-glycoprotein inhibitor tariquidar (Rottenberg *et al.*, 2008) or treatment with alternative PARPi, such as pamiparib that cannot be easily exported by MDR1 (Xiong *et al.*, 2020). Furthermore, increased drug efflux is one of the few mechanisms of PARPi resistance that has been confirmed in ATM-deficient cells to date. For example, the *ABCB1* locus is amplified in olaparib resistant ATM-deficient pancreatic ductal adenocarcinoma (PDAC), and qPCR analysis confirmed

this amplification directly translated to upregulation of MDR1 expression (Gout *et al.*, 2021).

1.5.4.2 Drug target-related effects

Altered PARP expression is another mechanism of PARPi resistance. PARP inhibitors induce cell death in HR-deficient tumours by inducing PARP trapping, therefore if PARP expression is downregulated less PARP trapping can occur. Point mutations in the DNA binding zinc finger domains of PARP1 were found in olaparib-resistant ovarian cancer patients which abolished PARP trapping and thus reduced sensitivity to the PARPi, talazoparib (Pettitt *et al.*, 2018). Furthermore, loss of PAR glycohydrolase (PARG) which removes PAR chains catalysed by PARP can restore PARylation to counteract PARPi mediated cytotoxicity. By restoring PARylation, PARG loss also increases PARP1 autoPARylation, resulting in reduced PARP trapping, conferring PARPi resistance (Gogola *et al.*, 2018). Gogola *et al.* identified PARG mutations in patients eligible for PARPi treatment, suggesting this could represent a pre-existing mechanism of PARPi resistance in patients (Gogola *et al.*, 2018). Furthermore, PARG loss has been identified as a major mechanism of PARPi resistance in BRCA2-deficient cells (Bhin *et al.*, 2023). This finding is significant as BRCA2-deficient cells have been shown to have distinct PARPi resistance mechanisms to BRCA1-deficient cells.

1.5.4.3 Restoration of replication fork protection

In addition to their roles in HR, BRCA1 and BRCA2 are required for RF protection. Deficiency in BRCA1/2 results in uncontrolled RF resection and collapse. Exposed DNA ends at stalled RFs are susceptible to degradation by nucleases such as MRE11, CtIP, EXO1 and DNA2, therefore RF protection can also be restored by

inhibiting the activity of these nucleases. One way this can achieved is through loss of RF reversal. Fork reversal is mediate by fork remodelers such as SMARCAL1. Deletion of SMARCAL1 remodels stalled RFs and restores RF stability, whilst minimising replication stress and decreasing the sensitivity of BRCA1/2 mutant cells to PARPi (Taglialatela *et al.*, 2017). Additionally, deletion of RF remodelling factors, such as PTIP and CHD4, prevent MRE11 recruitment to the RF leading to fork protection and PARPi resistance in BRCA2-deficient cells (Chaudhuri et al., 2016). Similarly, depletion of RADX, a RAD51 agonist restores fork stability by enhancing the recruitment of RAD51 to reinstate fork protection and confer PARPi resistance in BRCA2-deficient cells (Dungrawala *et al.*, 2017).

1.5.4.4 Single-strand DNA gap suppression

As described above ssDNA gaps are a key determinant of PARPi sensitivity, therefore, suppression of gap formation offers a potential mechanism of PARPi resistance. For example, PARPi resistant ovarian cancer cell lines showed suppressed ssDNA gap formation, suggesting that decreased gap accumulation can confer PARPi resistance (Cong *et al.*, 2021). As described above, loss of 53BP1 induces PARPi resistance through restoring HR in BRCA1-deficient cells. Alternatively, Cong *et al* observed that 53BP1 deletion reverses defective OF processing that causes ssDNA gap formation by engaging a backup lagging strand ligation pathway mediated by PARP1, XRCC1 and LIG3 (Cong *et al.*, 2021).

Another study showed that depletion of the nucleosome remodelling enzyme CHD4 confers chemotherapy resistance in BRCA2-deficieint PEO1 cells. CHD4 depletion protected cells from S1 nuclease following HU treatment, indicating that ssDNA gap suppression resulted in resistance in these cells (Panzarino *et al.*, 2021).

Furthermore, cellular sensitivity to PARPi can be restored in cells that have developed resistance by reinstating ssDNA gap accumulation through depletion of LIG3 required for OF processing (Paes Dias *et al.*, 2021). Together these findings highlight that mechanisms to restore gap filling or suppress ssDNA gap formation are important determinants of PARPi resistance.

Despite the evidence that restoration of fork protection and gap suppression may be the key determinants of PARPi sensitivity, a recent study has suggested that these factors may not be the principal determinants of PARPi sensitivity (Lim *et al.*, 2024). In this study the contribution of fork protection, gap suppression and HR to genome instability and PARPi sensitivity were elucidated using a BRCA2 separation-of-mutant mouse with functional HR but defective fork protection and accumulation of ssDNA gaps. The study showed fork-protection- and gap-suppression-deficient mice have minimal genome instability when compared to HR-deficient mice. Therefore, this paper concluded that HR-deficiency following loss of BRCA2 is the primary determinant of PARPi sensitivity in this context (Lim *et al.*, 2024).

1.5.4.5 Restoration of homologous recombination

One of the most common mechanisms of PARPi resistance is restoring HR through mutations that restore functional BRCA1/BRCA2. Secondary epigenetic or genetic events can occur within BRCA-mutated cancer cells to restore the reading frame of truncation mutants, leading to the expression of wild-type protein or functional BRCA variants. This is evidenced by the observation that prolonged treatment of BRCA2-mutant pancreatic cancer cell lines with PARPi resulted in the acquisition of secondary mutations restoring full length BRCA2 or domains critical for HR function (Sakai *et al.*, 2008). Reversion mutations in BRCA1 have also been observed in

patient derived xenograft mouse models of breast cancer. Sequencing of resistant tumours following prolonged PARPi treatment identified de novo secondary mutations restoring the BRCA1 open reading frame (ter Brugge *et al.*, 2016). Reversion mutations have been identified in approximately 20-25% of patients with acquired PARPi resistance (Domchek, 2017), highlighting this is a clinically relevant mechanism of PARPi resistance.

HR activity can also be restored in the absence of functional BRCA1 through re-wiring of the DDR. Multiple studies have highlighted that PARPi sensitivity in BRCA1-deifciency can be bypassed by concomitant loss of the key NHEJ regulator, 53BP1. This has been identified in patient derived xenograft models with acquired PARPi resistance (Cruz *et al.*, 2018), as well as tumour biopsies from PARPi-treated metastatic BRCA1-associated breast cancer patients (Waks *et al.*, 2020). Furthermore, staining of 53BP1 in archival tumour biopsies from ovarian cancer patients who had received PARPi revealed decreased 53BP1 expression was associated with reduced PARPi sensitivity (Hurley *et al.*, 2019).

53BP1 is an anti-resection factor and regulates the balance between NHEJ and HR. 53BP1 promotes NHEJ through the inhibition of DNA end-resection required for initiation of HR directed repair. Therefore, loss of 53BP1 facilitates BRCA1-indpendent DNA end-resection, restoring HR activity, enabling the resolution of PARPi-induced DSB, and conferring PARPi resistance. BRCA1-deficient mice with trp53bp1 inactivation had a low incidence of tumour development and near normal lifespan, highlighting that BRCA1 deficiency can be compensated through loss of 53BP1 (Cao et al., 2009). Loss of 53BP1 can also partially restore HR in BRCA1 null cells, demonstrating that BRCA1 function is not essential for HR (Bouwman *et al.*,

2010; Jaspers *et al.*, 2013). This mechanism is conserved in invertebrates, as disruption of the pro-NHEJ factor DNA-PKc can reactivate HR and confer PARPi resistance in EXO1-deficient cells (Kolb, Gunn and Lakin, 2017).

Furthermore, loss of 53BP1 has also been identified as a mechanism of PARPi resistance in ATM-deficient breast cancer cells (Hong *et al.*, 2016), highlighting this PARPi resistance mechanism could apply across multiple types of HR defects and cancer types. This is one of the only examples of PARPi resistance in ATM-deficiency investigated to date.

More recent studies have identified that the inactivation of downstream effectors of the 53BP1 pathway, including RIF1 and REV7 and the newly identified 53BP1 effector complex, shieldin is also associated with PARPi resistance via this mechanism of HR restoration (Chapman *et al.*, 2013; Xu *et al.*, 2015; Dev *et al.*, 2018). Reduced mRNA expression of the SHLD1 and SHLD2 shieldin complex components have been identified in PARPi resistant patient-derived xenografts (Dev *et al.*, 2018), indicating this could be a clinically relevant PARPi resistance mechanism. Despite this, loss of 53BP1 is unable to restore HR activity and thus confer PARPi resistance in the absence of BRCA2. For example, Bouwman *et al.* found that proliferation of mouse embryonic fibroblasts could be rescued by 53BP1 depletion in BRCA1- but not BRCA2- knockout cells (Bouwman *et al.*, 2010). It is thought that the DNA resection induced by 53BP1-knockout is sufficient to stimulate residual BRCA1-independent RAD51 foci formation to enable HR mediated repair. However, this loading is BRCA2-dependent, thus 53BP1 loss cannot rescue this effect in BRCA2-deficient cells (Nacson *et al.*, 2018). This is further supported by the findings that BRCA2-deficient mouse mammary tumours displaying PARPi resistance

are incapable of forming IR-RAD51-foci, indicating HR cannot be restored in this context (Bhin *et al.*, 2023).

1.5.4.6 Epigenetic resistance mechanisms

Epigenetic modifications have been shown to be important to PARPi resistance. For example, some patients can lose BRCA1 function through epigenetic silencing caused by hypermethylation of CpG sites close to the promoter region (Veeck *et al.*, 2010; Esteller *et al.*, 2000). Loss of BRCA1 promoter hypermethylation has the potential to restore BRCA1 function and induce PARPi resistance. This was demonstrated using the demethylating agent 5-azacytidine which reversed PARPi sensitivity in BRCA1-methylated breast cancer cell lines (Veeck *et al.*, 2010). Furthermore, in a study investigating BRCA1-methylated patient-derived xenograft models, >50% of PARPi resistant tumours were shown to have BRCA1 promoter demethylation (ter Brugge *et al.*, 2016). Alternatively, BRCA1 function can be restored and resistance cells can arise from de novo gene fusions which place BRCA1 under transcriptional control of a heterologous promoter (ter Brugge *et al.*, 2016).

Epigenetic histone modifications have also been implicated in mechanisms of PARPi resistance. Enhancer of zeste homolog 2 (EZH2) is a chromatin modifier responsible for tri-methylation of histone H3 at lysine 27 (H3K27me3). EZH2-mediated H3K27me3 at stalled RFs promotes the recruitment of the MUS81 endonuclease to promote fork degradation. Thereby, it was shown that loss of EZH2 prevented MUS81 recruitment following PARPi treatment in BRCA2-deficient cells, consequently preventing fork degradation and conferring PARPi resistance (Rondinelli *et al.*, 2017).

Furthermore, euchromatic histone-lysine *N*-methyltransferase 1 and 2 (EHMT1/2), which catalyses the mono- and di-methylation of histone H3 and lysine 9 (H3K9me/me2) is upregulated in PARPi-resistant HGSOC patients. Double knockdown or inhibition of EHMT1/2 in these resistant cells significantly increased their sensitivity to olaparib treatment through diminishing DSB repair. These findings were also confirmed in a patient-derived xenograft model (Watson *et al.*, 2019).

To further highlight the important contribution of the epigenetic landscape to PARPi resistance mechanisms, our lab has recently identified loss of the histone lysine methyltransferase SETD1A confers PARPi resistance in BRCA1-deficient cells (Bayley *et al.*, 2022). This will be discussed in further detail below.

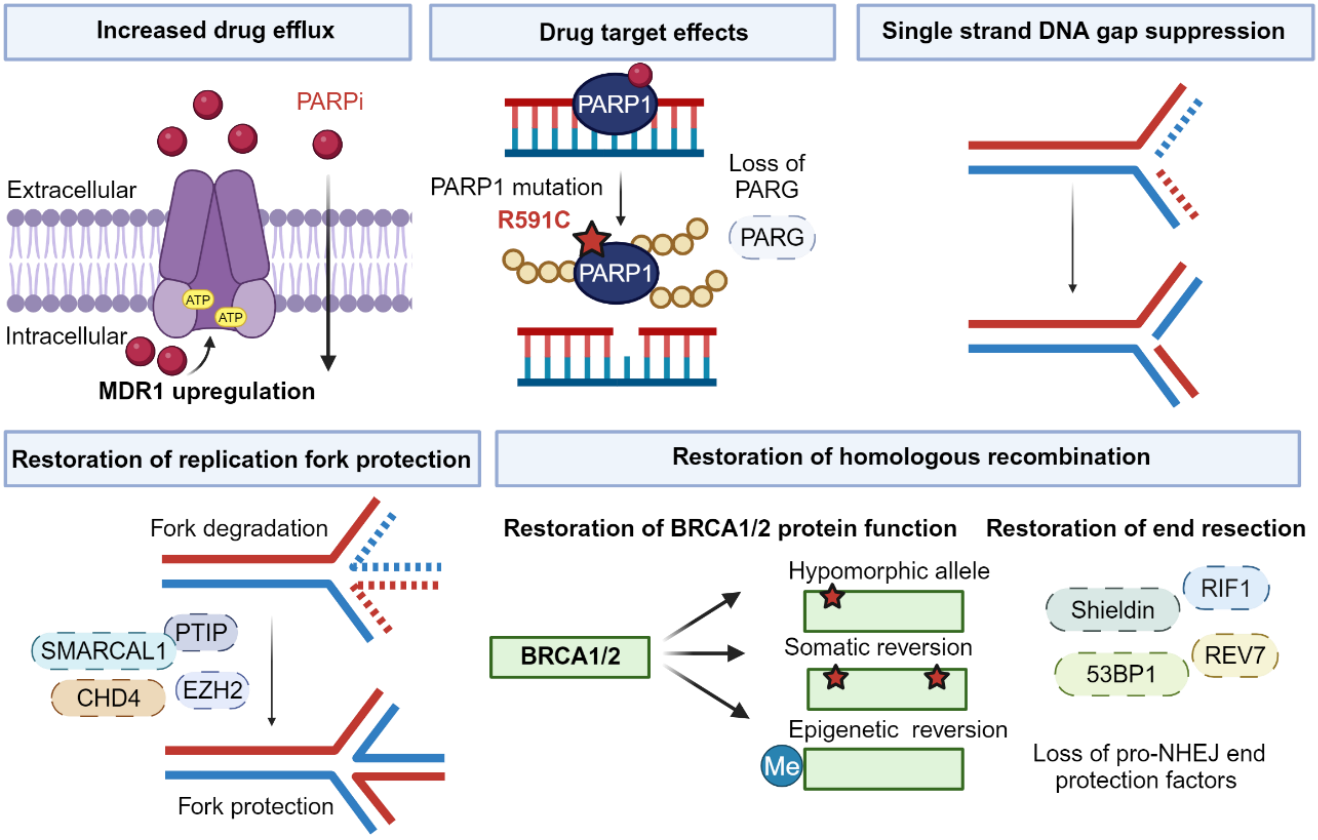

Figure 1.7- Mechanisms of resistance to poly (ADP-ribose) polymerase inhibitors.

Resistance is a key barrier to the success of PARP inhibitors in the clinic. PARPi resistance mechanisms can be split into five broad categories: increased drug efflux, drug target effects, single strand DNA gap suppression, restoration of replication fork protection and restoration of homologous recombination activity. Figure created with Biorender.

1.6 Histone lysine methylation

The N-terminal tails of histone proteins undergo extensive post-translational modifications on arginine and lysine residues, including phosphorylation, methylation, ubiquitination, and acetylation. Histone modifications are key epigenetic features that regulate many cellular processes through altering the charge density between histones and DNA, to impact chromatin structure and function and recruit non-histone proteins. As the focus of my thesis is the lysine methyltransferase SETD1A, this section will focus on histone lysine methylation.

Histone lysine methylation is catalysed by lysine methyltransferases (KMTs), which add methyl groups to lysine residues within histone tails using S-adenosyl-L-methionine as a methyl donor. Lysine methylation can exist in three states: mono (me1)-, di (me2)- and tri-methylation (me3). The addition of methyl groups does not modify the positive charge of the lysine side chains and only causes a small change in mass. However, lysine methylation alters the hydrogen binding potential of the methyl-lysine, which increases hydrophobicity and decreases the ability to donate hydrogen bonds. This increases incrementally as methylation state increases. Therefore, histone lysine methylation exerts its effects through effector molecules that specifically recognise and bind the methylated sites. Methyl binding proteins display methylation state specific recruitment and possess domains which read methylated lysine residues. These domains include bromo, MBT, PHD and PWWP motifs, Tudor domains, chromodomains and double chromodomains. Each methyl state recruits distinct downstream effectors containing specific reader domains.

1.6.1 H3K4 methylation

Both histones H3 and H4 can be methylated at various lysine residues. This thesis will specifically focus of methylation of histone H3 at lysine 4 (H3K4) due to its association with SETD1A. H3K4 methylation in humans in mainly catalysed by the highly conserved KMT2 family of lysine methyltransferases: KMT2A/ mixed-lineage leukaemia (MLL) 1, KMT2B/ MLL2, KMT2C/ MLL3, KMT2D/ MLL4, KMT2F/ SETD1A and KMT2G/ SETD1B (**Fig. 1.8**). Members of the KMT2 family exist in large, multisubunit complexes. Some of these interacting partners: WDR5, ASH2L, DPY30 and RBBP5 are common to all KMT2 family members. These common partners associate with the SET domain of KMT2s and are required for their H3K4 methyltransferase activity, as well as maintaining the integrity and stability of the complex.

Despite identical target sites KMT2 methyltransferases have non-redundant functions, highlighted by differing expression patterns, recruitment to different gene targets, distinct non-histone targets and differential phenotypes observed upon depletion in mice. This can be attributed to unique interacting proteins for each enzyme. Furthermore, as described above different KMT2 enzymes are capable of catalysing different methylation states. For example, SETD1A and its paralogue SETD1B are responsible for catalysing the majority of H3K4me3 in mammalian cells, whereas MLL1 and MLL2 can catalyse H3K4me1 and H3K4me2, but have low H3K4me3 activity and MLL3 and MLL4 are responsible for the majority of H3K4me1.

A second family of KMTs known as SET and MYND (myeloid-nervy-DEAF1) (SMYD) containing SMYD1, SMYD2 and SMYD3 also show H3K4me activity in addition to methylation at other histone residues (Spellmon *et al.*, 2015). Furthermore, KMT7

monomethylates H3K4 in addition to a wide range of non-histone proteins (Nishioka *et al.*, 2002).

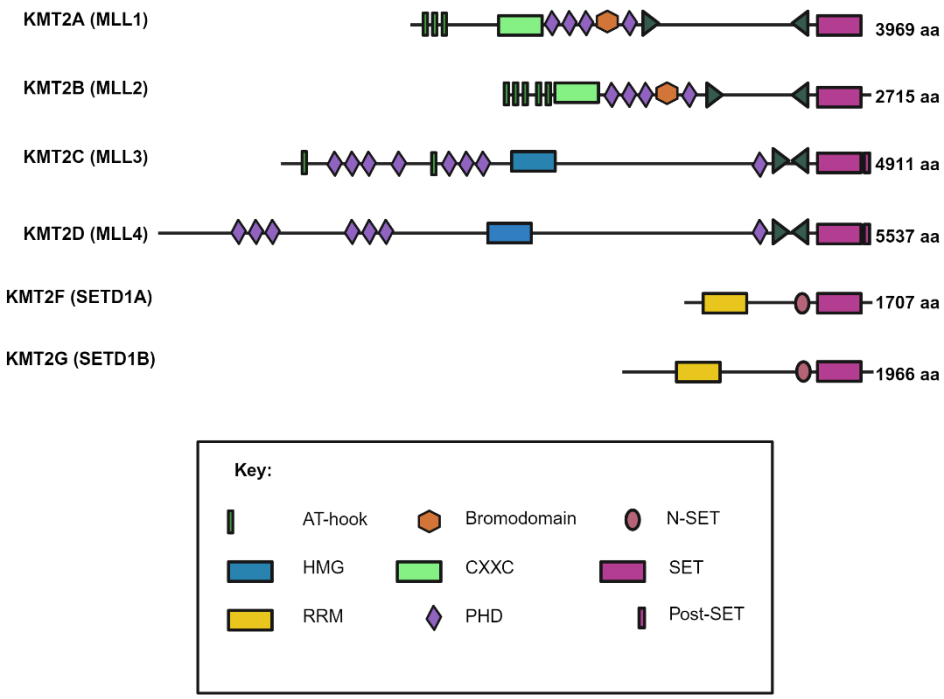

Figure 1.8- The KMT2 family.

Schematic representation of domain structures for each of the KMT2 histone lysine methyltransferases. aa (Amino acids); AT-hook (adenosine-thymidine-hook); CXXC (Zinc finger-CXXC domain); HMG (high mobility group); N-SET (N-terminal of SET); PHD (plant homeodomain); Post-SET, (C-terminal of SET); RRM (RNA recognition motif); SET (Su(var)3-9, Enhancer-of-zeste and Trithorax). Figure created with Biorender. Adapted from (Rao and Dou, 2015).

Lysine methylation is dynamic and reversible and can be subsequently removed by lysine demethylases (KDMs). Humans have six KDMs: KDM1A, KDM1B, KDM5A, KDM5B, KDM5C and KDM5D. The KDM1 family removes methyl groups from H3K4me1 and H3K4me2 only, whilst the KDM5 family can remove all three methylation states. As for KMTs, KDMs preferentially act at specific genomic locations (Hyun *et al.*, 2017).

1.7 SETD1A

1.7.1 Structure

SETD1A is the main KMT2 family methyltransferase expressed in human cells. It is comprised of 1707 amino acids, with three distinct functional domains: the SET domain, containing the catalytic subunit responsible for the methyltransferase activity, the N-terminal RNA interaction motif (RRM), and the C-terminal N-SET domain (Rao and Dou, 2015) (**Fig. 1.9**). The lysine methyltransferase activity of SETD1A is dependent upon the physical interactions between SETD1A and its associated interacting partners in a large multiunit complex known as the COMPASS complex. Some of these, as described above are common to all KMT2 family members, while other interacting proteins: CFP1, WDR82, and HCF1, are specific to the SETD1A COMPASS complex and dictate the functional specificity of SETD1A by recruiting it to distinct regions of the genome. CFP1 is responsible for recruiting SETD1A to promoter regions of the genome via binding to unmethylated CpG motifs through its CXXC DNA-binding domain to facilitate transcriptional activation. WDR82 binds phosphorylated RNA polymerase II to recruit SETD1A for transcription initiation (Lee and Skalnik, 2005; Dou *et al.*, 2006). Furthermore, SETD1A induces histone methylation and transcriptional activation at E2F-responsive promoters via interaction

with HCF1. Lastly, BOD1L has been identified as a novel co-factor of SETD1A which is required for H3K4me3 and has been implicated in the protection of RFs (Higgs *et al.*, 2018), as well as NHEJ-mediated DSB repair (Bayley *et al.*, 2022) (**Fig. 1.9**).

SETD1A and SETD1B share a high degree of homology within the RRM domain and C-terminal SET domain. However, the middle part of these paralogous proteins is less conserved, containing binding sites for enzyme specific interacting partners. SETD1A specifically interacts with HCF1 and BOD1L, whereas, SETD1B forms a specific complex with RBM15 and BOD1 (Porter *et al.*, 2013). SETD1A and SETD1B also have different localisation patterns. For example, the localisation of SETD1A within the nucleus does not overlap with SETD1B (Lee *et al.*, 2007). Additionally, SETD1B expression has been detected in the cytoplasm (Weerts *et al.*, 2021; Wang *et al.*, 2017b). Owing to these differences SETD1A and SETD1B have non-redundant functions, are recruited to different target sites, and regulate unique sets of genes, meaning in many instances loss of SETD1A cannot be rescued by SETD1B.

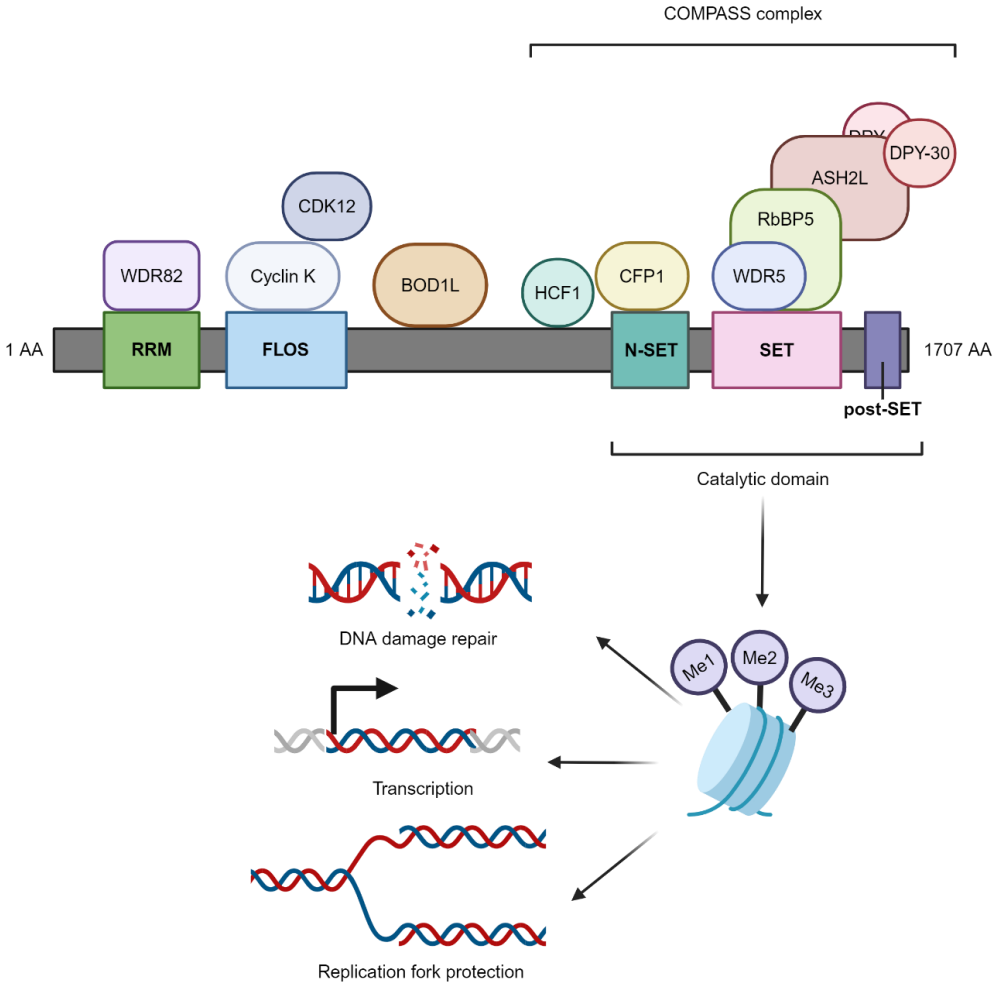

Figure 1.9- The structure and function of the SETD1A COMPASS complex.

SETD1A forms part of the COMPASS complex associating with WDR5, RbBP5, ASH2L, DPY30, CPF1 and WDR82. Furthermore, SETD1A specifically associates with BOD1L and HCF1. It was also identified that SETD1A interacts with cyclin K via the newly identified FLOS domain. Together this complex mediates the mono-, di- or tri-methylation of histone H3 at Lysine 4 to regulate cellular processes including DNA damage repair, transcription and replication. Figure created with Biorender.

1.7.2 SETD1A-dependent H3K4 methylation

SETD1A deposits H3K4me3 at specific genomic regions through sequence specific binding factors, association with transcriptional machinery and chromatin through histone modifications, and recruitment by RNA. For example, SETD1A-mediated H3K4 methylation is dependent on presence of the E3 ubiquitin protein ligase RNF20 dependent mono ubiquitination of H2B at lsyine123. In the absence of H2B ubiquitination an arginine rich motif present within the N-SET domain inhibits contact between the SET domain and the H3 tail to prevent methylation. Upon H2B ubiquitination this motif undergoes a conformational change allowing the SET domain to contact H3K4 (Hsu *et al.*, 2019). Conversely, H3R2 methylation performed by PRMT6 interferes with WDR5 binding to the H3 histone tail, preventing H3K4me3 (Hyllus *et al.*, 2007). H3K4me3 is also inversely correlated with H3K27me3, which inhibits the interaction of H3 with WDR5 and RBBP5. Consequently, H3K27 demethylation is a prerequisite for H3K4me3 (Kim *et al.*, 2013). The combination of these mechanisms works to specifically recruit SETD1A to the genome with different mechanisms working at different target genes to have functional consequences on a range of biological processes (Ruthenburg, Allis and Wysocka, 2007).

1.7.3 Biological function of SETD1A-dependent H3K4 methylation

1.7.3.1 Transcription

H3K4me3 is most well known as a marker of genomic regions undergoing active transcription. There is a correlation between the degree of H3K4me at specific genomic loci and gene expression levels. For example, H3K4me3 is associated with transcription start sites (TSS) and active promoter regions, whereas H3K4-me1 and -me2 are associated with enhancers and sites further within the gene body,

respectively. H3K4 methylation regulates transcription by recruiting chromatin remodelling and histone modifying enzymes to modulate the chromatin structure. For example, H3K4me3 facilitates the binding of the general transcription factor TAF3, a component of the RNA polymerase II preinitiation complex, at promoters.

SETD1A contributes to transcriptional activation through mediating H3K4me3, which is enriched at the TSSs and promoter regions, altering the chromatin state surrounding actively transcribed genes. Chromatin remodelling factors such as the NURF complex recognises H3K4me3 marks and create nucleosome free regions at the promoters, allowing for the recruitment of transcription factors (Wysocka *et al.*, 2006). This was demonstrated in a study by Li *et al.* who observed that loss of SETD1A resulted in decreased transcription of erythroid genes. This was due to reduced levels of H3K4me3, subsequently decreasing the recruitment of NURF to chromatin, preventing chromatin accessibility at erythroid promoters (Li *et al.*, 2016).

Multiple studies have highlighted the key role of SETD1A in regulating gene expression in various cancer types. For example, SETD1A regulates the transcription of cell cycle related genes such as FOXM1 in prostate cancer cells via binding to the E2F1 transcription factor. Suggesting that SETD1A drives cell proliferation and migration in mCRPC (Yang *et al.*, 2020b). Furthermore, SETD1A and its associated H3K4me3 have been identified as upregulated in human colorectal cancer cells and SETD1A knockdown resulted in altered expression of Wnt/β-catenin target genes. SETD1A mediates expression of genes in this pathway by being recruited to promoters of Wnt signalling genes though interaction with β-catenin. The role of SETD1A in gene expression was shown to be directly mediated through H3K4me3, as SETD1A knockdown in colorectal cancer cell lines significantly decreased the

enrichment of H3K4me3 at TSS of Wnt/β-catenin target genes, including MYC and TWIST2 (Salz *et al.*, 2014).

SETD1A is also a key regulator of gene expression in haemopoietic stem cells (HSCs). Transcriptomic profiling of SETD1A deleted cells revealed differential expression of genes related to DNA repair and stress response pathways. Furthermore, cells lacking SETD1A accumulated DNA breaks and failed to repair replicative stress, suggesting SETD1A coordinates the DNA damage response in HSCs (Arndt *et al.*, 2018).

In addition to regulating gene expression through H3K4 methylation, the non-enzymatic FLOS domain of SETD1A has also been shown to regulate gene expression in leukaemia cells. In this study they showed that the newly identified FLOS domain interacts with cyclin K to control expression of DNA damage response genes during S phase of the cell cycle (Hoshii *et al.*, 2018). This study highlights that SETD1A modulates gene expression via multiple mechanisms including both enzymatic and non-enzymatic functions.

1.7.3.2 Development

SETD1A plays a significant role in early embryonic development. This is highlighted by the fact that SETD1A deletion during early mouse embryonic development results in embryonic lethality at embryonic day 7.5. Furthermore, SETD1A is required for embryonic stem cell (ESC) viability, as ESCs cannot be derived in blastocysts with conditional SETD1A depletion. The same study found that SETD1A has unique roles in development in comparison to its paralogue SETD1B. SETD1B was shown to play a role in later stages of embryonic development and SETD1B knockout had no effect

on ESC survival. Furthermore, overexpression of SETD1B is unable to rescue the ESC defects following SETD1A knockout. Beyond embryonic development SETD1A was also shown to be required for the survival of adult mice with mice which died within 3 weeks of SETD1A knockout, highlighting the essential role for SETD1A mammalian development (Bledau *et al.*, 2014).

1.7.3.3 Haematopoiesis

SETD1A is also essential for the development of the hematopoietic system. The generation of haematopoietic stem and progenitor cells (HSPCs), which give rise to all blood lineages in adult organisms, is compromised in absence of SETD1A. For example, SETD1A deletion in mice resulted in the absence of definitive HSPCs during foetal development (Arndt *et al.*, 2018). Furthermore, global loss of SETD1A in adult mice results in a significant reduction in erythroid progenitor cells, suggesting a role for SETD1A in erythropoiesis (Li *et al.*, 2016).

1.7.3.4 DNA damage repair

H3K4 methylation mediates DNA damage repair through control of chromatin configuration to allow access of repair proteins to the DNA, furthermore methylated proteins act as docking sites for the recruitment of HR and NHEJ proteins (Wei *et al.*, 2018). Several studies have identified that SETD1A plays multiple, diverse roles within the DDR and disruption of SETD1A expression effects the ability of cells to recover from DNA damage. For example, upon depletion of SETD1A in HSCPs the transcription of genes associated with BER, NER, HR and NHEJ were significantly reduced. Furthermore, loss of SETD1A resulted in accumulation of DSBs after IR and a delay in repair kinetics, indicating an important role for SETD1A in the DDR (Arndt *et al.*, 2018). Hoshii *et al.* also found by chromatin immunoprecipitation-sequencing

that SETD1A is enriched at genes associated with the DDR, including *FANCD2*, *MLH1* and *ATR* in a mouse model of acute myeloid leukaemia (Hoshii *et al.*, 2022). The same group also found that a newly identified domain of SETD1A called the FLOS domain regulated the transcription of DDR genes, including FANCD2, through mechanisms relying on the interaction between SETD1A with cyclin K. (Hoshii *et al.*, 2018).

A less well-established role for SETD1A in the DDR is through its association with the E3 ubiquitin ligase enzyme RAD18 (Alsulami *et al.*, 2019), which is responsible for ubiquitinating PCNA at lysine 164 in response to DNA damage (Geng, Huntoon and Karnitz, 2010). As well as a physical interaction with RAD18, this study also revealed that knockdown of SETD1A could abolish the ubiquitination of PCNA following mitomycin C induced DNA damage, indicating a potential role for SETD1A in the maintenance of genome instability in response to replication stress (Alsulami *et al.*, 2019). However, further investigation is needed to verify this interaction.

SETD1A-dependent H3K4 methylation also plays a key role in promoting genomic stability by preventing DNA damage at stalled RFs. In cooperation with its co-factor BOD1L, SETD1A methylates H3K4 at stalled RFs, facilitating the FANCD2 mediated mobilisation of histones to promote RAD51-dependent fork protection. Methylated H3K4 at reversed RFs stabilises RAD51 and controls access of the chromatin remodelling factor CHD4 to reversed forks, protecting nascent DNA from uncontrolled resection by DNA2 (Higgs *et al.*, 2018).

Having identified the crucial role of SETD1A as an anti-resection factor during replication stress, the Higgs lab hypothesised that SETD1A may also act as a global

anti-resection factor at DSBs to promote NHEJ. This is also in keeping with findings in yeast showing that cells that cannot undergo H3K4me3 display a defect in DSB by NHEJ (Faucher and Wellinger, 2010).

As described above the 53BP1-RIF1-shieldin pathway is a critical determinant of DNA end-protection counteracting end-resection at DSBs by BRCA1. Loss of members of this pathway results in unstrained end-resection in G1 cells and impaired NHEJ. SETD1A, along with its co-factor BOD1L is required to recruit RIF1 to DSBs to enable efficient repair. Cells depleted of SETD1A, BOD1L or RIF1 also had an increased number of DSBs undergoing resection, as measured by native IdU foci, suggesting these factors act together to suppress inappropriate DNA resection at DSBs. This data suggested that SETD1A may act in concert with RIF1 and the 53BP1 pathway as a pro-NHEJ factor. This hypothesis was confirmed as depletion of SETD1A suppressed the fusion of dysfunctional telomeres in the absence of the shelterin subunit TRF2 (Bayley *et al.*, 2022). Bayley *et al.* then went on to show that the SETD1A-dependent recruitment of RIF1 to facilitate NHEJ was reliant on the H3K4 methyltransferase activity of SETD1A, as perturbation of H3K4 inhibited RIF1 foci formation following IR. In conclusion, this paper showed that SETD1A-dependent H3K4me3 facilitates the recruitment of RIF1 to DSBs, inhibiting DNA end-resection and promoting NHEJ through facilitation of the RIF1-53BP1-Sheildin pathway (Bayley *et al.*, 2022).

1.7.4 SETD1A in disease

1.7.4.1 Cancer

Unsurprisingly, due to the critical role of SETD1A in the DDR, ectopic expression of SETD1A is associated with a variety of human diseases, including the development

of human cancers. *SETD1A* mutations are most prevalent in large intestine, lung and endometrial cancers, with 15.6% of mutations occurring in the catalytic SET domain (Rao and Dou, 2015).

Amplification or mutations of *SETD1A* and increased mRNA expression have been identified in non-small cell lung carcinoma (NSCLC) and are associated with poor survival in these patients (Du *et al.*, 2021). Increased SETD1A has been shown to drive epithelial-mesenchymal transition (EMT) and enhanced DNA replication. These effects are achieved through elevated H3K4me3 upstream of oncogenes critical for lung tumour growth including CDC7 and TOP1 (Kang *et al.*, 2021b).

Other studies have found links between SETD1A and breast cancer. With 45% of breast cancers harbouring gain in copy number of SETD1A, and another 6.8% harbouring loss of copy number. Elevated SETD1A expression is associated with increased H3K4me3-mediated activation of genes linked to proliferation and invasion of breast cancer, including matrix metalloproteases, Six1 and cyclin A, promoting metastatic behaviour (Salz *et al.*, 2015).

Increased levels of SETD1A are also associated with lower overall survival in gastric cancer (Wu *et al.*, 2020). Elevated SETD1A drives tumorigenesis and gastric cancer progression through upregulation of HIF1α target genes, enhancing glycolysis. The same group have also shown that SETD1A contributes to gastric cancer cell migration, invasion and metastasis by inducing EMT through epigenetic reprogramming of the Snail transcription factor (Wu *et al.*, 2021).

1.7.4.2 Neurological defects

SETD1A is highly expressed in the adult mouse brain, specifically within the neocortex, indicating a potential role for SETD1A in neurodevelopment. This was confirmed in mice with SETD1A haploinsufficiency, which showed defects in the development of murine cortical axons, dendrites, and spines, resulting in significant cognitive defects. Reestablishing the expression of SETD1A in adult mice subsequently reversed these cognitive defects (Mukai *et al.*, 2019). This is further supported by Cameron *et al.* who showed SETD1A knockdown in human neural cell lines resulted in widespread changes in gene expression, particularly in genes involved in neurodevelopment, such as *DCX* and *DLX5 (Cameron et al., 2019)*.

As such, loss of function variants (LoF) in SETD1A have been identified in schizophrenia and other neurodevelopmental phenotypes (Singh *et al.*, 2016; Kummeling *et al.*, 2020; Cameron *et al.*, 2019). These patients displayed increased DDR activation following high dose hydroxyurea and severe nascent DNA degradation upon DNA damage induction, highlighting SETD1A-dependent DNA damage repair is defective in these cells (Kummeling *et al.*, 2020). Furthermore, a large-scale study conducted by Singh *et al.* identified LoF variants in SETD1A in patients with schizophrenia. Greater than 40% of these variants were a two-base deletion at the splice acceptor of exon 16, located upstream of the catalytic SET domain (Singh *et al.*, 2016), highlighting *SETD1A* as a candidate gene in schizophrenia.

1.7.5 SETD1A and PARPi resistance

As previously described, loss of pro-NHEJ factors such as 53BP1, RIF1 or REV7-shieldin confers resistance to PARPi by restoring HR. In accordance with the role of

SETD1A in regulating RIF1-dependent NHEJ and inhibiting DNA end-resection, further data from my lab also revealed that depletion of SETD1A attenuates the sensitivity of BRCA1-deficient cells to PARPi treatment, suggesting loss of SETD1A may offer a novel PARPi resistance mechanism. Furthermore, it was shown that cells deficient for both BRCA1 and SETD1A were able to recruit RAD51 to chromatin following PARPi, at least partially restoring functional HR (Bayley *et al.*, 2022). These phenotypes were also observed in cells with perturbed H3K4 methylation, either through mutation or overexpression of the KDM5A lysine demethylase, suggesting that PARPi resistance in BRCA1-deficient cells is driven by epigenetic modifications (Bayley *et al.*, 2022) (**Fig. 1.10**). These observations suggest that loss of SETD1A or associated H3K4me3 may provide a novel epigenetic mechanism of PARPi resistance in BRCA1-deficient cells by restoring HR, in a similar manner to loss of 53BP1, RIF1 or components of the shieldin complex.

A key area of outstanding research is to establish whether PARPi resistance induced by loss of SETD1A provides a general mechanism of resistance that can be applied to wider HR-deficient contexts. As discussed above, there is growing evidence that the efficacy of PARPi extends beyond BRCA1-deficiency to include ATM-deficient tumours. Despite this, the variable response of ATM-deficient tumours to PARPi in clinical trials highlights an urgent need to better understand mechanisms of PARPi resistance applicable to this genetic context. Therefore, in this thesis I ask whether SETD1A-induced PARPi resistance is specific to BRCA1-deficiency or whether it can also apply to ATM-deficient contexts.

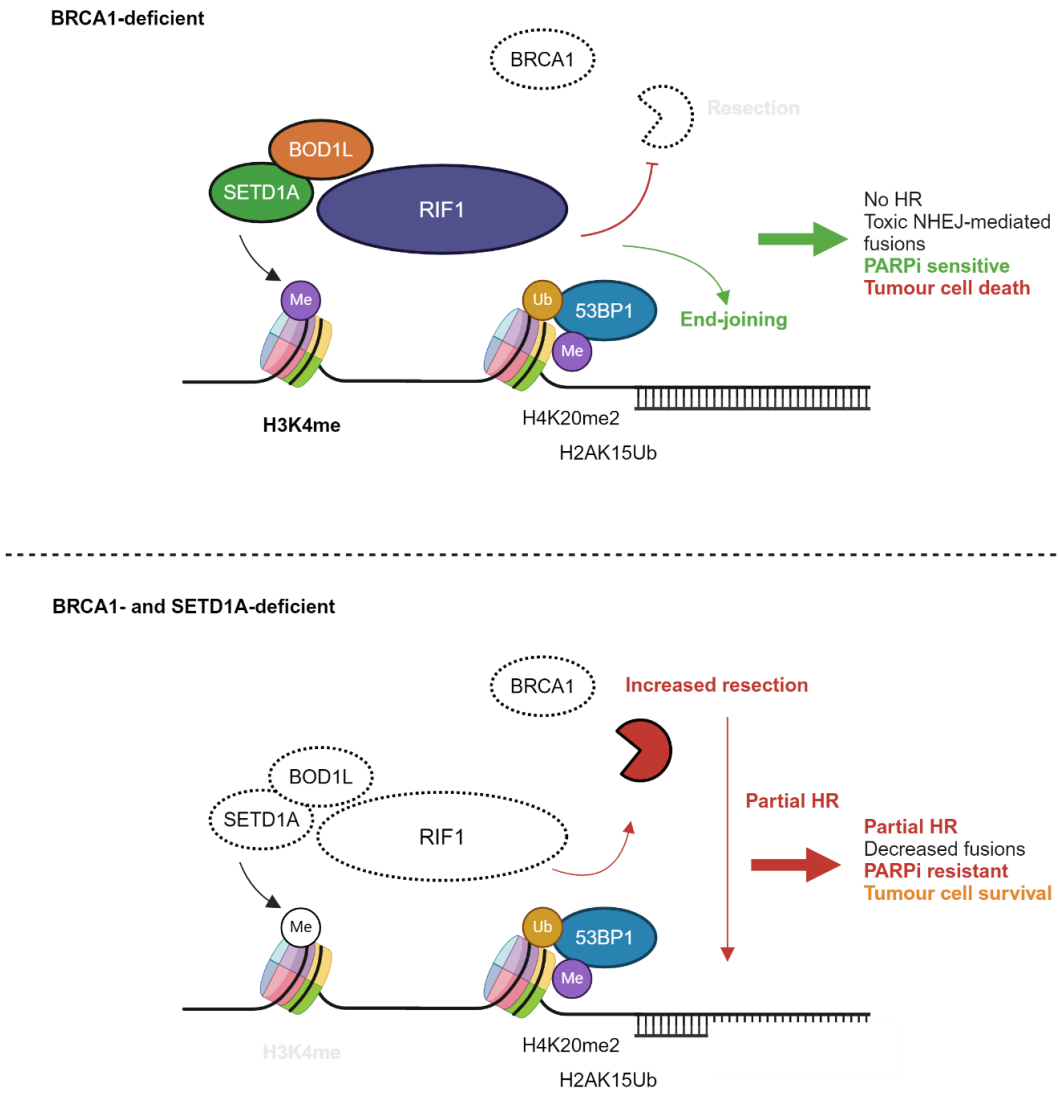

Figure 1.10- SETD1A facilitates RIF1-dependent non-homologous end joining driving PARPi resistance in BRCA1-deficient cells.

(Top) In G1 cells 53BP1 is recruited to sites of DSBs by binding to pre-existing H4K20me2 and H2AK15Ub. SETD1A and its co-factor BOD1L catalyse H3K4me to stabilise the recruitment of RIF1. This suppresses BRCA1-dependent resection and promotes NHEJ. In BRCA1-deficient cells, DNA end-resection and RAD51 loading are inhibited. Therefore, DNA damage cannot be repaired by homologous recombination (HR), resulting in sensitivity to PARP inhibition. (Bottom) In the absence of SETD1A, H3K4me levels are reduced and RIF1 recruitment is destabilised, leading to inappropriate resection of DSBs. In BRCA1-deficient cells loss of SETD1A partially restores HR, conferring cell survival and resistance to PARP inhibition. Figure created with Biorender. Adapted from (Bayley et al., 2022).

1.8 Hypothesis and aims

Hypothesis: SETD1A-dependent H3K4 methylation dictates PARP inhibitor sensitivity in BRCA1- and ATM-deficient cancers through restoring homologous recombination.

Aims:

The first aim of this thesis, explored in chapter three, is to establish whether loss of SETD1A provides a general mechanism of PARPi resistance that can be applied to ATM-deficient contexts. To this end I used ATM-depleted HeLa cells and assessed effects of SETD1A depletion on PARPi sensitivity and DDR kinetics using clonogenic survival assays and immunofluorescent microscopy techniques, respectively.

As discussed in chapter four, I then utilised BRCA1- and ATM-mutated cancer cell lines, along with survival analysis of HR-deficient cancers from cancer genomic databases to begin to establish the relevance of loss of SETD1A as a PARPi resistance mechanism in HR-deficient cancers.

In chapter five I then aimed to validate loss of SETD1A as a mechanism of PARPi resistance in an inducible CRISPR/Cas9 system.

Finally, in chapter six, I employed transcriptomic approaches such as RNA sequencing and qPCR to identify genes regulated by SETD1A in BRCA1- and ATM-deficient backgrounds. I then investigated the functional relevance of candidate genes in mediating PARPi resistance.

2. CHAPTER 2: MATERIALS AND METHODS

All chemicals were from Sigma-Aldrich, all cell culture reagents were from Gibco/Life technologies and all plasticware was from Corning, unless otherwise stated.

2.1 Mammalian cell culture

All cell lines were from ATCC, unless otherwise stated. HeLa, HeLa-H3-GFP (WT and K4A) (Higgs *et al.*, 2018; Sato *et al.*, 2012), A549 and MCF7 cell lines were cultured in Dulbecco's Modified Eagle's Medium (DMEM, 41966029) supplemented with foetal calf serum (FCS, 10270106) (10 % v/v) and penicillin-streptomycin (15140122) (1 % v/v). SKOV3 and U-2-OS Flp-In T-Rex cells (Stephen Taylor, University of Manchester) were cultured in McCoy's 5A media (26600023) supplemented with FCS (10 % v/v) and penicillin-streptomycin (1 % v/v). HCC1937 and H1395 cells (both from CLS Cell Lines Service) were cultured in RPMI-1640 (21875-034) supplemented with FCS (10 % v/v) and penicillin-streptomycin (1 % v/v). UWB1.289 cells were cultured in RPMI-1640, with 50 % Mammary Epithelial Cell Growth Medium (CC-3150, Clonetics™, Lonza) supplemented with FCS (3 % v/v). A Hela Kyoto cell line expressing inducible Cas9 (HeLa Kyoto iCas9) (Simon Boulton) was transduced with lentivirus made from pLentiGuide-Puro modified to contain a sgRNA targeting human SETD1A (gRNA #4 AGAGCCATCGGAAATTTCCG, gRNA #5 CGTATGCTCTATATGCACAG or gRNA #7 TATGTGCCGTAAGTACGGTG). HeLa Kyoto iCas9 cells were cultured in DMEM supplemented with tetracycline-free FCS (10 % v/v), penicillin-streptomycin (1 % v/v), and 0.5 µg/ml Puromycin (A11138-03). Where appropriate, Cas9 expression was induced with 1 µg/ml of doxycycline (14422, Cayman Chemical) for 48 hours. All cell lines were maintained at 37 °C and 5 % CO_2.

2.2 Creation of inducible U-2-OS Flp-In cells expressing FLAG-RBBP2

Tetracycline-inducible U-2-OS Flp-In cell lines expressing FLAG-RBBP2 or FLAG-RBBP2-H438A were generated according to the manufacturer's protocols (Thermo Fisher Scientific). Briefly, the parental U-2-OS Flp-In T-REx cell line was transfected with pOG44 Flp-recombinase expression vector and either pCDNA5-FRT-T/O-FLAG-RBBP2 or pCDNA5-FRT-T/O-FLAG-RBBP2-H438A at a 9:1 ratio using FuGENE® transfection reagent (Promega). Cells were selected in McCoys5A cell culture media with tetracycline-free FCS (10 % v/v), penicillin-streptomycin (1 % v/v) and 100 μg/ml hygromycin for 10 days. To induce expression of the protein of interest, cells were grown in McCoys5A cell culture media with tetracycline-free FCS (10 % v/v), penicillin-streptomycin (1 % v/v) and 100 μg/ml hygromycin for 3 days, then fresh media containing 1 μg/ml doxycycline for 48 hours. Untransfected U-2-OS Flp-In T-REx cells were used as a parental control.

2.3 siRNA transfection

Cells were seeded at a density of 5 x 10^5 cells per 6 cm dish one day prior to transfection. Cells were then transfected with ON-TARGETplus siRNAs (Dharmacon) (**Table 2.1**) at a final concentration of 100 nM in pre-warmed Opti-MEM (11058021, Gibco) and Oligofectamine transfection reagent (12251011, Invitrogen), according to the manufacturer's instructions. Transfected cells were rescued ~18 hours post transfection by the addition of complete growth medium supplemented with FCS or tetracycline free FCS (20 % v/v) without penicillin-streptomycin.

Table 2.1- siRNA oligonucleotide sequences.

Details of catalogue numbers and oligonucleotide sequences of the siRNAs used.

siRNA	Sequence
ON-TARGET plus Human SETD1A SMARTPool Cat# L-022793-01-0010	
J-022793-09	CGGAAAGAGCCAUCGGAAA
J-022793-10	CUCAGAAGGUGUACCGCUA
J-022793-11	AGUAUAUACCAGUCGAAGA
J-022793-12	ACAUAUGUUAAUAGCGCAA
ON-TARGET plus Human ATM SMARTPool Cat# L-003201-00-0005	
J-003201-11	GCAAAGCCCUAGUAACAUA
J-003201-12	GGUGUGAUCUUCAGUAUAU
J-003201-13	GAGAGGAGACAGCUUGUUA
J-003201-14	GAUGGGAGGCCUAGGAUUU
ON-TARGET plus Human BRCA1 SMARTPool Cat# L-003461-00-0005	
J-003461-09	CAACAUGCCCACAGAUCAA
J-003461-10	CCAAAGCGAGCAAGAGAAU
J-003461-11	UGAUAAAGCUCCAGCAGGA
J-003461-12	GAAGGAGCUUUCAUCAUUC
ON-TARGET plus Human RIF1 SMARTPool Cat# L-027983-01-0005	
J-027983-09	CCUCAAAUGAAAUGCGAAA
J-027983-10	UCACGUAGCCCUAAAUUUA
J-027983-11	GAAUCAAAUCUAAGGACUA
J-027983-12	GCAAGUUCCUGAUGAUUUA
ON-TARGET plus Human SETD1A – Set of 4 Cat# LQ-022793-01-0005	
SETD1A siRNA 1 J-022793-09	CUCAGAAGGUGUACCGCUA
SETD1A siRNA 2 J-022793-10	CUCAGAAGGUGUACCGCUA
SETD1A siRNA 3 J-022793-11	AGUAUAUACCAGUCGAAGA
SETD1A siRNA 4 J-022793-12	ACAUAUGUUAAUAGCGCAA
ON-TARGET plus Human EME1 SMARTPool Cat# L-016420	
J-016420-09	GAAUUUGCUCGCAGACAUA
J-016420-10	GUGCAGUUGUGAAUGCCUA
J-016420-11	CCGCAUUGGACCAGAACUA
J-016420-12	GCUAAGCAGUGAAAGUGAA
Control siRNA CTM-334043	
Control siRNA	CGUACGCGGAAUACUUCGDTDT

2.4 Western blotting

Cells were harvested by trypsinisation and pelleted at 1,200 x g for 5 minutes at room temperature, washed in PBS and cell pellets snap frozen in liquid nitrogen. Cells were then lysed on ice in UTB lysis buffer (8 M Urea, 50m M tris and 150 mM β-mercaptoethanol) followed by two cycles of sonication at 10 % power for 10 seconds using a Microson Ultrasonic Cell Disrupter (Misonix). Lysates were clarified by centrifugation at 12000 x g for 20 minutes at 4 °C. Lysate protein concentration was determined by Bradford protein assay (5000006, Bio-Rad) using bovine serum albumin standards (0-2 mg/ml), by measuring absorbance at 595 nm. Proteins were then diluted in Laemmli sample buffer (1610737EDU, Bio-Rad) supplemented with β-mercaptoethanol (10% v/v) and boiled at 95 °C for 10 minutes. Fifty micrograms of protein was resolved on a 6 % or biphasic 12 % and 6 % tris-bicine polyacrylamide gel at a constant current (0.025 A per gel) and transferred onto a nitrocellulose membrane at a constant current (0.2 A) for 18 hours. Membranes were blocked in 5 % dried milk in tris-buffered saline with 0.1% Tween 20 (TBST) for at least 1 hour, followed by overnight incubation at 4 °C with primary antibodies diluted in 5 % dried milk/TBST or 10 % BSA. Membranes were then washed three times for 10 minutes in TBST then incubated with horseradish peroxidase-conjugated (HRP) secondary antibodies diluted in 5 % dried milk/TBST for 1 hour at room temperature. Membranes were washed again three times in TBST for 10 minutes. Protein bands were visualised using ECL detection reagents (GERPN2209, Cytiva) and developed using Amersham Hyperfilm chemiluminescent film (28906846, Cytiva) or the Bio-Rad ChemiDoc imaging system.

2.5 Antibodies

The antibodies used in this study are detailed in **Table 2.2**

Table 2.2- Antibodies used in this study.

Antigen	Catalogue number	Manufacturer
ATM	Sc-53173	Santa Cruz Biotechnologies
BOD1L	N/A	Grant Stewart (Higgs *et al.*, 2015)
BRCA1	Sc-6954	Santa Cruz Biotechnologies
β-tubulin	86298	Cell signalling Technology
Cas9	844302	BioLegend
CENPF	58982	Cell signalling Technology
CHK1	Sc-8408	Santa Cruz Biotechnologies
P-CHK1 (Ser 345)	2348	Cell signalling Technology
CREB	Ab32515	Abcam
P-CREB (Ser 121)	SAB4503908	Sigma-Aldrich
EME1	Sc-53275	Santa Cruz Biotechnologies
FLAG (anti-DDDDK tag)	NBP1-06712	Novus Biologicals
H2A	07-16146	Millipore
γH2AX	05-636	Millipore
Histone H3	Ab1791	Abcam
H3K4me3	Ab8580	Abcam
KAP1	A300-274A	Bethyl Laboratories
P-KAP1 (Ser 824)	Ab70369	Abcam
Luciferase	Sc-745480	Santa Cruz Biotechnologies
Mitosin	610768	BD Biosciences
NBS1	14956	Cell signalling Technology
P-NBS1 (Ser 343)	Ab47272	Abcam
PARP1	Sc-74470	Santa Cruz Biotechnologies
RAD51	PC130	Calbiochem
RBBP2	Ab70892	Abcam
RIF1	A300-568A	Bethyl Laboratories
RPA	NA18	Millipore
P-RPA (Ser 4/8)	A300-245A	Bethyl Laboratories
SETD1A	A300-289A	Bethyl Laboratories
WDR5	A302-430A	Bethyl Laboratories
Alexa-fluor anti-mouse 488	A11029	Thermo Fisher Scientific
Alexa-fluor anti-rabbit 488	A11070	Thermo Fisher Scientific
Alexa-fluor anti-mouse 555	A532773	Thermo Fisher Scientific
Alexa-fluor anti-rabbit 555	A32794	Thermo Fisher Scientific
Anti-mouse-HRP	P0399	Dako
Anti-rabbit-HRP	P0447	Dako

2.6 Chromatin fractionation

Cells were harvested by trypsinisation as above and resuspended in chromatin fractionation (CF) buffer (20 mM Tris-HCl, 100 mM NaCl, 5 mM MgCl2, 10 % glycerol, 0.2 % IGEPAL CA-620, 0.5 mM DTT) supplemented with protease inhibitor cocktail and lysed on ice for 15 minutes. Lysates were then centrifuged at 2000 x g for 5 minutes at 4 °C. Supernatant was retained to form the soluble fraction, and the chromatin pellet was washed and resuspended in CF buffer before two cycles of sonication at 10 % power for 10 seconds. Protein concentration was determined by Bradford protein assay as above. Forty micrograms of whole cell lysate was analysed by SDS-PAGE and immunoblotting alongside 20 μg of both soluble and chromatin fractions. β-tubulin and Histone H3 were used as a negative and positive control for chromatin-bound protein, respectively.

2.7 Immunoprecipitation

Cell pellets from U-2-OS Flp-In-FLAG-RBBP2 or U-2-OS Flp-In-FLAG-RBBP2-H438A cells were harvested and lysed in NETN lysis buffer (250 mM NaCl, 50 mM Tris, pH 8, NP-40 (1 % v/v), 2 mM MgCl2, 90 units/ml benzonase and EDTA free protease inhibitor), by rotating for 30 minutes at 4 °C. Lysates were clarified by centrifugation at 44,000 x g for 30 minutes at 4 °C. Supernatant protein concentration was determined by Bradford protein assay as described above. Twelve microlitres of each sample was saved for an input sample.

Rabbit IgG antibody (X0903, Dako) was prebound to protein A beads (88845, Thermo Fisher Scientific) and rotated for 3 hours at 4 °C. One and a half milligrams of protein was incubated with 5 μg of IgG or anti-FLAG® M2 affinity gel (A2220, Millipore) and

rotated for 3 hours at 4 °C. Lysates were spun down at 3000 x g for 20 seconds and the supernatant was removed. Beads were washed three times in NTN wash buffer (100 mM NaCl, 20 mM Tris pH 7.4, NP-40 (0.05 % v/v) and protease inhibitor with EDTA). The supernatant was diluted in Laemmli sample buffer and boiled for 10 minutes at 95 °C. Samples were analysed by western blotting as described above.

2.8 Colony survival assays

Following transfection with indicated siRNAs, or after an additional 24-hour treatment with 1 μM AZD0156 (S8375, Selleckchem), transfected cells were seeded at low density and left overnight. Cells were then exposed to increasing concentrations (0, 0.2, and 2 μM) of olaparib (AZD2281) (S1060, Selleckchem) or equivalent volumes of dimethyl sulfoxide (DMSO) (D2650, Sigma Aldrich), and left to form colonies for 10 days, with olaparib replaced every 3 days. After 10-12 days colonies were stained with 0.5 % crystal violet solution (HT90132, Sigma-Aldrich) and enumerated. Alternatively, crystal violet stain was resolubilised with 0.1 % SDS for 1 hour with constant agitation and the absorbance measured at a wavelength of 595 nm. Data in either case was expressed as percentage survival normalised to an untreated control.

2.9 Immunofluorescence

2.9.1 Pre-extraction and fixation

Transfected cells were grown on glass coverslips at a density of 2 x 10^5 cells per well of a 6 well plate. Following the relevant treatment with inhibitors and/or genotoxic agents, cells were permeabilised with nuclear extraction buffer (20 mM NaCl, 3 mM MgCl2, 300 mM sucrose, 10 mM PIPES, 0.5 % Triton X-100, pH 6.8) for 5 minutes on

ice and then fixed with 4 % paraformaldehyde for 10 minutes at room temperature. Coverslips were then washed in PBS three times before blocking for at least 1 hour in PBS supplemented with FCS (10 % v/v) and sodium azide (0.1% v/v) at 4 °C prior to staining.

2.9.2 Staining and imaging

Fixed and permeabilised cells were incubated with primary antibodies diluted in PBS supplemented with FCS (3% v/v) for 1 hour at room temperature. Coverslips were then washed in PBS three times and then incubated with Alexa Fluor conjugated secondary antibodies diluted in PBS supplemented with FCS (3% v/v) for 1 hour in the dark at room temperature. Coverslips were then washed three times with PBS and then mounted onto slides with Duolink® *in situ* mounting medium with DAPI (DUO82040, Sigma-Aldrich). Images were taken using a Nikon E600 Eclipse equipped with a 60x oil lens, a Zyla 5.5 SCMOS camera (Andor) and NIS-Elements imaging software (Nikon). Foci numbers enumerated using ImageJ software. For each independent experiment at least 100 nuclei were counted per condition.

2.10 Homologous recombination assay

Homologous recombination was measured using a CRISPR-Cas9 based LMNA assay (Pinder, Salsman and Dellaire, 2015). In brief, HeLa cells were transfected with siRNA as described above. Forty-eight hours post transfection cells were seeded onto glass coverslips at high confluency. Cells with then transfected with 2 µg each of pLX330-LMNA-gRNA, pCR2.1-Clover-LMNA-donor and pRFP plasmids (Pinder, Salsman and Dellaire, 2015) using Lipofectamine™ 2000 (11668027, Invitrogen) according to the manufacturer's instructions. After 48 hours coverslips

were fixed for 10 minutes at room temperature in 4 % paraformaldehyde, followed by permeabilisation for 5 minutes at room temperature in PBS supplemented with Triton-X-100 (0.5 % v/v). Following this, coverslips were blocked with PBS supplemented with FCS (10 % v/v) for 30 minutes, before mounting on microscope slides with Duolink® *in situ* mounting medium with DAPI. Images were taken using a Nikon E600 Eclipse equipped with a 60x oil lens, a Zyla 5.5 SCMOS camera (Andor) and NIS-Elements imaging software (Nikon). Relative percentage homologous recombination was quantified by counting the number of green-ringed cells normalised to the efficiency of pRFP transfection. For each independent experiment at least 100 nuclei were counted per condition.

2.11 Metaphase spreads

Radial chromosomes were quantified in HeLa, H3-GFP and HeLa Kyoto iCas9 cells. Briefly, transfected cells were treated with 10 μM olaparib for 24 hours prior to harvesting. Three hours prior to harvesting cells were treated with 0.1 μg/ml Colcemid™ (15212012, Gibco). Cells were harvested by trypsinisation and treated with pre-warmed 0.075 M KCl and incubated at 37 °C for 10 minutes. Cells were then fixed in ice-cold methanol/ acetic acid (3:1) solution, and metaphases were dropped onto microscope slides pre-soaked in fixative solution. Slides were then placed on a heating block at 80 °C for 1 minute and allowed to dry overnight. Metaphase spreads were mounted with Duolink™ *in situ* mounting media containing DAPI. Images were taken using a Nikon E600 Eclipse equipped with a 100x oil lens, a Zyla 5.5 SCMOS camera (Andor) and NIS-Elements imaging software (Nikon). Radial chromosomes were quantified using ImageJ software. For each independent experiment at least 50 metaphases were analysed per condition.

2.12 Cloning

2.12.1 pET23a-RIF1

pET23a-RIF1 plasmid was created from a plasmid encoding GFP-tagged RIF1 (pCDNA5-FRT-T/O-eGFP-RIF1) obtained from Dan Durocher (Escribano-Díaz et al., 2013). RIF1 was subcloned from this vector into the *NotI-BamHI* sites of pET23a using primers (**Table 2.3**) by PCR to create pET23a-RIF1 (aa1-2446). PCR conditions were as follows: initial denaturation at 98 °C for 30 seconds, 32 cycles of 98 °C for 10 seconds, 68 °C for 30 seconds and 72 °C for 5 minutes and a finale extension step of 72 °C for 4 minutes.

2.12.2 pET23a-RIF1-ΔHEAT

pET23a-RIF1-ΔHEAT (aa978-2446) was created from pET23a-RIF1 using a Q5 site-directed mutagenesis kit (E0554S, New England Biolabs) and corresponding primers to remove the 5' end of RIF1 (**Table 2.3**). PCR conditions were as follows: initial denaturation at 98 °C for 30 seconds, 25 cycles of 98 °C for 10 seconds, 63 °C for 30 seconds and 72 °C for 4 minutes, and a final extension at 72 °C for 2 minutes. PCR products were transformed into NEB® 5-apha competent *E. coli* (C2987I, New England Biolabs) and ampicillin-resistant colonies selected. Plasmid DNA was then isolated from mini-cultures of these bacteria using the Nucleobond Xtra Maxi kit (740414.10, Macherey-Nagel) according to the manufacturer's protocol before screening as below.

2.12.2.1 Colony PCR

Ten colonies (clones 1-10) were selected for colony PCR to confirm HEAT repeat deletion using RIF1 primers 4 and 8 (**Table 2.3**). A positive control colony PCR was

also performed using primers 9 and 12 (**Table 2.3**). A negative no template control was also included. Colony PCR was performed using HotStarTaq® polymerase kit (203203, Qiagen) according to manufactures instructions. PCR conditions were as follows: initial activation at 95 °C for 15 minutes, 25 cycles of 94 °C for 30 seconds, 55 °C (Primers 4 and 8) or 50 °C (Primers 9 and 12) for 30 seconds and 72 °C for 2 minutes, with a final extension step at 72 °C for 2 minutes.

Ten microlitres of PCR product was analysed on 1 % agarose gel at 100 V for 1.5 hours with a 1 Kb gene ruler ladder (SM0311, Thermo Fisher Scientific).

2.12.2.2 Restriction digestion

Restriction digestion was carried out using *KpnI-HF* (R3142S, New England Biolabs) and *NotI-HF* (R3189S, New England Biolabs) enzymes and 10x cutsmart buffer (B7204S, New England Biolabs) according to manufacturer's instructions. Restriction reactions were incubated at 37 °C for 1 hour followed by heat inactivation at 65 °C for 20 minutes. Restriction fragment sizes of ~2804 bp and ~8187 bp for pET23a-RIF1 and ~ 2804 bp and ~5000 bp for pET23a-ΔHEATRIF1 were confirmed using agarose gel electrophoresis. Ten microlitres of pET23a-RIF1 or 20 µl pET23a-ΔHEATRIF1 restriction digestions were run on a 0.8 % agarose gel with the 1 Kb gene ruler ladder at 90 V for 1 hour.

2.12.3 pCDNA5-FRT-T/O-GFP-RIF1 1-411

Constructs encoding pCDNA5-FRT-T/O-eGFP-RIF1 and pCDNA5-FRT-T/O-GFP-RIF1 1-411 were obtained from Dan Durocher (Escribano-Díaz *et al.*, 2013). HEK293T cells were transfected using Lipofectamine™ 2000 (11668027, Invitrogen)

following manufacturer's instructions. Forty-eight hours post transfection cell lysates were harvested for histone pulldown assays.

Table 2.3- Oligonucleotide sequences for primers.

Oligonucleotide sequences of the primers used.

Primer	Sequence	Supplier
RIF1 pET23a forward	ATAAAGAATGCGGCCGCTAAACTAT AAATAGAATTTTCATGGGA	Sigma Aldrich
RIF1 pET23a reverse	CGCGGATCCGCGATGACGGCCAG GGGTCAG	Sigma Aldrich
ΔHEAT RIF1 forward	AAACAAAAATTTCTGCTCCTGTTG	Sigma Aldrich
ΔHEAT RIF1 reverse	ACCCATTTGCTGTCCACC	Sigma Aldrich
RIF1 primer 4	TCCTTTTTTTCCAAACATGC	Sigma Aldrich
RIF1 primer 8	CCGACTTGTAGGGTATGGGG	Sigma Aldrich
RIF1 primer 9	TCTAATACCACTGTTGCTGG	Sigma Aldrich
RIF1 primer 12	TCTCCTCACCCTCCTACTTC	Sigma Aldrich

2.13 Production of recombinant RIF1 protein

Recombinant full length or ΔHEAT RIF1 protein was produced from the pET23a-RIF1 or pET23a-ΔHEATRIF1 plasmids using the TnT® T7 Quick Coupled Transcription/Translation cell-free system (L1170, Promega). The reaction was prepared using 40 µl TnT® Quick Master Mix, 1 µl 1 mM methionine, 1 µl T7 TnT® PCR enhancer and 1 µg of pET23a-RIF1 or pET23a-ΔRIF1 plasmid DNA, in a final volume of 50 µl, and incubated at 30 °C for 75 minutes. Luciferase T7 control DNA was used as a positive control. Protein concentration was analysed against BSA standards on a tris-bicine polyacrylamide gel followed by staining with Coomassie blue (acetic acid (10 % v/v), methanol, (45 % v/v) and H_2O (45 % v/v) and 0.25 g Brilliant Blue G (27815, Sigma)) for 30 minutes on rocker at room temperature. Gel was then destained (acetic acid (10 % v/v), methanol, (45 % v/v) and H_2O (45 % v/v)) for 1 hour. Fresh destain was then added overnight.

2.14 Histone pulldowns

Lyophilised recombinant biotinylated histone H3 (31296, Active Motif) and histone H3K4me3 (Expressed Protein Ligation) (31282, Active Motif) were resuspended at 1 µg/µl in 25 mM Tris pH 7.5, 150 mM NaCl, 5 % glycerol. Two hundred nanograms of *in vitro* translated protein or HEK-29 cell lysate were mixed with 1 µg of recombinant histones in binding buffer (20 mM Tris pH 7.5, 150 mM KCl, 300 mM sucrose, 1 mM $MgCl_2$ and protease inhibitor cocktail) and rotated at 4 °C for 3 hours. Protein complexes were isolated via binding to streptavidin agarose beads (S1638, Sigma-Aldrich) and washed in binding buffer with 0.1 % Triton x-100. Samples were then analysed by western blotting as described above.

2.15 RNA-sequencing

HeLa Kyoto iCas9 cells expressing SETD1A gRNA #4 were transfected with control siRNA, ATM siRNA or BRCA1 siRNA as described above. Cas9 expression was induced with 1 µg/ml doxycycline for 48 hours, and cells were pelleted as above. Total RNA was extracted from cell pellets using a RNeasy kit (74104, Qiagen) with on-column DNase digestion (79254, Qiagen). RNA quality was confirmed using TapeStation (Agilent Technologies). mRNA was isolated using an NEBNext Poly(A) mRNA magnetic isolation module (E7490, New England Biolabs) and sequencing libraries were created using NEBNext Ultra II directional RNA library prep kit for Illumina (E7760, New England Biolabs). DNA libraries were validated with TapeStation (Agilent Technologies) and quantified using Qubit® 2.0 Fluorometer (Thermo Fisher Scientific). Libraries were pooled and sequenced on the Illumina NovaSeq 6000, and the resulting data was analysed by workflows on Galaxy https://usegalaxy.eu/ (Afgan *et al.*, 2018). RNA sequencing data can be accessed via

the NCBI Gene Expression Omnibus (GEO) using the accession number GSE271430.

2.16 Real-time quantitative polymerase chain reaction (RT-qPCR)

After cell lysis and RNA extraction as above, cDNA was synthesised from RNA using the High-Capacity cDNA Reverse Transcriptase kit (4368814, Applied Biosystems). Two micrograms of RNA was used per reverse transcriptase reaction. RNA was then quantified using NanoDrop Lite Spectrophotometer (Thermo Fisher Scientific).

For validation of RNA-sequencing data cDNA fragments were quantified using a custom TaqMan gene expression array (Applied Biosystems) (**Table 2.4**). Each reaction included 10 µl of cDNA and 10 µl of TaqMan™ Fast Advanced Master Mix (4444556, Applied Biosystems), and RT-qPCR was performed on a QuantStudio 5 PCR system (Thermos Fisher Scientific). Analysis was carried out of five independent biological repeats.

For other qPCR analysis, cDNA fragments were quantified using TaqMan gene expression assays (Applied Biosystems) (**Table 2.5**) using 2 µl cDNA, 1 µl TaqMan gene expression assay, 10 µl TaqMan™ Fast Advanced Master Mix and 7 µl nuclease-free water. RT-qPCR was performed as above, and data was obtained from three independent biological repeats. PCR conditions in all cases were as follows: UNG incubation at 50 °C for 2 minutes, followed by enzyme activation at 95 °C for 2 minutes, followed by 40 cycles of 95 °C for 1 second and 60 °C for 20 seconds. Quantification cycle (Cq) values were converted into relative quantities using the $2^{-\Delta\Delta Ct}$ method.

Table 2.4- Custom TaqMan gene expression array assay.

List of TaqMan probes and assays IDs used to validate RNA sequencing results by real-time quantitative polymerase chain reaction.

TaqMan probe	Assay ID
18s rRNA	Hs99999901_s1
GAPDH	Hs99999905_m1
HPRT	Hs99999909_m1
GUSB	Hs99999908_m1
BRCA1	Hs01556193_m1
ATM	Hs00175892_m1
SETD1A	Hs00322315_m1
TM2D3	Hs00365245_m1
C19orf54	Hs00418251_m1
TRMT1L	Hs00388276_m1
ITGAM	Hs00167304_m1
CHAC1	Hs00225520_m1
ACAD10	Hs00228886_m1
NLRX1	Hs04962648_m1
C22orf54	Hs00419781_m1
PTGR2	Hs01584044_m1
PEX10	Hs00538217_m1
TMEM143	Hs01553540_m1
C12orf66	Hs00329464_m1
OMA1	Hs00377028_m1
STX1B	Hs01041315_m1
CD180	Hs00194403_m1
EME1	Hs01103352_m1
RECQL5	Hs00696997_m1
ZFP41	Hs00403025_m1
ARL6IP6	Hs00611181_m1
IRF2BPL	Hs00766831_s1
LOC100287896	Hs01931732_s1
PEX12	Hs00704672_s1
DARS	Hs00154683_m1
PAAF1	Hs00228523_m1
RAD9B	Hs00332650_m1

Table 2.5-TaqMan gene expression assay IDs.

List of TaqMan probes and assays IDs used for real-time quantitative polymerase chain reactions.

TaqMan probe	Assay ID
GUSB	Hs00939627_m1
EME1	Hs01103352_m1
SETD1A	Hs00322315_m1
SETD1A	Hs00986930_m1

2.17 Cancer genomic data analysis

cBioPortal (https://www.cbioportal.org/) (Cerami *et al.*, 2012; Gao *et al.*, 2013) was used to access genomic data from TCGA lung adenocarcinoma, ovarian serous cystadenocarcinoma and METABRIC breast carcinoma datasets (Curtis *et al.*, 2012). In all cases, log2 mRNA expression of indicated genes was obtained from RNA sequencing datasets. Patients were stratified based on SETD1A mRNA expression using the following parameters: Low= homozygous SETD1A deletion or mRNA expression <=-2 standard deviations (SD) below mean; High= SETD1A mRNA expression >2 SD above mean. For Kaplan-Meir survival analysis ATM-, BRCA1- or BRCA2-deficient or -proficient cancer patients were selected (defined as homozygous deletion, mutation, or mRNA expression <=-2 SD below mean) and overall survival data obtained from cBioPortal. Patients were then stratified by low (bottom 50% mRNA expression) or high SETD1A (upper 50% mRNA expression) mRNA expression.

2.18 ChIP-sequencing data analysis

ChIP sequencing data of SETD1A from mouse embryonic stem cells was downloaded from the Gene Expression Omnibus (GEO: GSE93538) (Brown *et al.*,

2017). Reads were aligned to the mouse mm10 genome using Bowtie2 on the online Galaxy server (https://usegalaxy.eu/) (Afgan *et al.*, 2018). SETD1A peaks were called using EaSeq ChIP analysis software (https://easeq.net/) (Lerdrup *et al.*, 2016). Plots were created in IGV Genome Browser (Robinson *et al.*, 2011) for the selected genes.

2.19 Statistical analysis

Unless otherwise stated in figure legends, statistical differences were determined as follows. Statistical differences for radial chromosomes were determined by Kruskal-Wallis test with multiple comparisons. Clonogenic survival assays were analysed by two-way ANOVA. Kaplan-Meir survival plots were analysed by Log-rank Mantel-Cox text. Statistical differences for foci percentage, HR assays and immunoblot quantification, were determined by one-way ANOVA with post-hoc Tukey's test for multiple comparisons. For RNA-sequencing and qPCR validation, statistical differences were determined by a two-tailed Student's t-test. Statistical tests were performed using GraphPad Prism (GraphPad Software, LLC) and determined by comparison to control-treated samples unless otherwise stated. In all cases $*$ P =<0.05, $**$ P =<0.01, $***$ P=<0.001, **** P=<0.0001. Error bars represent standard deviation (SD) or standard error of the mean (SEM).

3. CHAPTER 3: LOSS OF SETD1A REDUCES OLAPARIB SENSITIVITY OF ATM-DEFICIENT CELLS

3.1 Introduction

Previous work demonstrated that loss of the lysine methyltransferase, SETD1A, decreased the sensitivity of BRCA1-deficient cells to the PARPi, olaparib. This was attributed to restoration of HR in the absence of SETD1A or upon perturbation of H3K4me, offering a potential new epigenetic mechanism of PARPi resistance (Bayley, Sweatman and Higgs, 2023).

However, there are multiple examples of HR-deficiency that drive synthetic lethality with PARPi; including alterations in BRCA2, RAD51 and ATM (McCabe *et al.*, 2006). For example, 80% of *ATM* mutated mCRPC patients responded to treatment with olaparib (Mateo *et al.*, 2015). Based on these findings olaparib was approved for mCRPC patients harbouring mutations in *ATM* or other DDR genes. These indications could be expanded in the future as loss of *ATM* sensitises a variety of other tumour types to PARPi, including haematological (Weston *et al.*, 2010), gastric (Kubota *et al.*, 2014), pancreatic (Perkhofer *et al.*, 2017) and lung (Schmitt *et al.*, 2017) cancer.

Despite the clinical approval and promising pre-clinical results, further clinical trials have shown variable sensitivity of ATM-deficient cells to PARPi, highlighting an urgent need to better understand mechanisms of PARPi resistance applicable to this genetic context. However, to date research into PARPi resistance mechanisms have focused on BRCA-deficiency. To gain further insights into PARPi resistance mechanisms relevant to ATM-deficiency, I assessed whether loss of the lysine

methyltransferase SETD1A could also convey PARPi resistance in the absence of ATM activity.

3.2 ATM inhibition or depletion reduces ATM kinase activity following exposure to ionising radiation

Firstly, I set out to investigate the effect of ATM silencing or inhibition on the HeLa cervical cancer cell line, before investigating response to PARPi. I transfected HeLa cells with control siRNA or those targeting ATM. Alternatively, cells were treated with 1 μM AZD0156 (a potent, selective inhibitor of ATM kinase (Riches *et al.*, 2019)) for 24 hours. Cells were then exposed to 3 Gy ionising radiation to induce DNA damage and harvested for immunostaining 8 hours post exposure. ATM activity was assessed through immunoblotting for downstream ATM phosphorylation targets in whole cell extracts.

AZD0156 treatment inhibited activation of ATM signalling following ionising radiation-induced DNA damage, highlighted by reduced phosphorylation of downstream ATM targets, including ATM-autophosphorylation, KAP1 and γH2AX. The reduced phosphoprotein expression was not due reduced expression of total protein (**Figs 3.1 A and B**). A similar decrease in the phosphorylation of downstream ATM targets was observed after ATM depletion using siRNA (**Figs 3.1 C and D**)**.** These results show that AZD0156 or siRNA transfection effectively reduce ATM-dependent DDR signalling.

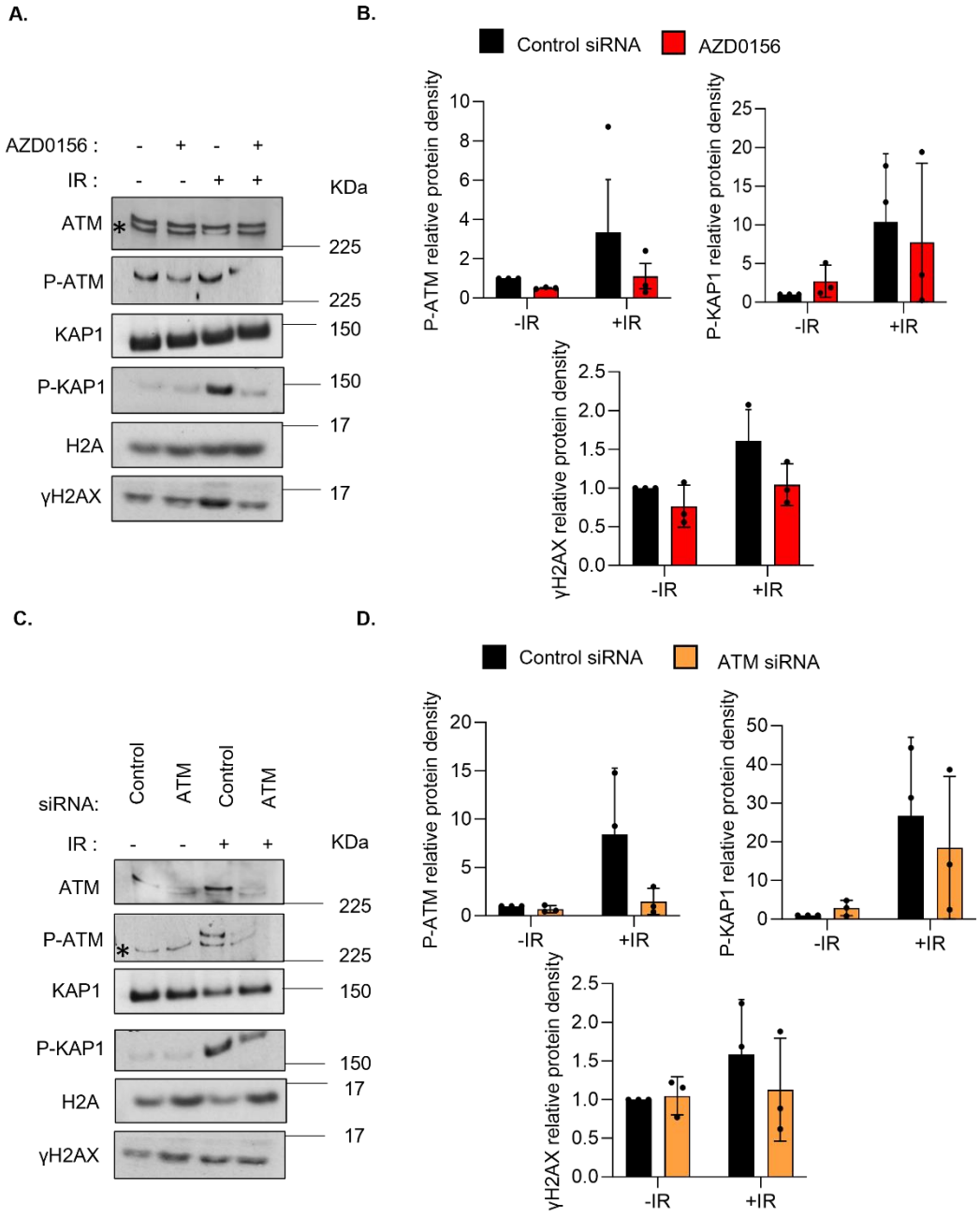

Figure 3.1- The effect of AZD0156 or ATM depletion on ATM-dependent DNA damage repair signalling following exposure to ionising radiation.

*(A.) HeLa cells were treated with ± 1 μM AZD0156 (C.) and/or indicated siRNAs and exposed to 3 Gy ionising radiation (IR). Whole cell lysates were harvested 8 hours post IR and immunoblotted with the indicated antibodies. *= nonspecific band. (B. and D.) Relative protein density of immunoblots quantified using ImageJ. All plots represent the mean ± SD from three independent biological repeats.*

3.3 SETD1A does not affect DNA damage induced ATM activation

A key step in the cellular response to DNA damage is ATM activation, illustrated by increased ATM-kinase activity following PARPi treatment (Aguilar-Quesada *et al.*, 2007). Therefore, I next assessed whether loss of SETD1A impacted ATM activation, following treatment with olaparib. HeLa cells were transfected with control or SETD1A siRNA and treated with 5 μM olaparib for 0-24 hours. ATM activity was assessed as described above.

As expected, SETD1A siRNA significantly decreased SETD1A protein expression. In addition, and in keeping with the role of ATM in the cellular response to PARPi treatment, ATM autophosphorylation and CHK1 phosphorylation incrementally increased over 24 hours of olaparib treatment. However, olaparib did not significantly impact PARP1 expression or the phosphorylation of H2AX or NBS1. In most cases, no additional changes were observed following SETD1A depletion (**Figs 3.2 A and B**). At 8 hours there was a slight decrease in the levels of phosphorylated ATM following loss of SETD1A compared to control cells, however this effect was lost after 24 hours of Olaparib treatment. This could indicate a slight delay in ATM autophosphorylation upon loss of SETD1A but this does not appear to have significant effects on downstream ATM signalling.

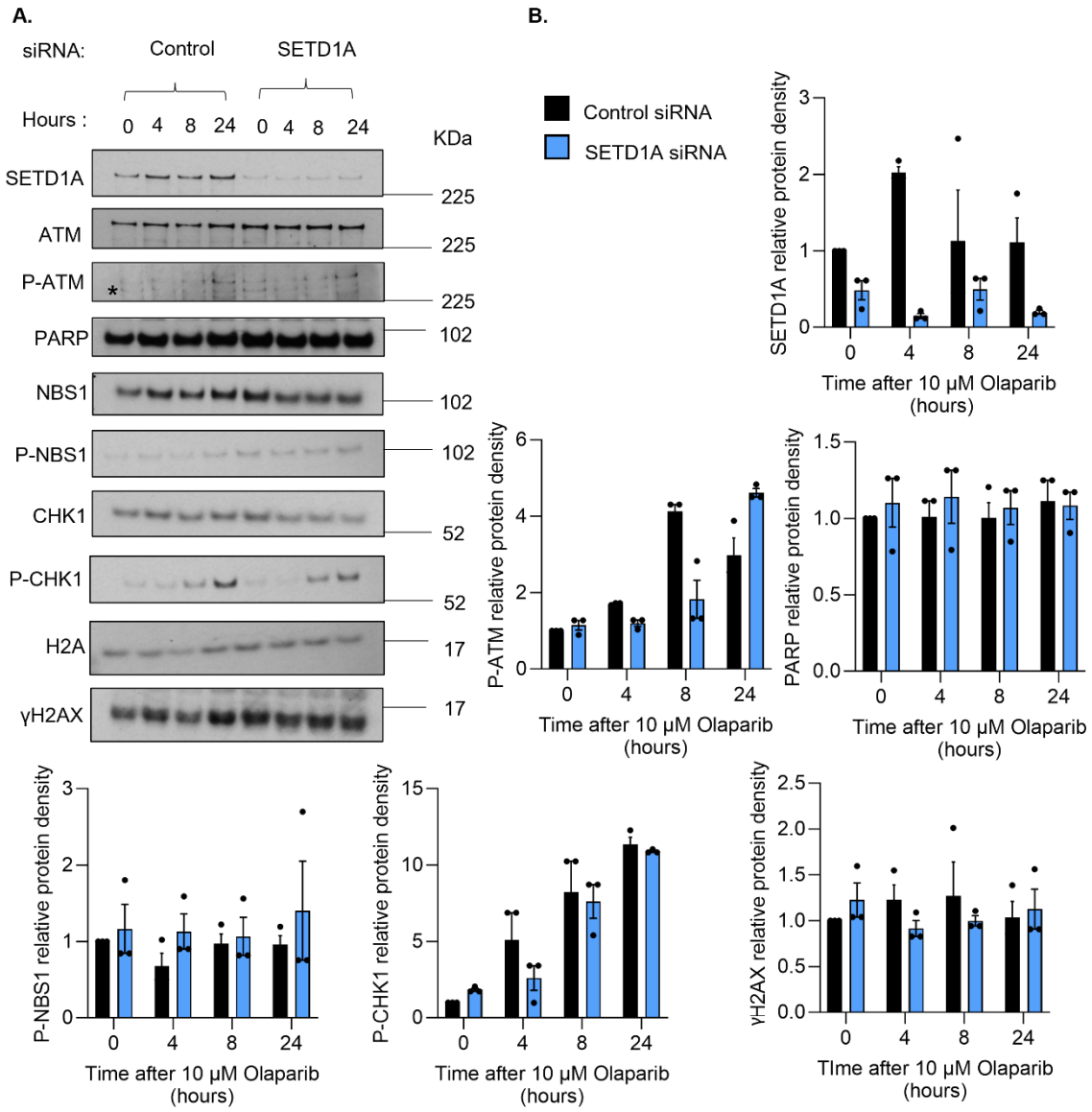

Figure 3.2- Loss of SETD1A does not affect ATM activation following PARP inhibition.

*HeLa cells were transfected with indicated siRNAs then exposed to 5 μM olaparib for indicated time(s). (A.) Whole cell lysates were immunoblotted using the indicated antibodies. *= nonspecific band. (B.) Relative protein densities of immunoblots quantified with ImageJ. All plots represent the mean ± SD from three independent biological repeats.*

3.4 SETD1A depletion reduces sensitivity of ATM-deficient cells to olaparib

Having confirmed ATM-kinase activity can be suppressed using AZD0156 and that loss of SETD1A does not affect ATM activation *per se*, I next set out to examine whether loss of SETD1A impacted sensitivity to PARP inhibitors in the absence of ATM activity. To this end, cells were depleted of SETD1A or treated ± 1 μM AZD0156 for 24 hours, and their sensitivity to olaparib was analysed using a clonogenic survival assay (**Fig. 3.3 A**).

As can be seen in (**Fig. 3.3 B**), siRNA knockdown of SETD1A was effective, as confirmed by western blot (**Fig. 3.3 B**). As previously observed (Bayley *et al.*, 2022), depletion of SETD1A alone induced minimal sensitivity to olaparib treatment. Furthermore, as expected, inhibition of ATM-kinase activity resulted in a significant increase in sensitivity to olaparib treatment. Whilst not statistically significant, co-depletion of SETD1A led to a 10% decrease in the sensitivity of ATM-inhibited cells to Olaparib (**Figs 3.3 C and D**). These results demonstrates that loss of SETD1A may reduce PARPi sensitivity in cells lacking ATM activity.

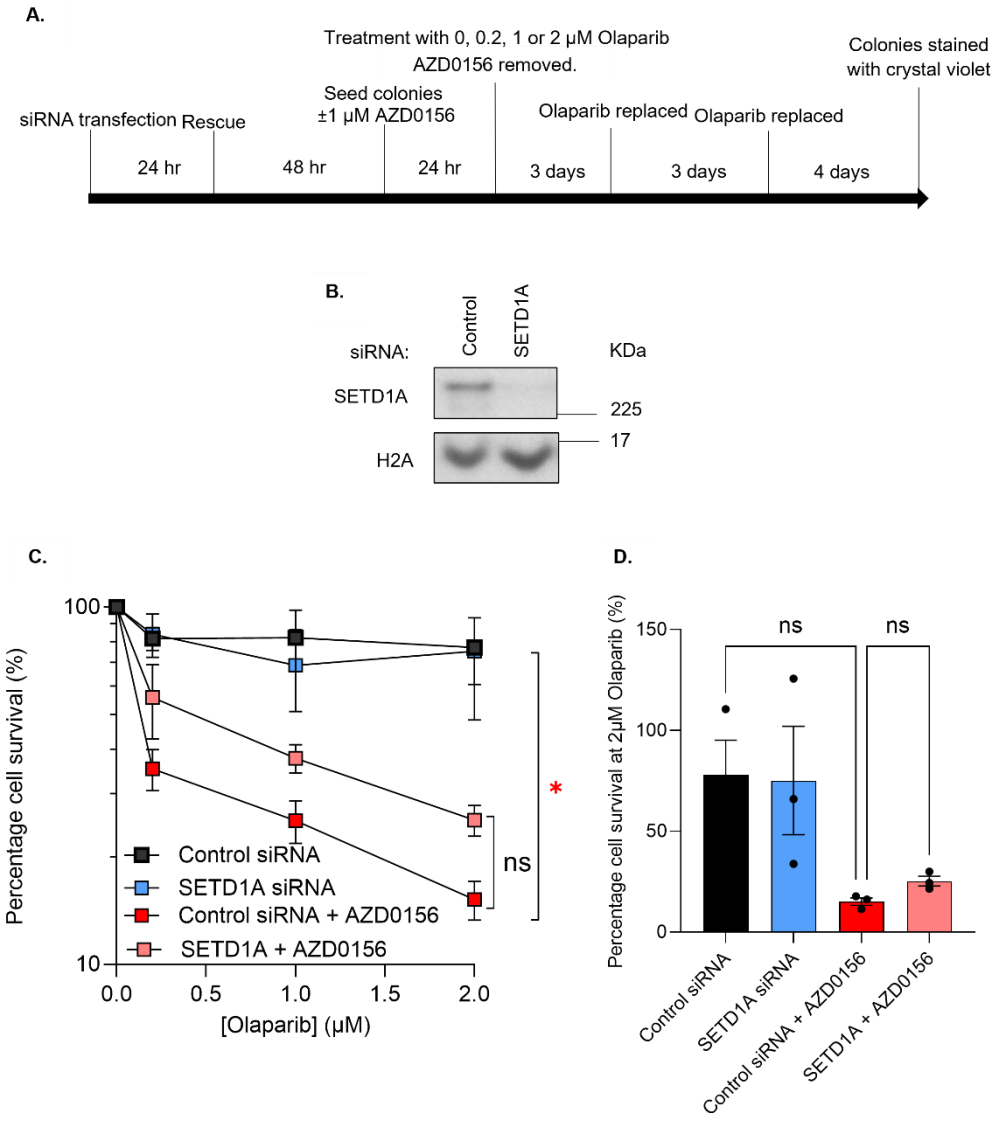

Figure 3.3- Loss of SETD1A reduces sensitivity of ATM-inhibited cells to olaparib treatment.

*(A.) Schematic of experimental time course. (B.) Whole cell extracts of HeLa cells treated with indicated siRNAs were immunoblotted with the indicated antibodies. (C.) Clonogenic survival of HeLa cells transfected with the indicated siRNAs ± 24-hour treatment with 1 μM of the ATM inhibitor AZD0156. Transfected HeLa cells were exposed to the indicated doses of olaparib for 10 days before staining with crystal violet and colonies counted. * = P <0.05 Control siRNA vs Control siRNA + AZD0156, ns= not significant Control siRNA + AZD0156 vs SETD1A siRNA + AZD015 as determined by a two-way ANOVA with post-hoc Tukey's test for multiple comparisons. (D.) Percentage cell survival from (C.) at 2 μM olaparib. Data points represent the mean ± SEM from three independent biological repeats. ns = not significant as determined by a one-way ANOVA with post-hoc Tukey's test for multiple comparisons.*

Although pharmacological inhibition of ATM with AZD0156 reduces ATM kinase activity, it does not decrease ATM expression; therefore, findings were confirmed using siRNA -mediated ATM knockdown. HeLa cells were transfected with control, SETD1A and/or ATM siRNAs, exposed to olaparib, and their survival assessed as above.

As before, depletion of ATM or SETD1A was confirmed by western blot (**Fig. 3.4 B**). As observed in previous experiments using ATM inhibitors, ATM knockdown also resulted in sensitivity to olaparib, although ATM knockdown did not induce as greater sensitivity compared to inhibition of kinase activity. In a similar manner to previous data, co-depletion of SETD1A reduced the sensitivity of ATM-deficient cells to olaparib treatment by ~20%, but this was not statistically significant (**Figs 3.4 C and D**). Together, these findings demonstrate that loss of SETD1A reduces sensitivity to PARPi treatment in ATM-deficient contexts.

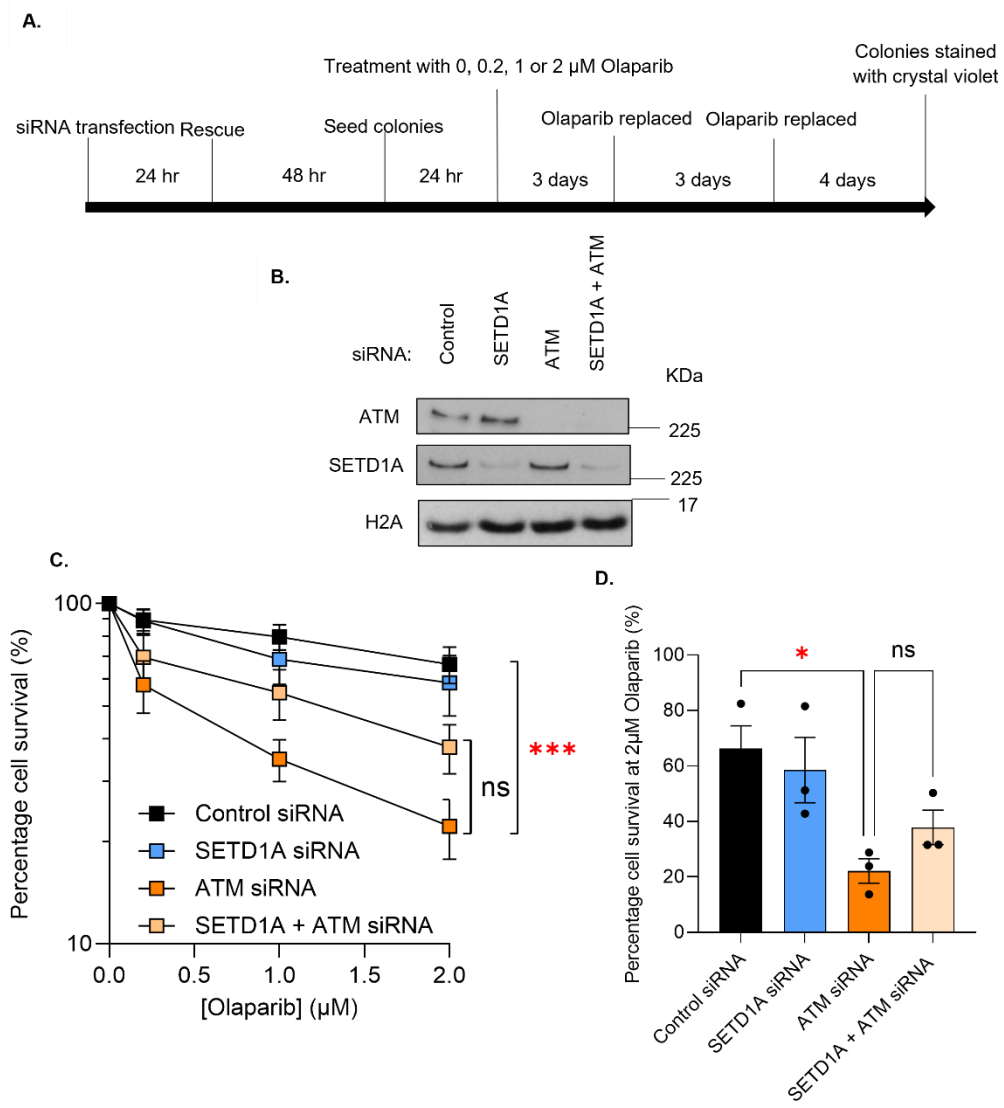

Figure 3.4- Loss of SETD1A reduces sensitivity of ATM depleted cells to olaparib treatment.

*(A.) Schematic of experimental time course. (B.) Whole cell extracts of HeLa cells treated with indicated siRNAs were immunoblotted with the indicated antibodies. (C.) Clonogenic survival curve for HeLa cells transfected with the indicated siRNAs. Transfected HeLa cells were exposed to the indicated doses of olaparib for 10 days before staining with crystal violet and colonies counted. ***= P < 0.001 Control siRNA vs ATM siRNA, ns= not significant ATM siRNA vs SETD1A siRNA + ATM siRNA as determined by a two-way ANOVA with post-hoc Tukey's test for multiple comparisons. (D.) Percentage cell survival from (C.) at 2 μM olaparib. Data points represent the mean ± SEM from three independent biological repeats. ns = not significant as determined by a one-way ANOVA with post-hoc Tukey's test for multiple comparisons.*

3.5 SETD1A depletion partially restores homologous recombination in ATM-deficient cells

A well characterised mechanism of PARPi resistance in HR-deficient cells is the BRCA1-independent restoration of HR. In BRCA1-deficient cells, loss of pro-NHEJ factors, such as 53BP1 (Escribano-Díaz *et al.*, 2013; Zimmermann *et al.*, 2013), RIF1 (Chapman *et al.*, 2013), REV7 and shieldin (Dev *et al.*, 2018; Noordermeer *et al.*, 2018; Xu *et al.*, 2015), can restore HR and confer PARPi resistance. Furthermore, in our earlier paper we showed that loss SETD1A could also restore HR in BRCA1-deficient cells (Bayley *et al.*, 2022). Therefore, I next investigated the effect of SETD1A loss on HR activity in ATM-deficient cells.

To examine this, I first assessed the formation of RAD51 foci as a surrogate marker of HR in cells lacking ATM and/or SETD1A. HeLa cells transfected with the appropriate siRNAs were seeded onto coverslips and treated with 5 μM olaparib ± 1 μM AZD0156 for 24 hours before being immunostained for RAD51. The number of cells expressing RAD51 foci were determined by immunofluorescence (**Fig. 3.5 A**).

As expected, inhibition or knockdown of ATM resulted in a defect in the formation of PARPi-induced RAD51 foci (most notable in ATM inhibited cells), although the defect was not as significant as that observed in BRCA1-deficient cells (Bayley *et al.*, 2022). Notably, co-depletion of SETD1A in ATM inhibited cells resulted in a significant increase in PARPi-induced RAD51 foci formation to levels comparable to control cells, suggesting that SETD1A depletion partially restores HR in ATM inhibited cells (**Figs 3.5 B and D**). A similar effect was observed in ATM knockdown cells however, this was not statistically significant (**Figs 3.5 C and E**).

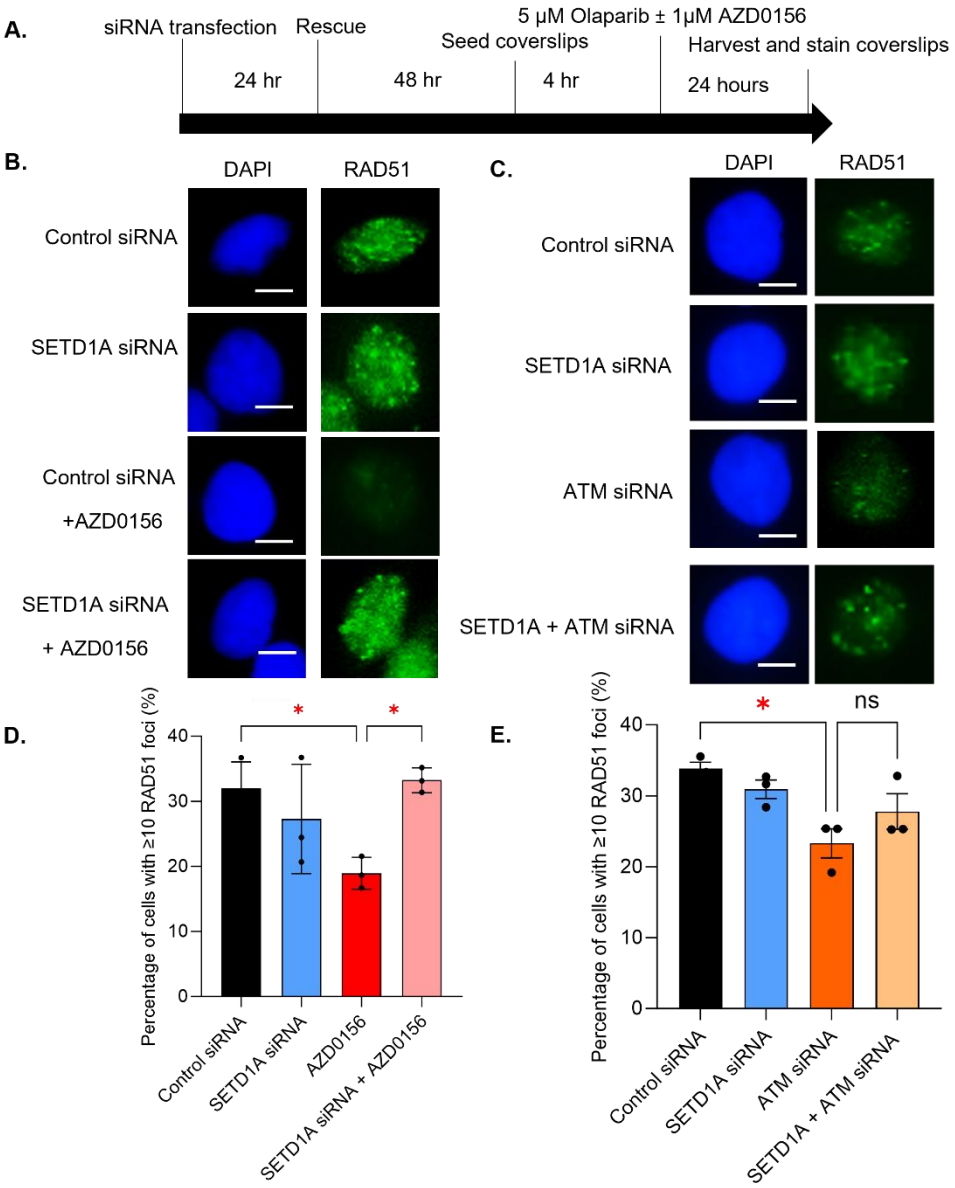

Figure 3.5- Loss of SETD1A restores RAD51 foci formation in ATM-deficient cells treated with olaparib.

*(C. and E.) HeLa cells were transfected with indicated siRNAs and exposed to 5 μM olaparib (B. and D.) ± 1 μM AZD0156 for 24 hours. Cells were immunostained for RAD51 foci and nuclei counterstained with DAPI. Foci formation was enumerated by fluorescent microscopy (A.). Schematic of experimental time course. (B. and C.) Representative immunofluorescent images (scale bar 10 μm). (D. and E.) Graphical representation of the percentage of cells with ≥ 10 RAD51 foci 24 hours post olaparib treatment. At least 100 cells were counted per condition. Results represent the mean ± SD from three biologically independent experiments. ns= not statistically significant, * = P < 0.05 as determined by a one-way ANOVA with post-hoc Tukey's test for multiple comparisons.*

These findings were also validated by directly measuring functional HR using a CRISPR-Cas9 based LMNA-HR assay (Pinder, Salsman and Dellaire, 2015). Briefly, this involves two plasmids: one encoding Cas9 and a gRNA to the *LMNA* gene, which induces site specific DSB formation, and a donor plasmid encoding a repair template with homology arms corresponding to regions of the LMNA gene flanked by a sequence for the monomeric green fluorescent protein, Clover. Cells undergoing functional HR, repair the DSB using the repair template, resulting in the incorporation of the fluorescent clover protein into the LMNA sequence and the appearance of green-fluorescent ringed nuclei (**Fig. 3.6 C**).

To assess HR levels, Hela cells were first transfected with control, SETD1A, ATM or BRCA1 siRNA ± 1 μM AZD0156, and then transfected with CRISPR-HR assay plasmids for 48 hours, before harvesting and processing for fluorescent microscopy (**Fig. 3.6 A**).

As expected, loss of BRCA1 or ATM knockdown/inhibition resulted in a significant decrease in the percentage of cells undergoing HR. Co-depletion of SETD1A in BRCA1- and ATM-deficient cells resulted in an increase in the percentage of cells undergoing HR (**Fig. 3.6 C**). However, this was not statistically significant, likely due to the variability seen between repeats. These findings provide further support to the notion that SETD1A depletion increases HR in BRCA1- and ATM-deficient cells.

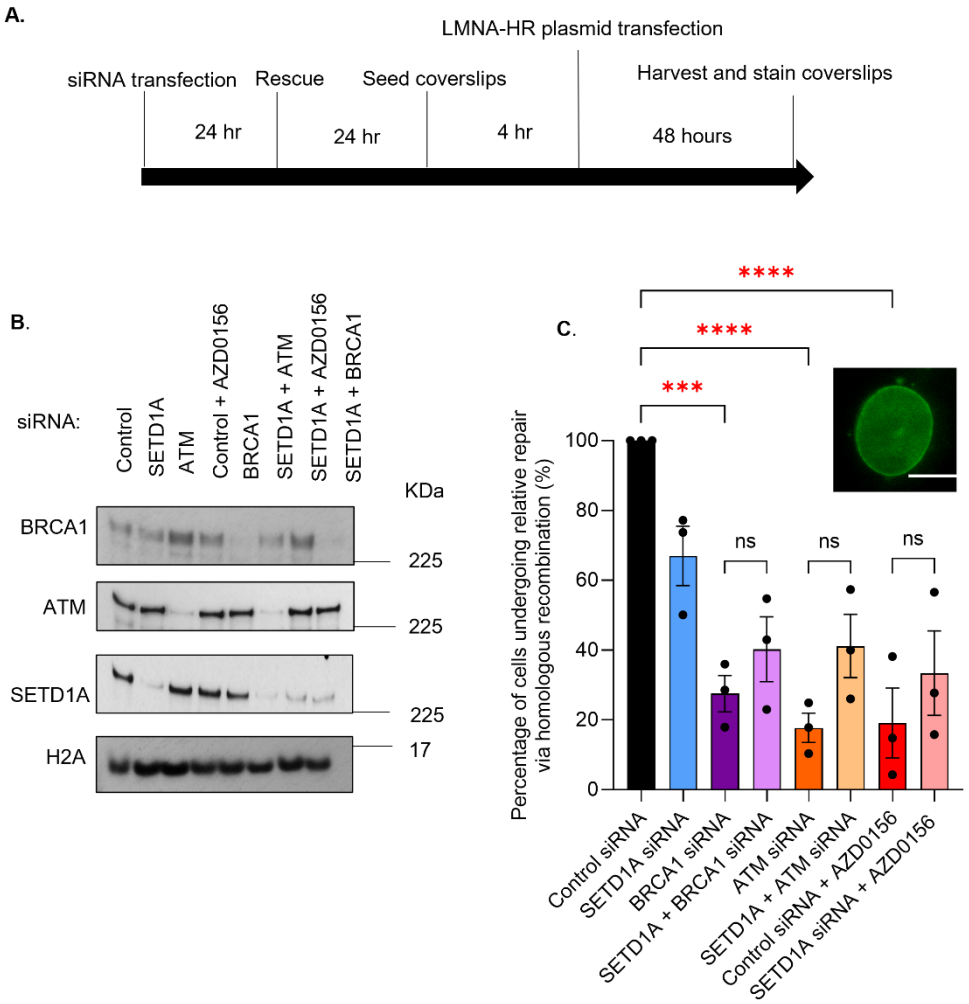

Figure 3.6- Loss of SETD1A increases HR in BRCA1- and ATM-deficient cells.

*HR was assessed using the CRISPR-Cas9 LMNA-HR system. HeLa cells were transfected with the indicated siRNAs ± 1 μM AZD0156 ATM inhibitor. Cells were later transfected with CRISPR-Cas9 HR plasmids encoding fluorescent nuclear Lamin A/C and a plasmid encoding red fluorescent protein (RFP). Relative percentage of cells expressing fluorescent Lamin and RFP were enumerated by fluorescent microscopy. (A.) Schematic representation of experimental time course. (B.) Whole cell extracts of HeLa cells treated with indicated siRNAs were immunoblotted with the indicated antibodies. (C.) The number of fluorescent Lamin expressing cells were normalised to RFP expression and is denoted in the graph as percentage relative repair by HR (inset illustrates a positive cell; scale bar 10 μm). At least 100 cells were counted per condition. Results represent the mean ± SEM from three biologically independent experiments. ***= P < 0.001, **** = P < 0.0001 as determined a one-way ANOVA with post-hoc Tukey test for multiple comparisons.*

3.6 SETD1A depletion decreases NHEJ-mediated radial formation in ATM-deficient cells

Olaparib-induced cell death in HR-deficient cells is driven by an increase in the formation of radial chromosomes, which is mediated by an increase in NHEJ (Patel, Sarkaria and Kaufmann, 2011). Given the role of SETD1A in regulating NHEJ-mediated DSB repair, I next assessed the effect of SETD1A depletion on radial chromosome formation in ATM- and BRCA1-deficient cells, using metaphase spreads. HeLa cells were transfected with indicated siRNAs ± 1 μM AZD0156 and radial chromosome formation was quantified in metaphase spreads (**Fig. 3.7 A**). As before, siRNA efficacy was confirmed by western blotting (**Fig. 3.7 B**).

Consistent with previous data, ATM- and BRCA1-deficient cells had significantly elevated numbers of chromosomal radials following olaparib treatment. Notably, this was significantly decreased upon co-depletion of SETD1A in both HR-deficient backgrounds (**Fig. 3.7 C**), providing further evidence that loss of SETD1A shifts DSB repair pathway usage from pro-NHEJ towards HR, restoring recombination in BRCA1- and ATM-deficient backgrounds.

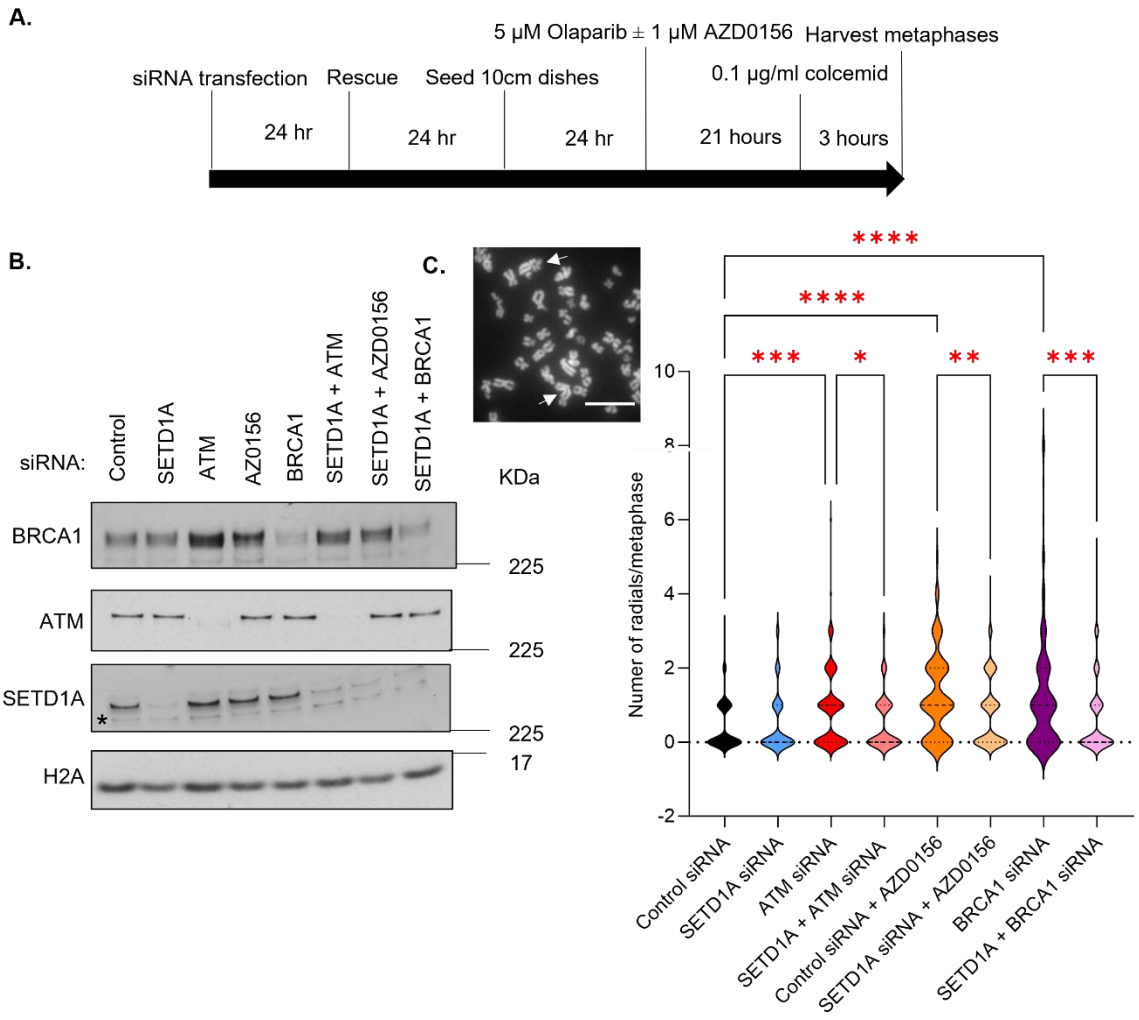

Figure 3.7- Loss of SETD1A decreases NHEJ-mediated radial formation in ATM- and BRCA1-deficient cells treated with olaparib.

*HeLa cells were transfected with the indicated siRNAs and treated with 5 μM olaparib for 24 hours ± 1 μM AZD0156. Radial chromosome formation was analysed in metaphase spreads by DAPI staining and light microscopy. (A.) Schematic of experimental time course (B.) Whole cell extracts of HeLa cells treated with indicated siRNAs were immunoblotted with the indicated antibodies. *= nonspecific antibody (C.) Graphical representation of number of radials/metaphases. At least 50 metaphases counted per condition (Scale bar 10μm). Data points represent mean ± SEM from three independent biological repeats. * = P < 0.05, ***= P < 0.001, **** = P < 0.0001 as determined by a Kruskal Wallis test with multiple comparisons.*

3.7 Perturbing H3K4 methylation reduces sensitivity of ATM-deficient cells to olaparib by partially restoring homologous recombination

SETD1A catalyses the mono-, di- and tri-methylation of lysine 4 of histone H3 (H3K4), which has important roles in protecting stalled RFs, regulating transcription and promoting DNA damage repair. In our previous paper we showed that perturbation of histone lysine methylation phenocopies loss of SETD1A in BRCA1-deficient cells (Bayley *et al.*, 2022). Therefore, one obvious question to answer is whether the lysine methyltransferase activity of SETD1A is involved in PARPi resistance in ATM-deficient contexts. To investigate this question, I used a HeLa cell line expressing either wild-type GFP-tagged histone H3 (H3-WT-GFP) or a lysine 4 to alanine mutant (H3-K4A-GFP), which perturbs methylation at lysine 4 (Higgs *et al.*, 2018; Sato *et al.*, 2012). These cells were transfected with control or ATM siRNA, and the cellular response to olaparib was examined by clonogenic survival assay (**Fig. 3.8 A**). As with previous experiments, efficient knockdown of ATM using siRNA was confirmed by western blot (**Fig. 3.8 B**).

As observed previously, H3-K4A-GFP cells displayed limited sensitivity to olaparib treatment. H3-WT-GFP cells showed a slight increase in PARPi sensitivity at the highest PARPi concentration but not to the same degree as ATM knockdown, which significantly sensitised H3-WT-GFP cells to olaparib treatment. On the other hand, knockdown of ATM in the H3-K4A-GFP cells phenocopied loss of SETD1A and conferred an increase in cellular survival following olaparib treatment (**Figs 3.8 C and D**). These findings demonstrate that loss of H3K4me3, which is catalysed by SETD1A, also influences PARPi sensitivity in ATM-deficient cells, suggesting SETD1A-induced PARPi resistance is dependent upon the histone lysine

methyltransferase activities of SETD1A, highlighting the importance of epigenetic mechanisms in the cellular response to PARP inhibition.

Next, I investigated whether changes in SETD1A-mediated histone methylation also underpinned HR restoration in ATM-deficient cells following loss of SETD1A. As before, I analysed RAD51 foci formation as a surrogate marker for HR (**Fig. 3.9 A**). In agreement with my previous findings, loss of ATM from H3-WT-GFP cells significantly reduced RAD51 foci formation, indicating compromised HR. Furthermore, loss of H3K4me3 through expression of the K4A mutant increased RAD51 foci formation, and thus HR in ATM-deficient cells following 5 μM olaparib treatment (**Figs 3.9 B and C**). These findings support the hypothesis that loss of SETD1A reduces the sensitivity of ATM-deficient cells to PARPi through restoration of HR because of reduced histone methylation.

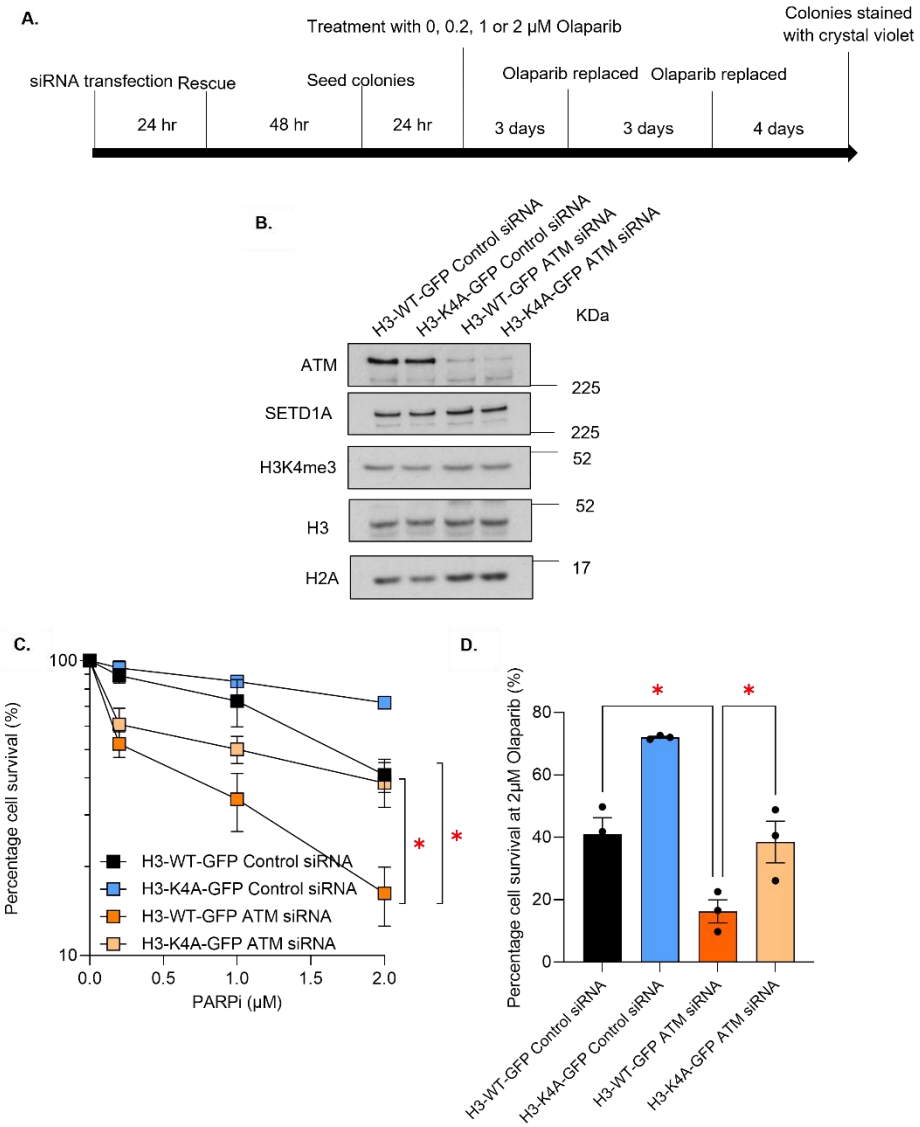

Figure 3.8- Loss of H3 lysine 4 tri-methylation reduces sensitivity of ATM depleted cells to olaparib treatment.

*H3-WT-GFP or H3-K4A-GFP cells were transfected with the indicated siRNAs. Transfected cells were exposed to the indicated doses of olaparib for 10 days, before staining with crystal violet and colonies counted. (A.) Schematic of experimental time course. (B.) Whole cell extracts of H3-WT-GFP and H3-K4A-GFP cells treated with indicated siRNAs were immunoblotted with the indicated antibodies. (C.) Clonogenic survival curve *= P < 0.05 H3-WT-GFP Control siRNA vs H3-WT-GFP ATM siRNA and H3-K4A-GFP ATM siRNA vs H3-WT-GFP ATM siRNA as determined by a two-way ANOVA with post-hoc Tukey's test for multiple comparisons. (D.) Percentage cell survival from (C.) at 2 μM olaparib. Data points represent the mean ± SEM from three independent biological repeats. * = P < 0.05 as determined by a one-way ANOVA with post-hoc Tukey's test for multiple comparisons.*

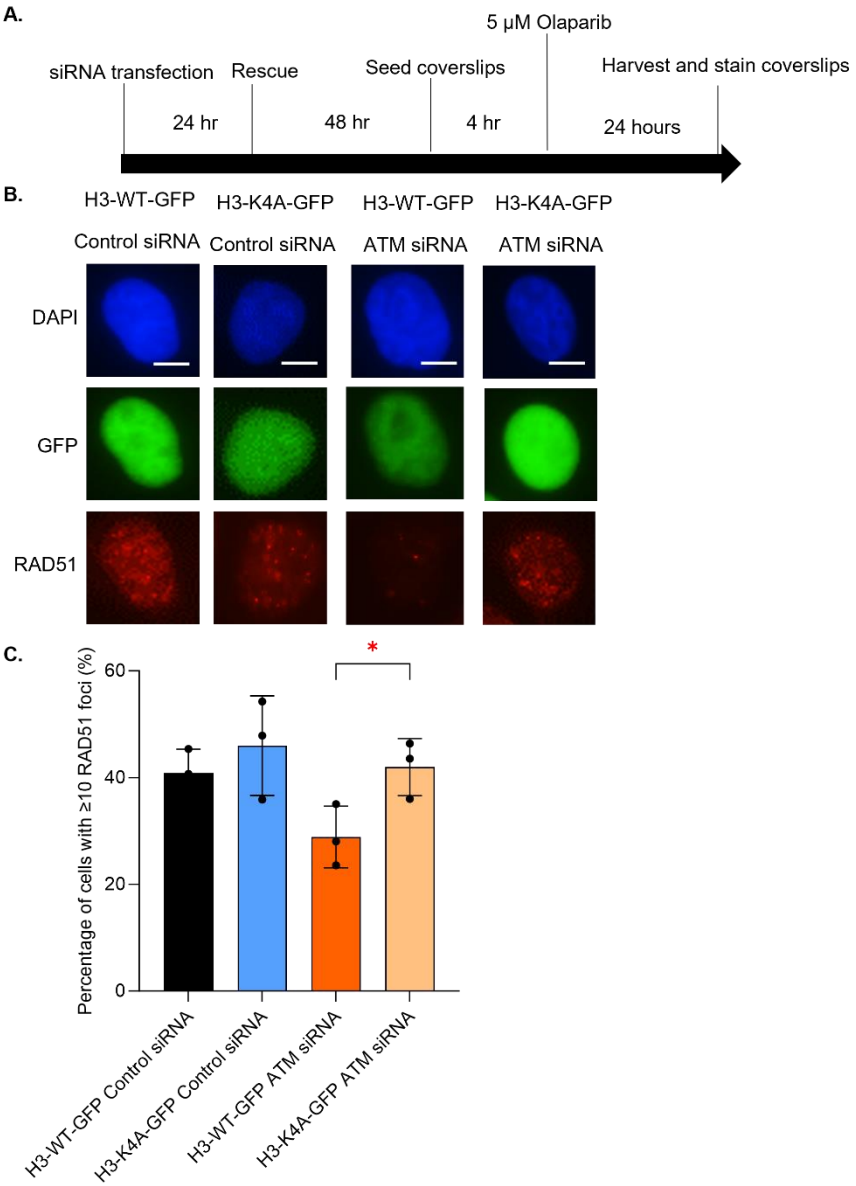

Figure 3.9- Loss of H3 lysine 4 tri-methylation restores RAD51 foci formation in ATM depleted cells treated with olaparib.

*H3-WT-GFP or H3-K4A-GFP cells were transfected with indicated siRNAs and exposed to 5 μM olaparib for 24 hours. Cells were immunostained for RAD51 foci and nuclei were counterstained with DAPI. Foci formation was enumerated by fluorescent microscopy (A.) Schematic of experimental time course. (B.) Representative immunofluorescent images (scale bar 10 μm) (C.) Graphical representation of the percentage of cells with ≥10 RAD51 foci 24 hours post olaparib treatment. At least 100 cells were counted per condition. Results represent the mean ± SD from three biologically independent experiments. * = P < 0.05 as determined by a one-way ANOVA with post-hoc Tukey's test for multiple comparisons.*

Finally, I assessed whether SETD1A-mediated histone methylation regulated the balance between HR and NHEJ in ATM-deficient cells. To this end, I performed metaphase spreads to determine the effect of abrogating H3K4me3 on chromosomal radial formation in ATM-deficient cells following olaparib treatment (**Fig. 3.10 A**). Consistent with my previous findings, loss of ATM in H3-WT-GFP cells significantly increased radial formation following olaparib treatment. On the other hand, expression of the K4A mutant significantly reduced olaparib-induced radial formation in ATM-deficient cells, indicative of decreased genomic instability and reduced cell death (**Fig. 3.10 C**). Taken together these findings highlight the key role of histone lysine methylation in mediating the cellular response to olaparib treatment in ATM-deficient cells. In summary, SETD1A influences PARPi sensitivity in ATM-deficient cells through restoring HR via a mechanism dependent on its H3K4 methyltransferase activity.

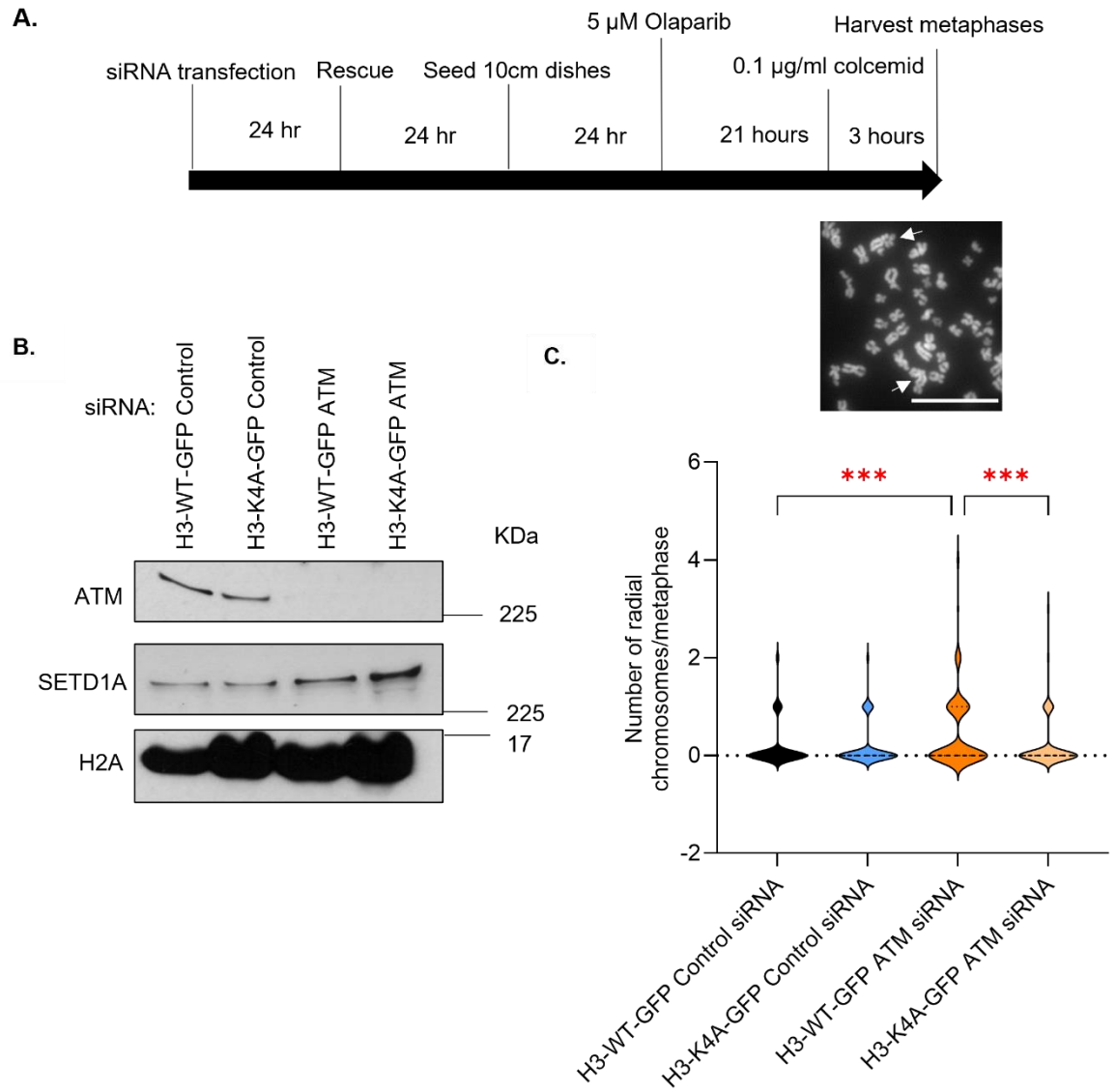

Figure 3.10- Loss of H3 lysine 4 tri-methylation decreases NHEJ-mediated radial formation in ATM depleted cells treated with olaparib.

*H3K4-WT-GFP or H3K4A-GFP cells were transfected with the indicated siRNAs and treated with 5 μM olaparib for 24 hours. Radial chromosome formation was analysed by DAPI staining and light microscopy. (A.) Schematic of experimental time course. (B.) Whole cell extracts of HeLa cells treated with indicated siRNAs were immunoblotted with the indicated antibodies. (C.) Graphical representation of number of radials/metaphases. At least 50 metaphases counted per condition (scale bar 10 μm). Data points represent mean ± SEM from three independent biological repeats. ***= P < 0.001, as determined by a Kruskal-Wallis test with multiple comparisons.*

3.8 Developing a RBBP2 overexpressing cell line

Lysine methylation is dynamic, and the methylation marks deposited by SETD1A are removed by the lysine specific demethylase enzyme, KDM5A, also known as, RBBP2 (Klose *et al.*, 2007). Overexpression of RBBP2 abrogates H3K4me, thus phenocopying loss of SETD1A or expression of the H3-K4A-GFP mutant cell line. To further validate my findings that SETD1A-induced PARPi resistance is dependent on H3K4me3, I aimed to repeat previous clonogenic survival and RAD51 experiments using a RBBP2 overexpressing cell line.

I generated a stable mammalian cell line with tetracycline inducible expression of FLAG-RBBP2 or a FLAG-RBBP2-H483A mutant using the U-2-OS Flp-In™ T-Rex system. RBBP2 overexpression was induced following 48-hour doxycycline treatment and confirmed by western blotting of whole cell lysates. As seen in (**Fig. 3.11 A**), doxycycline treatment induced FLAG expression in the FLAG-RBBP2 and -H483A cell lines, but not the parental cell line. Despite this, however, an increase in RBBP2 protein expression was not detected. Furthermore, in contradiction to the anticipated phenotype, induction of FLAG-RBBP2 lysine demethylase overexpression unexpectedly increased H3K4me3 (**Fig. 3.11 A**).

Next, I attempted to isolate the overexpressed FLAG-tagged RBBP2 proteins by performing a FLAG-tag immunoprecipitation, followed by western blotting for RBBP2. Following 48 hours doxycycline treatment the FLAG-tag was successfully immunoprecipitated in the RBBP2 WT and H483A cell line, whilst being absent from the un-transfected parental cell line. However, as before, RBBP2 protein expression was not detected in the immunoprecipitations of either cell line (**Fig. 3.11 B**).

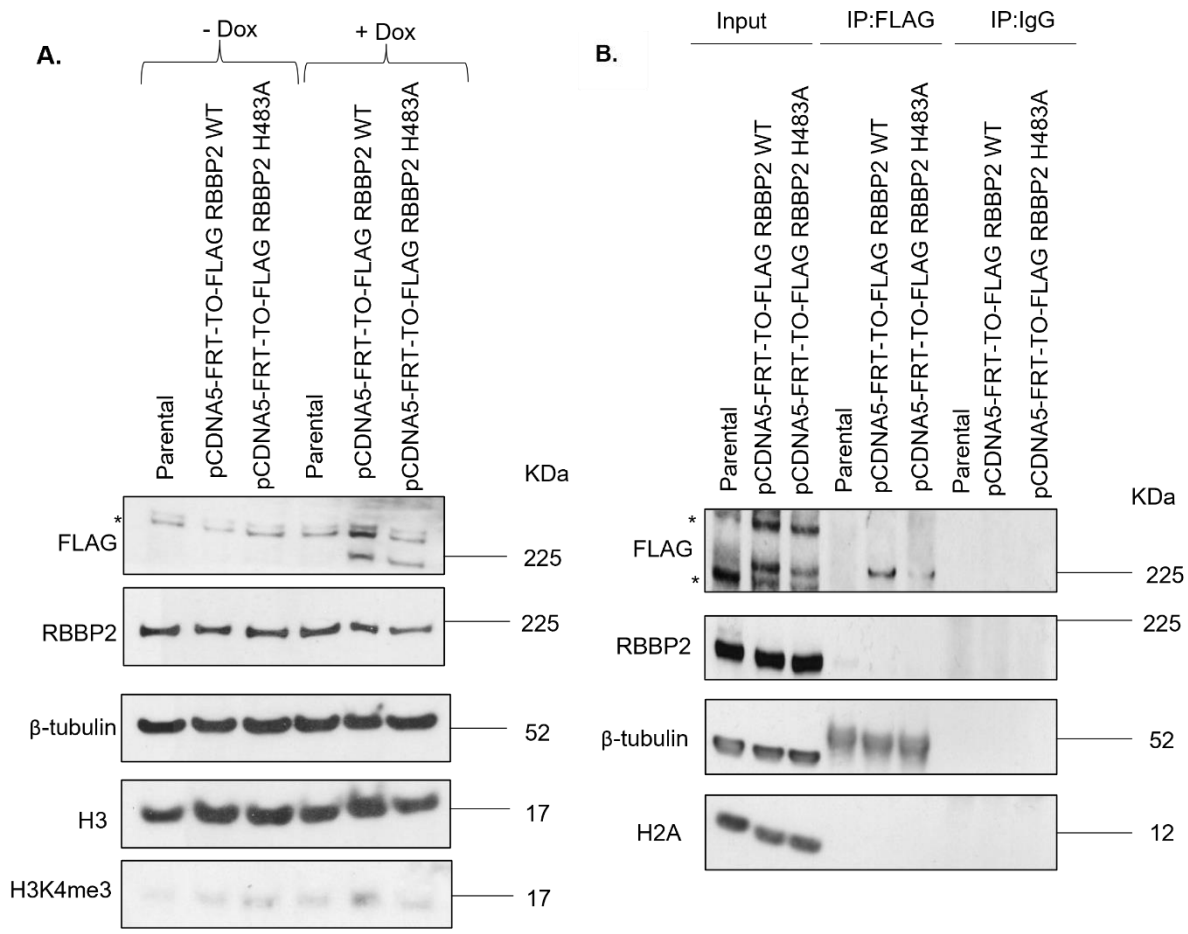

Figure 3.11- RBBP2 U-2-OS Flp-In T-Rex cell lines do not overexpress RBBP2 protein.

*Parental, RBBP2 wild-type (WT) or RBBP2 H483A mutant U-2-OS Flp-In T-Rex cell lines were treated doxycycline for 48 hours to induce transgene expression. (A.) Whole cell lysates were immunoblotted using the indicated antibodies. (B.) Immunoblot of FLAG/IgG immunoprecipitation using the indicated antibodies. *= nonspecific band.*

3.9 RIF1 associates with methylated H3K4 via N-terminal HEAT repeats

Together with previous findings, I have now shown loss of SETD1A, or associated H3K4me3 reduces the sensitivity of both BRCA1- and ATM-deficient cells to PARPi treatment, by increasing HR. It was previously shown that SETD1A mediates HR by regulating the recruitment of the downstream 53BP1 effector protein, RIF1, to the chromatin at DSBs, via H3K4me3. Mechanistically, loss of SETD1A can induce HR restoration and subsequent PARPi resistance by reducing the recruitment of RIF1 to DSBs, promoting inappropriate DNA end-resection (Bayley *et al.*, 2022).

Histone pulldown experiments using irradiated nuclear extracts suggested that RIF1 binds preferentially to methylated histone H3 (Bayley *et al.*, 2022). However, the presence of other interacting proteins facilitating RIF1 binding to H3K4me3 cannot be excluded. To further characterise whether the RIF1 recruitment to H3K4me3 occurs via a direct or indirect mechanism, I performed histone pulldown experiments with recombinant RIF1.

Recombinant RIF1 was produced using the cell-free TnT® Quick Coupled Transcription/Translation System (Promega). Firstly, I optimised the TnT protocol. As shown in **Fig. 3.12,** using the standard protocol, I failed to detect recombinant RIF1 protein expression by western blotting, despite expression of the luciferase positive control (**Fig. 3.12 A**). Following this, I increased plasmid concentration, volumes of the T7 enhancer (**Fig. 3.12 B**), and incubation temperature (**Fig. 3.12 C**). Notably, I found the addition of 1 µl of the T7 PCR enhancer successfully induced recombinant RIF1 expression, whereas, increasing the volume of T7 enhancer had no additional effect on the expression of recombinant RIF1 (**Fig. 3.12 B**). Furthermore, neither

decreasing the temperature, nor the addition of protease inhibitors, increased the yield of recombinant RIF1 (**Fig. 3.12 C**).

Having optimised the TnT reaction conditions, I bulked up the volume of recombinant RIF1 protein then performed a Coomassie staining to semi-quantify the concentration of RIF1 protein (**Fig. 3.12 D**).

Using the recombinant RIF1 produced from the TnT reaction I performed an *in vitro* histone pulldown assay to determine whether recombinant RIF1 directly interacts with methylated histone H3. Purified biotinylated histone H3 or H3K4me3 were incubated with recombinant RIF1, and pulldowns were analysed by immunoblotting for RIF1 and H3.

Recombinant RIF1 protein bound specifically to H3K4me3 in the cell free system, in the absence of any other factors. Furthermore, recombinant RIF1 did not interact with unmethylated histone H3 (**Fig. 3.13**). Together, these observations suggest a direct interaction between RIF1 and H3K4me3, with this interaction being dependent on the methylation status of the histone.

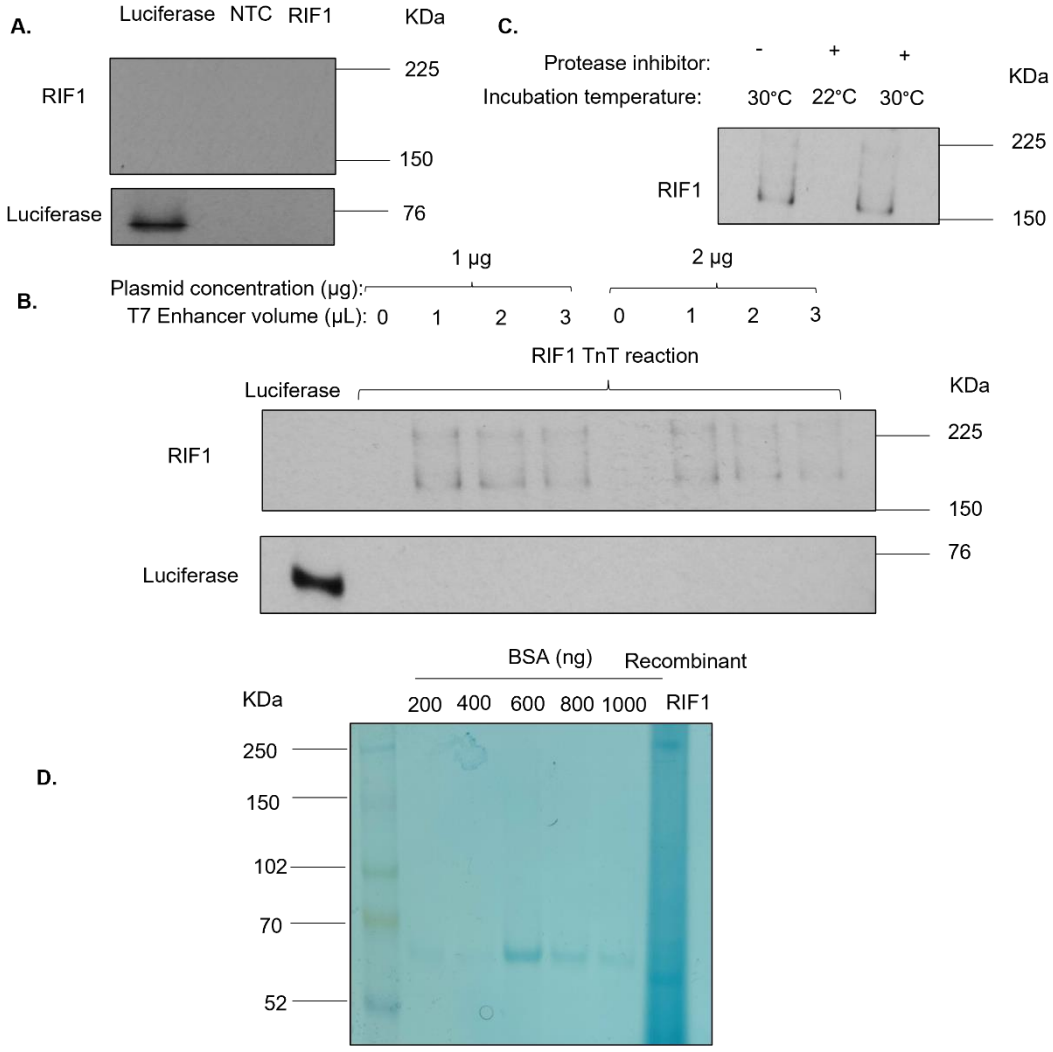

Figure 3.12- Optimisation of in vitro synthesis of recombinant RIF1 protein.

Full-length RIF1 protein was synthesised in vitro from the RIF1 pET-23a construct using the TNT® Quick Coupled Transcription/Translation System (Promega). Luciferase T7 control DNA and no template (NTC) were used for positive and negative controls, respectively. The standard TnT reaction comprised of 40 µl TNT ® Quick master mix, 1 µl 1 mM methionine, 1 µg plasmid DNA, made up to 50 µl with RNase free water. The reaction was incubated at 30 °C for 75 minutes. (A.) Western blot of Standard TnT® assay according to manufacturer's instructions. (B.) Western blot of TnT ® assay increasing plasmid concentration to 2 µg and addition of 0-3 µl of T7 enhancer. (C.) Western blot of TnT ® assay at 30 °C or 22 °C and addition of protease inhibitors. (D.) Recombinant RIF1 produced from TnT reaction was quantified using Coomassie staining compared to BSA standards (200-1000 ng).

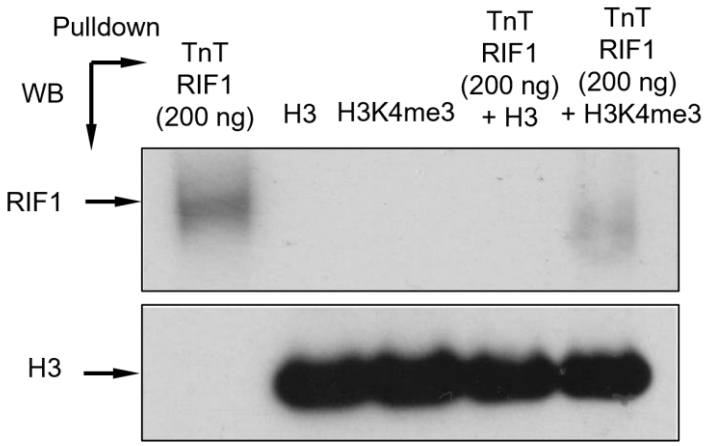

Figure 3.13- RIF1 directly associates with H3K4me3.

Full length recombinant RIF1 protein was synthesised in vitro from the RIF1 pET-23a construct using the TNT® Quick Coupled Transcription/Translation System (Promega). Recombinant RIF1 was incubated with purified biotinylated histone H3 or H3K4me3 and analysed by immunoblotting for RIF1 and H3. Data represents three independent experiments.

Having confirmed that RIF1 directly interacts with H3K4me3, I further investigated the nature of this interaction by determining the key domains involved. RIF1 contains two distinct regions: an N-terminal domain (AA 1-967), containing α helical HEAT (Huntingtin, Elongation factor 3, A subunit of protein phosphatase 2A and TOR) repeat domains, and a C-terminal domain (AA 2170-2446), which promotes RIF1 oligomerisation and interaction with the BLM helicase (Kobayashi *et al.*, 2019) (**Fig. 3.14 A**).

RIF1 HEAT repeats have been shown to be required for localisation of RIF1 to chromatin in yeast (Kobayashi *et al.*, 2019) and the formation of IR-induced RIF1 foci at sites of DNA damage in mammalian cells (Escribano-Díaz *et al.*, 2013). In addition to this, HEAT repeats present in other proteins have been shown to be able to bind H3K4me3 (Yuen, Slaughter and Gerton, 2017). Therefore, I hypothesised that the HEAT repeat domains of RIF1 may mediate the interaction between RIF1 and H3K4me3 to facilitate its recruitment to the chromatin at sites of DNA damage.

Using Q5-site directed mutagenesis, I deleted AA 1-976 from the pET23a-RIF1 construct to remove the N-terminal HEAT domain and create the pET23a-RIF1-ΔHEAT construct (**Fig. 3.14 A**). Successful deletion of the HEAT repeat region of RIF1 was confirmed using colony PCR with primers spanning the HEAT repeat domain (RIF1 primers 4 and 8). PCR product size was confirmed by agarose gel electrophoresis. WT pET23a-RIF1 is predicted to produce a PCR product of approximately 2000 bp, whereas successful deletion of the HEAT repeat domains should not produce any PCR product using these primers. As expected, WT pET23a-RIF1 produced a PCR product of approximately 2000 bp, whilst all clones of pET23a-RIF1-ΔHEAT (excluding clone 8) produced no PCR product, suggestive of successful

deletion of the HEAT repeat domain (**Fig. 3.14 B**). I performed a second colony PCR as a positive control for RIF1 construct expression, using RIF1 primers 9 and 12. This reaction should result in a PCR product of approximately 1500 bp in both pET23a-RIF1 and pET23a-RIF1-ΔHEAT. All samples, excluding the no template control produced the expected PCR product fragment size (**Fig. 3.14 C**).

To further validate successful deletion of the HEAT repeat domains, I performed restriction digestion reactions on four successful pET23a-RIF1- ΔHEAT clones, using the Kpn1 and NotI restriction enzymes. Following digestion, WT pET23a-RIF1 should produce fragments of ~2804 bp and ~8187 bp, whereas pET23a-RIF1- ΔHEAT should produce fragments of ~2804 bp and ~5000 bp. Fragment sizes were confirmed by agarose gel electrophoresis. As expected, both WT pET23a-RIF1 and pET23a-RIF1- ΔHEAT produced one fragment of approximately 3000 bp and there was a clear decrease in the larger fragment size in pET23a-RIF1- ΔHEAT compared to pET23a-RIF1, further indicating successful deletion of the HEAT repeat domains (**Fig. 3.15**).

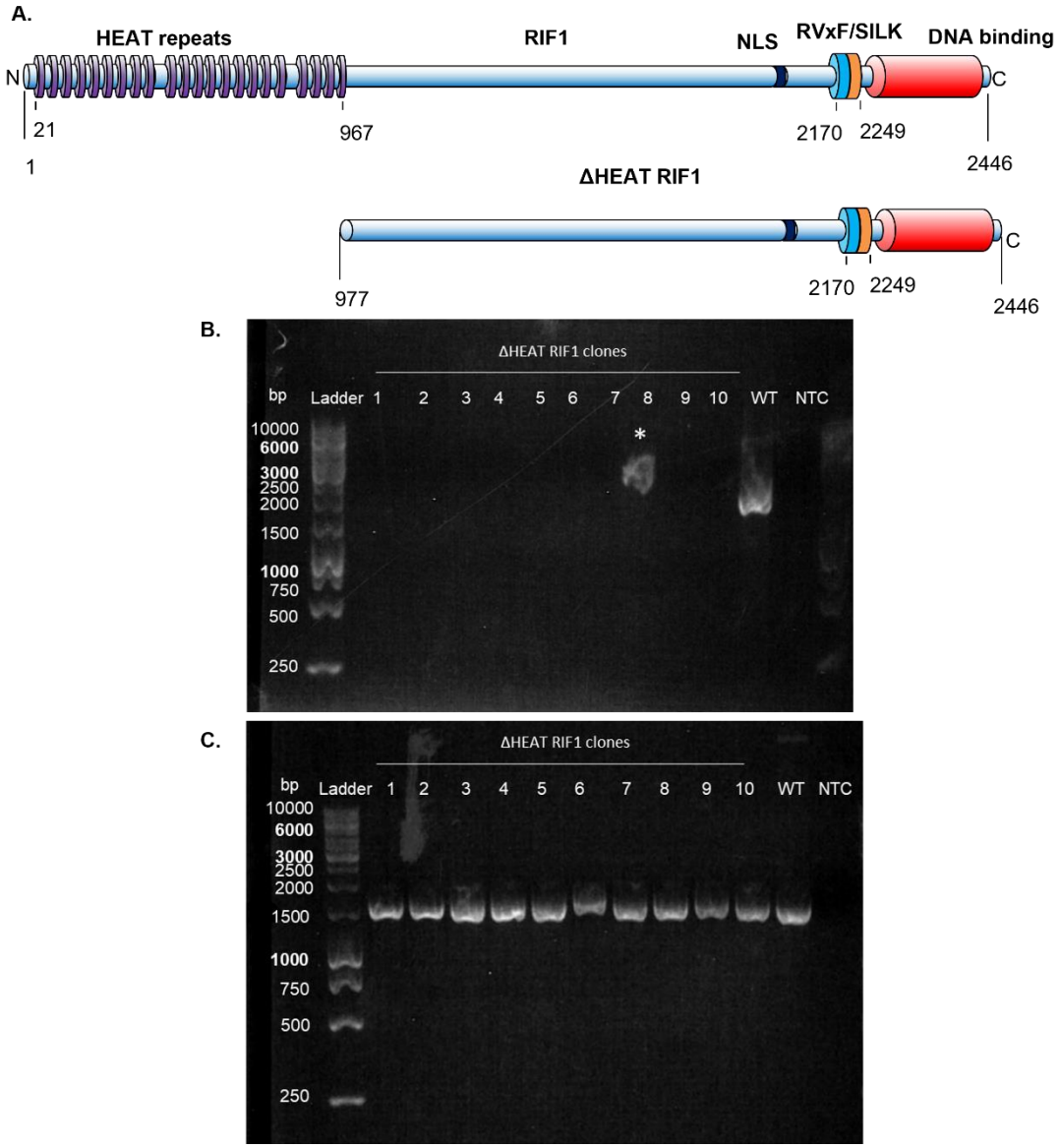

Figure 3.14- Colony PCR of pET23a-RIF1-ΔHEAT.

*pET23a-RIF1-ΔHEAT was created using the pET23a-RIF1 plasmid and site directed mutagenesis. (A.) Structure of full length and ΔHEAT RIF1. (B.) Transformed colonies were selected for colony PCR to confirm HEAT repeat deletion using RIF1 primers 4 and 8. (C.) RIF1 primers 9 and 12 were used a positive control for colony PCR. Clones 1-10 of pET23a-RIF1-ΔHEAT were compared to wild-type (WT) pET23a-RIF1 and a no template control (NTC). PCR products were analysed on a 1 % agarose gel with the 1 Kb gene rule ladder (Thermo Fisher Scientific). Gel ran at 100 V for 1.5 hours. *=unsuccessful HEAT repeat deletion.*

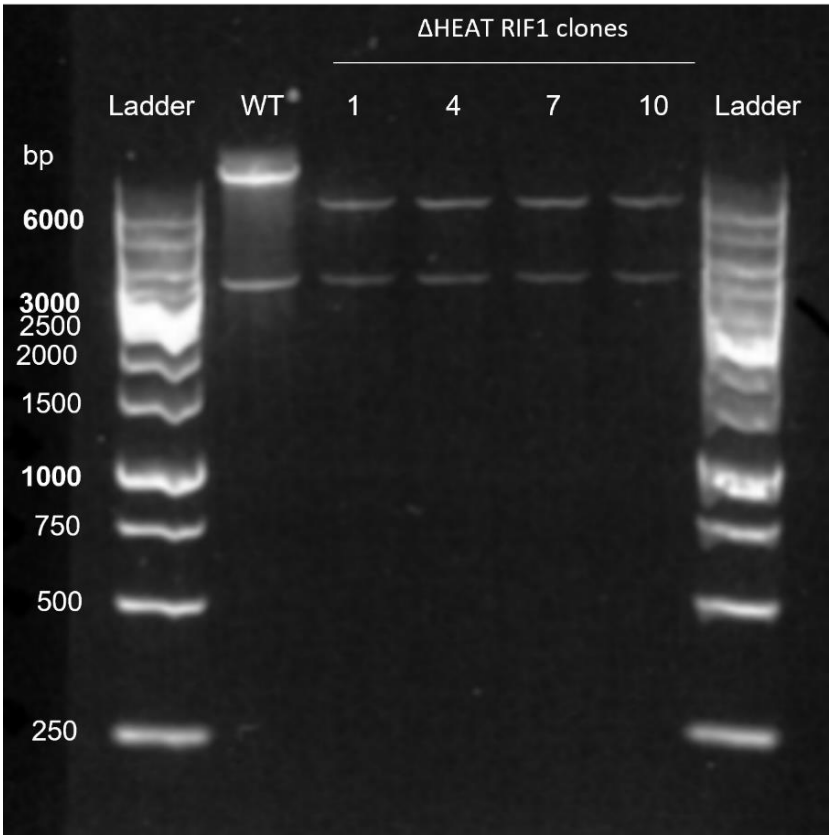

Figure 3.15- NotI and KpnI restriction digestion of pET23a-RIF1-ΔHEAT.

Four pET23a-RIF1-ΔHEAT clones produced by Q5 site-directed mutagenesis were validated using restriction digestion with KpnI and NotI. Restriction reactions were performed using cutsmart buffer (New England Biolabs) according to manufacturer's instructions. Restriction fragment size was confirmed by 0.8 % agarose gel electrophoresis compared to wild-type (WT) pET23a-RIF1 and 1Kb gene ruler ladder (Thermo Fisher Scientific).

Next, I produced recombinant ΔHEAT RIF1 protein using the pET23a-RIF1- ΔHEAT construct and the TnT reaction described above. To confirm whether the HEAT repeat domains of RIF1 mediate the interaction between RIF1 and H3K4me3 I performed a further histone pulldown experiment using full length and ΔHEAT RIF1 incubated with purified biotinylated histone H3K4me3. As hypothesised, full length RIF1 showed direct binding to H3K4me3 whereas, deletion of the N-terminal HEAT repeats of RIF1 abrogated this binding (**Fig. 3.16**).

Previous work from the lab further validated the role of the N-terminal HEAT repeat domains in mediating the interaction between RIF1 and H3K4me3. A sub region of the HEAT repeats (AA 1-411) was expressed in HEK-293 cells transfected with pCDNA5-FRT-T/O-GFP-RIF1 or pCDNA5-FRT-T/O-GFP-RIF1 1-411 (Bayley *et al.*, 2022) (**Fig. 3.17 A**). As before, full length RIF1 interacted with H3K4me3. Furthermore, expression of a sub-region (AA-1-411) of the HEAT repeat domains was sufficient to support the interaction between RIF1 and H3K4me3 in mammalian cells (**Fig 3.17. B**). This provides further evidence to support the role of H3K4me3 in recruiting RIF1 to the chromatin via interaction with the N-terminal HEAT repeat domain.

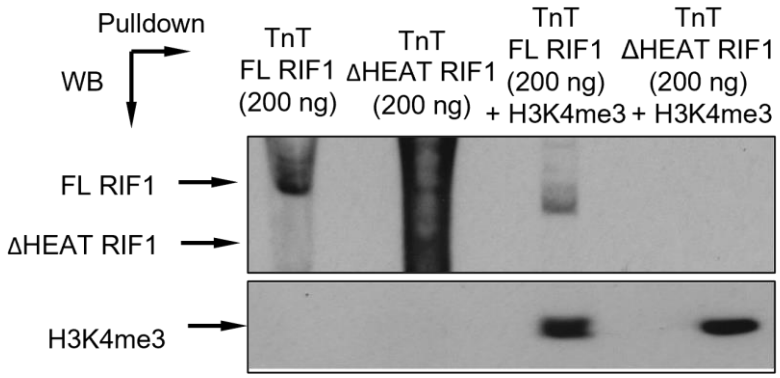

Figure 3.16- RIF1 directly binds to H3K4me3 through HEAT repeat domains.

Full length or ΔHEAT RIF1 recombinant protein was synthesised in vitro from the RIF1 pET23a or ΔHEAT RIF1 pET23a construct using the TNT® Quick Coupled Transcription/Translation System (Promega). Recombinant full length (FL) RIF1 or ΔHEAT RIF1 were incubated with purified biotinylated histone H3K4me3 and immunoblotted for RIF1 or H3K4me3. Data represents three independent experiments.

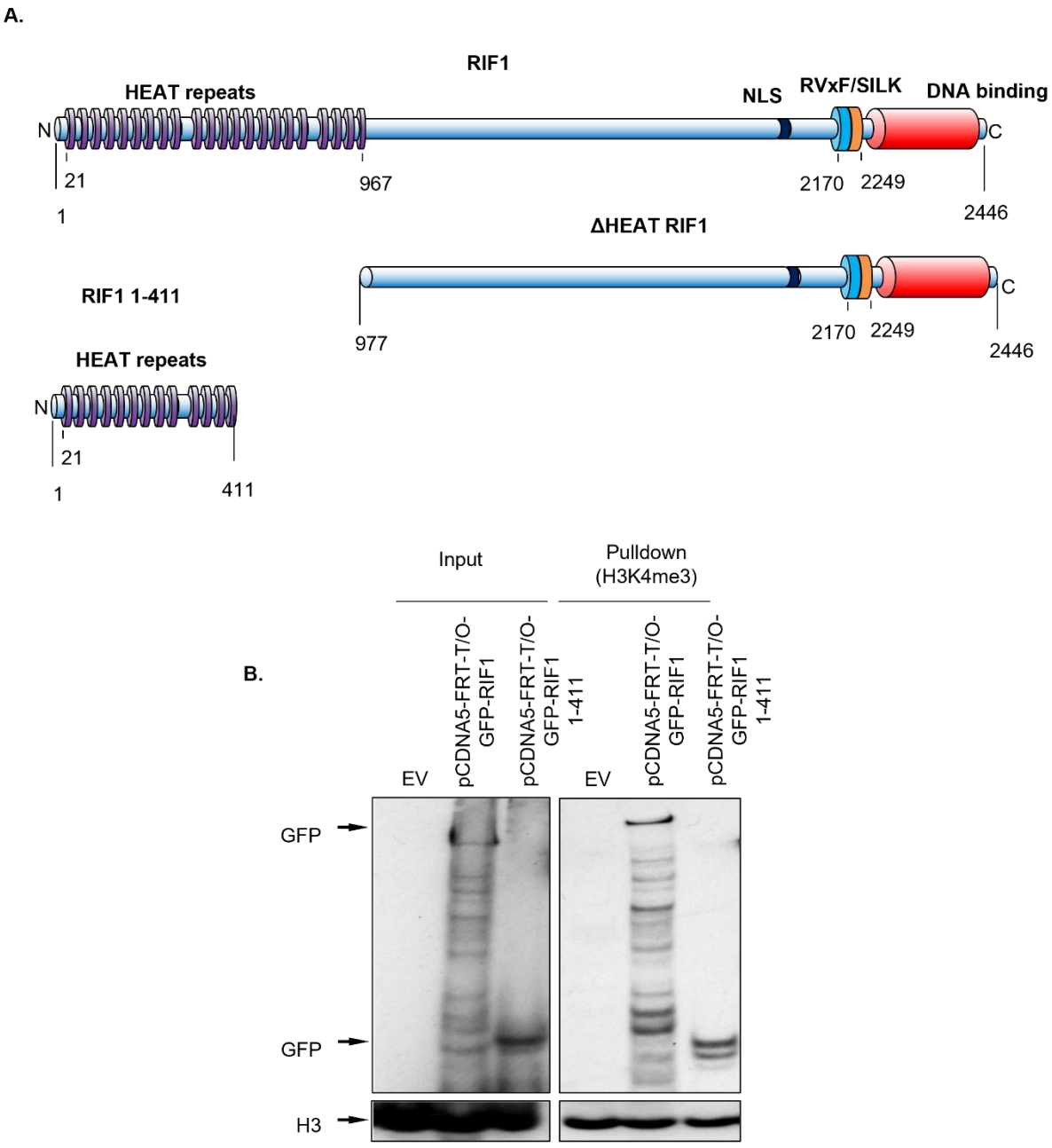

Figure 3.17- RIF1 1-411 associates with H3K4me3.

(A.) Schematic of full length, ΔHEAT and AA 1-411 RIF1 structure. (B.) HEK-293 cells were transfected with plasmids expressing the indicated RIF1 proteins, left for 48 h, and cell lysates incubated with purified biotinylated histones and analysed by immunoblotting. Data represents at least two independent experiments (Bayley et al., 2022).

3.10 Discussion

In this chapter, I aimed to improve our understanding of PARPi resistance mechanisms in genetic contexts beyond BRCA1-deficiency by expanding the relevance of loss of SETD1A a novel epigenetic mechanism of PARPi resistance to ATM-deficient cellular models.

3.10.1 The ATM inhibitor AZD0156 reduces ATM kinase activity

In line with numerous previous findings, inhibition of ATM activity by AZD0156 or ATM depletion sensitised HeLa cells to olaparib treatment, supporting the notion that ATM-deficiency correlates with PARPi sensitivity (Weston *et al.*, 2010; Williamson *et al.*, 2010). These findings provide further support for the rationale of targeting ATM-deficient tumours with PARP inhibition or using ATM inhibition to potentiate the effects of PARPi treatment.

Chemical inhibition of ATM resulted in a greater sensitisation to olaparib treatment compared to ATM depletion by siRNA, suggesting chemical inhibition was more efficient in abrogating ATM activity in comparison to ATM knockdown. This is also reflected in the fact that ATM inhibited cells displayed a more significant RAD51 defect compared to ATM knockdown cells. Western blot analysis of siRNA efficacy supports this hypothesis as ATM siRNA induced sufficient, but not complete ATM knockdown and therefore, some residual ATM activity may remain contributing to slightly reduced PARPi sensitivity. This observation demonstrates that the level of ATM-kinase activity correlates with PARPi sensitivity. These findings have consequence for treatment of ATM-deficient cancers, as the type of ATM mutation could influence the level of sensitivity/resistance to treatment. This highlights the

importance of identifying the effect of patient ATM mutations on ATM-kinase function prior to treatment with PARPi.

ATM activation is an important component of the cellular response to the DNA damage induced by PARPi, as ATM signalling is induced at several time points following PARPi treatment (Bryant and Helleday, 2006). In this context, the cellular response to PARPi was not affected by depletion of SETD1A alone. These findings are supported by the observation that loss of SETD1A does not change PARPi sensitivity in HR-proficient cells (Bayley *et al.*, 2022). Therefore, we can conclude that depletion of SETD1A has no effect on ATM activation and signalling following DNA damaged induction.

3.10.2 Loss of SETD1A reduces sensitivity of ATM-deficient cells to olaparib by restoring homologous recombination

This chapter presents that loss of SETD1A reduces the sensitivity of ATM-deficient cells to PARPi treatment. The current findings establish loss of SETD1A as a potential novel mechanism of PARPi resistance in ATM-deficient cells, building upon our labs previous work demonstrating these findings in BRCA1-deficient contexts (Bayley *et al.*, 2022). Therefore, loss of SETD1A offers a conserved mechanism of PARPi resistance across both BRCA1- and ATM-deficient cells and could potentially apply to further HR-deficient contexts that show synthetic lethality with PARPi. Identification of a broadly applicable mechanism of resistance is useful when developing biomarkers of PARPi response in the clinic. Despite this, data currently under review shows this mechanism is not extended to cells lacking BRCA2 (Sweatman *et al.*, 2024). This can be attributed to the distinct roles of BRCA1, ATM and BRCA2 during HR. BRCA1 and ATM promote initial steps of HR and DNA end-

resection, and loss can be overcome by loss of competing pathways e.g. 53BP1 and RIF1, and as shown here SETD1A. Whereas, BRCA2 is indispensable for RAD51-dependent recombination. These findings are consistent with multiple studies demonstrating loss of pro-NHEJ factors cannot drive PARPi resistance in BRCA2-deficient cells (Bouwman *et al.*, 2010) (Bhin *et al.*, 2023). Instead, loss of PARG expression or BRCA2 reversion mutations are the most common mechanisms of resistance in BRCA2-deficient tumours (Bhin *et al.*, 2023). These findings highlight that loss of proteins even within the same DNA damage repair pathways can have different impacts on PARPi resistance patterns.

Understanding the underlying mechanisms responsible for inducing PARPi resistance is important to develop methods of overcoming resistance and improve patient outcomes. A well-established mechanism of PARPi resistance is restoration of HR, supported by previous findings that loss of SETD1A restores HR in BRCA1-deficient cells that show reduced PARPi sensitivity (Bayley *et al.*, 2022). Consistent with these previous results, loss of SETD1A also restored HR in ATM-deficient cells, as demonstrated through RAD51 foci and Cas9-nickase mediated recombination assays. These findings are supported by previous studies showing that loss of another pro-NHEJ, 53BP1, induces PARPi resistance in ATM-deficient cells through restoration of HR (Hong *et al.*, 2016).

Consistent with the degree of sensitivity to PARPi treatment, ATM inhibition induced a more significant defect in RAD51 foci formation in comparison to siRNA-mediated knockdown. This is consistent with previous studies demonstrating that ATM loss does not cause a complete HR defect (Neeb *et al.*, 2021). One explanation is that cells lacking ATM accumulate unresolved RAD51 foci, representing incomplete

dysfunctional recombination (Köcher et al., 2013). Alternatively, incomplete depletion of ATM transcripts in ATM knockdown cells may result in residual ATM activity sufficient to perform HR.

To mitigate the effects of unresolved RAD51 foci accumulation, a CRISPR-Cas9 based assay was used to directly quantify the effect of SETD1A loss on functional HR. As expected, both BRCA1 and ATM depletion (by knockdown or inhibition) significantly reduced the percentage of cells undergoing HR directed repair. These findings support the theory that RAD51 foci can still be recruited despite defective HR. Furthermore, co-depletion of SETD1A in BRCA1- and ATM-deficient cells restored HR activity to up to 40% of control levels, consistent with RAD51 foci results. Our findings suggest that loss of SETD1A only partially restores HR, this is consistent with partial reversal of PARPi sensitivity observed using clonogenic survival assays. Previous studies showed that BRCA1 was indispensable for DNA end-resection, but its later roles in promoting RAD51 loading cannot be fully compensated by loss of factors such as 53BP1 (Nacson *et al.*, 2018). A similar role for ATM would explain why only partial restoration of HR is observed. Although, the increase in HR activity after SETD1A depletion in BRCA1- and ATM-deficient cells was not statistically significant, this finding is likely still of biological significance, as previous studies have found an increase in RAD51 foci of only 10% in olaparib resistant cells (Jaspers et al., 2013).

As well as HR, NHEJ has also been shown to play a key role in the cellular response to PARPi. For example, NHEJ regulates the formation of radial chromosome structures in HR-deficient cells treated with PARPi, driving the accumulation of genomic instability and ultimately cell death (Patel, Sarkaria and Kaufmann, 2011).

Depletion of SETD1A decreased the formation of chromosomal radials in both BRCA1- and ATM-deficient cells in response to olaparib treatment. These findings are indicative of decreased error-prone NHEJ, suggesting loss of SETD1A decreases the level of genomic instability in HR-deficient cells following PARP inhibition. These results are consistent with the role of SETD1A as an end-protection factor facilitating RIF1-dependent NHEJ (Bayley *et al.*, 2022). This also supports previous findings that disabling NHEJ, by genetic or pharmacological approaches, can rescue synthetic lethality following PARP inhibition in cell lines lacking BRCA1 (Bunting *et al.*, 2010). Importantly, these findings were also recapitulated in ATM-deficient cell lines, in which PARPi hypersensitivity could be rescued through inhibition of DNA-PKc (Patel, Sarkaria and Kaufmann, 2011). These findings highlight the importance of the balance between HR and NHEJ in PARPi sensitivity. Loss of SETD1A in HR-deficient cells shifts the balance of DSB repair towards HR and away from NHEJ to induce PARPi resistance.

In addition to regulating NHEJ, SETD1A is known to protect stalled replication forks from DNA2-dependent degradation. As a result, loss of SETD1A produces a deficiency in fork protection (Higgs *et al.*, 2018). An alternative mechanism of PARPi resistance established in BRCA1-deficient cells is restoration of replication fork protection (Ray Chaudhuri *et al.*, 2016). However, this mechanism does not correspond to PARPi resistance in the absence of SETD1A, as depletion of SETD1A in BRCA1-deficient cells does not restore fork protection, suggesting that the resistance to PARPi is specifically due to restoration of HR (Bayley *et al.*, 2022). In the case of loss of SETD1A, these findings demonstrate that restoration of HR can override loss of fork protection in relation to PARPi sensitivity in BRCA1- and ATM-

deficient contexts. Taken together, these observations highlight the multifactorial nature of PARPi resistance and highlights that multiple resistance mechanisms may exist within one cell, whilst the same mechanisms may have different influences dependent on the underlying genetic context.

Due to the established role of SETD1A as an end-protection factor promoting DSB repair via NHEJ, these observations establish loss of SETD1A akin to loss of members of the 53BP1 pathway and components of the shieldin complex, which have already been well characterised in PARPi resistance (Chapman *et al.*, 2013; Zimmermann *et al.*, 2013). Furthermore, the role of SETD1A in facilitating RIF1-dependent NHEJ implies that deficiencies in HR present in ATM-deficient cells can also be overcome by compromising the 53BP1-RIF1-shieldin pathway. This is in agreement with a previous study demonstrating loss of 53BP1 also acts as a PARPi resistance mechanism in ATM-deficient cells (Hong *et al.*, 2016). However, these findings are in contradiction with another study which showed loss of 53BP1 cannot suppress the PARPi sensitivity of ATM-deficient mouse embryonic stem cells (Balmus *et al.*, 2019). This is likely due to the necessary role of ATM in activating the 53BP1-RIF1 axis via 53BP1 phosphorylation. These differences highlight that the genetic background/tumoral nature of models used to study PARPi resistance mechanisms can impact results. Nevertheless, these findings suggest that perturbation of pro-NHEJ pathways by loss of SETD1A drives PARPi resistance in multiple genetic contexts, offering a conserved mechanism for PARPi resistance across BRCA1- and ATM-deficient cells. In the future it will be of interest to investigate whether loss of other pro-NHEJ such as RIF1, REV-7 and the Shieldin complex also reduce PARPi sensitivity in ATM-deficient contexts.

3.10.3 Loss of H3K4 methylation reduces PARPi sensitivity in ATM-deficient cells

Another significant finding highlighted in this chapter is that the methylation of H3K4 also confers PARPi resistance in ATM-deficient cells. Perturbation of H3K4me using the H3-K4A-GFP system phenocopied SETD1A loss, alleviating PARPi sensitivity, restoring HR and decreasing PARPi induced radial formation in absence of ATM. Thereby linking both SETD1A and H3K4me to PARPi resistance in HR-deficient contexts. However, we have not yet shown whether SETD1A-dependent H3K4me underpins PARPi resistance in ATM-deficient cells. This should be investigated in the future using a methyltransferase dead SETD1A mutant lacking the catalytic SET domain, which has previously shown to be required for the recruitment of RIF1 to DSBs to facilitate NHEJ (Bayley *et al.*, 2022).

Unexpectedly, H3-WT-GFP cells did show greater sensitivity to 2 μM olaparib treatment compared to H3-K4A-GFP in the presence of ATM. However, this does not detract from the fact sensitivity was significantly further decreased in the H3-WT-GFP cells upon depletion of ATM. This observation could be due to effects of the GFP tag, which will increase the molecular mass of the histones and could impair their physiological function. This could be resolved in future studies by removing the GFP tag from the histones.

Unfortunately, we could not validate the contribution of H3K4 methylation to PARPi resistance as we were unable to confirm RBBP2 overexpression using the U-2-OS Flp-In TRex system. Although, doxycycline treatment induced FLAG expression, overexpression of RBBP2 could not be detected. Despite this, endogenous RBBP2 could be detected in all cell lines confirming antibody efficacy. Thus, I hypothesise

that the FLAG tag masks the epitope recognised by the RBBP2 antibody in the fusion proteins. In the future, the FLAG tag could be removed to alleviate this effect or the RBBP2 constructs could be introduced into cells by transient transfection. Previous studies have utilised this approach to show that RBBP2 overexpression reduces H3K4 methylation levels independently of loss of SETD1A and effects the recruitment of RIF1 to DSBs in a similar manner to loss of SETD1A (Bayley *et al.*, 2022).

Abrogation of histone methylation in these experiments did not produce a global change in H3K4me3 detectable by western blotting. An explanation for this could be that changes in histone methylation occur more locally, for example at the promoters of specific SETD1A regulated genes. This is supported by previous studies showing that SETD1A depletion does not significantly alter total H3K4 methylation and histone H3 levels in breast cancer cell lines (Tajima *et al.*, 2015), indicating that SETD1A is not critical for maintenance of overall H3K4 methylation.

We have yet to show whether loss of H3K4me3 specifically catalysed by SETD1A is responsible for reduced PARPi sensitivity in ATM-deficient cells. Previous work has shown that exogenous expression of full length SETD1A could reinstate normal RIF1 and BRCA1 foci formation following ionising radiation in SETD1A depleted cells, but not a variant lacking the catalytic SET domain. Establishing that SETD1A-dependent H3K4 methylation is required to regulate end protection and facilitate NHEJ, thus it is also likely to be responsible for influencing PARPi sensitivity (Bayley *et al.*, 2022). We could use this add back system in conjunction with clonogenic survival assays to confirm whether there is a direct link between the histone-mutant and SETD1A phenotypes in relation to PARPi sensitivity and determine whether loss of SETD1A-dependent H3K4 methylation underpins PARPi resistance in HR-deficient cells.

In addition to SETD1A, other KMT2 family members, including SETD1B or KMT2A – D, are responsible for H3K4 methylation. Previous work from our lab showed that depletion of these other KMT2 family members had no effect on RIF1 or RPA foci formation following ionising radiation (Bayley *et al.*, 2022). These findings suggest a specific role for SETD1A in RIF1-dependent NHEJ, therefore depletion of these other KMTs is unlikely to influence PARPi sensitivity. Nevertheless, a role for these other KMTs in PARPi response in this context should be ruled out by performing clonogenic survival assays following specific depletion of these methyltransferases.

The important contribution of epigenetic mechanisms of PARPi resistance have been demonstrated numerous times previously. For example, in a similar manner to loss of 53BP1, acetylation of 53BP1 can also inhibit NHEJ by negatively regulating its recruitment to DSBs, leading to PARPi resistance in BRCA1-deficient cells (Guo *et al.*, 2017). More specifically epigenetic modifications of histones are also known to influence PARPi sensitivity. For instance, PARPi resistant HGSOC cancer cells display a global increase in H3K9me, accompanied by overexpression of the EHMT1/2 methyltransferases (Watson *et al.*, 2019). Loss of EZH2 reduces H3K27me3, preventing the recruitment of crossover junction endonuclease MUS81 to RFs to suppress fork degradation in BRCA2-deficient cells and confer PARPi resistance (Rondinelli *et al.*, 2017). More recently, two other members of KMT2 family of lysine methyltransferases have been implicated in PARPi resistance. Genetic alterations in KMT2C and KMT2A were identified in BRCA1- and BRCA2-associated mouse models of PARPi resistant breast cancer (Bhin *et al.*, 2023). In this study we build upon these previous findings, identifying a further potential novel epigenetic

PARPi resistance mechanism mediated by loss of H3K4 methylation and its associated methyltransferase, SETD1A.

3.10.4 H3K4 tri-methylation directly interacts with RIF1 through the N-terminal HEAT repeat domains

Previously, loss of SETD1A was shown to confer PARPi resistance in BRCA1-deficient cells as a result of failure to recruit RIF1, arising from defective H3K4 methylation and subsequent loss of binding of RIF1 to H3K4me3 at sites of damage (Bayley *et al.*, 2022). My findings provide further evidence in support of this model, demonstrated by histone pulldown experiments with recombinant RIF1, I confirmed that RIF1 directly binds to H3K4me3, and this binding is dependent on the methylation status of histone H3. Additional results revealed that the N-terminal HEAT repeat domains of RIF1 mediated the interaction between RIF1 and H3K4me3. In **Fig 3.16** full length recombinant RIF1 appeared at a higher molecular weight in the pulldown lane compared to the input sample. A potential explanation is that the input sample has undergone a posttranslational modification that is not present in the histone pulldown sample, therefore the pulldown process may be enriching for the unmodified forms of recombinant RIF1. This would indicate that recombinant RIF1 only interacts with H3K4me3 in its unmodified form. There is previous evidence to show posttranslational modifications regulate RIF1 binding, for example, RIF1 phosphorylation at the RVxF/SILK domain disrupts its interaction with protein phosphatase 1 (Davé *et al.*, 2014) .

Together this data supports a model whereby RIF1 binds to H3K4me3 deposited by SETD1A via its N-terminal HEAT repeats to facilitate its localisation at DSBs. This observation supports previous findings that the N-terminal HEAT repeat domains of

RIF1 are required for its recruitment to DSBs (Escribano-Díaz *et al.*, 2013). Although, HEAT repeats are not considered canonical methyl-binding domains, studies have shown that HEAT-repeat domains present in condensin are able to bind to methylated H3K4 (Yuen, Slaughter and Gerton, 2017). Further evidence identified HEAT repeats mediate the interaction of RIF1 with phosphorylated 53BP1 and the shieldin complex (Setiaputra *et al.*, 2022; Sifri *et al.*, 2023), highlighting their importance in regulating DNA repair via NHEJ. Collectively, these findings show that N-terminal HEAT repeats of RIF1 can read the epigenetic status of chromatin surrounding DSBs via binding to H3K4me3 deposited by SETD1A to control the DDR.

A limitation of this approach, however, is we have not confirmed that ΔHEAT RIF1 is properly folded into its final protein conformation, structural studies should be conducted in the future to confirm this. Another important avenue for further investigation will be to characterise the precise nature and timing of RIF1 recruitment to H3K4 methylation. Using the recombinant TnT system I could express different fragments of the HEAT repeat domain of RIF1 to identify the minimal fragment required for the interaction between RIF1 and H3K4me3. Furthermore, to investigate the importance of methylation status, including mono-, di-, and tri-methylation of H3K4 for this interaction, histone pulldown experiments should be repeated using different methylation states of recombinant histone H3 proteins.

Collectively, these findings support the model in which SETD1A facilitates NHEJ by directly recruiting RIF1 to the chromatin at DSBs via its interaction with H3K4me3. Subsequently, depletion of SETD1A reduces the level of methylated histone H3 present at damaged chromatin, consequently preventing the recruitment of RIF1 to

the DSB. This leads to loss of DNA end-protection and uncontrolled resection of the break, allowing HR to be restored, thus giving rise to partial PARPi resistance in BRCA1- and ATM-deficient contexts.

To summarise, in this chapter I have demonstrated that loss of SETD1A reduces PARPi sensitivity in ATM-deficient cells, expanding upon previous findings in BRCA1-deficient contexts. This suggests that loss of SETD1A is not specific to BRCA1-deficiency and can be applied to multiple HR-deficient contexts, expanding the clinical relevance of this resistance mechanism to multiple tumour types. In this case, reduced PARPi sensitivity was attributed to restoration of HR upon loss of SETD1A in ATM-deficient cells. This positions SETD1A with other pro-NHEJ factors such as 53BP1, RIF1 and the shieldin complex whose loss have been well established as mechanisms of PARPi resistance through restoration of HR. These findings support the limited previous research in ATM-deficient cells to highlight that perturbation of pro-NHEJ pathways influences PARPi sensitivity in this context. Another significant finding is that methylation of H3K4 also reduces PARPi sensitivity in HR-deficient cells, providing another epigenetic mechanism of PARPi resistance. In combination, these findings solidify a model for SETD1A-induced PARPi resistance in which loss of SETD1A reduces the methylation of H3K4 at sites of DSBs. As a result, RIF1 recruitment is decreased and DSB end-protection is lost. This allows for DNA end-resection to occur in the absence of BRCA1, restoring HR and rescuing PARPi sensitivity.

4. CHAPTER 4: LOSS OF SETD1A REDUCES OLAPARIB SENSITIVITY IN A SUBSET OF HR-DEFICIENT CANCER CELL LINES

4.1 Introduction

In earlier work, loss of SETD1A was shown to reduce the PARPi sensitivity of ATM- (Chapter three) and BRCA1- deficient (Bayley *et al.*, 2022) HeLa cells by restoring HR. However, one outstanding question is whether SETD1A loss represents a clinically relevant PARPi resistance mechanism in HR-deficient tumours. Therefore, I aimed to extend my findings from HeLa cells to breast, ovarian and lung cancer cell lines bearing pathogenic *BRCA1* or *ATM* mutations, focusing on UWB1.289, HCC1937, and H1395 cells.

Additionally, I aimed to examine the effects of SETD1A loss on the survival outcomes of HR-deficient cancer patients. The lack of treatment information available from cancer genomic databases precludes definitive bioinformatic verification of SETD1A depletion as a PARPi resistance mechanism. Instead, I aimed to broadly examine the effects of SETD1A loss on patient survival, using data from HR-proficient and -deficient cancer patients in publicly available cancer genomics datasets.

4.2 SETD1A depletion reduces sensitivity of BRCA1-deficient cancer cell lines to olaparib through restoring homologous recombination

Firstly, I aimed to extend earlier findings from HeLa cells into cancer cell lines bearing pathogenic *BRCA1* mutations. UWB.1289 is a HGSOC cell line possessing the germline *BRCA1* 594delC mutation, which has been identified in women with familial breast and ovarian cancer (DelloRusso *et al.*, 2007). This alteration introduces a stop at codon 845 of *BRCA1*, resulting in lack of wild-type BRCA1 protein expression.

Firstly, I performed clonogenic survival assays in UWB1.289 cells following olaparib treatment in the presence/absence of SETD1A (**Fig. 4.1 A**). The *BRCA1*-proficient SKOV3 ovarian cancer line was used as a cancer type matched control. In both cases, cell lines were transfected with control or SETD1A siRNA and protein depletion was confirmed by western blot (**Fig. 4.1 B**). As expected, *BRCA1*-mutated UWB1.289 cells displayed notable sensitivity to olaparib treatment, whilst *BRCA1*-proficient SKOV3 cells did not. Consistent with previous findings in HeLa cells, depletion of SETD1A reduced the sensitivity of UWB1.289 cells to olaparib but had no effect on SKOV3 cells (**Figs 4.1 C and D**).

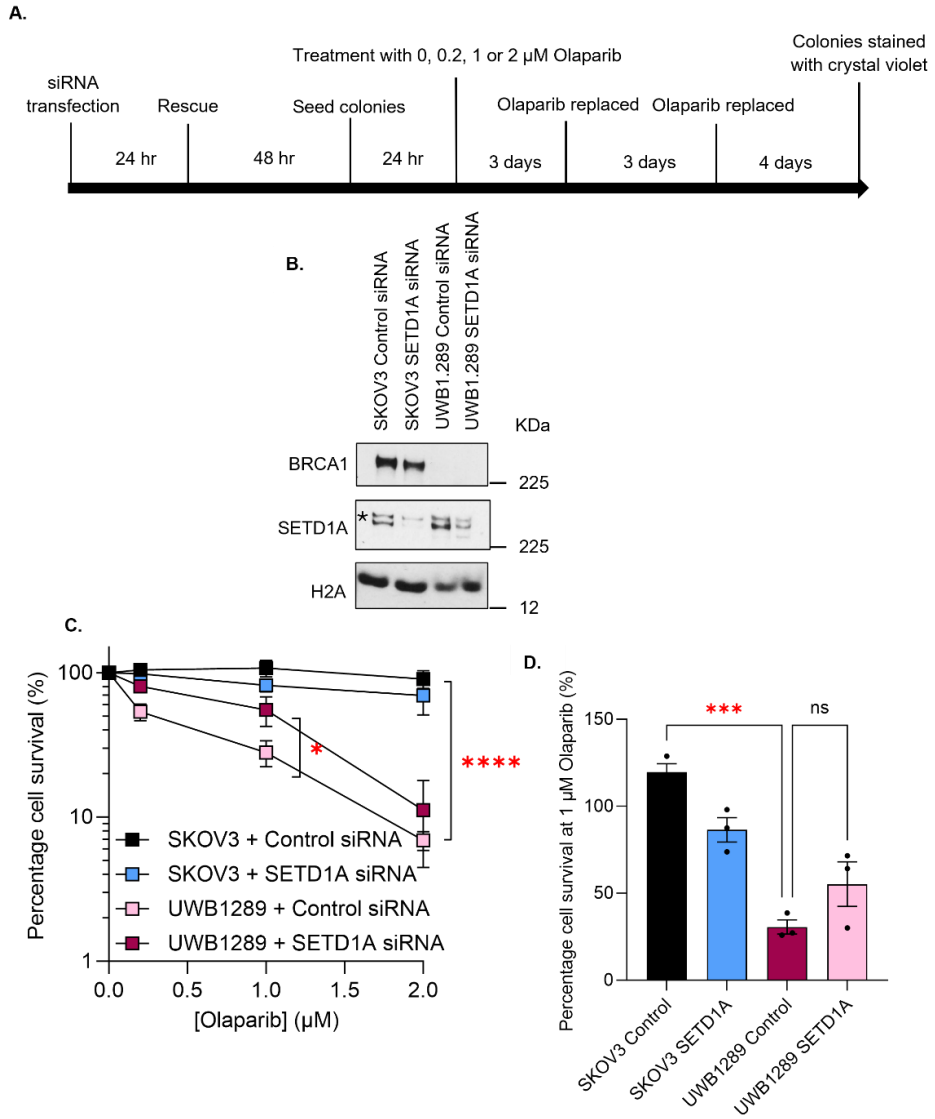

Figure 4.1- Loss of SETD1A reduces sensitivity of BRCA1 mutant ovarian cancer cells to olaparib treatment.

*(A.) Schematic of experimental time course. (B.) Whole cell extracts of cells treated with indicated siRNAs were immunoblotted with the indicated antibodies. *=nonspecific band. (C.) Clonogenic survival of SKOV3 and UWB1.289 cells transfected with the indicated siRNAs. Transfected cells were exposed to the indicated doses of olaparib for 10 days before staining with crystal violet and colonies counted. (D.) Percentage cell survival from (C.) at 1 μM of olaparib. Data points represent the mean ± SEM from three independent biological repeats. * = P <0.05, **** = P <0.0001 as determined by a two-way ANOVA with Tukey's test for multiple comparisons. ns= not statistically significant, *** = P <0.001 as determined by a one-way ANOVA with Tukey's test for multiple comparisons.*

Next, I examined whether this reduced PARPi sensitivity was associated with restored HR, as measured by RAD51 foci formation (**Fig. 4.2 A**). As predicted, given their BRCA1 status, UWB1.289 cells showed a significant defect in PARPi-induced RAD51 foci formation, which was restored to control levels upon depletion of SETD1A. However, no such defect was seen in the SKOV3 cells, and SETD1A depletion had no restorative effect (**Figs 4.2 B and C**). Taken together, these findings further support the conclusion that SETD1A depletion induces PARPi resistance in cells harbouring *BRCA1* mutations by partially restoring HR.

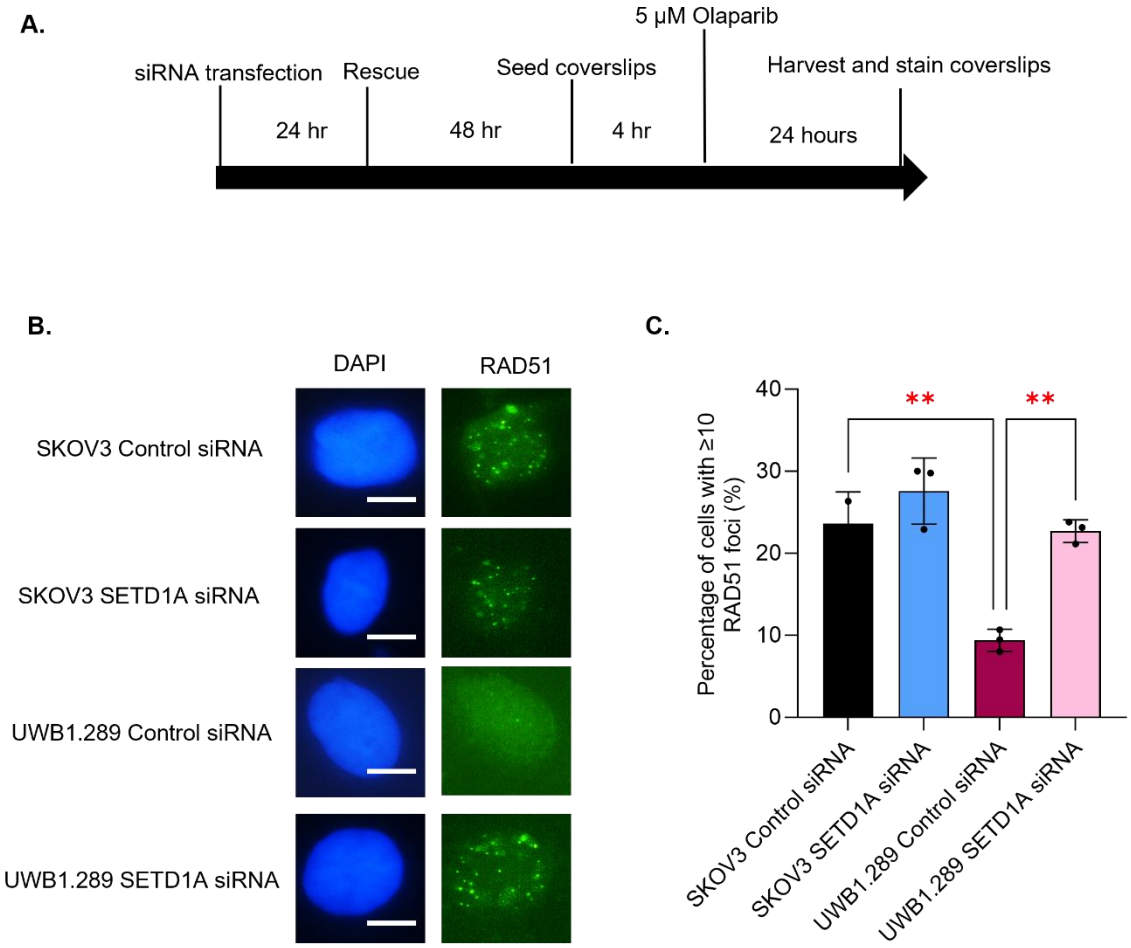

Figure 4.2- Loss of SETD1A restores RAD51 foci formation in BRCA1 mutated ovarian cancer cells treated with olaparib.

*SKOV3 and UWB1.289 cells were transfected with indicated siRNAs and exposed to 5 μM olaparib for 24 hours. Cells were immunostained with an antibody to RAD51 and counterstained with DAPI. Foci formation was enumerated by fluorescent microscopy. (A.) Schematic of experimental time course. (B.) Representative immunofluorescent images (scale bar 10 μm). (C.) Graphical representation of the percentage of cells with ≥10 RAD51 foci 24 hours post olaparib treatment. At least 100 cells were counted per condition. Results represent the mean ± SD from three biologically independent experiments. ** = P < 0.01 as determined by a one-way ANOVA with post-hoc Tukey's test for multiple comparisons.*

These findings were then extended to *BRCA1*-mutant HCC1937 breast cancer cells. HCC1937 is a cell line derived from a primary ductal breast carcinoma possessing a homozygous germline *BRCA1* 5382insC mutation, which results in truncated BRCA1 protein expression (Tomlinson *et al.*, 1998).

We intended to use MCF7 cells as a cancer type matched BRCA1-proficient control cell line, however we excluded these from the clonogenic survival analysis as they showed an unexpectedly high degree of PARPi sensitivity. Therefore, a caveat to the following data is a lack of an appropriate parental control. As a result, we cannot comment on the relative sensitivity of HCC1937 cells to Olaparib treatment in comparison to a non-sensitive BRCA1-proficient cell line. Despite this, and consistent with my previous findings in HeLa and UWB1.289 cell lines, depletion of SETD1A reduced the sensitivity of the HCC1937 breast cancer cell line to olaparib treatment (**Fig. 4.3**).

Consistent with their *BRCA1* status and PARPi sensitivity, HCC1937 cells also displayed reduced RAD51 foci formation after PARPi exposure, whilst the *BRCA1* wild-type MFC7 cells did not display this defect. As before, SETD1A depletion resulted in a significant increase in PARPi-induced RAD51 foci formation in HCC1937 cells, but not in MCF7s (**Fig. 4.4**). These findings provide further support that SETD1A depletion confers PARPi resistance in BRCA1-deficient cells cancer cell lines by partially restoring HR.

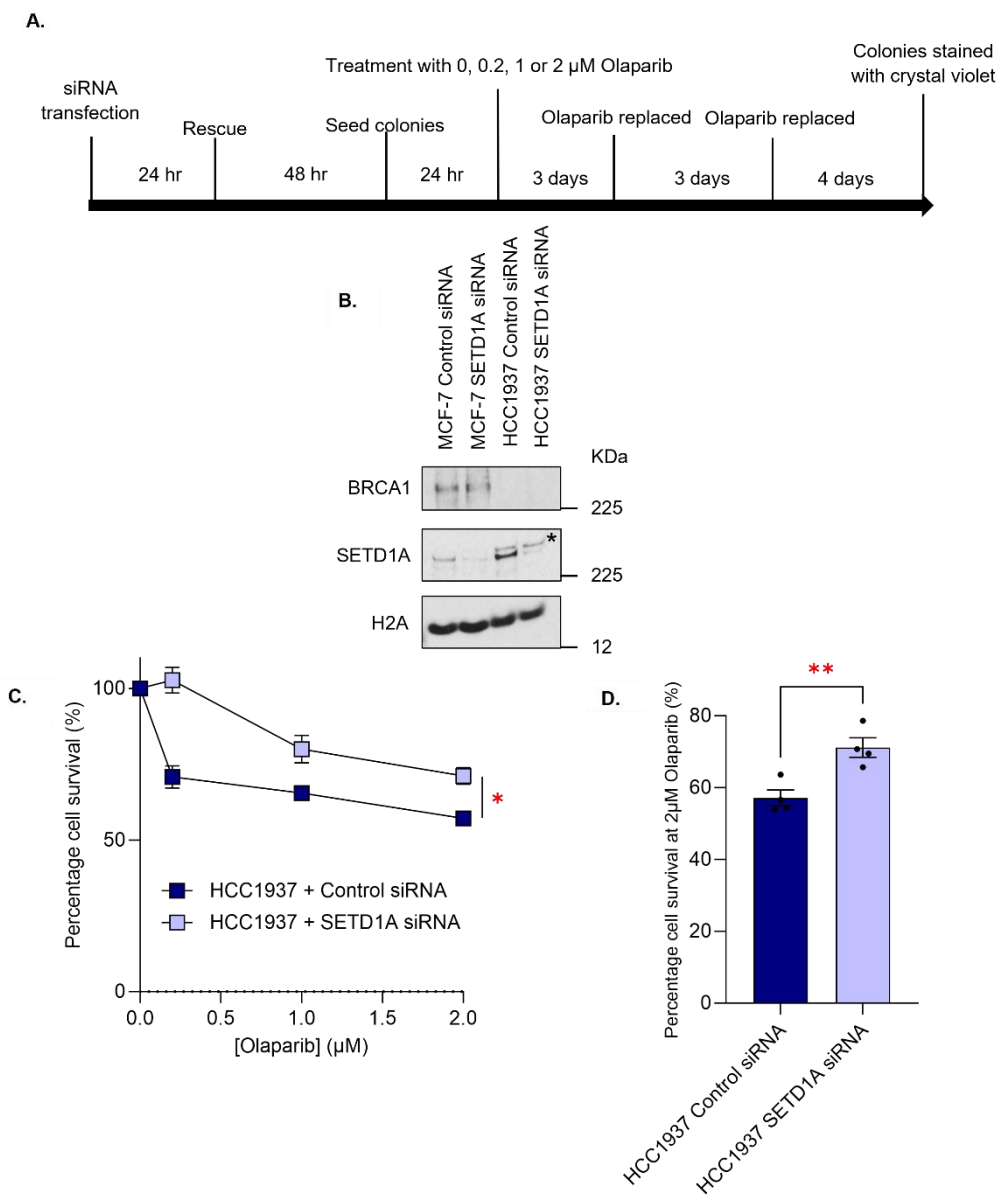

Figure 4.3- Loss of SETD1A reduces sensitivity of BRCA1 mutant breast cancer cells to olaparib treatment.

*(A.) Schematic of experimental time course. (B.) Whole cell extracts of cells treated with indicated siRNAs were immunoblotted with the indicated antibodies. *= nonspecific band. (C.) Clonogenic survival curve for HCC1937 cells transfected with the indicated siRNAs. Transfected cells were exposed to the indicated doses of olaparib for 10 days before staining with crystal violet and colonies counted. (D.) Percentage cell survival from (C.) at 2 μM olaparib. Data points represent the mean ± SEM from three independent biological repeats. * = P <0.05 as determined by a two-way ANOVA with Tukey's test for multiple comparisons. ** = P <0.01 as determined by a two-tailed Students t-test.*

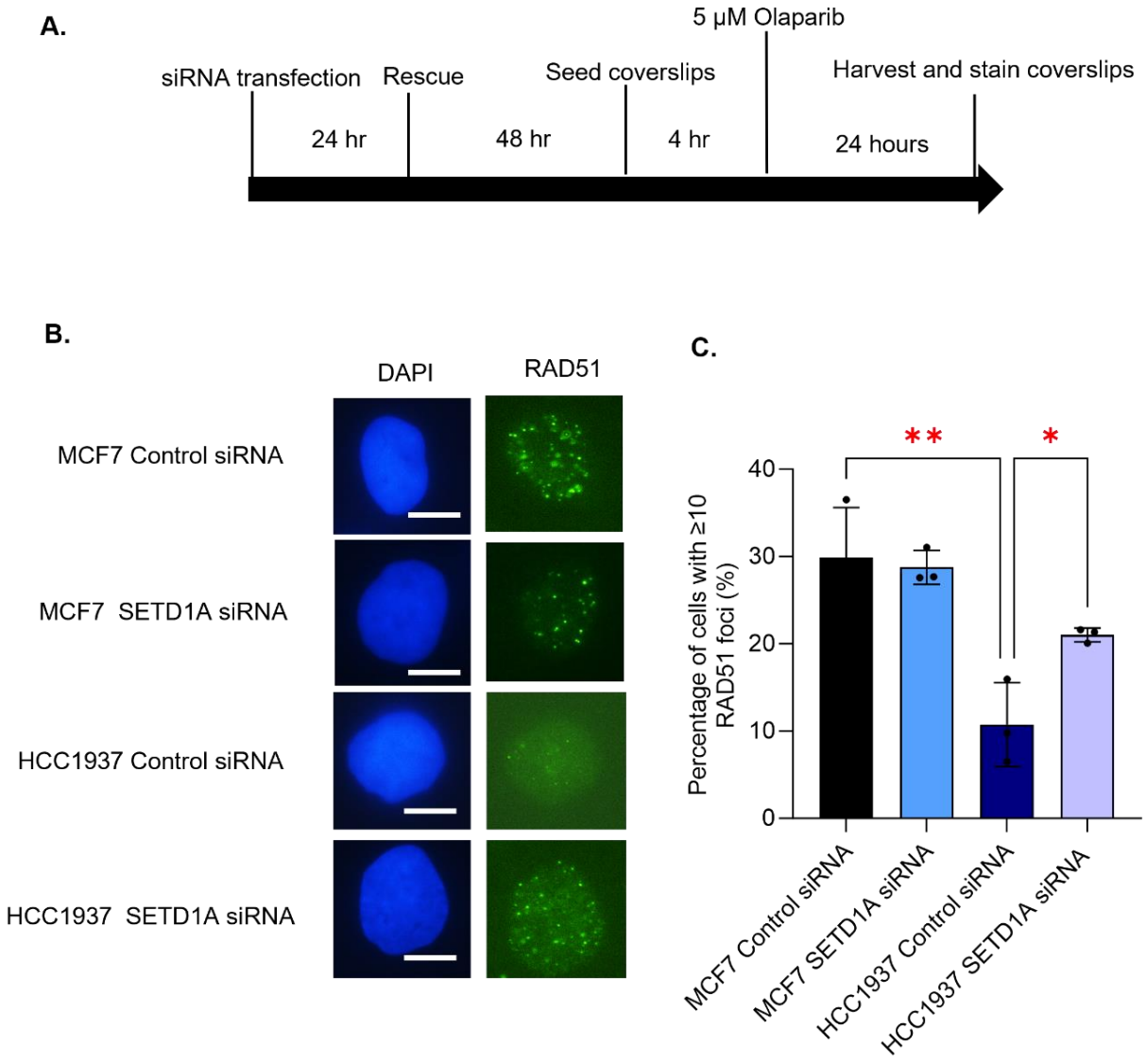

Figure 4.4- Loss of SETD1A restores RAD51 foci formation in BRCA1 mutated breast cancer cells treated with olaparib.

*MCF7 and HCC1937 cells were transfected with indicated siRNAs and exposed to 5 μM olaparib for 24 hours. Cells were immunostained with an antibody to RAD51 and counterstained with DAPI. Foci formation was enumerated by fluorescent microscopy. (A.) Schematic of experimental time course. B. Representative immunofluorescent images (scale bar 10 μm). (C.) Graphical representation of the percentage of cells with ≥10 RAD51 foci 24 hours post olaparib treatment. At least 100 cells were counted per condition. Results represent the mean ± SD from three biologically independent experiments. * = P < 0.05, **= P <0.01 as determined by a one-way ANOVA with Tukey's test for multiple comparisons.*

4.3 SETD1A depletion does not affect sensitivity of an ATM-deficient lung cancer cell line to olaparib

Having demonstrated that loss of SETD1A reduces PARPi sensitivity in *BRCA1*-mutated cancer cell lines, I next aimed to extend these findings into models of ATM-deficiency. Since genomic analyses revealed that low SETD1A mRNA expression correlated with significantly reduced overall survival in ATM-mutated NSCLC patients (**Fig. 4.7**), I utilised the *ATM* mutated H1395 NSCLC cell line. H1395 cells possess a homozygous *ATM* A7996G missense mutation present at the N-terminus of the PI3K domain, which results in low levels of ATM expression and functional impairment of ATM kinase activity (Davies *et al.*, 2005).

In contradiction to my previous finding in BRCA1-mutated cancer cell lines and ATM-deficient HeLa cells, clonogenic survival assays demonstrated that loss of SETD1A had no impact on PARPi sensitivity in ATM-mutated H1395 cells (**Figs 4.5 C and D**). Due to difficulties forming quantifiable colonies, this data is limited by the lack of parental or ATM-proficient cancer type matched control, therefore comments cannot be made on the relative sensitivity of H1395 to PARPi treatment.

Next, I investigated whether this discrepancy was due to a defect in HR. The *ATM*-proficient A549 cell line was used as a cancer type matched control (**Fig. 4.6 A**). As expected, H1395 cells showed a defect in RAD51 foci formation consistent with the known pro-HR role of ATM, whilst A549 cells displayed no such defect. Interestingly, loss of SETD1A increased RAD51 foci formation in H1395 cells, although this was not statistically significant (**Figs 4.6 B and C**), suggesting increased HR activity. Together these findings imply that whilst HR activity increases upon loss of SETD1A, this does not confer reduced sensitivity to PARPi in H1395 cells.

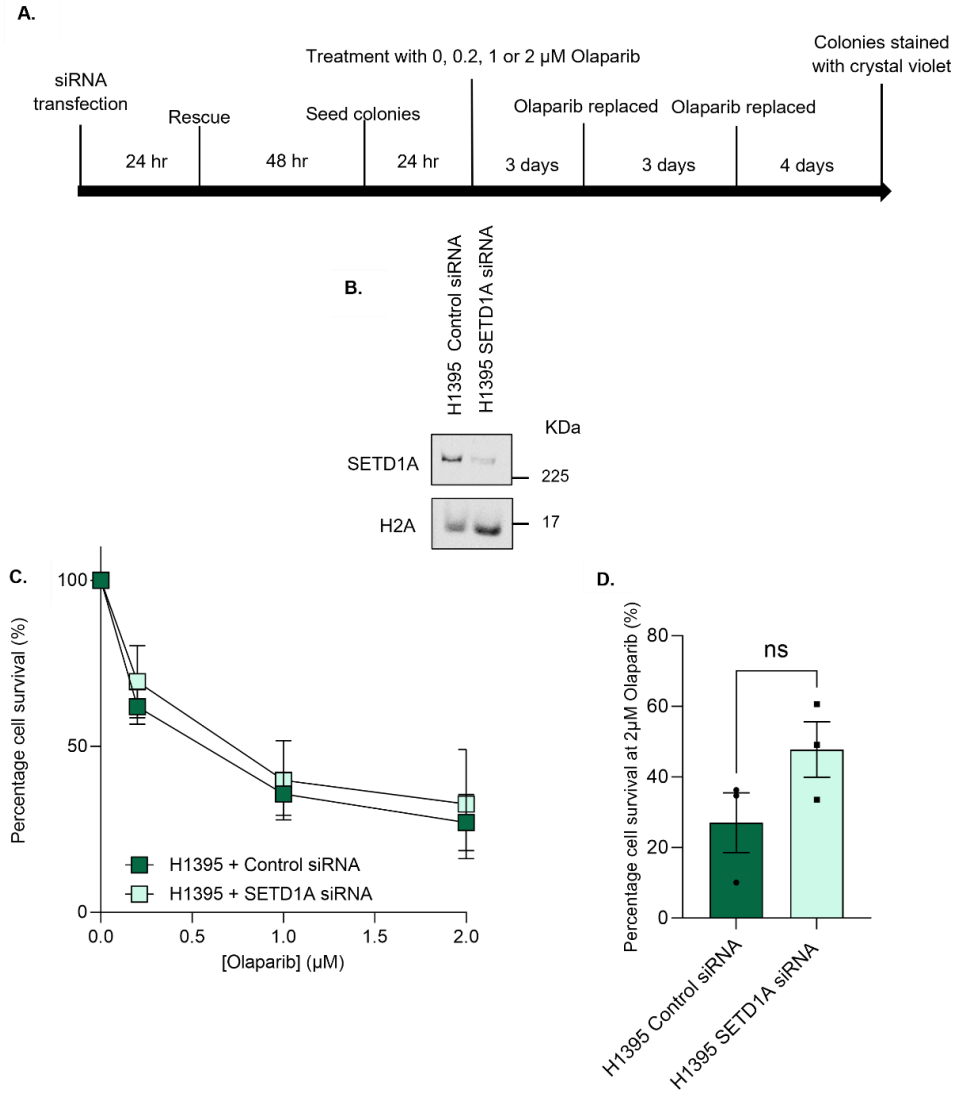

Figure 4.5- Loss of SETD1A has no effect on the sensitivity of ATM mutant lung cancer cells to olaparib treatment.

(A.) Schematic of experimental time course. (B.) Whole cell extracts of cells treated with indicated siRNAs were immunoblotted with the indicated antibodies. (C.) Clonogenic survival curve for H1395 cells transfected with the indicated siRNAs. Transfected cells were exposed to the indicated doses of olaparib for 10 days before staining with crystal violet and colonies counted. (D.) Percentage cell survival from (C.) at 2 μM olaparib. Data points represent the mean ± SEM from three independent biological repeats. ns= not statistically significant as determined by a two-tailed Students t-test.

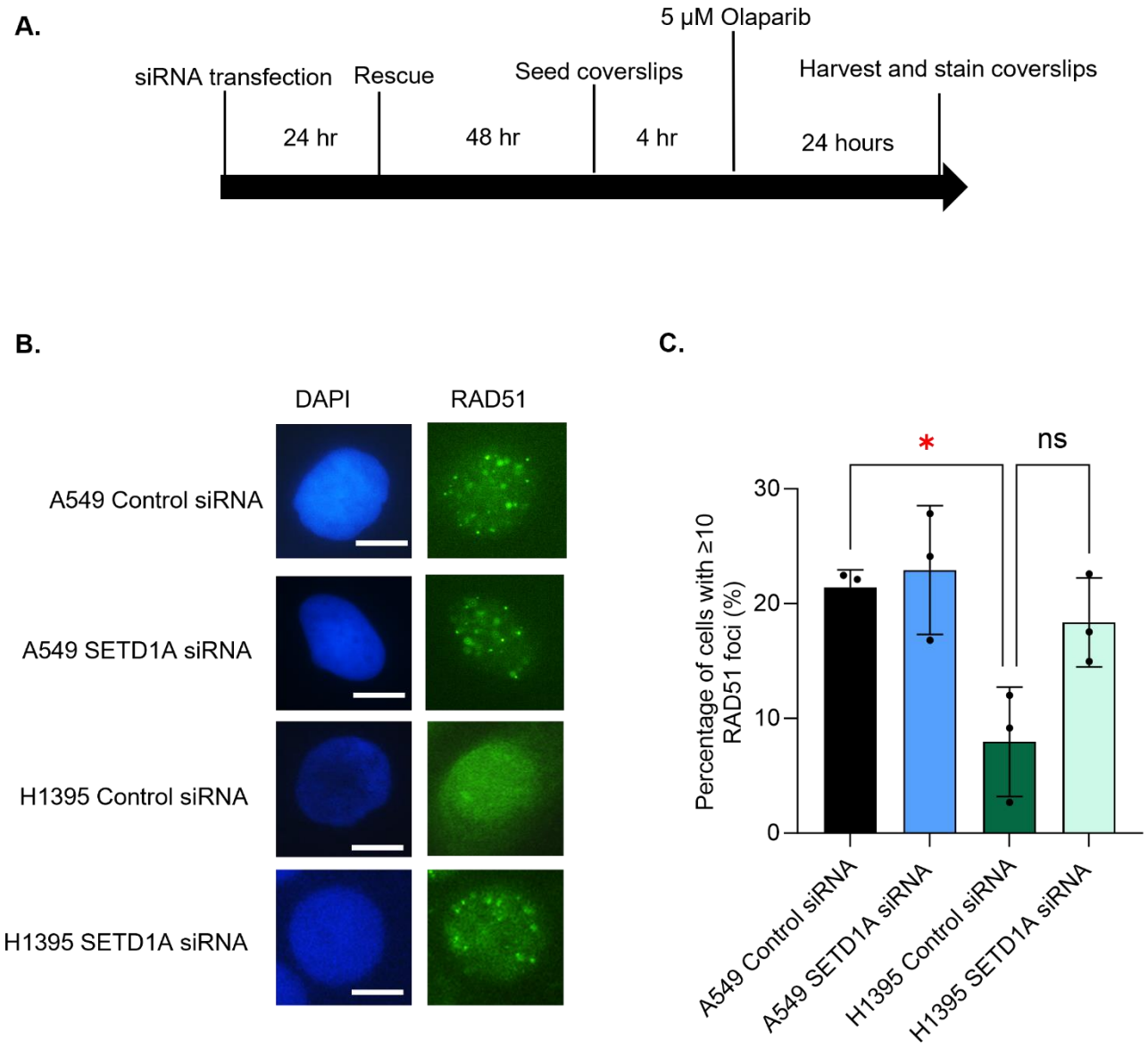

Figure 4.6- Loss of SETD1A does not restore RAD51 foci formation in ATM mutated lung cancer cells treated with olaparib.

*A549 and H1395 cells were transfected with indicated siRNAs and exposed to 5 μM olaparib for 24 hours. Cells were immunostained with an antibody to RAD51 and counterstained with DAPI. Foci formation was enumerated by fluorescent microscopy. (A.) Schematic of experimental time course. (B.) Representative immunofluorescent images (scale bar 10 μm). (C.) Graphical representation of the percentage of cells with ≥10 RAD51 foci 24 hours post olaparib treatment. At least 100 cells were counted per condition. Data points represent the mean ± SD from three biologically independent experiments. ns= not statistically significant, * = P < 0.05 as determined by a as determined by a two-tailed Students t-test.*

4.4 Low SETD1A mRNA expression is associated with poor overall survival in some HR-deficient cancer types

To determine the significance of these results in patients, I examined whether SETD1A levels correlated with patient survival in a range of HR-deficient/proficient cancer types. I first identified ATM-, BRCA1- and BRCA2-deficient patients diagnosed with lung, ovarian or breast cancer, as well as corresponding HR-proficient patients, using data obtained from The Cancer Genome Atlas (TCGA) cancer genomics program (https://www.cancer.gov/tcga) or the Molecular Taxonomy of Breast Cancer International Consortium (METABRIC) (Curtis *et al.*, 2012) via the CBioPortal online cancer genomic database (Cerami *et al.*, 2012; Gao *et al.*, 2013) (https://www.cbioportal.org/). I then stratified patients by SETD1A mRNA expression using RNA-sequencing data and performed Kaplan-Meir survival analyses (**Fig. 4.7**).

This analysis revealed that *BRCA1*-deficient breast (**Fig. 4.7 C**) and ovarian (**Fig. 4.7 E**) and *ATM*-deficient lung adenocarcinoma patients (**Fig. 4.7 D**) with low SETD1A mRNA expression had poorer overall survival compared to those with higher levels of SETD1A. This was most notable in *ATM*-deficient lung adenocarcinoma, where low SETD1A expression corresponded to a statistically significant decrease in overall survival (**Fig. 4.7 D**). These findings show survival of both BRCA1- and ATM-deficient cancer patients can be triaged be SETD1A expression, supporting earlier findings that loss of SETD1A reduces cellular survival following PARPi in backgrounds of BRCA1-or ATM-deficiency. On the other hand, low expression of SETD1A had no impact on the survival of patients with wild-type BRCA1 (**Fig. 4.7 A**) or ATM (**Fig. 4.7 B**), or in BRCA2-deficient cancer patients (**Fig. 4.7 F**), indicating that SETD1A expression only correlates with survival in selected HR-deficient tumour types.

A.

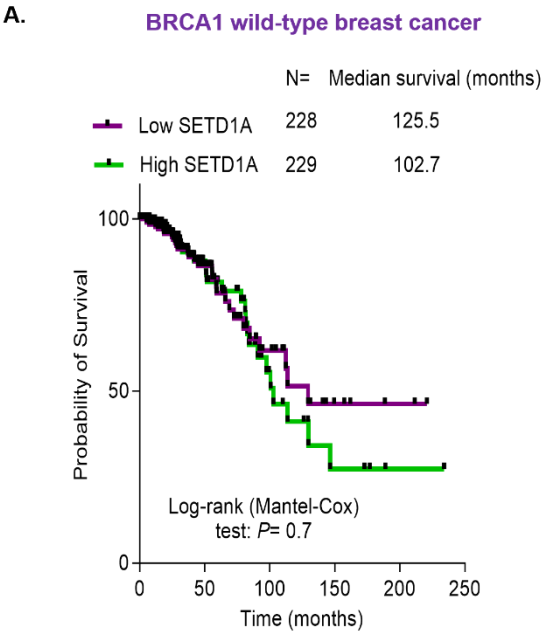
BRCA1 wild-type breast cancer
N= Median survival (months)
Low SETD1A 228 125.5
High SETD1A 229 102.7
Probability of Survival
Log-rank (Mantel-Cox) test: P= 0.7
Time (months)

B.

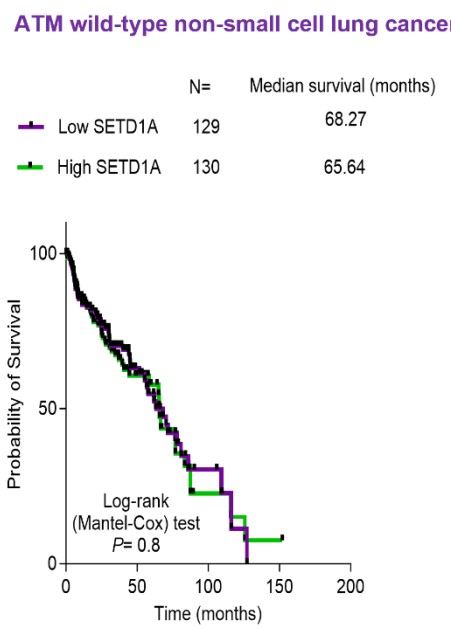
ATM wild-type non-small cell lung cancer
N= Median survival (months)
Low SETD1A 129 68.27
High SETD1A 130 65.64
Probability of Survival
Log-rank (Mantel-Cox) test P= 0.8
Time (months)

C.

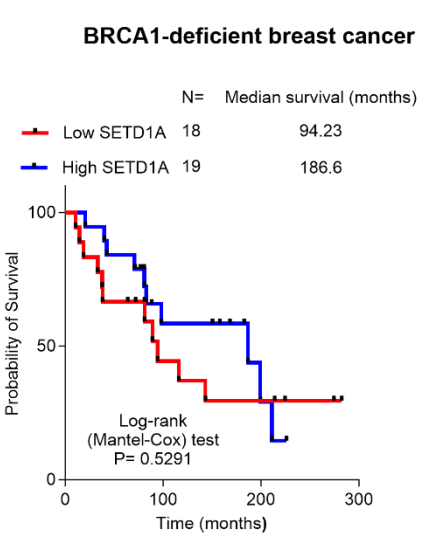
BRCA1-deficient breast cancer
N= Median survival (months)
Low SETD1A 18 94.23
High SETD1A 19 186.6
Probability of Survival
Log-rank (Mantel-Cox) test P= 0.5291
Time (months)

D.

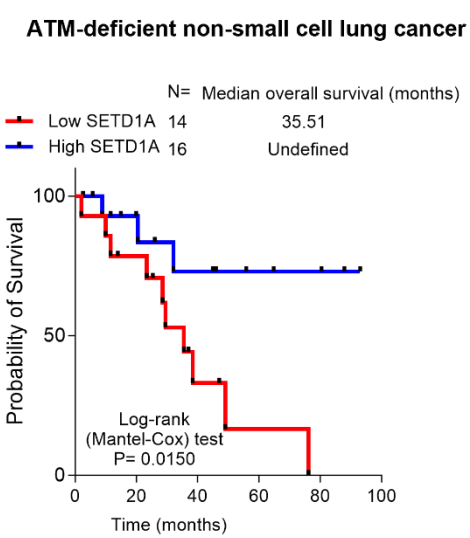
ATM-deficient non-small cell lung cancer
N= Median overall survival (months)
Low SETD1A 14 35.51
High SETD1A 16 Undefined
Probability of Survival
Log-rank (Mantel-Cox) test P= 0.0150
Time (months)

E.

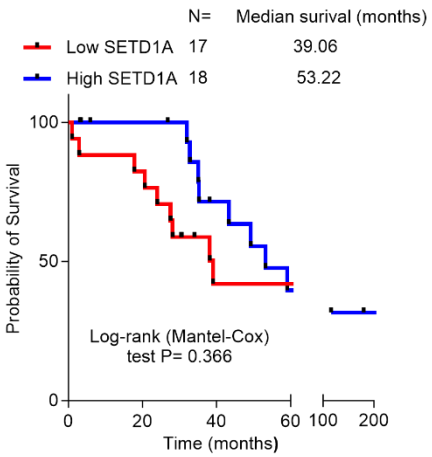
BRCA1-deficient ovarian cancer
N= Median surival (months)
Low SETD1A 17 39.06
High SETD1A 18 53.22
Probability of Survival
Log-rank (Mantel-Cox) test P= 0.366
Time (months)

F.

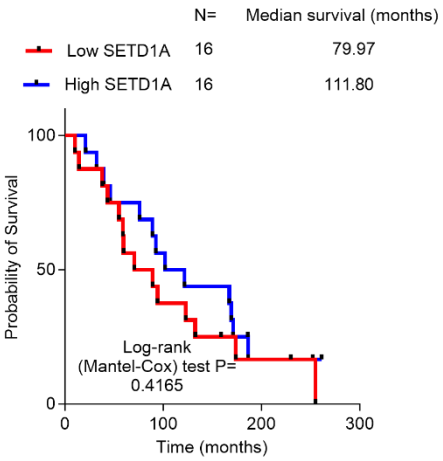
BRCA2-deficient breast cancer
N= Median survival (months)
Low SETD1A 16 79.97
High SETD1A 16 111.80
Probability of Survival
Log-rank (Mantel-Cox) test P= 0.4165
Time (months)

Figure 4.7- Downregulation of SETD1A expression is associated with poorer overall survival in ATM- and BRCA1-deficient tumours.

Kaplan-Meir plots of patients with the following HR-deficient/proficient cancers stratified by low versus high SETD1A expression: (A.) BRCA1 wild-type breast cancer from the METABRIC database. (B.) ATM wild-type non-small cell lung cancer from the TCGA database. (C.) BRCA1-deficient breast cancer from the METABRIC database. (D.) ATM-deficient non-small cell lung cancer from the TCGA database. (E.) BRCA1-deficient ovarian cancer from the TCGA database. (F.) BRCA2-deficient breast cancer from the TCGA database. HR gene-deficient patients were defined as homozygous deletion, mutation, or mRNA expression <=-2 SD below mean of the indicated HR-related genes. All data was obtained from the CBioPortal database https://www.cbioportal.org/. Patients with lower SETD1A mRNA expression (<median mRNA expression; red or purple line) were compared to those with higher SETD1A mRNA expression (>median mRNA expression; blue or green line). Curve comparisons were performed using the Log-rank (mantel-Cox) test.

4.5 Discussion

In this chapter I had two aims: to extend my previous observations from BRCA1- or ATM-deficient HeLa cells, in which SETD1A loss restored HR and conferred PARPi resistance, to HR-deficient cancer cell line models, and to examine the impact of SETD1A expression on the survival of HR-deficient cancer patients.

4.5.1 Low SETD1A reduces PARPi sensitivity in BRCA1-mutated cancer cell lines by restoring homologous recombination

In this chapter, I have shown that the *BRCA1*-mutated ovarian cancer cell line, UWB1.289 is sensitive to treatment with the PARPi olaparib. These results are in concordance with several previous studies showing UWB1.289 cells display sensitivity to PARPi treatment (Dickson *et al.*, 2021; Sharma Saha *et al.*, 2021; Lee *et al.*, 2023). Furthermore, reconstitution of BRCA1 expression has been shown to reduce cytotoxicity of UWB1.289 cells following PARPi treatment, demonstrating that the increased sensitivity of UWB1.289 to olaparib is due to loss of wild-type BRCA1 function (Deng *et al.*, 2022). There is contradictory evidence as to whether HCC1937 cells show sensitivity to PARPi treatment with some studies showing significant PARPi sensitivity (Drew *et al.*, 2010; Bosnjak *et al.*, 2021), whilst other studies have questioned the sensitivity of HCC1937 cells to PARP inhibition. For example, Lehmann *et al*. found that HCC1937 cells were sensitive to the PARPi veliparib but not olaparib, suggesting other factors in addition to *BRCA1* status determine sensitivity to this PARPi (Lehmann *et al.*, 2011). Due to the lack of BRCA1-proficient cancer type matched control I was unable to comment on the relative sensitivity of HCC1937 cells to Olaparib treatment compared to a non-sensitive cell line. To

improve the interpretation of this data I would need to perform survival analysis of HCC1937 cells alongside a BRCA1 reconstituted cell line in the future.

Differences in PARPi sensitivity observed between studies could be attributed to different methodologies used to measure cellular survival. For instance, one study demonstrated that measuring the antiproliferative effects of olaparib using the MTT assay only showed a 24.8 % growth inhibition in HCC1937 cells, whereas colony formation assays showed significantly greater inhibition of 75 % (Pierce *et al.*, 2013). This highlights that cellular sensitivity can vary largely, dependent on the specific cell viability assay used to measure it. I selected colony survival assays to measure cell viability in this thesis, as they directly measure the ability of a single cell to proliferate to form a colony, as opposed to MTT assays, which indirectly measure viability by quantifying cellular metabolism.

Loss of SETD1A also increased HR-mediated repair in both UWB1.289 and HCC1937 cells. Both cell lines displayed defects in RAD51 foci formation, which is consistent with their PARPi sensitivity and lack of functional BRCA1 protein expression. This is in accordance with previous findings showing HCC1937 cells failed to form RAD51 foci following ionising radiation, validating their HR-deficient status (Gu *et al.*, 2016). Similarly, studies have confirmed UWB1.289 cells HR-deficient status by measuring RAD51 foci following DNA damage (Sharma Saha *et al.*, 2021) or adenovirus-based HR reporter assays (Lee *et al.*, 2023). Despite this, in contradiction with the findings in this chapter, other studies have shown that although UWB1.289 cells possess a pathogenic *BRCA1* mutation, they retain greater than 50 % functional HR status, a similar level to BRCA1-profient SKOV3 cells (Meijer *et al.*, 2024). This study would suggest there is discrepancy between BRCA1 mutation

status and functional HR activity and that an alternative mode of action is responsible for PARPi sensitivity/resistance in UWB1.289 cells. The discrepancies between studies determining the HR status are likely attributed to differences in the methodologies used to determine HR status.

Consistent with my previous observations that BRCA1-deficiency increases NHEJ-mediated chromosomal radial formation following olaparib treatment, studies have shown PARPi treatment activates DSB repair by NHEJ in UWB1.289 cells, as demonstrated by increased DNA-PKc phosphorylation (Deng *et al.*, 2022). Furthermore, treatment with the DNA-PK inhibitor, NU7441, significantly upregulated RAD51 foci formation, restoring HR in the UWB1.289 cell lines (McCormick *et al.*, 2017). These observations support a mechanism by which loss of SETD1A confers PARPi resistance in UWB1.289 cells by decreasing NHEJ activation in parallel to restoring HR. We could confirm this hypothesis in the future by measuring radial chromosome formation following SETD1A loss in these *BRCA1*-mutated cancer cell lines.

4.5.2 Low SETD1A did not affect PARPi sensitivity in an ATM-mutated NSCLC cell line

In the previous chapter I extended loss of SETD1A as a novel mechanism of PARPi resistance to ATM-deficient HeLa cells, however, colony survival analyses demonstrated that loss of SETD1A had no effect on PARPi sensitivity in *ATM*-mutated H1395 NSCLC cells, despite restoring HR. As discussed above a key limitation of this analysis is a lack of parental control which means the relative sensitivity of H1395 cells to PARPi treatment cannot be determined. Future experiments reconstituting functional ATM activity in these ATM-mutated cell lines are

required to further confirm the impact of SETD1A depletion on PARPi sensitivity in this cell line.

Despite this, these findings may therefore suggest that HR status alone does not correspond to PARPi sensitivity in H1395 cells, and there could be additional mechanisms co-occurring alongside ATM-deficiency determining PARPi sensitivity. This prediction is evidenced by the TOPARP-B trial investigating the use of olaparib in ATM-deficient tumours. This study showed detection of ATM alterations alone might not be sufficient to identify PARPi sensitivity and that the synthetic lethality in ATM-deficient cells treated with PARPi depends on cellular background and molecular events co-occurring with ATM loss. For example, in addition to the *ATM* mutation, the H1395 cancer cell line possesses mutations in *BRAF*, a gene mutated in 3-5% of NSCLC (Perrone *et al.*, 2022). Therefore, the presence of these additional mutations could also have implications for PARPi sensitivity in this cell type. To confirm whether loss of SETD1A confers PARPi resistance in ATM-mutated cancer types, an expanded panel of *ATM* mutated cancer cell lines should be investigated, encompassing other cancer types with different mutational landscapes.

4.5.3 Low SETD1A mRNA expression is associated with poor overall survival in some HR-deficient cancer types

I also demonstrated that the survival of BRCA1- or ATM-deficient cancer patients could be triaged by SETD1A expression, whereby reduced SETD1A expression correlated with reduced overall survival. This was particularly evident for ATM-deficient NSCLC. SETD1A has been associated with NSCLC progression in multiple studies (Kang *et al.*, 2021b; Du *et al.*, 2021). However, these studies suggested that high expression of SETD1A correlates with poor prognosis in NSCLC (Wang *et al.*,

2021; Du *et al.*, 2021). This discrepancy may be because my analyses were performed on NSCLC with ATM aberrations, whilst these previous studies included all patients regardless of HR status. This suggests that the stratification of NSCLC by SETD1A expression is markedly influenced by ATM status and indicates that loss of SETD1A has specific consequences in HR-deficient cells.

Although, SETD1A expression correlated with patient survival in ATM mutated NSCLC cancer patients, SETD1A depletion did not influence cellular survival in *ATM*-mutated NSCLC cell lines. As discussed above, co-occurring mutations in other genes could have significant influence on survival in this cancer type. Further investigation of cancer genomics data showed 9 % of ATM-deficient NSCLCs also possess a *BRAF* mutation, with greater than 60 % of these mutations occurring in patients with high SETD1A expression. Therefore, *BRAF* mutation status could also be linked to SETD1A expression and contribute to improved survival in these patients.

Additionally, we found that reduced SETD1A expression did not influence survival in BRCA2-deficienct or HR-proficient cancers. These findings are in keeping with unpublished findings showing that loss of SETD1A cannot restore HR to induced PARPi resistance in BRCA2-deficient (Sweatman *et al.*, 2024) or HR-proficient HeLa cells. This can be attributed to the differing roles of ATM, BRCA1 and BRCA2 in HR. Whilst ATM and BRCA1 promote end-resection and the initial steps of HR and their loss can partially be overcome by loss of competing pathways, BRCA2 is absolutely required for RAD51-dependent recombination. This is in keeping with multiple studies demonstrating that loss of pro-NHEJ factors cannot drive PARPi resistance in BRCA2-deficient cells (Bhin *et al.*, 2023; Gogola, Rottenberg and Jonkers, 2019).

A key limitation of this survival analysis is the small patient numbers available for analysis. Furthermore, clinical information regarding anti-cancer therapies was not publicly available, thus I was unable to stratify patients based on PARPi response. Therefore, the interaction between HR status, SETD1A expression, PARPi treatment and overall patient survival could not be analysed. Hopefully, increased use of PARPi to treat a wider range of cancer types in the clinic will result in more clinical data available, allowing this analysis to be extended in the future.

In the future I would also extend this chapter by repeating experiments in a broader range of HR-deficient cancer cell lines, such as the *BRCA1*-mutant triple negative breast cancer cell line, MDA-MB-436, which has been shown to have an increased response to PARPi in comparison to HCC937 (Keung *et al.*, 2020). Furthermore, with access to tissue sections from BRCA1- and ATM-deficient cancer patients treated with PARPi we could perform immunohistochemical staining for SETD1A expression to further validate whether SETD1A expression correlates with response to treatment with PARPi in the clinic. Additionally, by measuring SETD1A expression in HR-deficient cancers over the course of treatment, we could also determine whether low SETD1A expression is a pre-existing or acquired mechanism of PARPi resistance.

In summary, the findings presented in this chapter firmly establish that loss of SETD1A drives PARPi resistance, particularly in BRCA1-deficient contexts and expands the relevance of this proposed PARPi resistance mechanism to cancer-type appropriate models of HR-deficiency. However, further investigations are required to confirm whether loss of SETD1A is a potentially clinically relevant mechanism of PARPi resistance, specifically in the context of ATM-deficiency. Based on this data we

predict low SETD1A expression could potentially provide a biomarker for patient prognosis in patients with BRCA1- or ATM-deficiencies.

5. CHAPTER 5: CHARACTERISING CELL LINES WITH INDUCIBLE CAS9-MEDIATED GENE EDITING OF SETD1A

5.1 Introduction

Previously, I demonstrated that SETD1A knockdown using siRNA reduced PARPi sensitivity of ATM-deficient cells by restoring HR. siRNA transiently silences targets by degrading mRNA transcripts, thus the biggest limitations of this approach are incomplete knockdown of the target mRNA and potential off-target effects (Jackson *et al.*, 2006). Considering this, I sought to validate our previous findings with an alternative system, which employed CRISPR-Cas9 to genetically edit SETD1A and deplete functional gene expression.

This system uses a single guide RNA (gRNA), which recognises the target gene in a sequence specific manner through complementary base pairing. This directs the CRISPR-associated protein (Cas9) to generate DSBs at specific genomic regions upstream of a conserved DNA sequence downstream of the cut site called the protospacer adjacent motif (PAM). These breaks are subsequently repaired by error-prone NHEJ, which can induce insertions/deletions that alter the reading-frame and generate premature termination codons in the target gene. The nascent mRNA is then degraded by the nonsense-mediated decay system, leading to disrupted expression of the target gene (Asmamaw and Zawdie, 2021).

However, SETD1A appears to be an essential gene, illustrated by the fact that homozygous knockout in mice causes early embryonic lethality (Tusi *et al.*, 2015). Furthermore, SETD1A was shown to be essential for the proliferation of numerous cancer cells lines through CRISPR loss-of-function screens in the DepMap portal,

where it has been characterised as a ‘common essential gene’ (Tsherniak *et al.*, 2017). As a result, creating a stable *SETD1A* knockout cell line is technically difficult and can only be achieved in cells also depleted of p53 (Kang *et al.*, 2021a). Instead, we therefore induced a conditional SETD1A deletion using a doxycycline inducible Cas9 system (Simon Boulton). In this system Cas9 expression is under the control of a tetracycline operator containing promoter. In the absence of doxycycline, Cas9 expression is suppressed, however, following doxycycline treatment, the tetracycline operator-containing Cas9 promoter is activated to induce Cas9 expression and subsequent Cas9 mediated gene editing of SETD1A (Zhang *et al.*, 2019).

5.2 Creation and characterisation of HeLa Kyoto inducible Cas9 SETD1A gRNA cell lines

To create the inducible Cas9-mediated SETD1A edited cell line, HeLa Kyoto cells expressing a doxycycline inducible Cas9 (iCas9) were transduced with pre-existing lentivirus containing three different sgRNA targeting human *SETD1A.* These gRNAs targeted different exons of *SETD1A* (**Fig. 5.1**). Additionally, a non-targeting control (NTC) gRNA which does not target any known human gene was used as a negative control for SETD1A depletion.

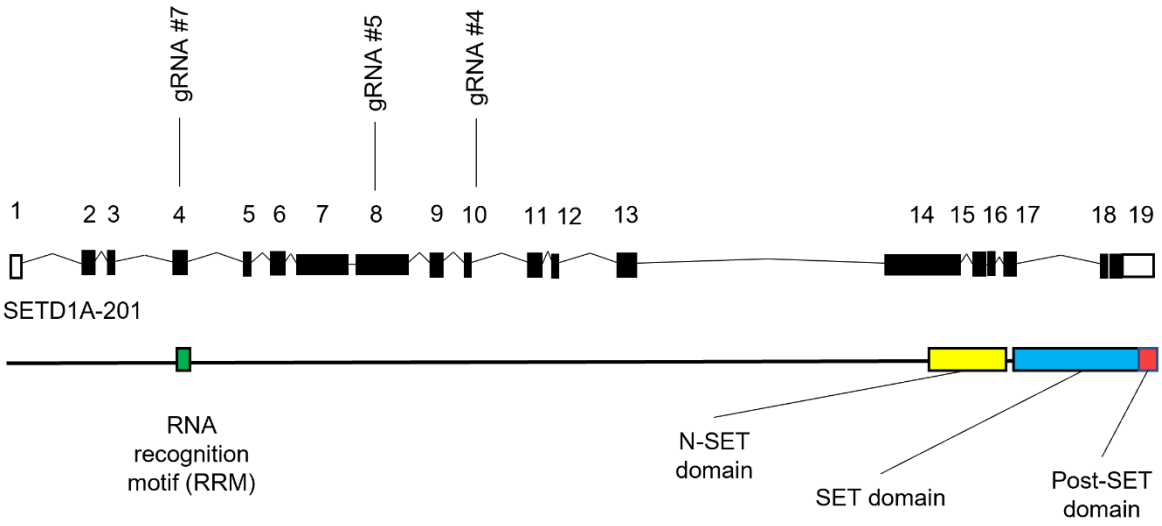

Figure 5.1- SETD1A exons targeted by gRNAs.

Schematic of the exons of SETD1A targeted by the three individual gRNAs transfected into HeLa Kyoto iCas9 cell lines. Transcript information and domain annotations were obtained from ensembl genome browser https://useast.ensembl.org/index.html.

Firstly, I assessed the impact of SETD1A gene editing on protein expression by western blotting using HeLa Kyoto iCas9 cells expressing SETD1A gRNA. Upon addition of doxycycline to induce Cas9-mediated gene editing of SETD1A, two different gRNAs (#4 or #5) demonstrated significant reduction of SETD1A protein expression, whilst no change in SETD1A protein expression was observed using the NTC gRNA (**Figs 5.2 A and B).** Furthermore, Cas9-mediated gene editing of SETD1A had no impact on the expression of key interacting proteins: RIF1, BOD1L or WDR5 (**Figs 5.2 A, C, E and F**), as well as ATM (**Figs 5.2 A and D).** Surprisingly, given its role as a H3K4 methyltransferase, the expression of global H3K4me3 was also unchanged following Cas9-mediated gene editing of SETD1A (**Figs 5.2 A and G**).

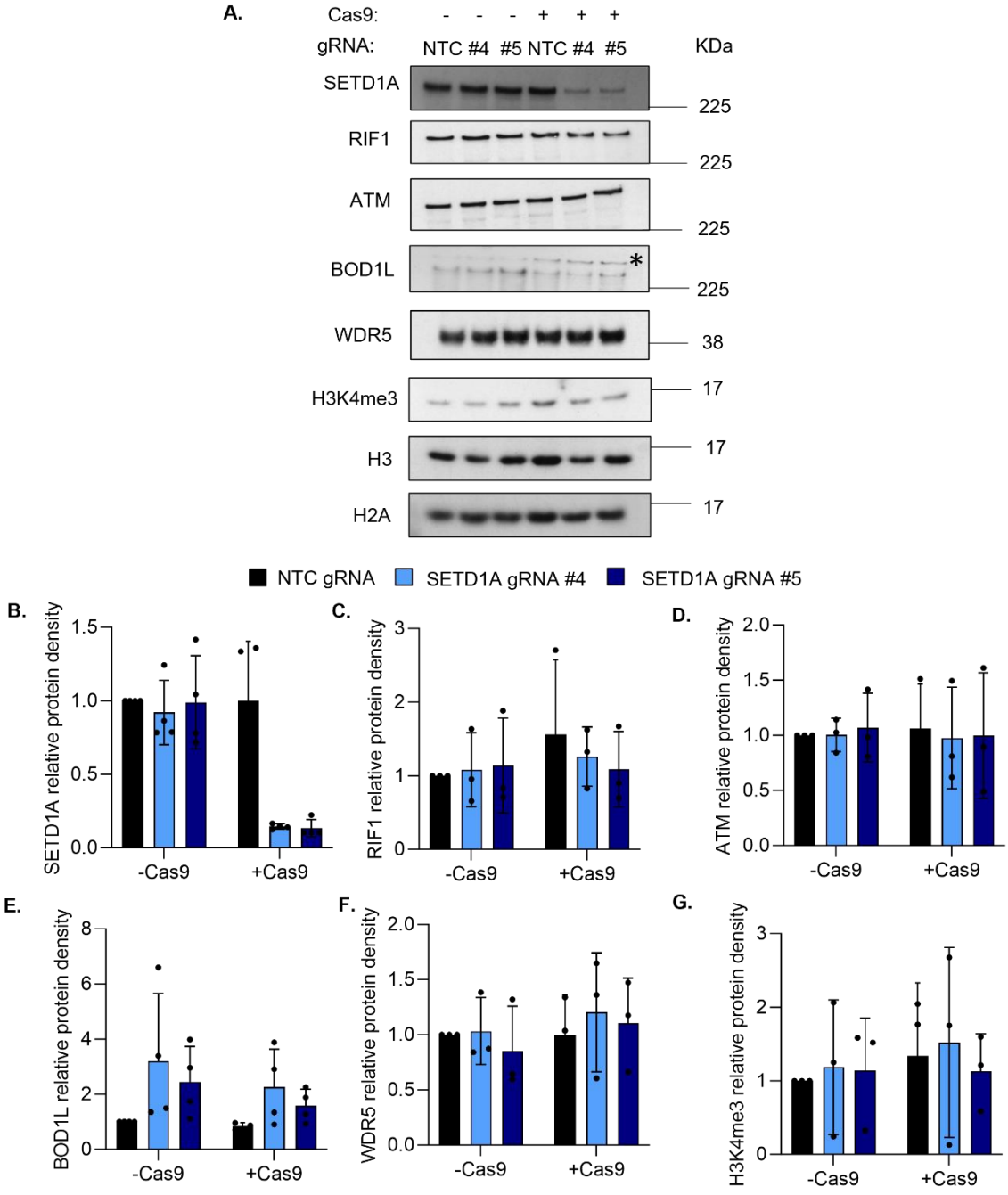

Figure 5.2- Cas9-mediated gene editing of SETD1A significantly reduces SETD1A protein expression.

*(A.) Hela Kyoto iCas9 cell lines expressing SETD1A gRNA #4 or #5, or a non-targeting control (NTC) were treated for 72 hours ± 1 µg/ml doxycycline. After 72 hours the cells were harvested and whole cell extracts were immunoblotted using the indicated antibodies. (B-G.) Immunoblot quantification from (A.) using ImageJ. All plots represent the mean ± SD from three independent biological repeats. *= nonspecific band.*

5.3 Cas9-mediated gene editing of SETD1A reduces RIF1 foci formation and increases BRCA1 foci formation following ionising radiation

As mentioned previously, SETD1A knockdown reduces RIF1 foci formation and increases BRCA1 foci formation in G1 cells following IR (Bayley *et al.*, 2022). To validate these cell lines further, I aimed to recapitulate these findings in the HeLa Kyoto iCas9 cells. BRCA1 and RIF1 foci formation were measured following ionising radiation in G1 cells (**Fig. 5.3 A**), as under normal conditions end resection is suppressed in G1, protecting DNA ends to favour NHEJ. Thus, under normal conditions RIF1 foci should be formed in G1 but BRCA1 foci should be absent in response to DNA damage. However, previous studies have shown loss of end protection factors, such as SETD1A leads to unrestrained end-resection of G1 breaks, characterised by accumulation of BRAC1 foci (Bayley *et al.*, 2022).

In accordance with knockdown, Cas9-mediated gene editing of SETD1A using gRNA #4 or #5 significantly increased IR-induced BRCA1 foci (**Figs 5.3 B and D**) and markedly decreased RIF1 foci formation (**Figs 5.3 C and E**) in G1 cells. Together, these findings suggest that SETD1A gene editing has similar effects on DNA repair kinetics in comparison to siRNA mediated knockdown. Both gRNA #4 and #5 produced similar levels of SETD1A depletion and RIF1 foci recruitment, therefore we chose to use gRNA #4 going forward with future experiments.

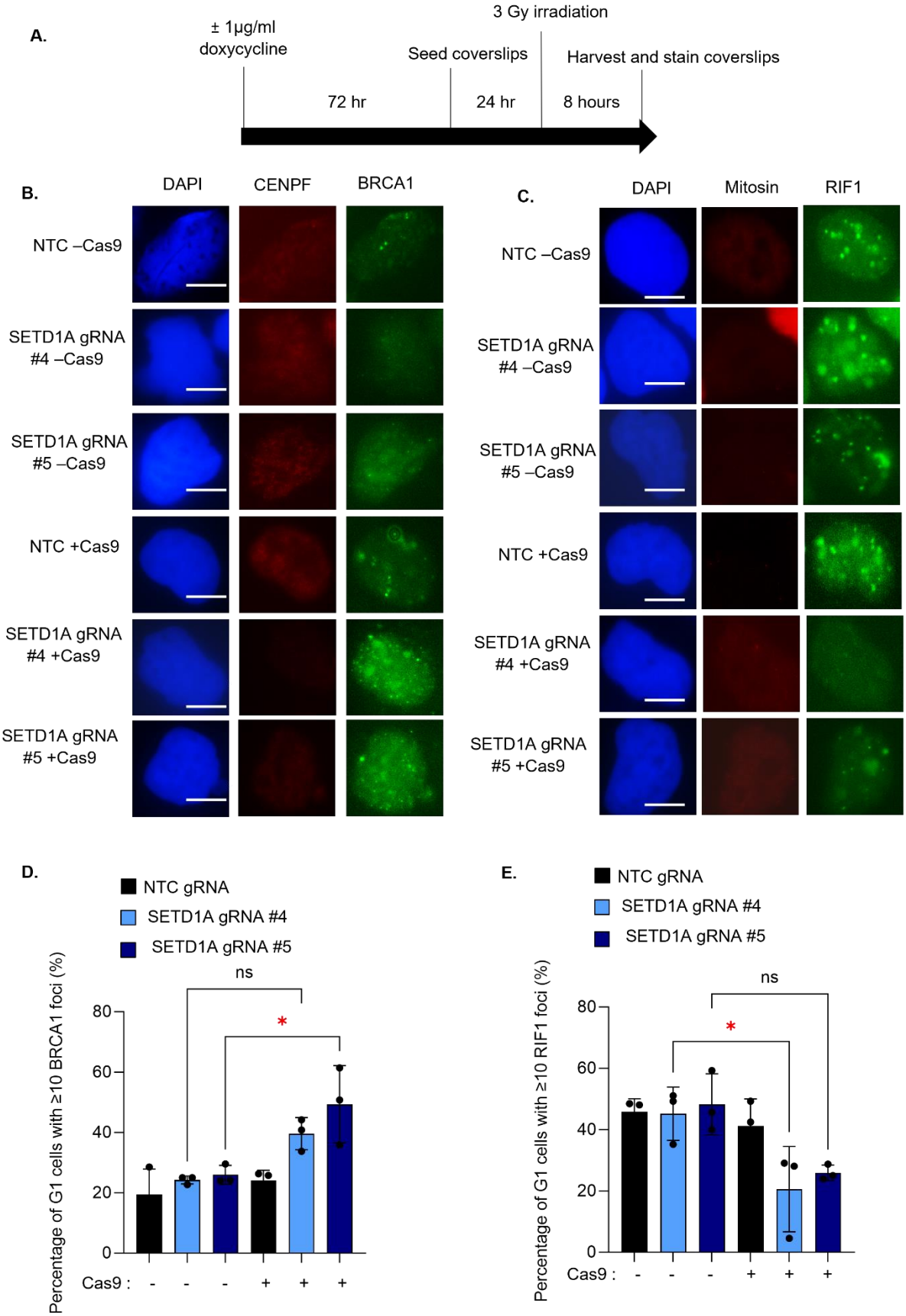
A.
± 1µg/ml doxycycline
3 Gy irradiation
Seed coverslips
Harvest and stain coverslips
72 hr
24 hr
8 hours
B.
DAPI
CENPF
BRCA1
NTC –Cas9
SETD1A gRNA #4 –Cas9
SETD1A gRNA #5 –Cas9
NTC +Cas9
SETD1A gRNA #4 +Cas9
SETD1A gRNA #5 +Cas9
C.
DAPI
Mitosin
RIF1
NTC –Cas9
SETD1A gRNA #4 –Cas9
SETD1A gRNA #5 –Cas9
NTC +Cas9
SETD1A gRNA #4 +Cas9
SETD1A gRNA #5 +Cas9
D.
NTC gRNA
SETD1A gRNA #4
SETD1A gRNA #5
ns
*
Percentage of G1 cells with ≥10 BRCA1 foci (%)
80
60
40
20
0
Cas9 : - - - + + +
E.
NTC gRNA
SETD1A gRNA #4
SETD1A gRNA #5
ns
*
Percentage of G1 cells with ≥10 RIF1 foci (%)
80
60
40
20
0
Cas9 : - - - + + +

Figure 5.3- Cas9-mediated gene editing of SETD1A increases BRCA1 foci and decreases RIF1 foci formation following ionising radiation.

*Hela Kyoto iCas9 cells expressing SETD1A gRNA #4 or #5, or a non-targeting control (NTC) were treated for 72 hours ± 1 μg/ml doxycycline. Cells were harvested 8 hours post exposure to 3 Gy IR and immunostained for RIF1 or BRCA1. G1 cells were identified as CENPF/mitosin negative and nuclei counterstained with DAPI. (A.) Schematic of experimental time course. (B and C.) Representative immunofluorescent images (scale bar 10 μm). (D and E.) Quantification of the percentage of G1 cells with ≥10 RIF1 or BRCA1 foci 8-hour post IR. At least 100 cells were counted per condition. Data points represent the mean ± SD from three independent biological repeats. ns= not statistically significant, * = P <0.05 as determined by a one-way ANOVA with post-hoc Tukey's test for multiple comparisons.*

5.4 Cas9-mediated gene editing of SETD1A increases sensitivity of ATM-deficient cells to olaparib

Next, I aimed to assess the effect of SETD1A depletion, by Cas9-mediated gene editing, on PARPi sensitivity in the absence of ATM. To keep experimental conditions consistent with previous experiments using siRNA-mediated depletion of SETD1A, induction of Cas9 expression was reduced from 72- to 48-hours. I confirmed, by western blotting, that reducing length of doxycycline treatment was sufficient to induce Cas9 protein expression and decrease SETD1A expression in cells expressing SETD1A gRNA #4. As before, SETD1A gene editing had no impact on the expression of SETD1A interacting proteins (**Fig. 5.4**).

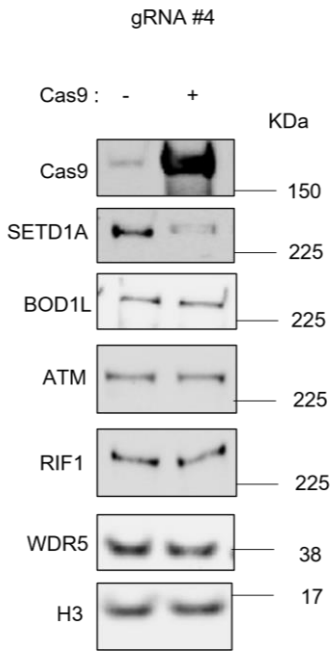

Figure 5.4- Forty-eight hours of Cas9 expression is sufficient to substantially reduce SETD1A levels.

Hela Kyoto iCas9 cells expressing SETD1A gRNA #4 were treated for 48 hours ± 1 μg/ml doxycycline. After 48 hours the cells were harvested and whole cell extracts were immunoblotted using the indicated antibodies. Blot representative of three independent biological repeats.

Next, I investigated cellular response to PARP inhibition. HeLa Kyoto iCas9 cells expressing gRNA #4 or a NTC were transfected with control or ATM siRNA and treated ± 1 μg/ml doxycycline to induce Cas9-mediated gene editing of SETD1A. Cells were then plated at low density, and I performed clonogenic survival assays as described above (**Fig. 5.5 A**). As before, gene editing of SETD1A was confirmed by western blot (**Fig. 5.5 B**).

As expected, prior to Cas9 induction, expression of the NTC or gRNA #4 did not influence PARPi sensitivity, whereas ATM knockdown significantly increased sensitivity to olaparib treatment. In control siRNA treated cells SETD1A gene editing conferred a small decrease in cellular survival at higher olaparib concentrations. However, the most notable finding was that Cas9-mediated gene editing of SETD1A further increased the olaparib sensitivity of ATM depleted cells (**Figs 5.5 C and D**). This contradicts earlier findings where siRNA mediated depletion of SETD1A reduced PARPi-sensitivity in ATM-deficient cells. Together these findings highlight significant differences in PARPi response in ATM-deficient cells following these two methods of genetic manipulation.

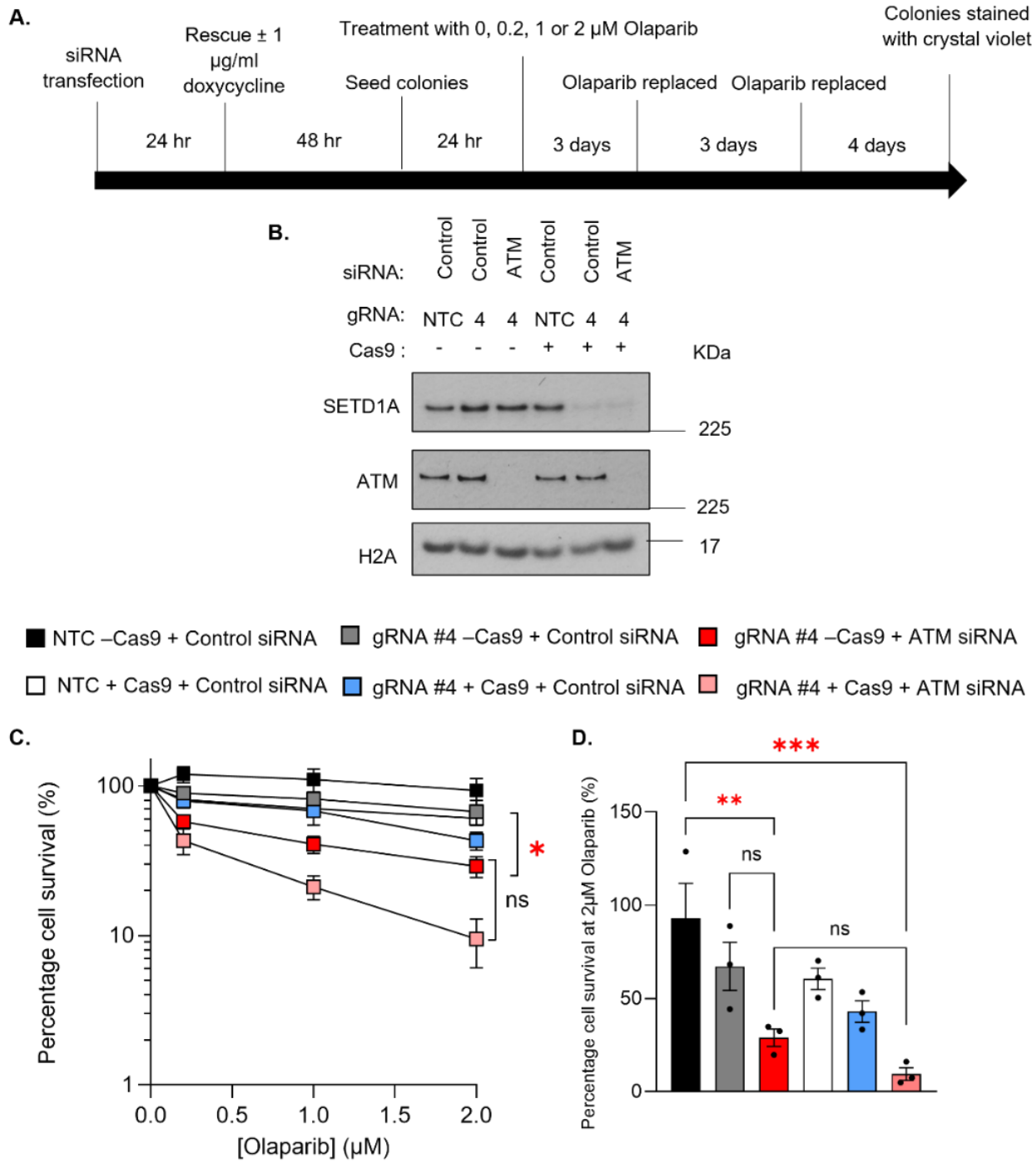
A.
siRNA transfection
Rescue ± 1 µg/ml doxycycline
Treatment with 0, 0.2, 1 or 2 µM Olaparib
Seed colonies
Olaparib replaced
Olaparib replaced
Colonies stained with crystal violet
24 hr
48 hr
24 hr
3 days
3 days
4 days
B.
siRNA: Control Control ATM Control Control ATM
gRNA: NTC 4 4 NTC 4 4
Cas9 : - - - + + +
KDa
SETD1A
225
ATM
225
H2A
17
NTC –Cas9 + Control siRNA
gRNA #4 –Cas9 + Control siRNA
gRNA #4 –Cas9 + ATM siRNA
NTC + Cas9 + Control siRNA
gRNA #4 + Cas9 + Control siRNA
gRNA #4 + Cas9 + ATM siRNA
C.
Percentage cell survival (%)
100
10
1
0.0
0.5
1.0
1.5
2.0
[Olaparib] (µM)
*
ns
D.
Percentage cell survival at 2µM Olaparib (%)
150
100
50
0
***
**
ns
ns

Figure 5.5- Cas9-mediated gene editing of SETD1A increases sensitivity of ATM-deficient cells to olaparib treatment.

*(A.) Schematic of experimental time course. (B.) Whole cell extracts of HeLa Kyoto cells treated with indicated siRNAs were immunoblotted with the indicated antibodies. (C.) Clonogenic survival curve for HeLa Kyoto iCas9 cells expressing SETD1A gRNA #4, or a non-targeting control (NTC) transfected with the indicated siRNAs ± 48-hour treatment with 1 µg/ml doxycycline. Cells were then exposed to the indicated doses of olaparib for 10 days before staining with crystal violet and colonies counted. *= P < 0.05 gRNA #4 -Cas9 + Control siRNA vs gRNA #4 -Cas9 + ATM siRNA, ns= not significant gRNA #4 -Cas9 + ATNM siRNA vs gRNA #4 +Cas9 + ATM siRNA as determined by a two-way ANOVA with post-hoc Tukey's test for multiple comparisons (D.) Percentage cell survival from (C.) at 2 µM olaparib. Data points represent the mean ± SEM from three independent biological repeats. ns= not statistically significant, ** = P <0.01, *** = P < 0.001 as determined by a one way ANOVA with post-hoc Tukey's test for multiple comparisons.*

5.5 Cas9-mediated gene editing of SETD1A restores homologous recombination in ATM-deficient cells

Previously, PARPi resistance was attributed to restored HR following SETD1A depletion. Therefore, I next investigated whether the increased PARPi sensitivity observed following Cas9-mediated gene editing of SETD1A in ATM-deficient cells was due to a persistent defect in HR. As before, RAD51 foci formation was used as a surrogate for HR activity (**Fig. 5.6 A**) and gene editing efficacy was confirmed by western blot (**Fig. 5.6 C**).

Expression of gRNA #4 or the NTC alone had no effect on RAD51 foci formation following olaparib treatment. On the other hand, ATM knockdown induced a significant defect in PARPi-induced RAD51 foci formation, which was restored to control levels following Cas9-mediated SETD1A gene editing (**Figs 5.6 D and E**). This is in accordance with previous results following SETD1A knockdown but inconsistent with survival data following Cas9-mediated gene editing of SETD1A. I then validated these findings using the LMNA-CRISPR HR assay to measure functional HR repair (**Fig. 5.6 B**). In two independent repeats we also observed SETD1A depletion by Cas9 gene editing restored the HR defect observed in ATM-deficient cells (**Fig. 5.6 F**). Together these results show that SETD1A depletion by Cas9-mediated gene editing restores HR in ATM-deficient cells despite increasing PARPi sensitivity.

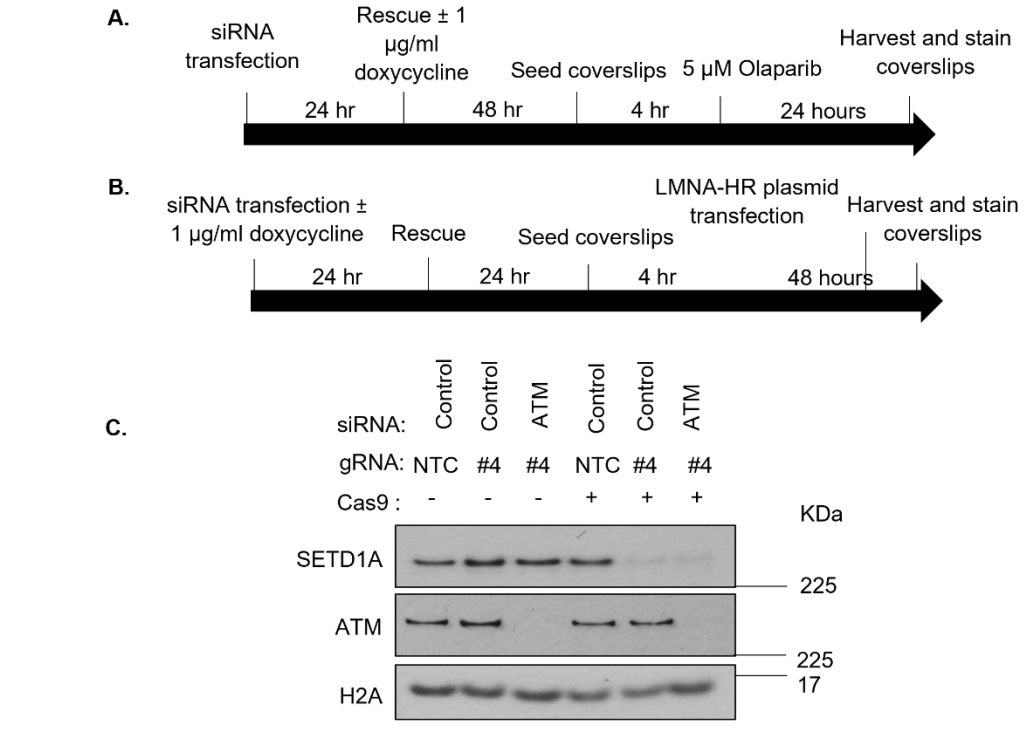
A.
siRNA transfection
Rescue ± 1 µg/ml doxycycline
Seed coverslips
5 µM Olaparib
Harvest and stain coverslips
24 hr
48 hr
4 hr
24 hours
B.
siRNA transfection ± 1 µg/ml doxycycline
Rescue
Seed coverslips
LMNA-HR plasmid transfection
Harvest and stain coverslips
24 hr
24 hr
4 hr
48 hours
C.
siRNA: Control Control ATM Control Control ATM
gRNA: NTC #4 #4 NTC #4 #4
Cas9 : - - - + + +
KDa
SETD1A
225
ATM
225
H2A
17

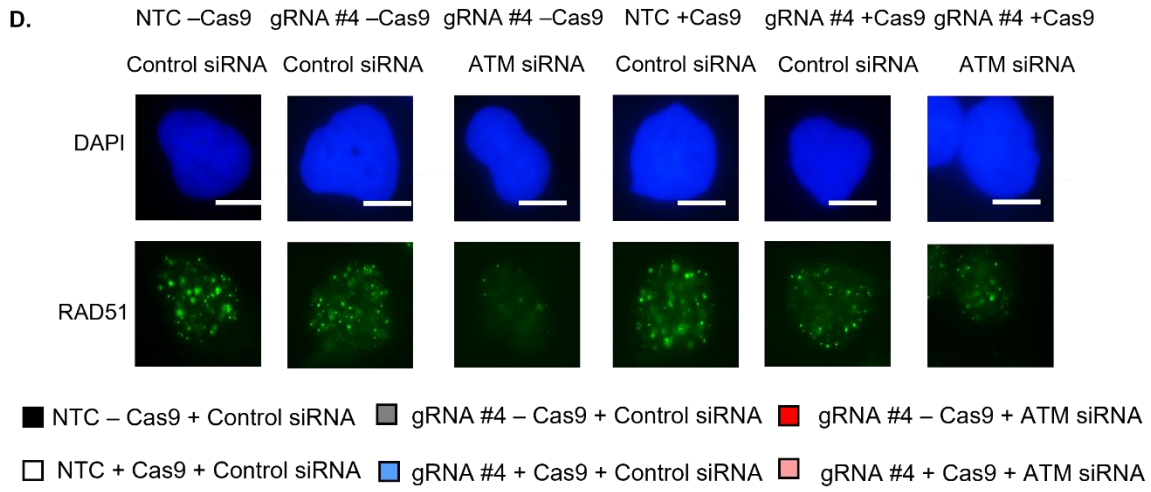
D.
NTC –Cas9
gRNA #4 –Cas9
gRNA #4 –Cas9
NTC +Cas9
gRNA #4 +Cas9
gRNA #4 +Cas9
Control siRNA
Control siRNA
ATM siRNA
Control siRNA
Control siRNA
ATM siRNA
DAPI
RAD51
NTC – Cas9 + Control siRNA
gRNA #4 – Cas9 + Control siRNA
gRNA #4 – Cas9 + ATM siRNA
NTC + Cas9 + Control siRNA
gRNA #4 + Cas9 + Control siRNA
gRNA #4 + Cas9 + ATM siRNA

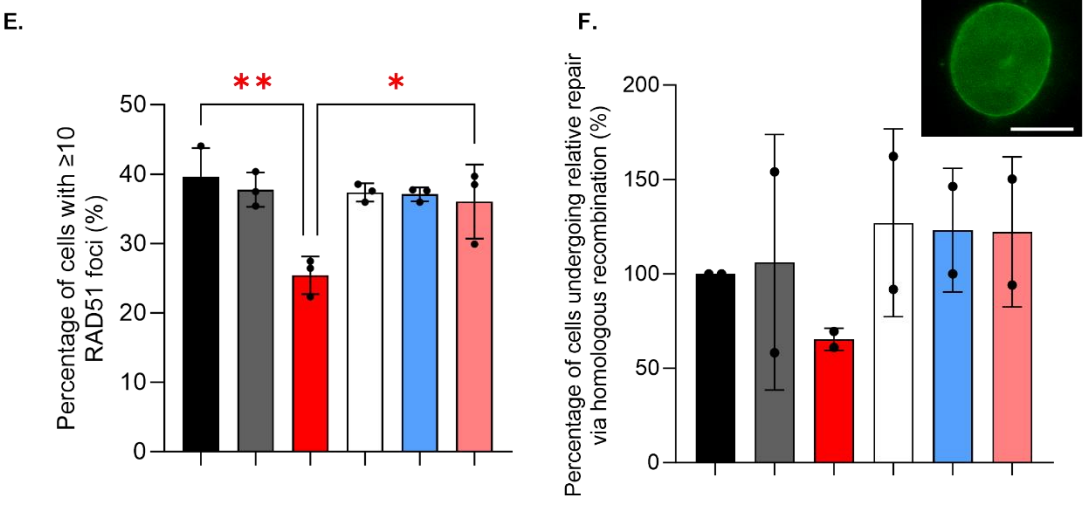
E.
**
*
Percentage of cells with ≥10 RAD51 foci (%)
0
10
20
30
40
50
F.
Percentage of cells undergoing relative repair via homologous recombination (%)
0
50
100
150
200

Figure 5.6- Cas9-mediated gene editing of SETD1A increases RAD51 foci formation and restores HR in ATM-deficient cells treated with olaparib.

*HeLa Kyoto iCas9 cell lines expressing SETD1A gRNA #4, or a non-targeting control (NTC) were transfected with the indicated siRNAs. Cells were treated with ± 1 μg/ml doxycycline for 48 hours to induce Cas9 expression and (A.) exposed to 5 μM olaparib for 24 hours, then immunostained with an antibody to RAD51 and counterstained with DAPI. Foci formation was enumerated by fluorescent microscopy or (B) transfected with CRISPR-Cas9 HR plasmids encoding fluorescent nuclear Lamin A/C and a plasmid encoding red fluorescent protein (RFP). Relative percentage of cells expressing fluorescent Lamin and RFP were enumerated by fluorescent microscopy. (C.) Whole cell extracts of Hela Kyoto iCas9 cells were immunoblotted by indicated antibodies. (D.) Representative immunofluorescent images of RAD51 foci (scale bar 10 μm). (E.) Graphical representation of the percentage of cells with ≥10 RAD51 foci 24 hours post olaparib treatment. Results represent the mean ± SD from three biologically independent experiments. * = P < 0.05, ** = P <0.01 as determined by a one-way ANOVA with post-hoc Tukey's test for multiple comparisons. (F.) Graphical representation of percentage relative repair by HR. The number of fluorescent Lamin expressing cells were normalised to RFP expression. Results represent the mean ± SEM from two biologically independent experiments (scale bar 10 μm). In both cases at least 100 cells were counted per condition.*

5.6 Cas9-mediated gene editing of SETD1A does not decrease NHEJ-mediated radial formation in ATM-deficient cells

Previously, SETD1A depletion reduced PARPi-induced NHEJ-mediated radial chromosome formation in ATM-deficient cells, indicating a shift in DSB repair pathway use from NHEJ to HR. Therefore, I wanted to investigate the effect of Cas9-mediated gene editing of SETD1A on NHEJ-mediated radial formation using metaphase spreads (**Fig. 5.7 A**).

Consistent with our previous findings, ATM-deficient cells had a significant increase in olaparib-induced radial formation. However, unlike SETD1A knockdown, the levels of these radials remained unchanged following SETD1A depletion by Cas9-mediated gene editing (**Fig. 5.7 C**). This finding indicates that genomic instability persists following Cas9-mediated gene editing of SETD1A in ATM-deficient cells, which in keeping with clonogenic survival data is likely to drive increased cell death in this context.

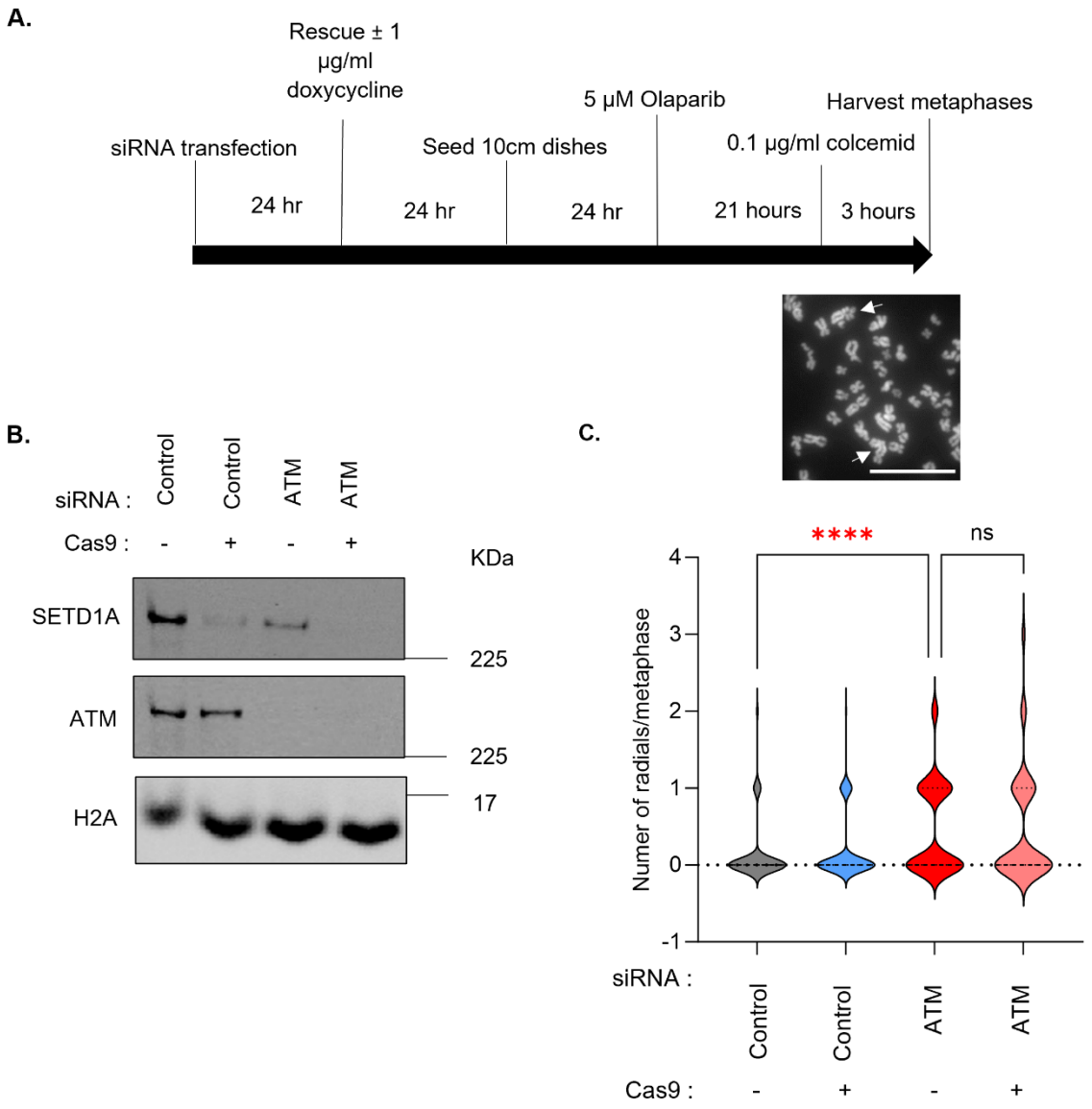

Figure 5.7- Cas9-mediated gene editing of SETD1A does not decrease NHEJ-mediated radial formation in ATM-deficient cells treated with olaparib.

*HeLa Kyoto iCas9 cells expressing SETD1A gRNA #4 were transfected with the indicated siRNAs and treated with ± 1 µg/ml doxycycline for 48 hours and 5 µM olaparib for 24 hours. Radial chromosome formation was analysed by DAPI staining and light microscopy. (A.) Schematic of experimental time course (B.) Whole cell extracts of HeLa cells treated with indicated siRNAs were immunoblotted with the indicated antibodies. (C.) Graphical representation of number of radials/metaphases (scale bar 10 µm). At least 50 metaphases were counted per condition. Data points represent mean ± SEM from two independent biological repeats. ns= not statistically significant, ****= P < 0.0001 as determined by a Kruskal-Wallis test with multiple comparisons.*

5.7 Cas9-mediated SETD1A gene editing of SETD1A alters PARP1 levels on chromatin

As described above, PARP trapping is another determinant of PARPi sensitivity. Therefore, I hypothesised that Cas9-mediated gene editing of SETD1A may increase the level of PARP trapping on damaged chromatin leading to increased PARPi sensitivity in ATM-deficient cells. To investigate this, gRNA #4 cells were treated with doxycycline for 48 hours to induce Cas9 expression ± ATM inhibitor and/or olaparib treatment for 24 hours. Cells were then fractionated, and chromatin-bound proteins analysed by immunoblotting (**Fig. 5.8 A**).

As expected, olaparib treatment increased PARP1 levels on the chromatin, confirming that olaparib effectively traps PARP1 under these conditions. In contrast, both inhibition of ATM and/or SETD1A gene editing decreased the levels of chromatin-bound PARP. Furthermore, combining SETD1A gene editing and ATM inhibition further decreased PARP1 chromatin levels (**Fig. 5.8 B**). For all conditions the levels of PARP1 in the whole cell fraction remained largely unchanged showing this difference was not due to changes in the levels of total PARP1 protein (**Fig. 5.8 A**). Despite this, changes in chromatin bound PARP1 did not correlate with PARPi sensitivity. For example, ATM inhibition significantly increases PARPi sensitivity but reduces PARP1 levels in the chromatin fraction. Furthermore, combining ATM inhibition with Cas9-mediated gene editing of SETD1A resulted in the lowest level of PARP trapping but the greatest PARPi sensitivity. These findings indicate that whilst loss of SETD1A and/or ATM inhibition affects the level of PARP on chromatin following olaparib treatment, PARP trapping is not the underlying mechanism of the

increased PARPi sensitivity observed following Cas9-mediated gene editing of SETD1A in ATM-deficient cells.

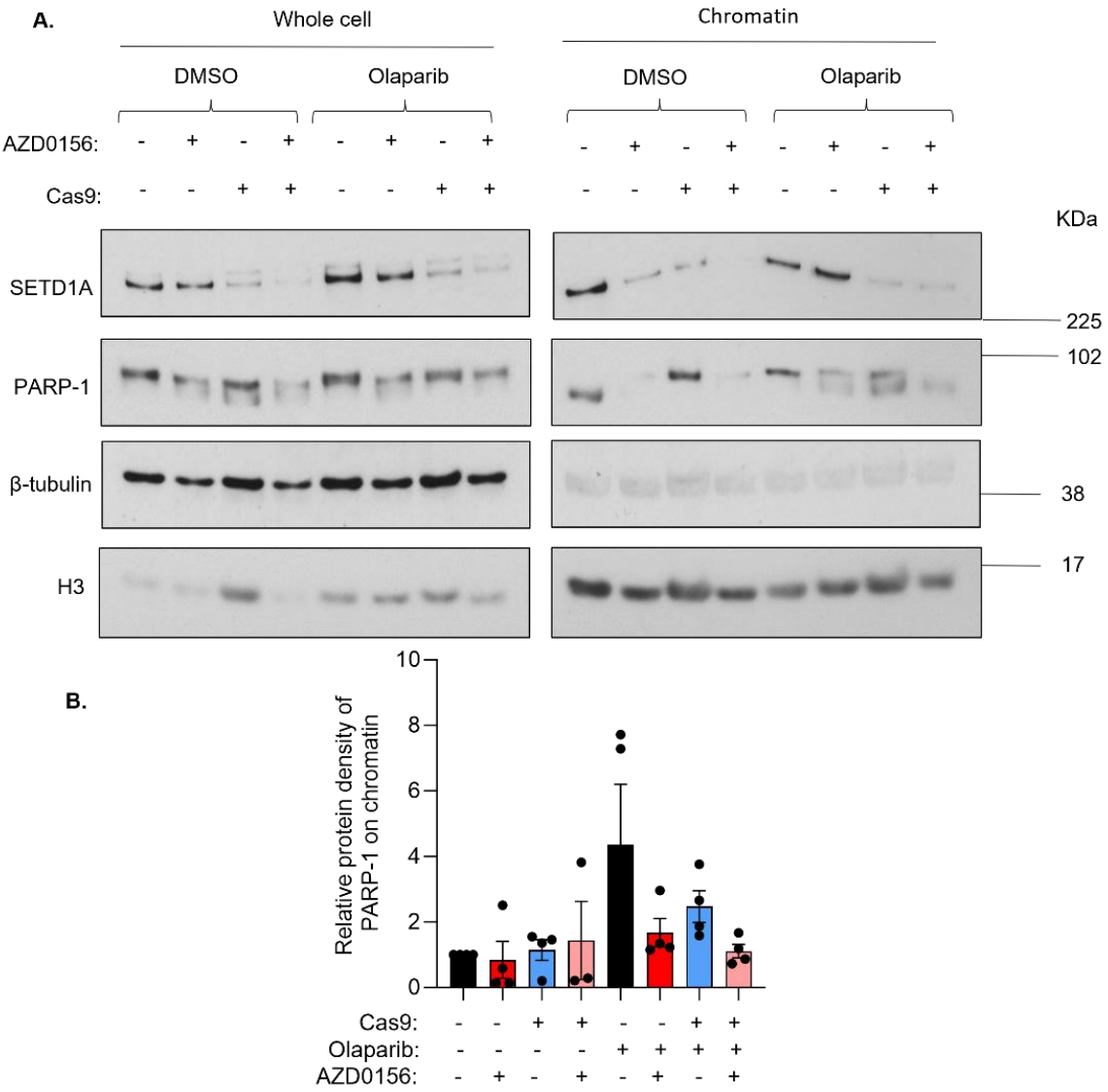

Figure 5.8- Cas9-mediated gene editing of SETD1A and/or ATM inhibition reduces PARP1 levels on chromatin.

HeLa Kyoto iCas9 cells expressing SETD1A gRNA #4 were treated with ± 1 µg/ml doxycycline for 48 hours to induce Cas9 expression. Cells were then treated with 10 µM olaparib ± 1 µM AZD0156 for 24 hours, and chromatin fractions isolated. (A.) Western blot analysis of whole cell, nuclear soluble and chromatin bound fractions using the indicated antibodies. (B.) Quantification of PARP1 levels in the chromatin binding fraction relative to total PARP1 expression in the whole cell lysate and normalised to the untreated control. Band signal intensity was quantified using ImageJ. Data points represent mean ± SD from three independent biological repeats.

5.8 Cas9-mediated gene editing of SETD1A with gRNA #7 increases sensitivity of ATM-deficient cells to olaparib

So far, the findings presented in this chapter largely contradict the results observed following SETD1A knockdown. To determine whether these unexpected findings were specific to gRNA #4, which targets SETD1A at exon 10, I aimed to validate results using an alternative SETD1A gRNA #7 which targets SETD1A at exon 4 (**Fig. 5.1 A**).

Firstly, I confirmed that gRNA #7 induced sufficient depletion of SETD1A protein expression (**Fig. 5.9**) and the expected RIF1 and BRCA1 foci phenotypes following ionising radiation (**Fig. 5.10**).

Next, I investigated the cellular response to PARPi using clonogenic survival assays (**Fig. 5.11 A**). Consistent with gRNA #4, prior to Cas9 induction gRNA #7 had no significant impact on PARPi sensitivity. Cas9-mediated gene editing of SETD1A alone significantly increased PARPi sensitivity, particularly at higher concentrations of olaparib but not to the same degree as ATM knockdown. As before, combining Cas9-mediated gene editing of SETD1A with ATM-deficiency resulted in further sensitisation to olaparib treatment (**Figs 5.11 C and D**). These findings further support that Cas9-mediated gene editing of SETD1A hypersensitises ATM-deficient cells to PARPi and this effect is not gRNA specific.

Furthermore, as observed with gRNA #4, Cas9-mediated gene editing of SETD1A using gRNA #7 restored the RAD51 foci defect present in ATM-deficient cells (**Fig. 5.12**) but failed to reduce NHEJ-mediated radial formation (**Fig. 5.13**).

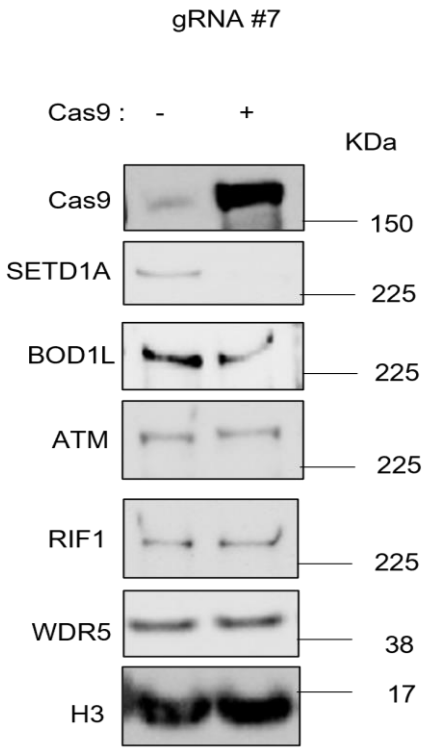

Figure 5.9- Forty-eight hours of Cas9 expression is sufficient to substantially reduce SETD1A levels using gRNA #7.

Hela Kyoto iCas9 cell line expressing SETD1A gRNA #7 was treated for 48 hours ± 1 µg/ml doxycycline. After 48 hours the cells were harvested and whole cell extracts were immunoblotted using the indicated antibodies. Blots representative of three independent biological repeats.

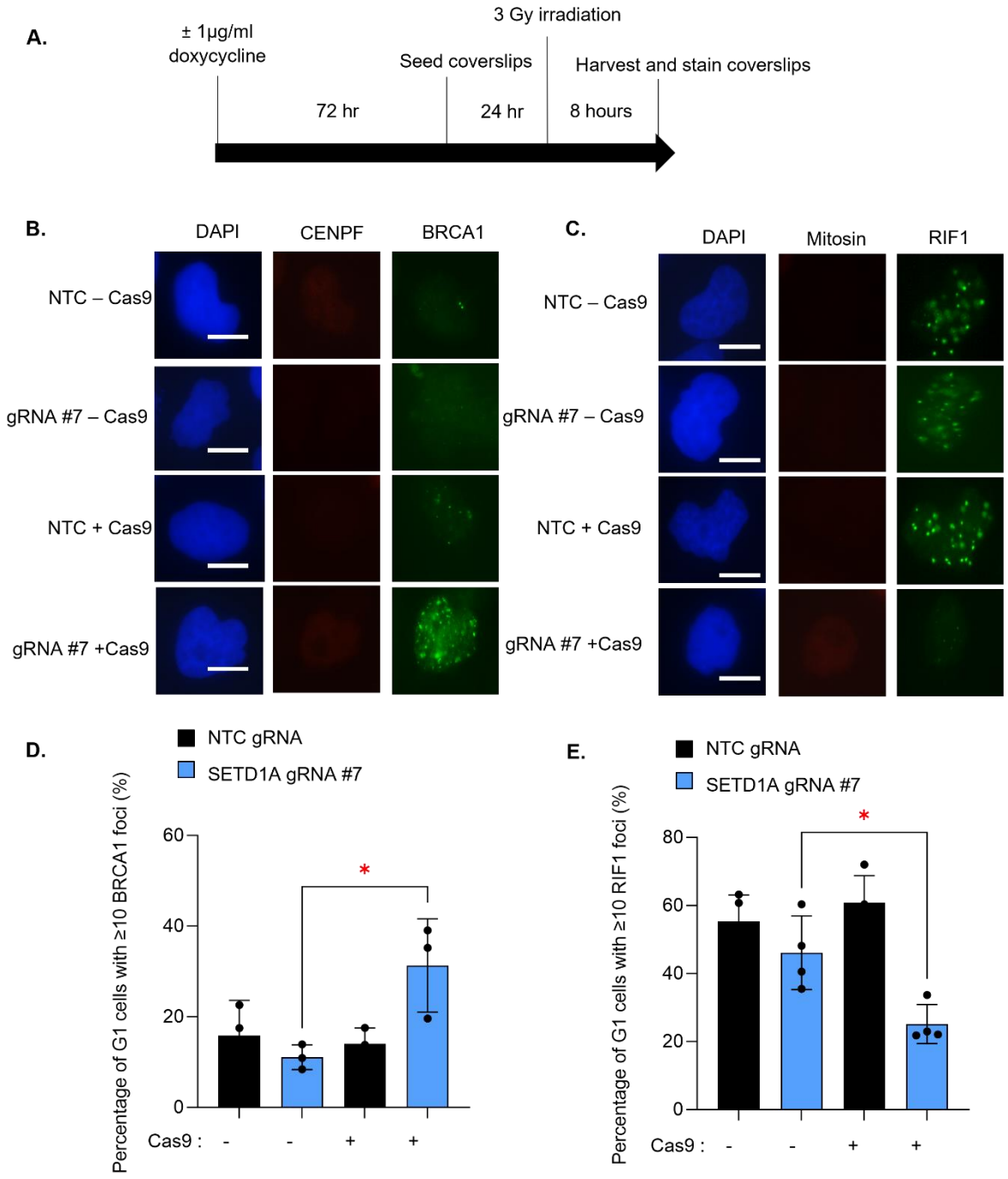
A.
± 1µg/ml doxycycline
3 Gy irradiation
Seed coverslips
Harvest and stain coverslips
72 hr
24 hr
8 hours
B.
DAPI
CENPF
BRCA1
NTC – Cas9
gRNA #7 – Cas9
NTC + Cas9
gRNA #7 +Cas9
C.
DAPI
Mitosin
RIF1
NTC – Cas9
gRNA #7 – Cas9
NTC + Cas9
gRNA #7 +Cas9
D.
NTC gRNA
SETD1A gRNA #7
Percentage of G1 cells with ≥10 BRCA1 foci (%)
60
40
20
0
*
Cas9 : - - + +
E.
NTC gRNA
SETD1A gRNA #7
Percentage of G1 cells with ≥10 RIF1 foci (%)
80
60
40
20
0
*
Cas9 : - - + +

Figure 5.10- Cas9-mediated gene editing of SETD1A using gRNA #7 increases BRCA1 foci and decreases RIF1 foci formation following ionising radiation.

*Hela Kyoto iCas9 cells expressing SETD1A gRNA #7 or a non-targeting control (NTC) were treated for 72 hours ± 1 µg/ml doxycycline. Cells were harvested 8 hours post exposure to 3 Gy IR and immunostained for RIF1 or BRCA1. G1 cells were identified as CENPF/mitosin negative and nuclei counterstained with DAPI. (A.) Schematic of experimental time course. (B and C.) Representative immunofluorescent images (scale bar 10 µm). (D and E.) Quantification of the percentage of G1 cells with ≥10 BRCA1 or RIF1 foci 8-hour post IR. At least 100 cells were counted per condition. Data points represent the mean ± SD from three independent biological repeats. * = P <0.05 as determined by a one-way ANOVA with post-hoc Tukey's test for multiple comparisons.*

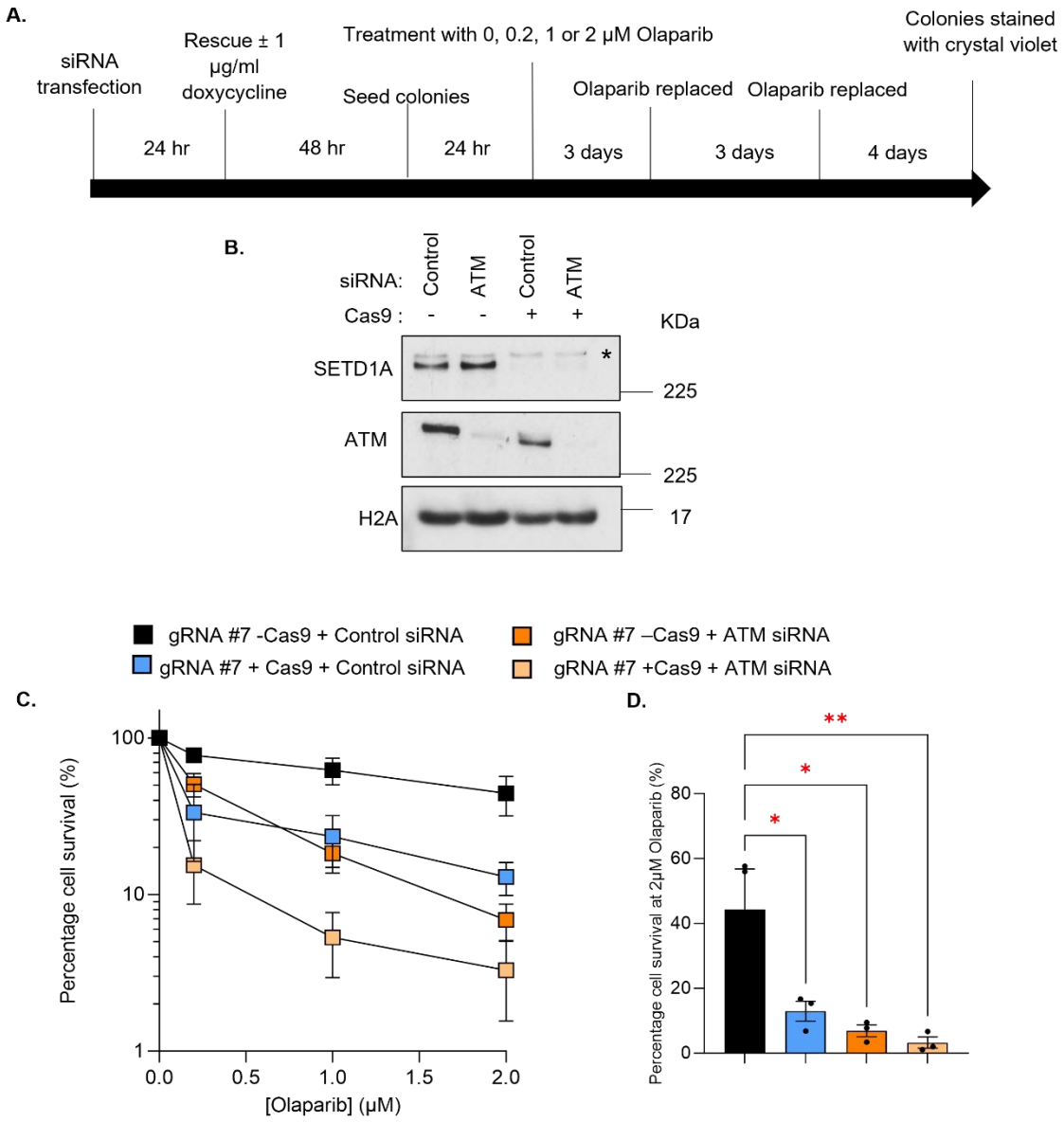

Figure 5.11- Cas9-mediated gene editing of SETD1A using gRNA #7 increases the sensitivity of ATM-deficient cells to olaparib treatment.

*(A.) Schematic of experimental time course. (B.) Whole cell extracts of HeLa Kyoto iCas9 cells treated with indicated siRNAs were immunoblotted with the indicated antibodies. *= nonspecific band. (C.) Clonogenic survival curve for HeLa Kyoto iCas9 cells expressing SETD1A gRNA #7 transfected with the indicated siRNAs ± 48-hour treatment with 1 µg/ml doxycycline. Cells were then exposed to the indicated doses of olaparib for 10 days before staining with crystal violet and colonies counted. (D.) Percentage cell survival from (C.) at 2 µM olaparib. Data points represent the mean ± SEM from three independent biological repeats. *= P < 0.05, ** = P <0.01 as determined by a one-way ANOVA with post-hoc Tukey's test for multiple comparisons.*

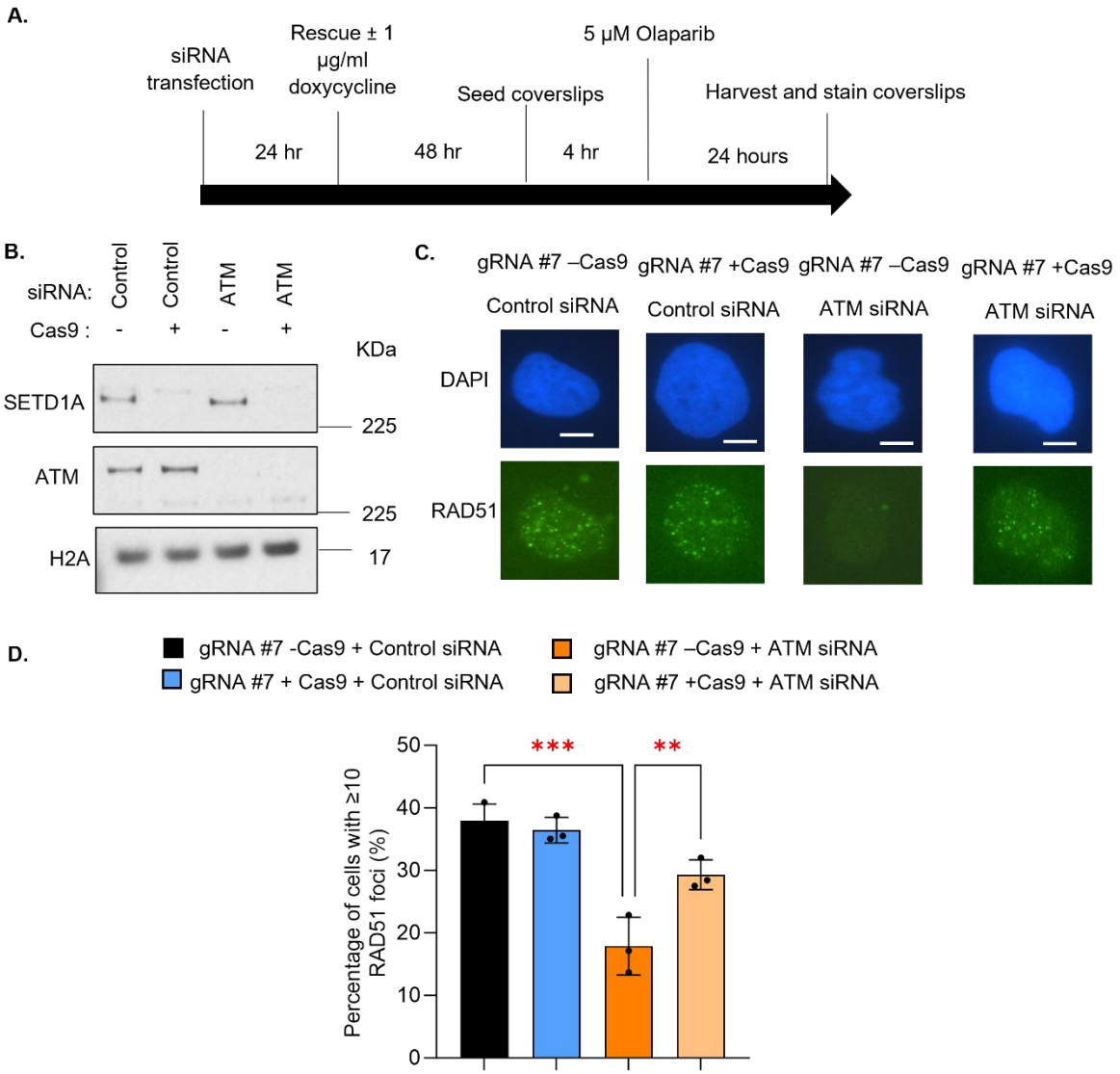

Figure 5.12- Cas9-mediated gene editing of SETD1A using gRNA #7 increases RAD51 foci formation in ATM-deficient cells treated with olaparib.

*HeLa Kyoto iCas9 cell line expressing SETD1A gRNA #7 were transfected with the indicated siRNAs. Cells were treated with ± 1 µg/ml doxycycline for 48 hours to induce Cas9 expression and exposed to 5 µM olaparib for 24 hours. Cells were immunostained with an antibody to RAD51 and counterstained with DAPI. Foci formation was enumerated by fluorescent microscopy (A.) Schematic of experimental time course. (B.) Whole cell extracts of Hela Kyoto iCas9 cells were immunoblotted by indicated antibodies. (C.) Representative immunofluorescent images (scale bar 10 µm). (D.) Graphical representation of the percentage of cells with ≥10 RAD51 foci 24 hours post olaparib treatment. At least 100 cells were counted per condition. Results represent the mean ± SD from three biologically independent experiments. ** = P <0.01. *** = P <0.001 as determined by a one-way ANOVA with post-hoc Tukey's test for multiple comparisons.*

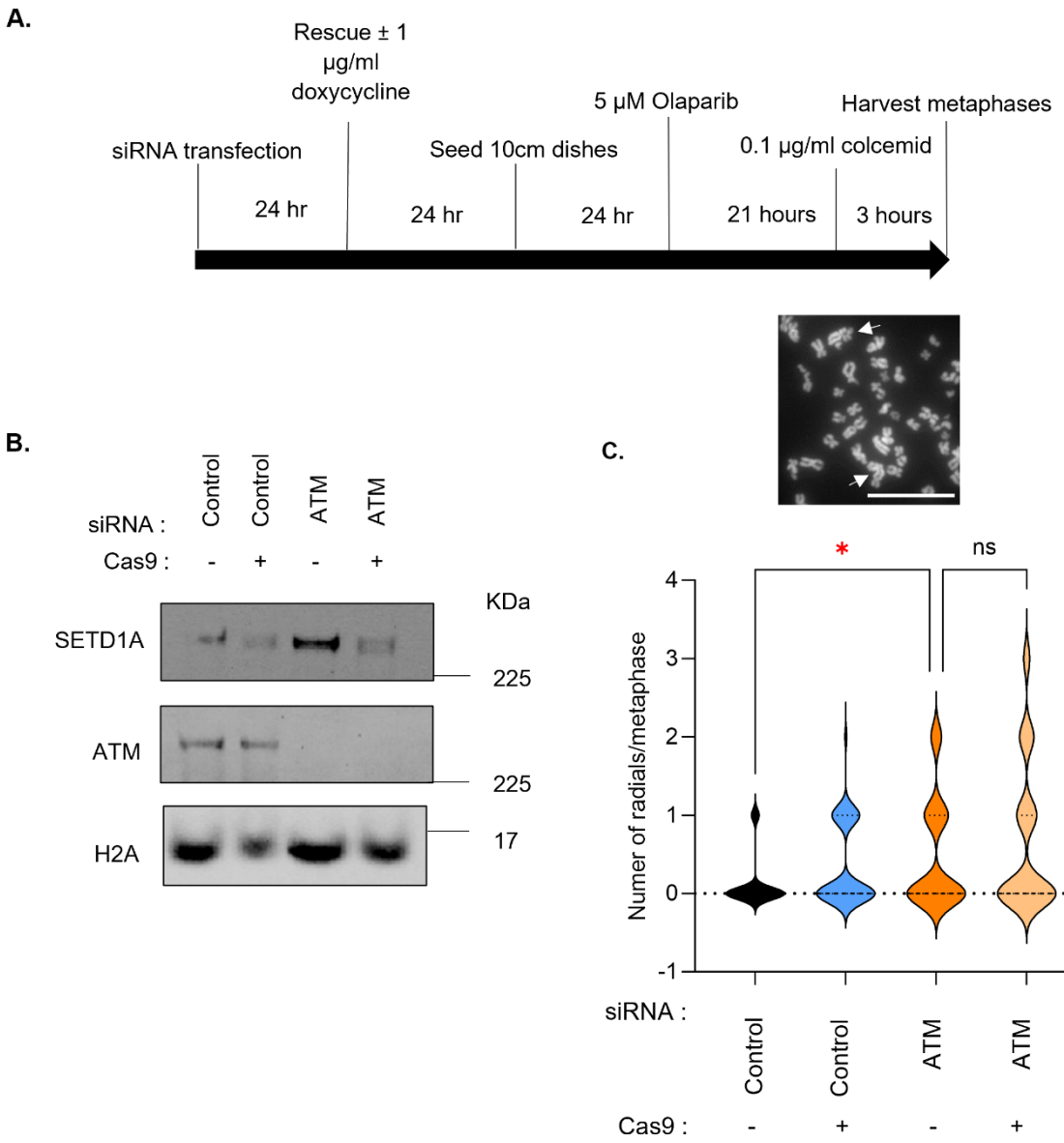

Figure 5.13- Cas9-mediated gene editing of SETD1A using gRNA #7 does not decrease NHEJ-mediated radial formation in ATM-deficient cells treated with olaparib.

*HeLa Kyoto iCas9 cells expressing SETD1A gRNA #7 were transfected with the indicated siRNAs and treated with ± 1 µg/ml doxycycline for 48 hours and 5 µM olaparib for 24 hours. Radial chromosome formation was analysed by DAPI staining and light microscopy. (A.) Schematic of experimental time course. (B.) Whole cell extracts of HeLa cells treated with indicated siRNAs were immunoblotted with the indicated antibodies. (C.) Graphical representation of number of radials/metaphases (Scale bar 10 µm). At least 50 metaphases were counted per condition. Data points represent mean ± SEM from two independent biological repeats. ns= not statistically significant, * = P < 0.05 as determined by a Kruskal-Wallis test with multiple comparisons.*

5.9 Investigating the impact of SETD1A gRNA targeting on transcript expression

To reconcile the differences in PARPi response between SETD1A knockdown and Cas9-mediated gene editing in ATM-deficient cells, I investigated the impact of the mRNA transcripts targeted by the two different systems of SETD1A depletion. SETD1A has four different protein coding transcripts: SETD1A-201, -204, -205 and -202 (**Fig. 5.14**). SETD1A gRNA #4 targets exon 10, thus does not target transcripts SETD1A-204 and -202, whilst gRNA #7 targets exon 4 so does not target SETD1A-202. On the other hand, the SMARTPool siRNA used for SETD1A knockdown is made up of four siRNAs which target all known protein coding transcripts (**Fig. 5.14**).

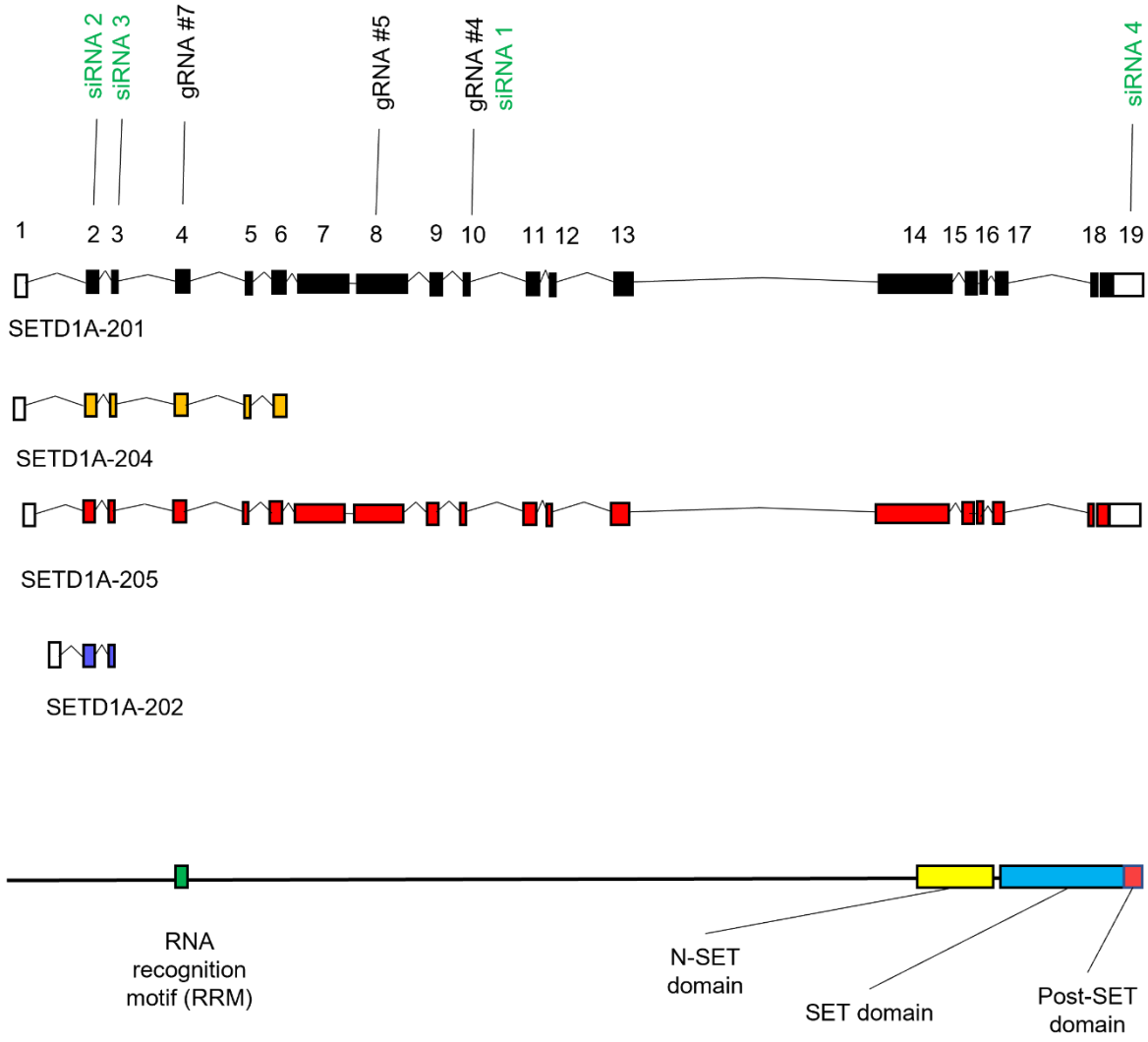

Figure 5.14- SETD1A gRNAs do not target all SETD1A transcripts.

Schematic showing transcripts targeted by SETD1A siRNAs (green) and gRNAs (black). The SETD1A gene encodes four protein coding transcripts. SETD1A-201 and -205 encode the full length SETD1A protein whilst -204 and -202 produce short 3' truncated transcripts. Transcript information obtained from ensembl genome browser https://useast.ensembl.org/index.html.

Based on (**Fig. 5.14**), I hypothesised that the persistence of the truncated transcripts following Cas9-mediated gene editing of SETD1A could underpin the increased sensitivity observed in ATM-deficient cells. To investigate this, we determined the abundance of individual SETD1A transcripts in gRNA #4 and gRNA #7 cell lines by qPCR using two SETD1A TaqMan probes: Hs00322315_m1, which spans exons 3 and 4 and Hs00986930_m1, which spans exons 10 and 11. As such Hs00322315_m1 will amplify all SETD1A transcripts, whilst Hs00986930_m1 will only amplify SETD1A-201 and SETD1A-205. By subtracting the expression of Hs00986930_m1 from Hs00322315_m1 I quantified the expression of SETD1A-204 and SETD1A-202 (**Fig. 5.15 A**).

qPCR analysis revealed that in both the gRNA #4 and gRNA #7 cell lines the SETD1A-204 and -202 transcripts make up > 60 % of total SETD1A transcript expression. Cas9-mediated gene editing of SETD1A using gRNA #4 or #7 decreased total SETD1A mRNA and of the remaining SETD1A mRNA not targeted for degradation ~86% was attributed to the small SETD1A-204 and SETD1A-202 transcripts in gRNA #4 cells vs ~70% in gRNA #7 cells (**Fig. 5.15 B**). As gRNA #7 supposedly targets exon 4 this indicates most of the remaining expression is formed of SETD1A-202. These results show SETD1A-204 and-202 make up a significant percentage of SETD1A expression in the HeLa Kyoto iCas9 SETD1A cell lines. Furthermore, in keeping with their targeting of exon 10 and exon 4, respectively these truncated transcripts are not fully depleted by Cas9-mediated gene editing of SETD1A using gRNA #4 or #7.

SETD1A knockdown using SMARTPool siRNA reduced total SETD1A transcript level to a comparable degree to Cas9-mediated gene editing. However, consistent with

targeting all SETD1A transcripts, SMARTPool siRNA resulted in a larger decrease in the small SETD1A transcripts in comparison to Cas9-mediated gene editing using gRNA #4. On the other hand, gRNA #7 and SMARTPool siRNA produced a similar degree of small transcript depletion. No further significant difference in transcript expression was observed when Cas9-mediated gene editing or knockdown was combined (**Fig. 5.15 B**).

SETD1A knockdown using SETD1A siRNA 2 resulted in the smallest decrease in SETD1A transcript expression overall, suggesting targeting multiple exons with a SMARTPool siRNA is more effective for transcript depletion. Furthermore, combining SETD1A siRNA 2 with Cas9-mediated gene editing did not significantly alter transcript expression levels (**Fig. 5.15 B**).

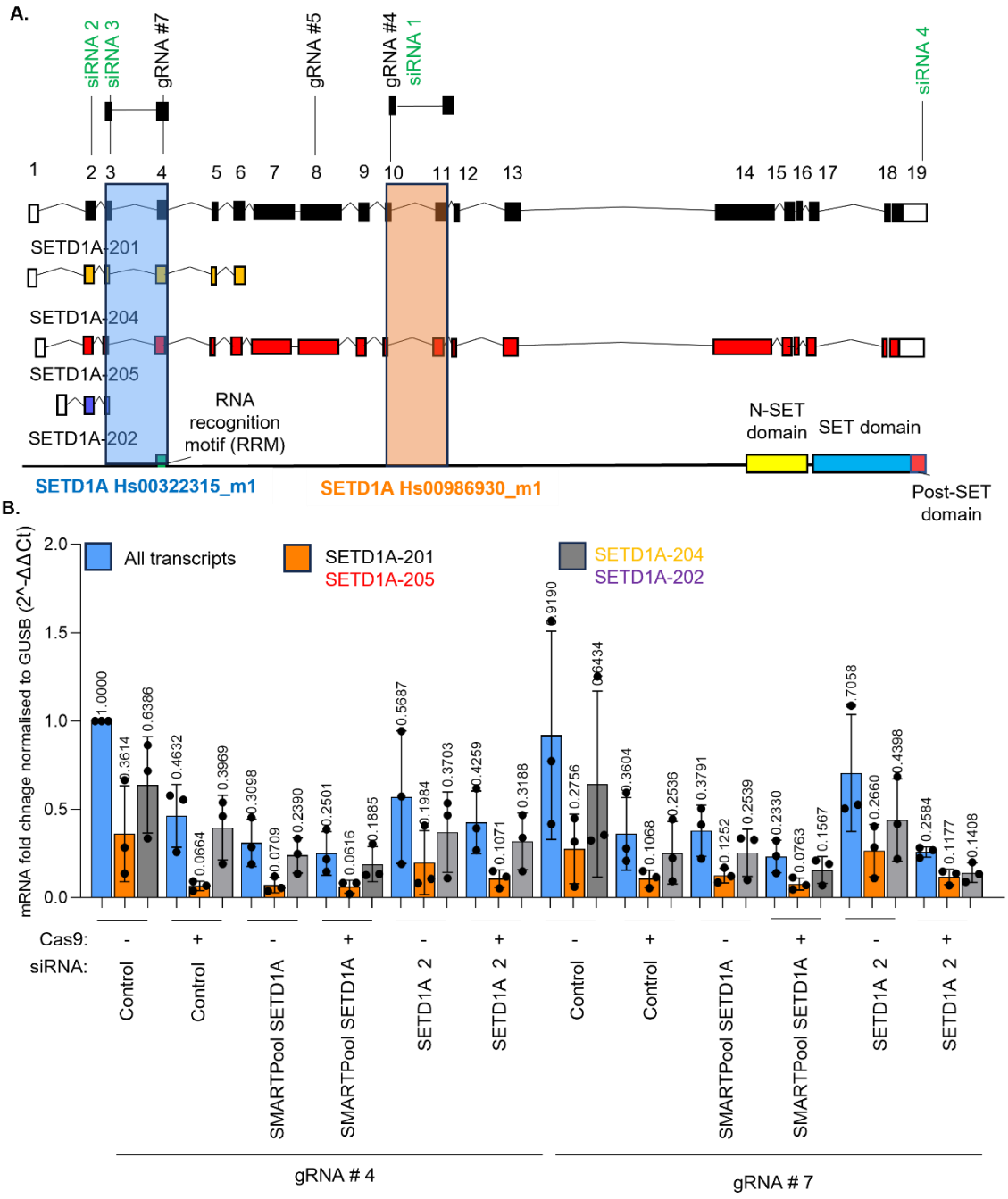
A.
siRNA 2
siRNA 3
gRNA #7
gRNA #5
gRNA #4
siRNA 1
siRNA 4
1 2 3 4 5 6 7 8 9 10 11 12 13 14 15 16 17 18 19
SETD1A-201
SETD1A-204
SETD1A-205
SETD1A-202
RNA recognition motif (RRM)
N-SET domain
SET domain
Post-SET domain
SETD1A Hs00322315_m1
SETD1A Hs00986930_m1
B.
mRNA fold chnage normalised to GUSB (2^-ΔΔCt)
All transcripts
SETD1A-201
SETD1A-205
SETD1A-204
SETD1A-202
Cas9:
siRNA:
Control
SMARTPool SETD1A
SETD1A 2
gRNA # 4
gRNA # 7

Figure 5.15- SETD1A-204 and -202 transcripts are abundant in HeLa Kyoto iCas9 cell lines.

(A.) Schematic showing transcripts targeted by SETD1A siRNAs (green) and gRNAs (black). Exons targeted by PCR probes Hs00322315_m1 and Hs00986930_m1, highlighted in blue and orange, respectively. (B.) HeLa Kyoto iCas9 cells expressing SETD1A gRNA #4 or gRNA #7 were transfected with control, SETD1A SMARTPool or individual SETD1A 2 siRNA. SETD1A knockout was induced by treatment with ± 1 µg/ml doxycycline. After 48 hours the cells were harvested and RNA extracted. mRNA was isolated and mRNA levels of SETD1A-201, -204, -205 and -202 (Hs00322315_m1), SETD1A-201 and -205 (Hs00986930_m1) or SETD1A-204 and -202 (Hs00322315_m1 minus Hs00986930_m1) transcripts was determined by qPCR. mRNA expression fold change normalised to GUSB was calculated using the 2^-ΔΔCt method. Data points represent the mean ± SD from three biologically independent experiments.

5.10 Combining Cas9-mediated gene editing and knockdown of SETD1A further sensitises ATM-deficient cells to olaparib

Since not all SETD1A transcripts are targeted for degradation in gRNA #4 and #7 cell lines, I hypothesised the transcripts not targeted for degradation may underpin the increase in PARPi sensitivity observed following Cas9-mediated gene editing of SETD1A in ATM-deficient cells. To examine this, I combined SETD1A siRNA transfection in gRNA #4 cells to further deplete SETD1A expression. By assessing the individual oligonucleotides that make up the SMARTPool siRNA used for SETD1A knockdown I identified SETD1A siRNA 2 targets exon 2, thus eliminating the SETD1A-204 and -202 protein coding transcripts (**Fig. 5.15 A**).

Whilst combining SETD1A siRNA 2 and gRNA #4 didn't result in any further significant reduction in SETD1A expression at the mRNA level as measured by qPCR (**Fig. 5.15 B**), SETD1A siRNA 2 did reduce SETD1A protein expression (**Figs 5.16 A and B**) and decrease IR-induced RIF1 foci formation in G1 cells. The other individual SETD1A siRNAs examined did not produce a marked decrease in RIF1 foci formation (**Figs 5.16 C and D**). This is an unexpected finding, suggesting SETD1A depletion only reduces RIF1 foci formation using specific oligonucleotide sequences. However, this finding is based on one experiment and further biological repeats are needed to confirm these results. Furthermore, combining SETD1A siRNA 2 with gRNA #4 and/or ATM siRNA also significantly decreased RIF1 foci formation (**Figs 5.17 B and C**).

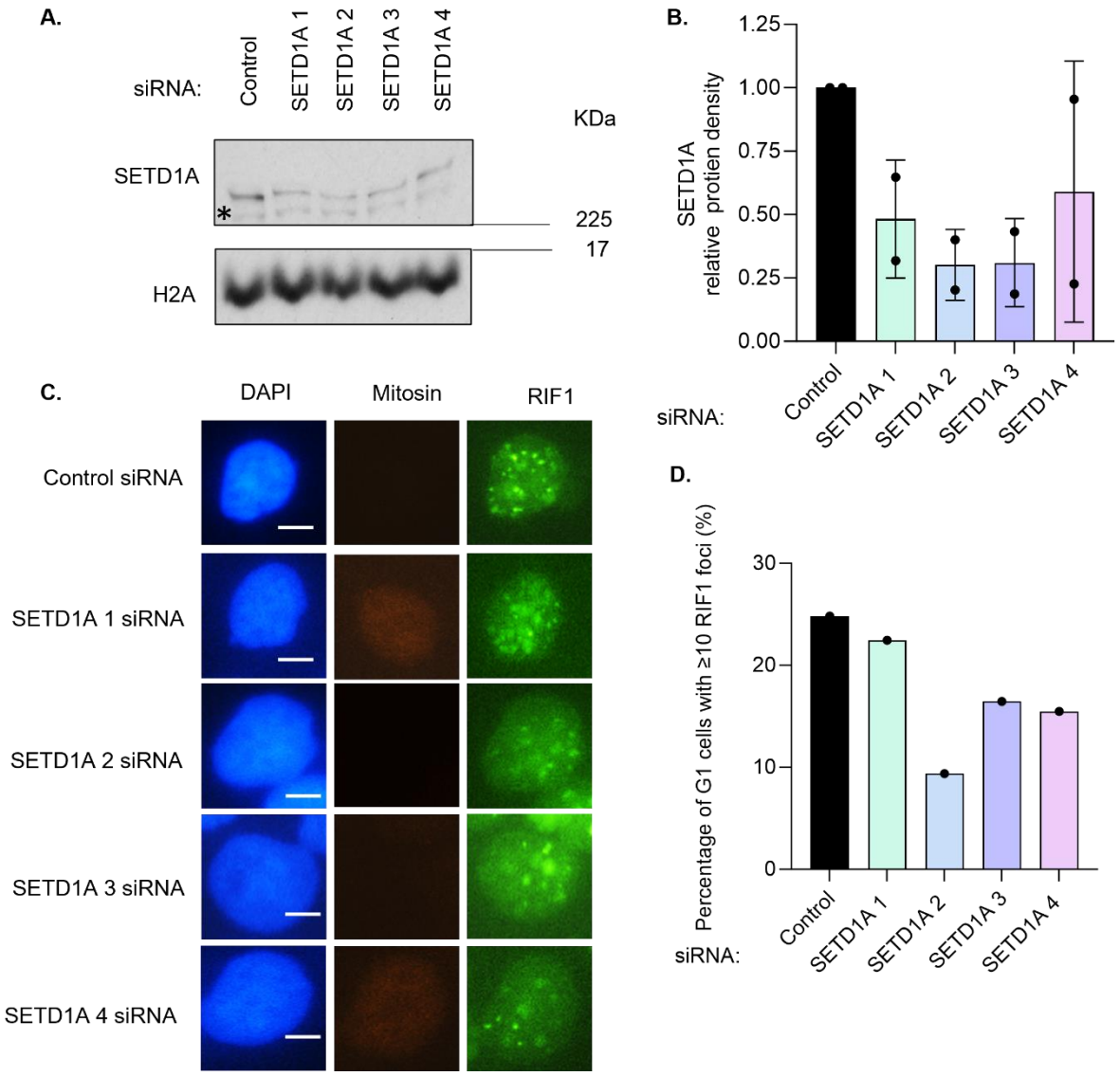

Figure 5.16- SETD1A siRNA 2 decreases SETD1A protein expression and RIF1 foci formation in G1 cells following ionising radiation.

*(A.) Whole cell extracts of HeLa cells treated with indicated siRNAs were immunoblotted with the indicated antibodies. *= nonspecific band. (B.) Quantification of blot in (A.) using ImageJ. Data points represent the mean ± SD from two independent biological repeats. Hela cells transfected with indicated siRNAs were harvested 8 hours post exposure to 3 Gy IR and immunostained for RIF1. G1 cells were identified as mitosin negative and nuclei counterstained with DAPI. (C.) Representative immunofluorescent images (scale bar 10 μm). At least 100 cells were counted per condition. (D.) Quantification of the percentage of G1 cells with ≥10 RIF1 foci 8-hour post IR. Data point represents the mean from one biological repeat.*

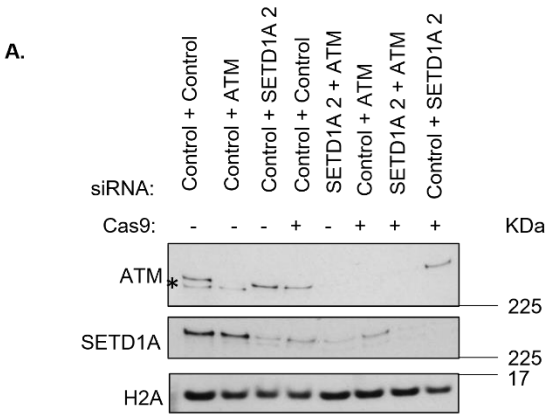
A.
siRNA:
Control + Control
Control + ATM
Control + SETD1A 2
Control + Control
SETD1A 2 + ATM
Control + ATM
SETD1A 2 + ATM
Control + SETD1A 2
Cas9: - - - + - + + +
KDa
ATM
*
225
SETD1A
225
17
H2A

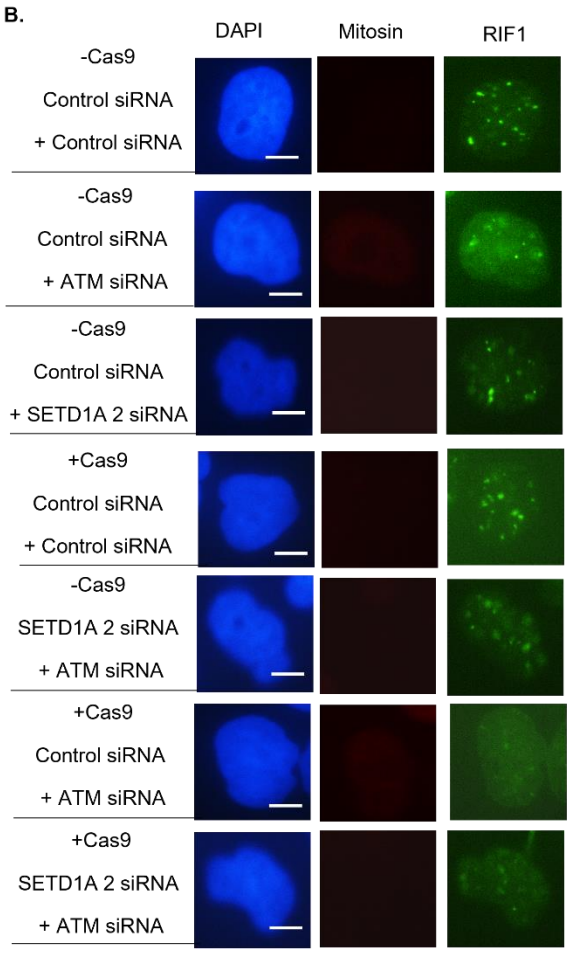
B.
DAPI
Mitosin
RIF1
-Cas9
Control siRNA
+ Control siRNA
-Cas9
Control siRNA
+ ATM siRNA
-Cas9
Control siRNA
+ SETD1A 2 siRNA
+Cas9
Control siRNA
+ Control siRNA
-Cas9
SETD1A 2 siRNA
+ ATM siRNA
+Cas9
Control siRNA
+ ATM siRNA
+Cas9
SETD1A 2 siRNA
+ ATM siRNA

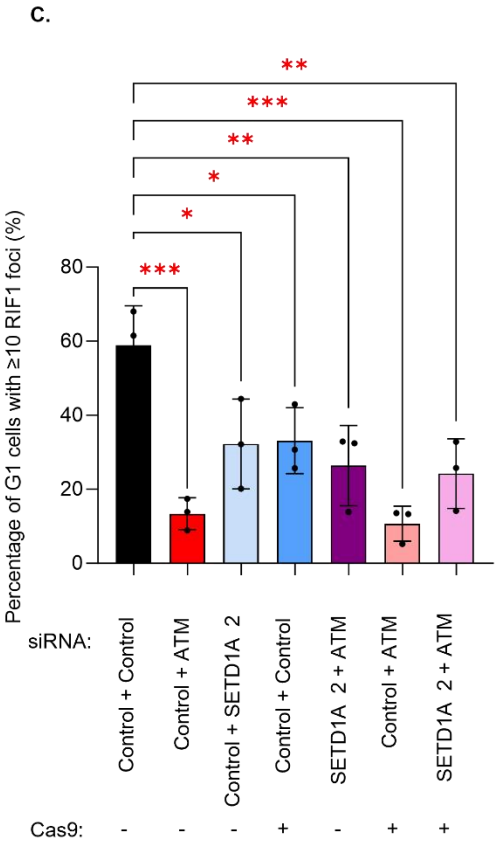
C.
Percentage of G1 cells with ≥10 RIF1 foci (%)
0
20
40
60
80
**
***
**
*
*
***
siRNA:
Control + Control
Control + ATM
Control + SETD1A 2
Control + Control
SETD1A 2 + ATM
Control + ATM
SETD1A 2 + ATM
Cas9: - - - + - + +

Figure 5.17- Analysing the effect of SETD1A siRNA 2 on RIF1 foci formation in G1 cells following ionising radiation in combination with SETD1A gRNA #4 and/or ATM- depletion.

*Hela Kyoto iCas9 cell lines expressing SETD1A gRNA #4, were transfected with indicated siRNAs and treated for 72 hours ± 1 µg/ml doxycycline. Cells were harvested 8 hours post exposure to 3 Gy IR and immunostained for RIF1. G1 cells were identified as mitosin negative and nuclei counterstained with DAPI. (A.) Whole cell extracts of HeLa Kyoto iCas9 cells treated with indicated siRNAs were immunoblotted with the indicated antibodies. *=nonspecific band (B.) Representative immunofluorescent images (scale bar 10 µm). At least 100 cells were counted per condition. (C.) Quantification of the percentage of G1 cells with ≥ 10 RIF1 foci 8-hour post IR. Data points represent the mean ± SD from three independent biological repeats. * = P <0.05, **= P < 0.01, *** = P <0.001 as determined by a one-way ANOVA with post-hoc Tukey's test for multiple comparisons.*

I then assessed the effect of combining Cas9-mediated gene editing and knockdown of SETD1A on PARPi sensitivity (**Fig. 5.18 A**) and HR activity (**Fig. 5.19 A**) of ATM-deficient cells.

Firstly, as seen on multiple occasions, ATM-deficient cells displayed sensitivity to olaparib treatment. SETD1A knockdown using SETD1A siRNA 2 conferred a slight decrease in PARPi sensitivity in ATM-deficient cells, in keeping with our previous findings using SMARTPool SETD1A siRNA. As before, Cas9-mediated gene editing of SETD1A did not rescue PARPi sensitivity of ATM-deficient cells, however, in this case they were not significantly more sensitive than ATM-deficient cells alone. We hypothesised that decreasing residual SETD1A transcript expression by combining SETD1A siRNA 2 with Cas9-mediated gene editing of SETD1A would reduce PARPi sensitivity in ATM-deficient cells. Surprisingly, however, combining Cas9-mediated gene editing of SETD1A and knockdown further sensitised ATM-deficient cells to olaparib treatment (**Figs 5.18 C and D**).

As previously observed, ATM-deficient cells showed a defect in RAD51 foci formation, which was subsequently restored to control levels when SETD1A was depleted by Cas9-mediated gene editing or knockdown. Interestingly however, when combined, Cas9-mediated gene editing and SETD1A knockdown failed to restore RAD51 foci levels, indicative of a persistent HR-defect (**Figs 5.19 C and D**).

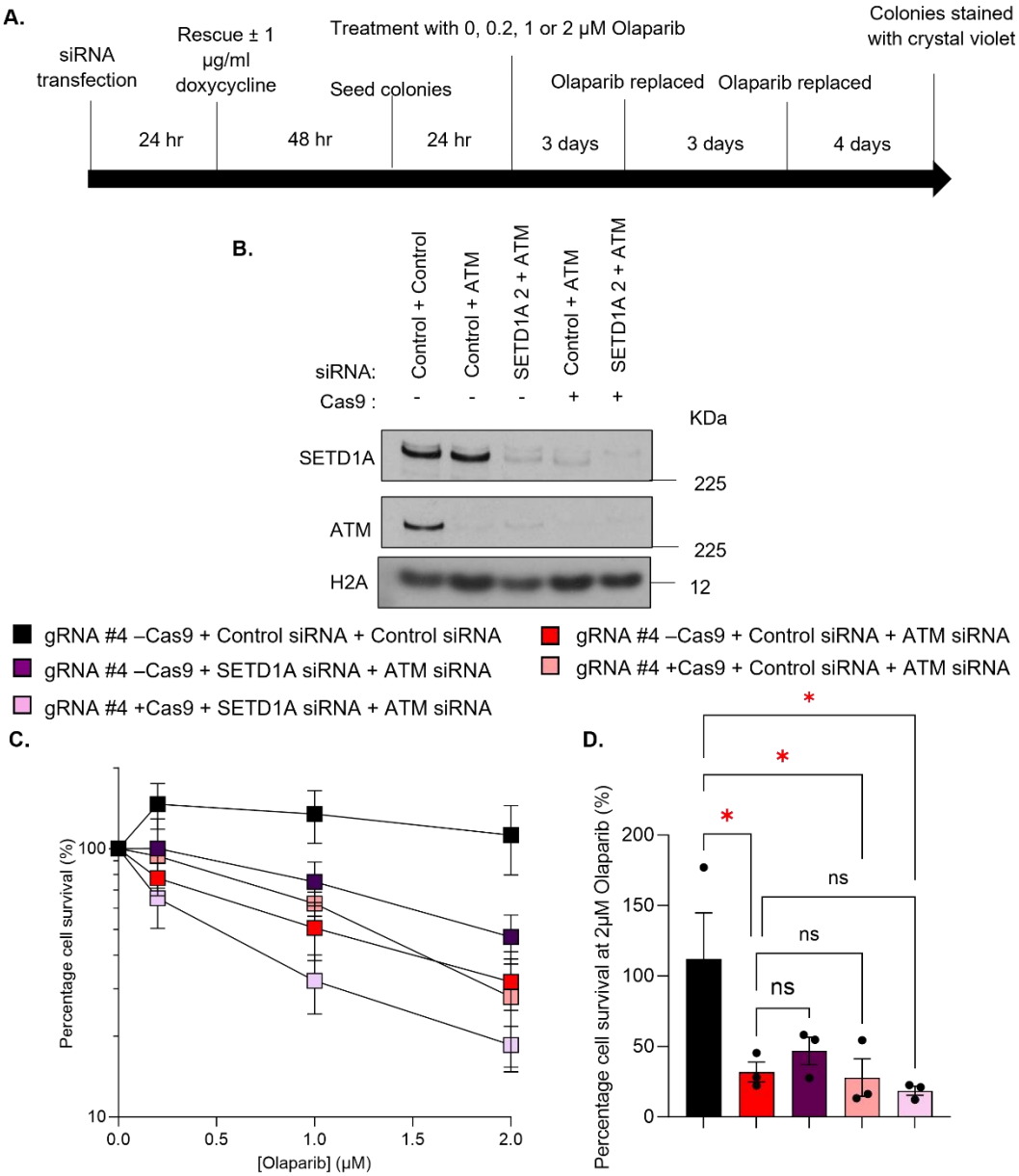

Figure 5.18- Combining Cas9-mediated gene editing of SETD1A with siRNA further increases sensitivity of ATM-deficient cells to olaparib treatment.

*(A.) Schematic of experimental time course. (B.) Whole cell extracts of HeLa Kyoto iCas9 cells treated with indicated siRNAs were immunoblotted with the indicated antibodies. (C.) Clonogenic survival curve for HeLa Kyoto iCas9 cells expressing SETD1A gRNA #4 were transfected with the indicated siRNAs ± 48-hour treatment with 1 µg/ml doxycycline. Cells were then exposed to the indicated doses of olaparib for 10 days before staining with crystal violet and colonies counted. (D.) Percentage cell survival from (C.) at 2 µM olaparib. Data points represent the mean ± SEM from three independent biological repeats. ns= not statistically significant, * = P <0.05 as determined by a one-way ANOVA with post-hoc Tukey's test for multiple comparisons.*

A.

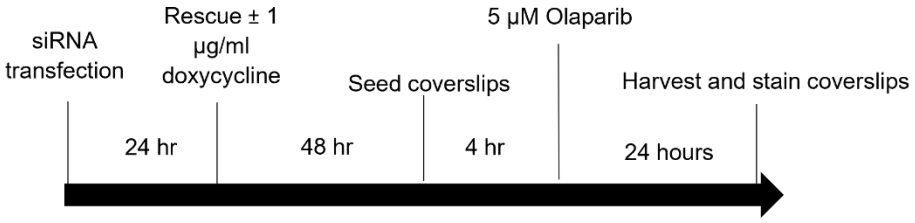
siRNA transfection
Rescue ± 1 µg/ml doxycycline
Seed coverslips
5 µM Olaparib
Harvest and stain coverslips
24 hr
48 hr
4 hr
24 hours

B.

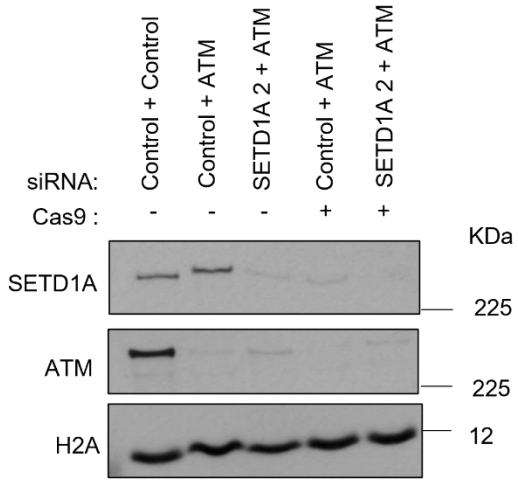
siRNA:
Cas9 :
Control + Control
Control + ATM
SETD1A 2 + ATM
Control + ATM
SETD1A 2 + ATM
- - - + +
KDa
SETD1A
225
ATM
225
H2A
12

C.

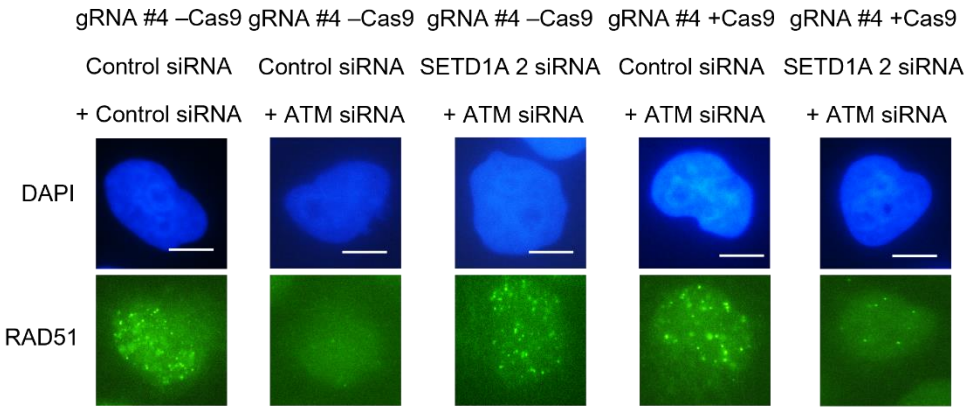
gRNA #4 –Cas9 Control siRNA + Control siRNA
gRNA #4 –Cas9 Control siRNA + ATM siRNA
gRNA #4 –Cas9 SETD1A 2 siRNA + ATM siRNA
gRNA #4 +Cas9 Control siRNA + ATM siRNA
gRNA #4 +Cas9 SETD1A 2 siRNA + ATM siRNA
DAPI
RAD51

D.

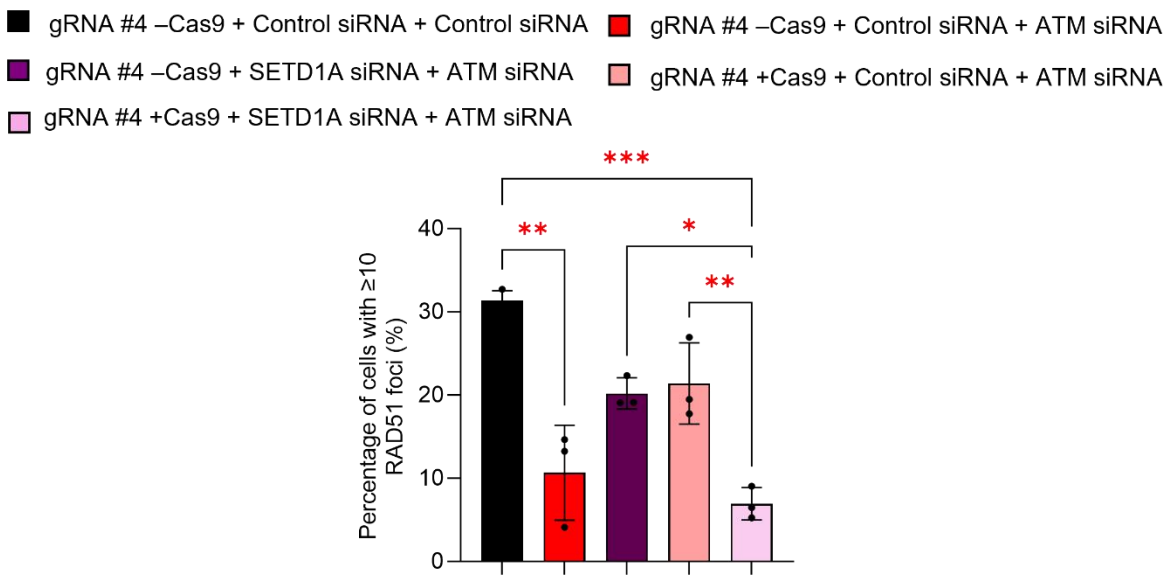
gRNA #4 –Cas9 + Control siRNA + Control siRNA
gRNA #4 –Cas9 + Control siRNA + ATM siRNA
gRNA #4 –Cas9 + SETD1A siRNA + ATM siRNA
gRNA #4 +Cas9 + Control siRNA + ATM siRNA
gRNA #4 +Cas9 + SETD1A siRNA + ATM siRNA
***
**
*
**
Percentage of cells with ≥10 RAD51 foci (%)
40
30
20
10
0

Figure 5.19- Combining Cas9-mediated gene editing of SETD1A with siRNA further decreases RAD51 foci formation in ATM-deficient cells treated with olaparib.

*HeLa Kyoto iCas9 cell line expressing SETD1A gRNA #4 were transfected with the indicated siRNAs. Cells were treated with ± 1 µg/ml doxycycline for 48 hours to induce Cas9 expression and exposed to 5 µM olaparib for 24 hours. Cells were immunostained with an antibody to RAD51 and counterstained with DAPI. Foci formation was enumerated by fluorescent microscopy (A.) Schematic of experimental time course. (B.) Whole cell extracts of Hela Kyoto iCas9 cells were immunoblotted by indicated antibodies. (C.) Representative immunofluorescent images (scale bar 10 µm). (D.) Graphical representation of the percentage of cells with ≥10 RAD51 foci 24 hours post olaparib treatment. At least 100 cells were counted per condition. Results represent the mean ± SD from three biologically independent experiments. * = P <0.05, ** = P <0.01. *** = P <0.001 as determined by a one-way ANOVA with post-hoc Tukey's test for multiple comparisons.*

5.11 Combining Cas9-mediated gene editing and knockdown of SETD1A further depletes SETD1A and increases p53 protein expression

Combining Cas9-mediated gene editing and knockdown of SETD1A exacerbated PARPi sensitivity and HR deficiency in ATM-deficient cells. Based on these observations I hypothesised that the level of residual SETD1A protein expression following different methods of SETD1A depletion influences PARPi sensitivity in ATM-deficient contexts. To investigate this, I assessed SETD1A protein levels by western blotting following SETD1A knockdown, Cas9-mediated gene editing or a combination of both.

Prior to induction of Cas9 expression, control or ATM siRNA transfected cells showed normal SETD1A expression. As expected, Cas9 induction or transfection with SETD1A siRNA 2 significantly reduced SETD1A protein expression levels. Furthermore, supporting our hypothesis, combining Cas9 induction with SETD1A knockdown further decreased SETD1A protein expression, so that it was undetectable by western blot after a 30 second exposure (**Fig. 5.20**).

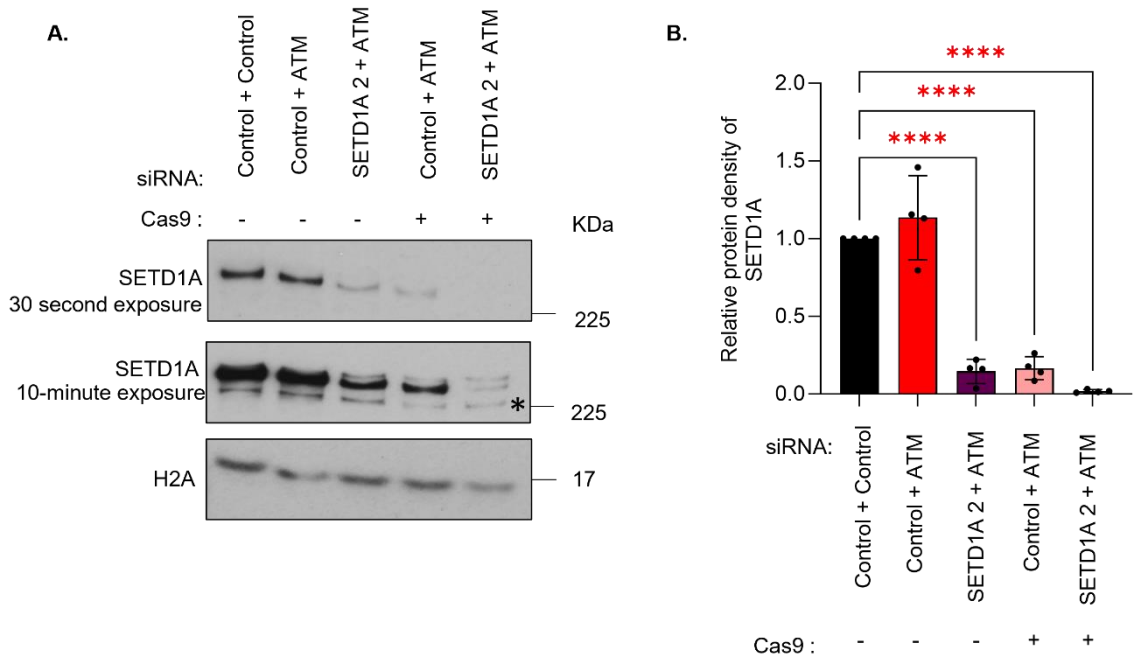

Figure 5.20- Combining Cas9-mediated gene editing with SETD1A siRNA further decreases SETD1A protein expression.

*HeLa Kyoto iCas9 cell line expressing SETD1A gRNA #4 were transfected with the indicated siRNAs. Cells were treated with ± 1 µg/ml doxycycline for 48 hours to induce Cas9 expression. (A.) Whole cell extracts of Hela Kyoto iCas9 cells were immunoblotted by indicated antibodies *= nonspecific band. (B.) Quantification of western blot using ImageJ. Results represent the mean ± SD from four biologically independent experiments. **** = P <0.0001 as determined by a one-way ANOVA with post-hoc Tukey's test for multiple comparisons.*

The tumour suppressor gene p53 (*TP53*) controls cell division and development by transcriptionally regulating the CDK inhibitor p21 and becomes activated in response to a range of cellular stimuli, including DNA damage. Overexpression of wild-type p53 in tumours has been shown to induce growth arrest and cell death via apoptosis (Marei *et al.*, 2021). As such, I hypothesised that the increased sensitivity to PARPi observed upon combining SETD1A knockdown with Cas9-mediated gene editing in ATM-deficient cells may be a result of increased p53 activity in response to DNA damage, resulting in increased cell cycle arrest and apoptosis.

To test this hypothesis, the same cells from (**Fig. 5.20**) were also immunoblotted for p53 expression and γH2AX levels. Combining Cas9-mediated gene editing of SETD1A with knockdown in ATM-depleted cells resulted in a significant increase in p53 expression (**Figs 5.21 A and B**). However, no change in γH2AX expression was observed across the conditions (**Figs 5.21 A and C**). These results indicate that complete deficiency of SETD1A could increase cell growth arrest and apoptosis through increased p53 expression.

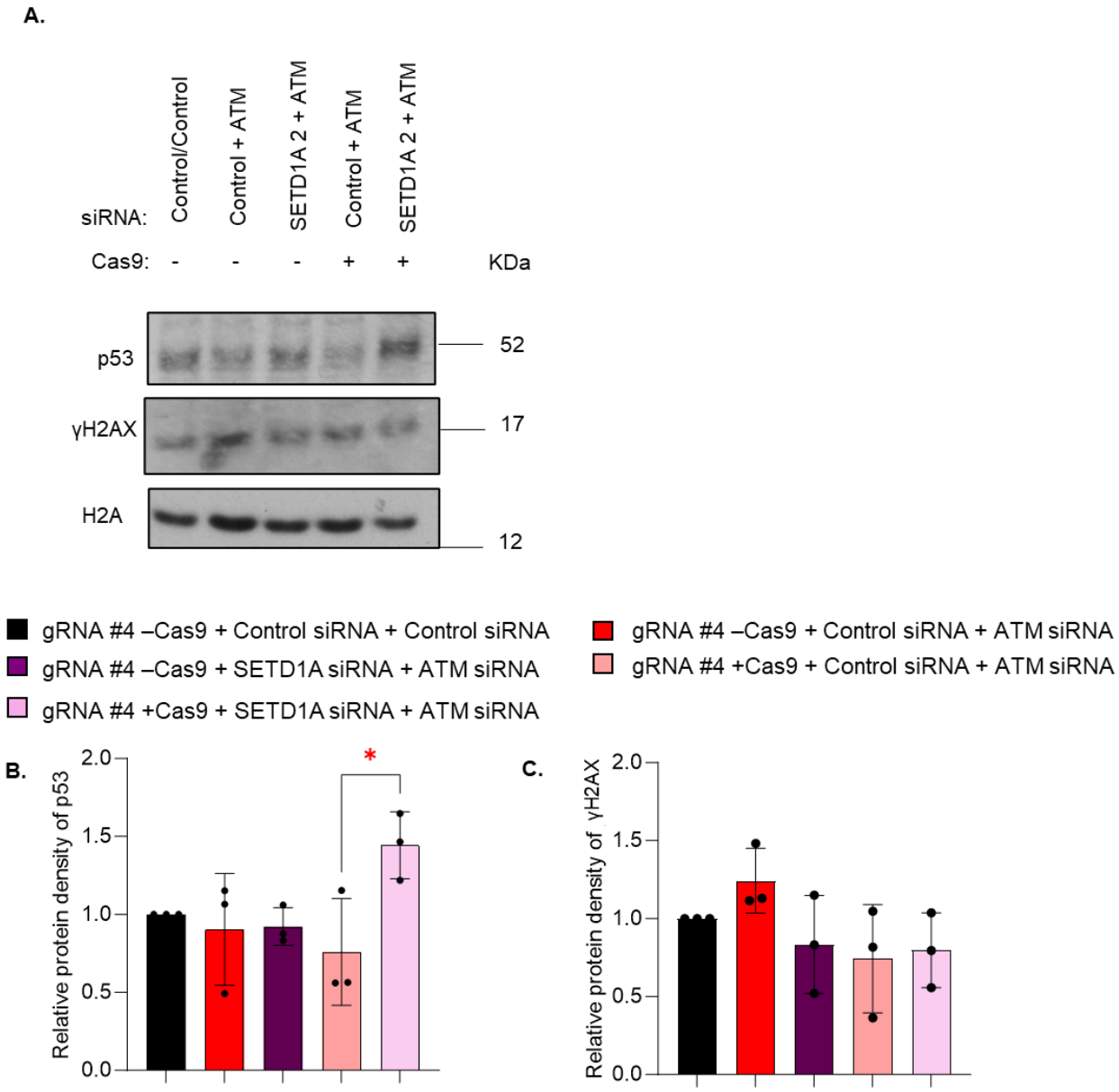

Figure 5.21- Combining Cas9-mediated gene editing with SETD1A siRNA increases p53 expression in ATM-deficient cells.

*HeLa Kyoto iCas9 cell line expressing SETD1A gRNA #4 was transfected with the indicated siRNAs. Cells were treated with ± 1 µg/ml doxycycline for 48 hours to induce Cas9 expression. (A.) Whole cell extracts of Hela Kyoto iCas9 cells were immunoblotted by indicated antibodies. (B. and C.) Quantification of western blot in (A.) using ImageJ. Results represent the mean ± SD from three biologically independent experiments. * = P <0.05 as determined by a one-way ANOVA with post-hoc Tukey's test for multiple comparisons.*

5.12 Discussion

5.12.1 Cas9-mediated gene editing of SETD1A decreases RIF1 recruitment in response to DNA damage

In this chapter, we show notable reduction of SETD1A expression by all three gRNAs using an inducible CRISPR/Cas9 system. Furthermore, these cell lines showed low background Cas9 expression, which was upregulated upon doxycycline treatment, allowing us to conditionally control gene editing. Despite this, reduced SETD1A expression did not change global H3K4me3 expression. This is supported by previous studies observing no effect on total H3K4me3 protein expression (Tajima *et al.*, 2019), or its presence at TSSs (Hoshii *et al.*, 2018) following SETD1A knockdown. This suggests the effects of SETD1A are limited to specific genetic targets rather than global methylation changes. Additionally, the expression of SETD1A was not required for the stability of other COMPASS complex members and interacting proteins such as RIF1 and WDR5. This corresponds with previous findings showing SETD1A depletion did not affect RIF1 protein expression, indicating SETD1A is not required to stabilise RIF1 (Bayley *et al.*, 2022).

Further validating this CRISPR-Cas9 system we found that all gRNAs significantly reduced RIF1- and increased BRCA1-foci formation in response to DNA damage. This supports the previously identified role for SETD1A in preventing BRCA1-dependent end-resection through the recruitment of RIF1 to chromatin at DSBs (Bayley *et al.*, 2022). These initial findings suggested that Cas9-mediated gene editing of SETD1A produced the same phenotypes as SETD1A knockdown and recapitulated our previous findings.

5.12.2 Cas9-mediated gene editing of SETD1A increases PARPi sensitivity of ATM-deficient cells due to accumulation of chromosomal radials

Although Cas9-mediated gene editing of SETD1A recapitulated many of the phenotypes of SETD1A knockdown, it unexpectedly resulted in increased olaparib sensitivity in ATM-deficient cells. This strongly contradicts our previous findings and highlights that the choice of method for genetic manipulation of SETD1A significantly influences PARPi sensitivity. Although PARPi sensitivity was increased, Cas9-mediated gene editing of SETD1A also increased HR in ATM-deficient cells, suggesting that HR status is not indicative of PARPi sensitivity in these cell lines. This conclusion is supported by drug screening data from the Cancer Cell Line Encyclopaedia which revealed that genomic alterations in HR-related genes and HR-deficiency scores are not correlated with sensitivity to PARP inhibitors (Takamatsu, Murakami and Matsumura, 2024).

On the other hand, SETD1A gene editing did not decrease NHEJ-mediated radial formation in ATM-deficient cells, indicating persistence of PARPi-induced genomic instability. This is consistent with studies showing the accumulation of radial structures drives PARPi induced genome instability and cell death in HR-deficient cells (Patel, Sarkaria and Kaufmann, 2011).These findings suggest that the inability to repair these lesions is a more important determinant of PARPi sensitivity than HR status in this context.

Another key determinant of PARPi sensitivity in HR-deficient cells is the level of PARP1 trapping on chromatin (Pettitt *et al.*, 2018). However, in this case changes in the level of PARP1 on the chromatin following SETD1A and/or ATM depletion did not correlate with PARPi sensitivity. This suggests that whilst both SETD1A and ATM

appear to influence the level of PARP1 present at the chromatin, PARP trapping is not a significant influence of PARPi sensitivity in this specific genetic context.

In summary, these findings support a model in which Cas9-mediated gene editing of SETD1A is unable to rescue PARPi-induced genomic instability in ATM-deficient cells due to persistence of NHEJ-mediated radial chromosome structures, which are repaired by a mechanism independent of HR. The differences between SETD1A gene editing and knockdown in driving the accumulation or resolution of these structures, respectively should be investigated in the future.

5.12.3 Phenotypic differences between Cas9-mediated gene editing of SETD1A and knockdown

The significant differences in PARPi sensitivity observed between the two systems for SETD1A depletion could be explained by siRNA-mediated off-target effects or differences in the level of gene depletion achieved. For example, siRNA transfection can result in variable knockdown efficiency due to targeting of the mRNA transcripts, in comparison to Cas9-mediated gene editing which depletes functional gene expression by interrupting the open reading frame to induce truncation mutations. Therefore, whilst I attempted to mitigate this effect using SMARTPool siRNA targeting multiple SETD1A transcripts, greater levels of residual protein expression following SETD1A knockdown could explain these differences in PARPi sensitivity. These results suggest ATM-deficient cells may require some residual SETD1A expression for cell survival. As combining Cas9-mediated gene editing of SETD1A with knockdown further decreased SETD1A protein expression and PARPi sensitivity in ATM-deficient cells, this would indicate that these cells need a residual level of SETD1A protein expression for survival.

Phenotypic differences between gene knockout and knockdown have been previously demonstrated (El-Brolosy and Stainier, 2017; Karakas *et al.*, 2007; Rossi *et al.*, 2015). This has been attributed to genetic compensation resulting from upregulation of related genes as a direct consequence of loss of protein function following genetic knockout. These upregulated genes can modulate the targeted pathway to partially or fully rescue the desired outcome (El-Brolosy and Stainier, 2017). For example, mice with loss of the *Rpl22* ribosomal gene showed upregulation of the *Rpl21l1* paralogue which is normally inhibited by RPL22. As a result of loss of this negative feedback loop these mice showed no translational defects (O'Leary *et al.*, 2013). Furthermore, another study found that knockdown of the CDK inhibitor p21 by RNAi in MCF-10A cells resulted in distinct gene expression patterns in comparison to p21 knockout following TGFβ exposure (Karakas *et al.*, 2007). Together, these studies highlight how choice of method for gene manipulation can influence findings through upregulation of compensatory mechanism. Therefore, it is possible that loss of functional SETD1A protein expression following Cas9-mediated gene editing upregulates compensatory pathways resulting in increased PARPi sensitivity in ATM-deficient cells. For example, other KMT2 family members may become upregulated or KDM expression may be downregulated to compensate for reduced H3K4me3 levels following Cas9-mediated SETD1A deletion. This hypothesis could be confirmed by blotting for these enzymes in HeLa Kyoto iCas9 SETD1A gRNA cell lines.

5.12.4 Cas9-mediated gene editing of SETD1A does not target all protein coding SETD1A transcripts

Using qPCR we showed the SETD1A-204, and -202 transcripts account for a significant proportion of SETD1A expression in the HeLa Kyoto cell lines. Furthermore, we showed these transcripts are not targeted by the gRNAs used in this study. Currently, we do not know the functional consequences these small transcripts could have for PARPi sensitivity. Since SETD1A-204 possess the RRM domain, this transcript could bind to an array of coding and non-coding RNAs to regulate mRNA stability independent of histone methyltransferase activity (Amin *et al.*, 2023).Additionally, the RRM domain also binds WDR82 to mediate the interaction of SETD1A with RNA polymerase II phosphorylated at serine 5 of the C-terminal domain (Lee and Skalnik, 2008), therefore this transcript has the potential to target SETD1A to TSSs. As a result, the presence of SETD1A-204 could be responsible for differences in PARPi sensitivity observed between SETD1A knockdown and Cas9-mediated gene editing. However, this hypothesis was ruled out as targeting this transcript using the alternative gRNA #7 or combining gRNA #4 with SETD1A siRNA did not reduce PARPi sensitivity in ATM-deficient cells.

In the future further investigation of transcript expression using qPCR probes specifically designed to detect each individual SETD1A transcript will be required to further validate the abundance of each specific transcript in these HeLa Kyoto iCas9 cell lines.

5.12.5 Combining knockdown and Cas9-mediated gene editing of SETD1A further exacerbates PARPi-sensitivity in ATM-deficient cells

Having shown that SETD1A-202 and -204 are not targeted by gRNA #4 we investigated the effect of further depleting SETD1A expression with an siRNA targeting exon 2 of SETD1A (SETD1A siRNA 2). Although transfection of gRNA #4 cells with siRNA 2 did not further decrease SETD1A mRNA expression shown in (**Fig. 5.17**), we observed a significant reduction in protein expression. This could potentially be a result of specificity of the PCR primers used to detect SETD1A transcripts. Furthermore, it should be noted that the SETD1A antibody (A300-289, Bethyl Laboratories) detects a region of human SETD1A between residue 1200 and 1250, thus this antibody would not be able to detect the proteins encoded by the SETD1A-202 and -204 transcripts. Therefore, the decrease in SETD1A protein expression observed upon transfection with siRNA 2 is unlikely to be due to a decrease in SETD1A-202 and -204 specifically, but instead due to a further reduction in other SETD1A transcripts. In the future we would need to repeat western blots using an antibody which recognised an alternative epitope of SETD1A near the c-terminus to determine the specific effects on SETD1A-202 and -204 protein expression.

Nevertheless, combining gRNA #4 with siRNA 2 further exacerbated the PARPi sensitivity of ATM-deficient cells. However, in this case combining SETD1A knockdown and knockout could not restore the RAD51 defect observed in ATM-deficient cells, indicating defective HR. These findings imply that some residual SETD1A protein expression is required for the survival of ATM-deficient cells in response to olaparib treatment and the induction of PARPi resistance relies on a low

level of residual SETD1A protein expression. Together these findings indicate that PARPi sensitivity is determined by a delicate balance of SETD1A expression in HR-deficient cells.

5.12.6 Combining knockdown and Cas9-mediated gene editing of SETD1A increases p53 protein expression

We also observed that combining gRNA #4 and siRNA 2 significantly increased p53 protein expression. In theory HeLa cell lines should have diminished p53 functionality due to the presence of human papilloma virus (HPV)-18, which degrades transcriptionally active p53 to reduce protein expression (Ajay, Meena and Bhat, 2012). Despite this, our findings suggest that HeLa cells may retain a low level of p53 protein expression, which is further upregulated following SETD1A depletion. Previous studies have shown treatment with small molecule nuclear export inhibitors enabled accumulation of transcriptionally active p53 in the nucleus allowing for re-expression of functional p53 and the induction of apoptotic cell death in HeLa cells (Hietanen *et al.*, 2000). Our findings are also in keeping with the fact that constitutive SETD1A knockout is viable in H1299 NSCLC cells, due to their lack of expression of the p53 protein (Kang *et al.*, 2021a). Additionally, studies have linked SETD1A to regulation of p53 expression (Hoshii *et al.*, 2018). For example, a recent study showed downregulation of SETD1A expression increased p53 expression and phosphorylation in transformed follicular lymphoma (Zhuang *et al.*, 2024).

We hypothesise that increased p53 expression following complete depletion of SETD1A may cause increased PARPi sensitivity through induction of apoptosis. Previously, p53 overexpression has been shown to induce significant apoptosis in HeLa cells due to upregulation of pro apoptotic Bcl-2associated XX protein (Bax) and

Bcl-2 homologous antagonist killer (Bak) (Sun *et al.*, 2018). Furthermore, Smeby *et al.* observed p53 signal transduction was upregulated in response to PARPi and p53 wild-type colorectal cancer cells display increased sensitivity to PARPi compared to p53 mutant counterparts (Smeby *et al.*, 2020).No difference in γH2AX expression was observed following loss of SETD1A, suggesting the increased p53 expression observed was not due to increased DNA damage signalling upon SETD1A depletion. Future investigations assessing whether SETD1A depletion results in increased apoptosis in olaparib treated cells should be performed utilising Annexin V and PI quantification by flow cytometry or by assessment of caspase 3/7 cleavage.

In conclusion, we have demonstrated that Cas9-mediated gene editing of SETD1A significantly increases PARPi sensitivity in ATM-deficient cells, contradicting our previous findings following SETD1A knockdown. We attributed this unexpected finding to the ability of these cells to resolve PARPi-induced genomic instability. Furthermore, it appears the level of residual SETD1A expression following genetic manipulation is an important factor in PARPi sensitivity through regulation of p53 protein expression. In the future it will be interesting to investigate the effect of these different methodologies of genetic manipulation on p53 activity and apoptosis.

6. CHAPTER 6: TRANSCRIPTIONAL REGULATION BY SETD1A DRIVES PARP INHIBITOR RESISTANCE

6.1 Introduction

SETD1A is an important epigenetic regulator of transcription (Lee and Skalnik, 2008; Yang *et al.*, 2020b; Salz *et al.*, 2014; Hoshii *et al.*, 2022) due to its role depositing H3K4me3 marks at the promoter regions of actively transcribed genes (Bernstein *et al.*, 2005). SETD1A can also regulate transcription by interaction with cyclin K mediated through the FLOS domain, promoting RNA polymerase II phosphorylation and gene expression (Hoshii *et al.*, 2018). Consequently, multiple studies have shown that loss of SETD1A results in large changes in gene expression in multiple cell types (Cameron *et al.*, 2019; Hoshii *et al.*, 2022; Salz *et al.*, 2014). More specifically, it has been shown deletion of SETD1A results in transcriptional changes in pathways related to the DNA repair and stress response, including HR, NHEJ, RF protection, as well as BER, in stem cells (Arndt *et al.*, 2018) and mouse models of leukaemia (Hoshii *et al.*, 2022). Based on these previous studies, I was interested in investigating the effect of SETD1A depletion of gene expression patterns in HR-deficient cells.

6.2 SETD1A depletion results in differential gene expression in HR-deficient backgrounds

To investigate the effect of loss of SETD1A on gene expression in HR-deficient and -proficient backgrounds, I performed RNA-sequencing analysis using HeLa Kyoto iCas9 gRNA# 4 cells transfected with control, ATM or BRCA1 siRNA (**Fig. 6.1**). Surprisingly, loss of SETD1A had limited impact on gene expression in both HR-

proficient and -deficient cells, suggesting SETD1A is not a major transcriptional regulator in these specific genetic contexts. Because of this, I employed less stringent cut-off values for log fold change and p-value of 0.5 and 0.06, respectively to identify additional potentially relevant differentially expressed genes (DEGs) that were just under the thresholds for significance. In control siRNA transfected cells, SETD1A depletion resulted in a significant 1.5-fold change downregulation of 12 transcripts and upregulation of one transcript (**Fig. 6.2 A**). In ATM siRNA transfected cells, loss of SETD1A downregulated the expression of 16 transcripts and upregulated the expression of one transcript (**Fig. 6.2 B**). Finally, in BRCA1-siRNA treated cells, 10 transcripts were significantly downregulated, whilst one transcript was upregulated following SETD1A depletion (**Fig. 6.2 C**).

To identify commonly deregulated genes in HR-proficient or -deficient contexts I compared DEGs following loss of SETD1A in BRCA1-deficient, ATM-deficient, and HR-proficient backgrounds (**Fig. 6.2 D**). Five DEGs were shared between all backgrounds irrespective of HR gene status, suggesting these genes are dependent on SETD1A for their expression. One out of five of these genes (*TM2D3*) was upregulated upon SETD1A depletion, whilst the remaining DEGs (*C19orf54*, *TRMT1L*, *PEX12* and *C12orf66*) were downregulated. Other DEGs were specifically deregulated in Control-, ATM- or BRCA1- siRNA backgrounds. Additionally, one gene (*EME1*) was commonly downregulated upon SETD1A depletion in both ATM- and BRCA1-deficient cells but did not meet the threshold for fold change in control siRNA transfected cells, despite showing a statistically significant difference in normalised counts (**Fig. 6.3 A**). Normalised counts of SETD1A-dependent differentially expressed genes are shown in (**Fig. 6.3**).

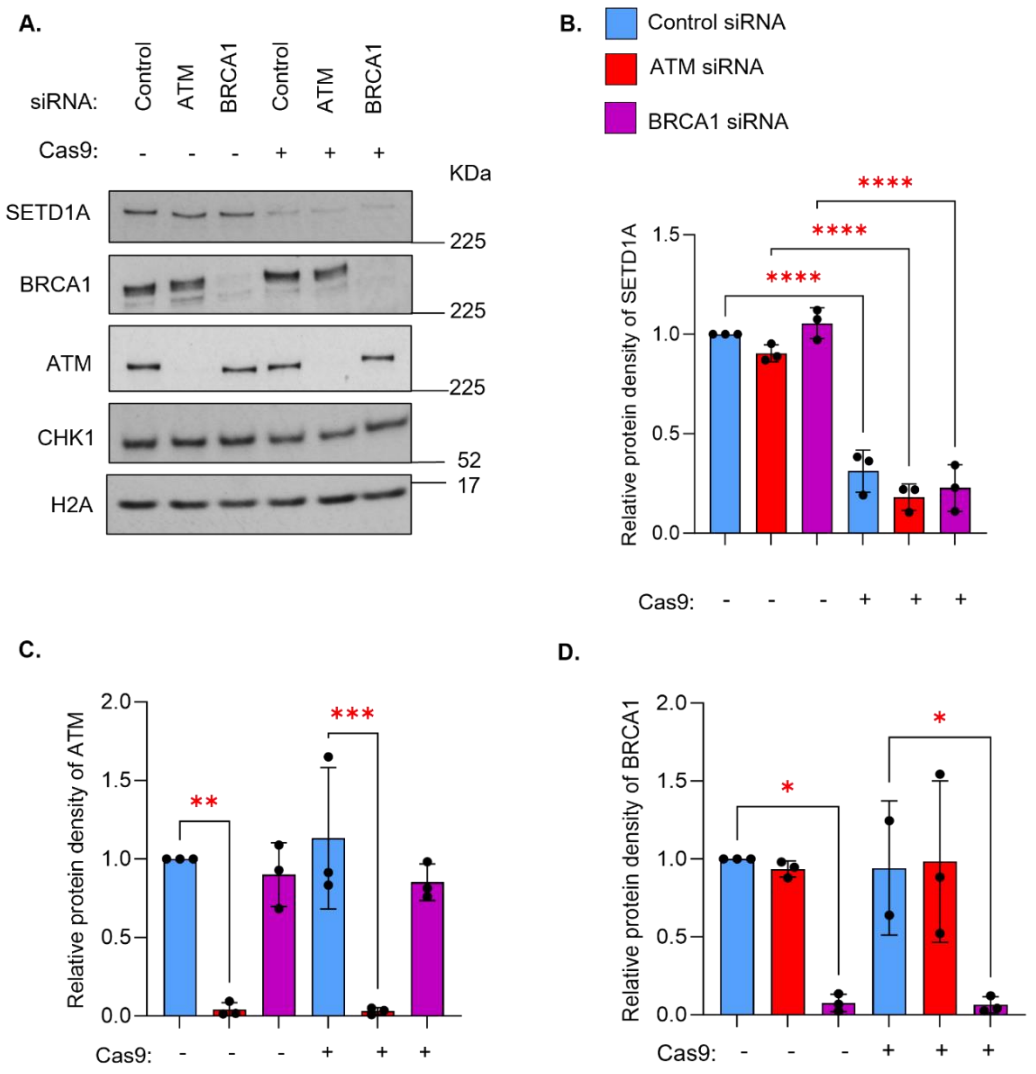

Figure 6.1- ATM or BRCA1 was depleted in HeLa Kyoto iCas9 SETD1A gRNA #4 cell lines.

*(A.) HeLa Kyoto iCas9 cell line expressing SETD1A gRNA #4 was transfected with control, ATM or BRCA1 siRNA. SETD1A gene editing was induced by treatment with ± 1 µg/ml doxycycline. After 48 hours the cells were harvested and whole cell extracts were immunoblotted using the indicated antibodies. (B.-D.) Immunoblot quantification from (A.) using ImageJ. All plots represent the mean ± SD from three independent biological repeats. * = P <0.05, ** = P <0.01, *** = P <0.001, **** = P <0.0001 as determined by a one-way ANOVA with post-hoc Tukey's test for multiple comparisons.*

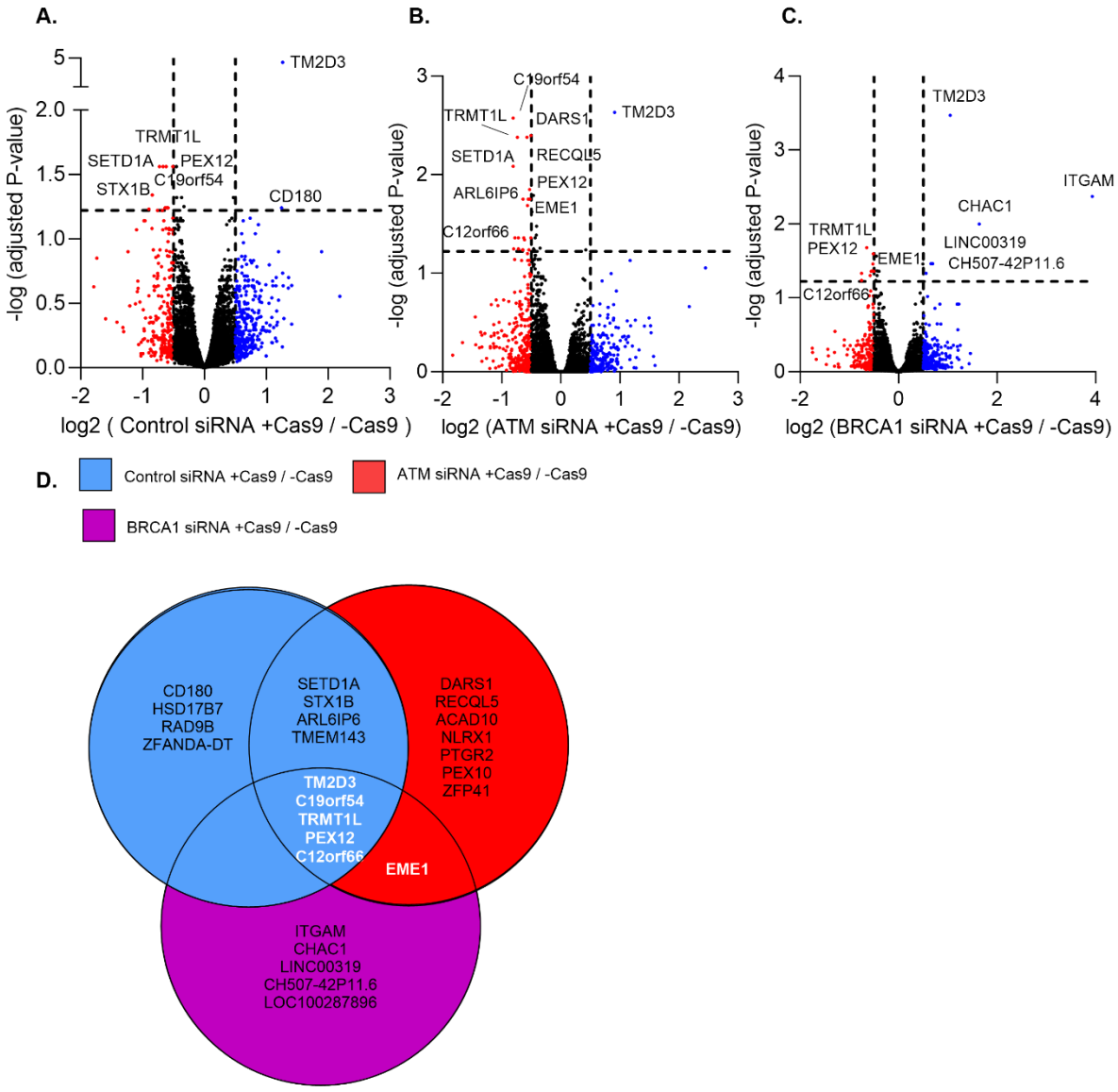

Figure 6.2- SETD1A drives expression of EME1 in ATM- and BRCA1-deficient cells.

(A.-C.) HeLa Kyoto iCas9 cells expressing SETD1A gRNA #4 were transfected with control, ATM or BRCA1 siRNA. SETD1A gene editing was induced by treatment with ± 1 µg/ml doxycycline. After 48 hours the cells were harvested and RNA extracted. Gene expression was analysed using RNA-seq and differential gene expression is displayed as a volcano plot. Significantly upregulated genes are highlighted in blue and significantly downregulated genes are highlighted in red. Cut-off values of differentially expressed genes were log2 fold change = 0.5 and -log (adjusted P-value) = 1.22. Data points represent means from three independent repeats. (D) Venn diagram of overlapping differentially expressed genes from A-C.

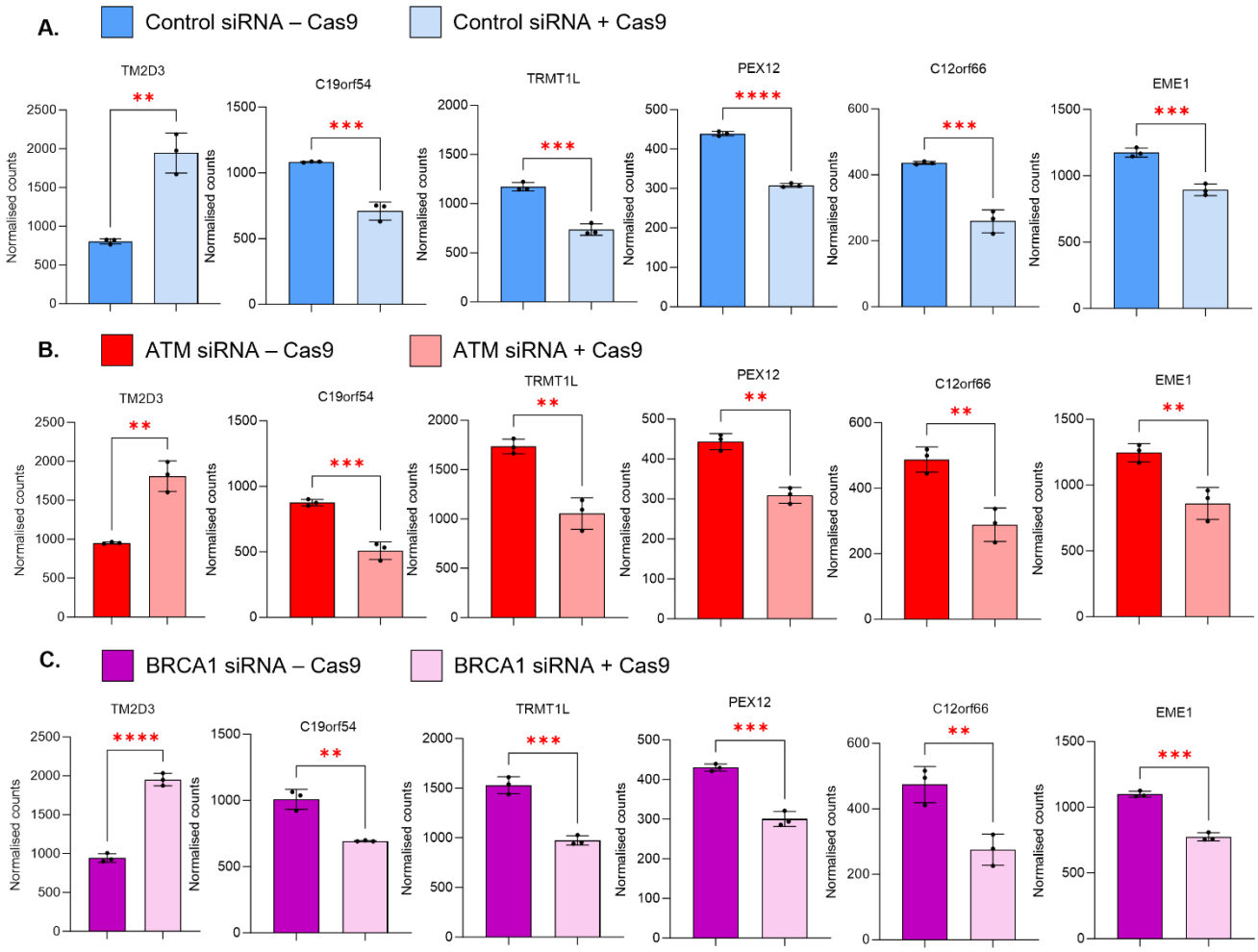

Figure 6.3- Normalised counts of SETD1A-dependent differentially expressed genes.

*HeLa Kyoto iCas9 cells expressing SETD1A gRNA #4 were transfected with control, ATM or BRCA1 siRNA. SETD1A gene editing was induced by treatment with ± 1 µg/ml doxycycline. After 48 hours the cells were harvested and RNA extracted. Gene expression was analysed using RNA-seq. Normalised counts for differentially expressed genes in (Fig. 6.2) calculated by DESeq2 according to median of ratios method. (A.) Control siRNA +iCas9/ -Cas9. (B.) ATM siRNA +iCas9/ -Cas9. (C.) BRCA1 siRNA +iCas9/ -Cas9. Data points represent the mean ± SD from three biologically independent experiments. ** = P < 0.01, ***= P < 0.001, ****= P < 0.0001 as determined by a as determined by a two-tailed Students t-test.*

As we used less stringent cut-off values for thresholds of significance, and only observed a small number of significant DEGs in the RNA-sequencing, it was important to independently verify these findings by qPCR. We also tested additional samples from each cell type to confirm biological repeatability of these findings. All DEGs identified in RNA sequencing also showed significant fold change by qPCR, except for *PEX12*, which did not meet minimum cut off value for relative fold change (**Fig. 6.4**). Similarly to RNA-seq count data (**Fig 6.3 A**), EME1 expression also showed a statistically significant difference following SETD1A depletion in control siRNA treated cells but did not meet the minimum cut off relative fold change (**Fig. 6.4 A**). To determine how well RNA- sequencing data correlated with the qPCR validation I compared Log2 fold change of the DEGs determined by both methods. **Fig. 6.5** highlights that Log2 fold change of DEGs corresponds well with qPCR validation.

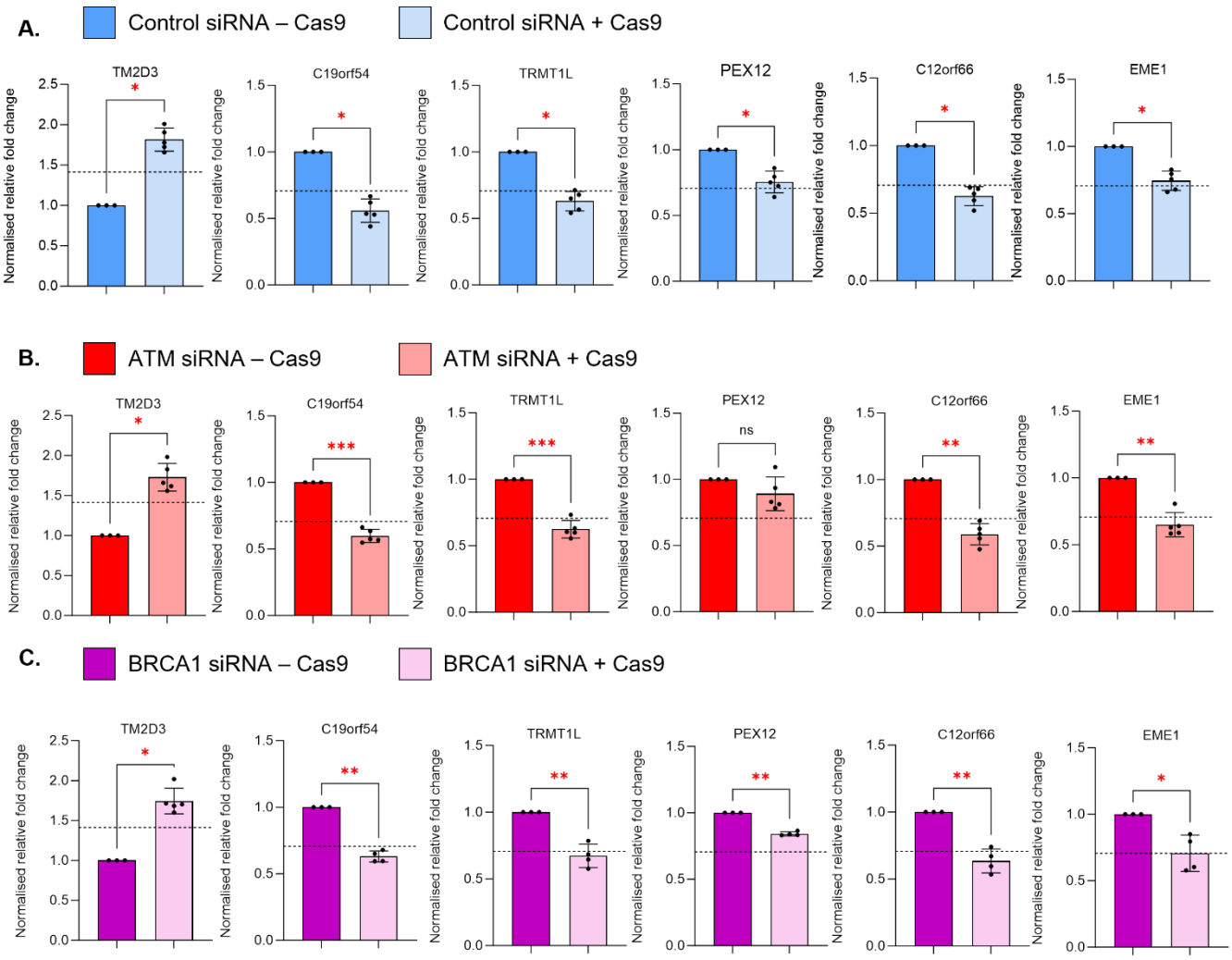

Figure 6.4- Validation of RNA-sequencing hits by qPCR.

*HeLa Kyoto iCas9 cells expressing SETD1A gRNA #4 were transfected with control, ATM or BRCA1 siRNA. SETD1A gene editing was induced by treatment with ± 1 µg/ml doxycycline. After 48 hours the cells were harvested and RNA extracted. mRNA was isolated and mRNA levels of the denoted transcripts determined by qPCR. (A.) Control siRNA +iCas9/ -Cas9. (B.) ATM siRNA +iCas9/ -Cas9. (C.) BRCA1 siRNA +iCas9/ -Cas9. mRNA expression fold change normalised to GUSB calculated using the 2^-ΔΔCt method. Dotted line represents fold change cut off at 1.414214 for upregulated genes and 0.707107 for downregulated genes. Data points represent the mean ± SD from five biologically independent experiments. * = P < 0.05, ** = P < 0.01, ***= P < 0.001, as determined by a as determined by a two-tailed Students t-test.*

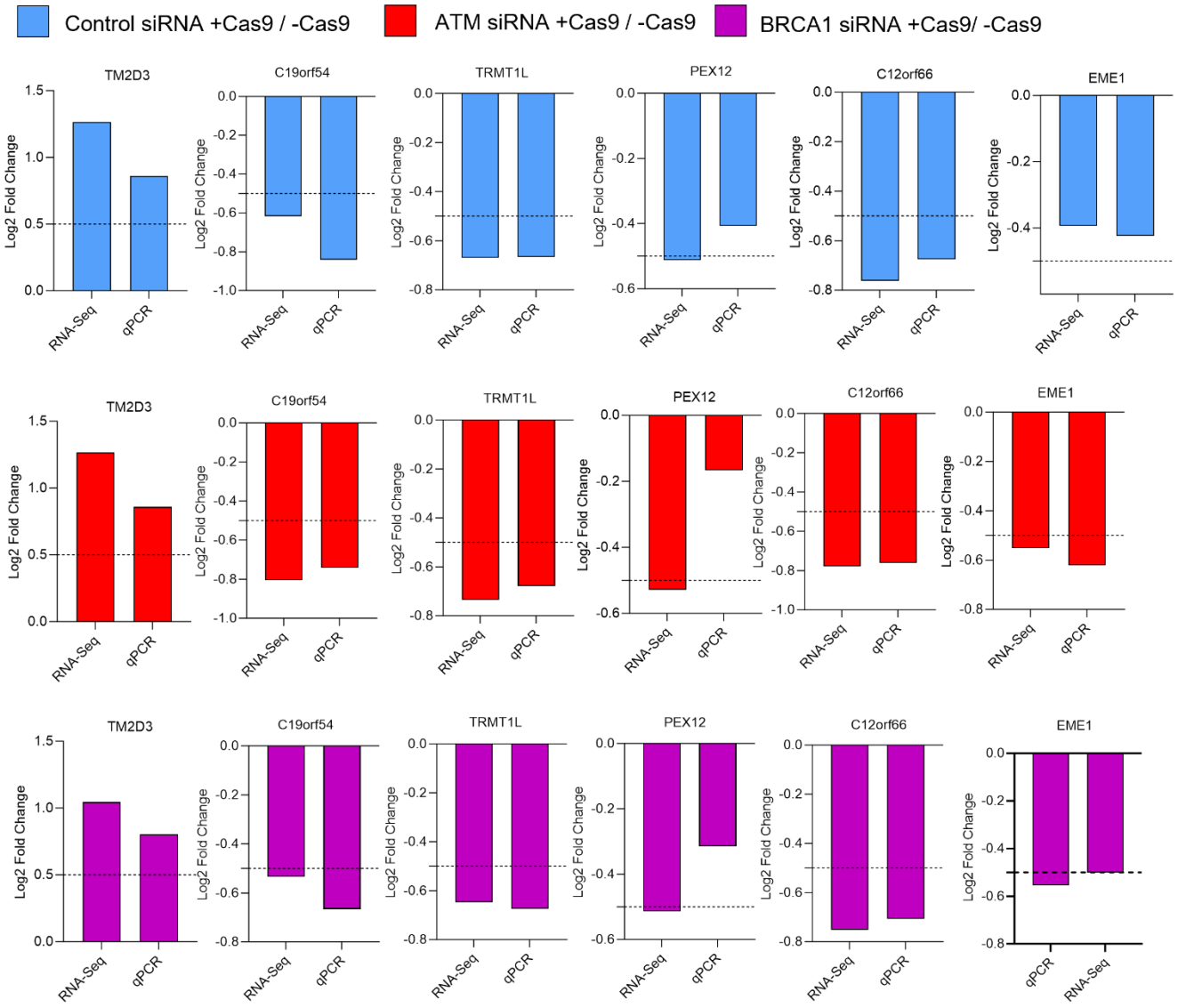

Figure 6.5- Log2 fold change of differentially expressed genes corresponds with qPCR validation.

Log2 fold change of differentially expressed genes from (Fig. 6.2) compared to log2 fold change from qPCR validation in (Fig. 6.4). Dotted line represents log2 fold change cut-off at 0.5 for upregulated genes and -0.5 downregulated genes. If bars cross dotted line, the cut-off threshold has been reached.

6.3 SETD1A is enriched at transcription start sites of SETD1A-dependent differentially expressed genes

As SETD1A regulates transcription by mediating H3K4me3 marks at the TSSs of actively transcribed genes, I investigated the presence of SETD1A at TSSs of the DEGs identified from our RNA-sequencing analysis using pre-existing mouse SETD1A ChIP-seq datasets. SETD1A was highly enriched at TSSs of SETD1A-dependent genes including *Tm2d3*, *Trmt1l*, *Pex12* and *Eme1 (***Figs 6.6 B-E***)*. I also assessed enrichment at *Nkd2*, a gene whose expression did not change upon SETD1A depletion, suggesting *Nkd2* expression is not regulated by SETD1A. As expected, there was no enrichment for SETD1A at the TSS of *Nkd2* (**Fig. 6.6 A**).

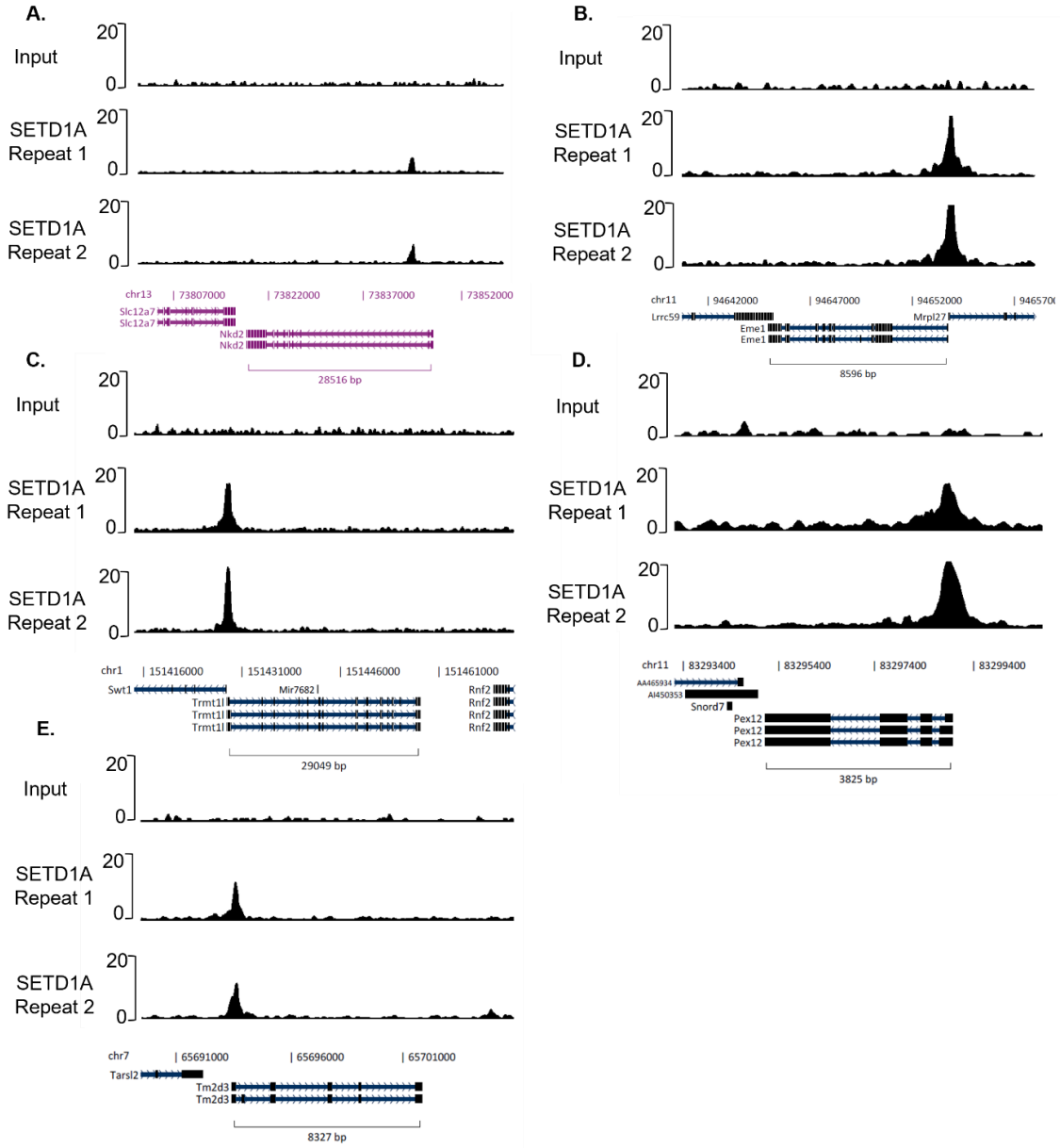

Figure 6.6- SETD1A is enriched at transcription start sites of differentially expressed genes.

Chromatin immunoprecipitation profiles of murine Setd1a over the transcription start sites (TSS) of genes from Fig. 6.2. (A.) Nkd2 (B.) Eme1 (C.) Trmt1l (D.) Pex12 (E.) Tm2d3. ChIP-Seq datasets taken from (Brown et al., 2017) were mapped to mm10 using Bowtie2 on the online galaxy platform (https://usegalaxy.eu/) . SETD1A peaks identified using EASeq ChIP sequencing analysis software (https://easeq.net/. The TSS and termination site of each gene are in located in the first and last exon (black box), respectively. Arrows indicate direction of transcription of the gene from the TSS as annotated by the integrative genomics viewer (IGV) using the NCBI reference sequence database.

6.4 Differentially expressed genes are deregulated in cancer patients with altered SETD1A expression

Next, I analysed data from cancer genomic datasets to investigate whether SETD1A expression correlated with DEG expression in tumours. First, I stratified lung adenocarcinoma, breast carcinoma or ovarian carcinoma patients by SETD1A mRNA expression then assessed the levels of each DEG. Some of the DEGs identified in the RNA-Seq analysis were also deregulated in a subset of cancer patients. For example, consistent with previous analyses, lung, breast and ovarian cancer patients with low levels of SETD1A (<-2 SD log2 mRNA expression) had significantly decreased expression of C19orf54, which was also downregulated in RNA-seq analysis. Furthermore, patients with low levels of SETD1A showed significantly increased expression of *TM2D3* (the only DEG identified as upregulated upon SETD1A deletion in RNA-sequencing analysis) in lung and breast cancer (**Fig. 6.7**). There also appeared to be an association between SETD1A and EME1 expression in lung and breast cancer, as patients with higher SETD1A expression also had higher mRNA levels of EME1.These results highlight that SETD1A expression correlates with the expression of some DEGs in certain cancer types.

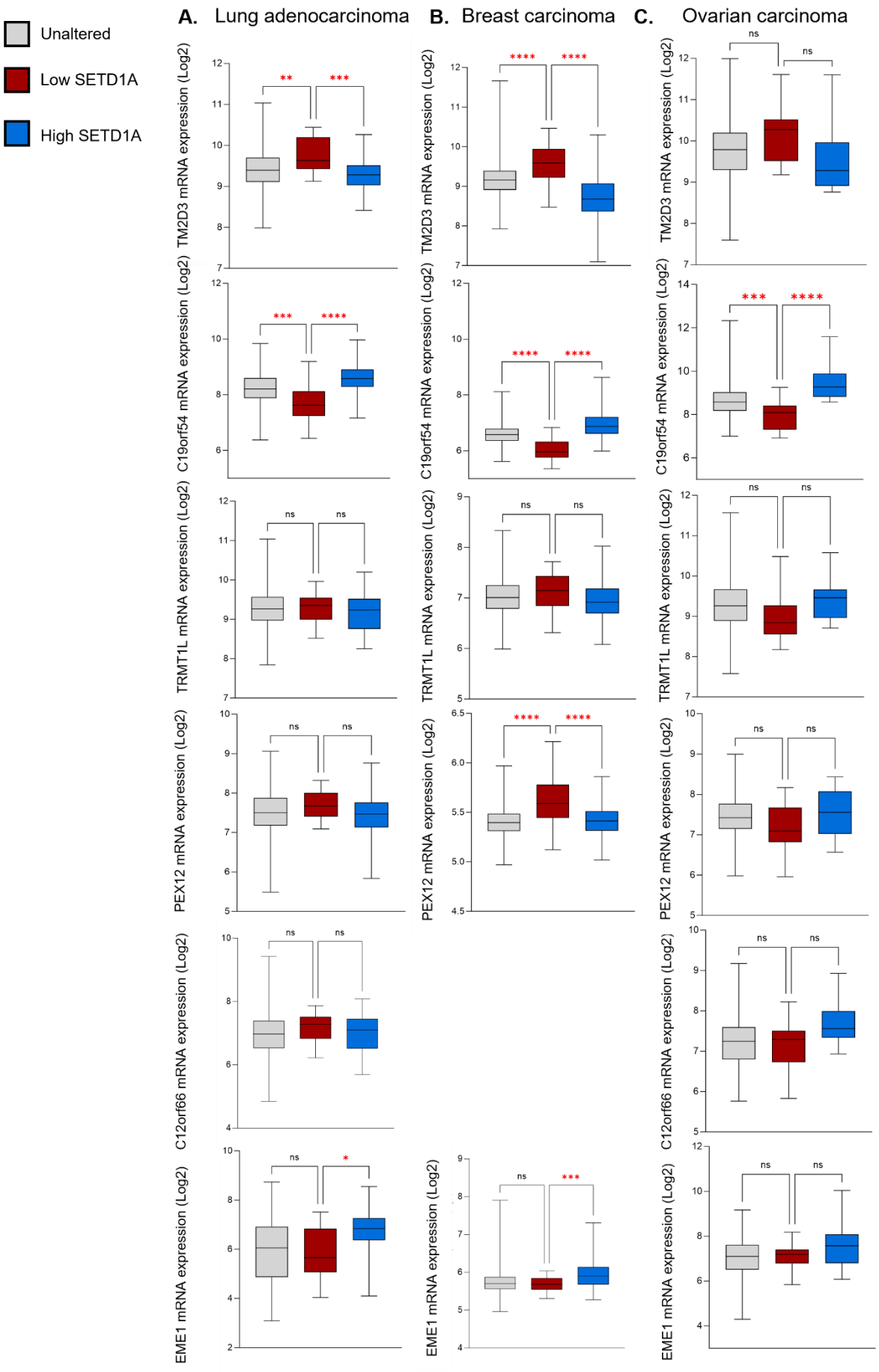
Unaltered
Low SETD1A
High SETD1A
A. Lung adenocarcinoma
B. Breast carcinoma
C. Ovarian carcinoma
TM2D3 mRNA expression (Log2)
C19orf54 mRNA expression (Log2)
TRMT1L mRNA expression (Log2)
PEX12 mRNA expression (Log2)
C12orf66 mRNA expression (Log2)
EME1 mRNA expression (Log2)
ns
*
**
***
****

Figure 6.7- Differentially expressed genes are deregulated in cancer patients with altered SETD1A expression.

*Log2 mRNA expression of DEGs identified from RNA-sequencing analysis in (A.) lung adenocarcinoma (B.) breast carcinoma or (C.) ovarian carcinoma patients triaged by SETD1A expression. Low= homozygous SETD1A deletion or mRNA expression <=-2 SD below mean; high= SETD1A mRNA expression >2 SD above mean. ns= not statistically significant, * = P < 0.05, ** = P < 0.01, ***= P < 0.001, ****= P < 0.0001 as determined by a one-way ANOVA with Tukey's test for multiple comparisons.*

6.5 SETD1A mediates EME1 expression

RNA-sequencing analysis identified EME1 was downregulated following loss of SETD1A expression in ATM- and BRCA1-deficient cells. We also observed a significant difference in HR-proficient cells, although this did not meet the minimum cut-off threshold for fold change in expression. Therefore we wanted to further validate the role of SETD1A in EME1 transcription in both HR-proficient and -deficient backgrounds. Firstly, I investigated the effect of SETD1A depletion on EME1 protein expression in HR-proficient cell lines by western blotting, which demonstrated SETD1A deletion significantly decreased EME1 protein expression (**Figs 6.8 A and B**), suggesting SETD1A may regulate EME1 expression independent of HR-status.

Next, as SETD1A is thought to regulate gene expression through H3K4me3, I hypothesised abrogating H3K4 methylation would also deregulate EME1 expression. To investigate this, I utilised the H3-WT-GFP and H3-K4A-GFP cell lines, as first described in chapter 3, treated with control, ATM or BRCA1 siRNA. As predicted, perturbing H3K4 methylation with H3-K4A-GFP significantly reduced EME1 mRNA expression levels in cells depleted of BRCA1, however, this effect was not observed in control or ATM siRNA treated cells (**Fig. 6.8 C**). In fact, abrogation of H3K4me appeared to increase EME1 expression in control siRNA treated cells, suggesting there could be an alternative method beyond H3K4me3 in which SETD1A may regulate EME1 transcription.

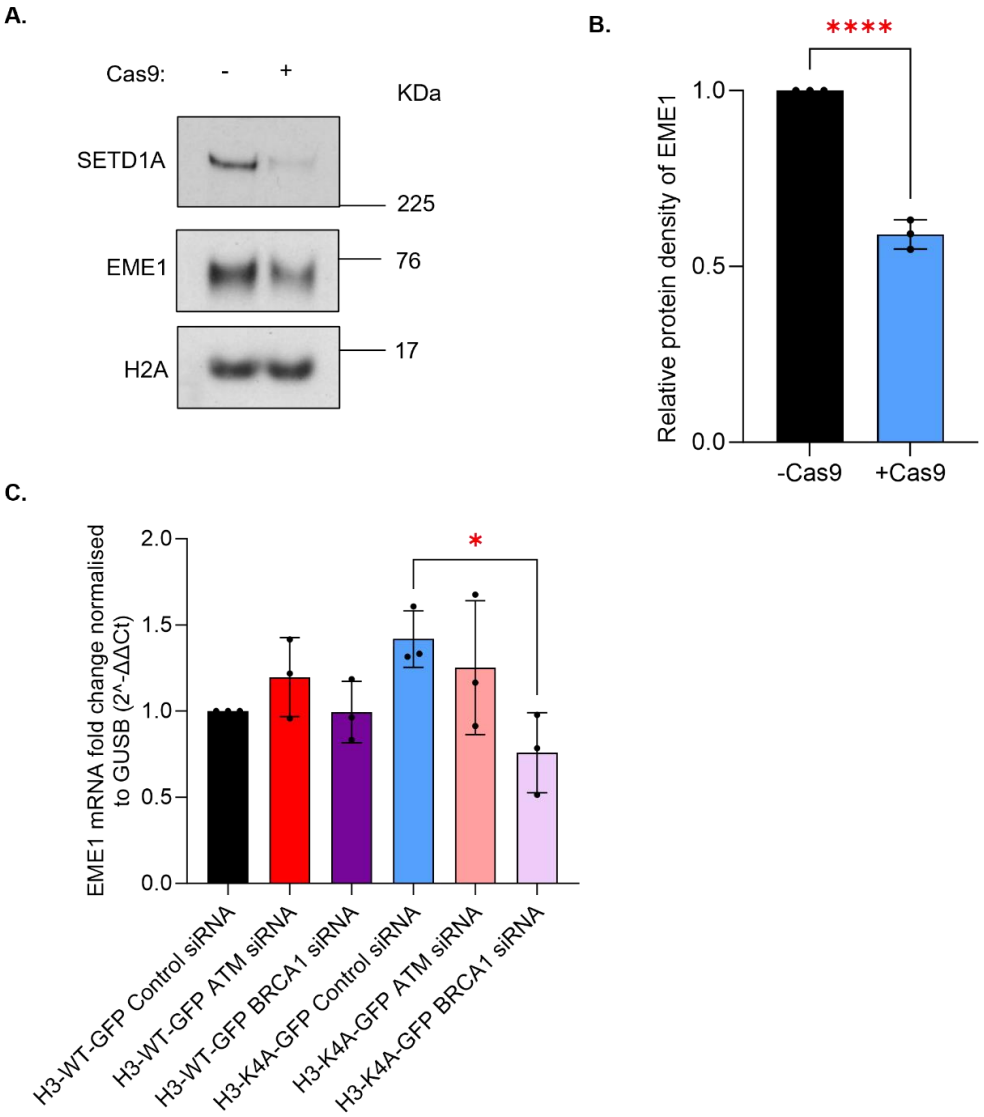

Figure 6.8- SETD1A and H3K4me3 regulate EME1 protein or mRNA expression.

*(A.) HeLa Kyoto iCas9 cell line expressing SETD1A gRNA #4 was treated with ± 1 µg/ml doxycycline for 48 hours to induce SETD1A gene editing. Cells were harvested and whole cell extracts were immunoblotted using the indicated antibodies. (B.) Immunoblot quantification from (A.) using ImageJ. (C.) H3-WT-GFP or H3-K4A-GFP cells were transfected with the indicated siRNAs. Cells were harvested and RNA extracted. mRNA levels of EME1 transcripts were determined by qPCR. mRNA expression fold change normalised to GUSB was calculated using the 2^-ΔΔCt method. All plots represent the mean ± SD from three independent biological repeats. * = P <0.05 as determined by a two-tailed Students t-test. **** = P <0.0001 as determined by a one-way ANOVA with post-hoc Tukey's test for multiple comparisons.*

To investigate whether SETD1A also regulates EME1 expression in HR-deficient cancer cells, I measured EME1 protein and mRNA expression in *BRCA1*- and *ATM*-mutated cancer cell lines. As expected, EME1 protein expression was downregulated when SETD1A was depleted from *BRCA1*-mutated UWB1.289 ovarian cancer and HCC1937 breast cancer cells or *ATM*-mutated H1395 lung cancer cells (**Figs 6.9 A and B**). These findings were further validated at the mRNA level in the *BRCA1*-mutated cancer types (**Fig. 6.9 C**), suggesting the transcriptional regulation of EME1 by SETD1A is conserved across multiple cancer types.

As SETD1A localises to the chromatin at sites of DSBs we next wanted to assess whether EME1 also associated with chromatin in a SETD1A-dependent manner. To investigate this, we performed western blotting following chromatin fractionation, using PARP1 as a chromatin control. The results show that EME1 is expressed in the chromatin fraction of HeLa cells and that this is reduced upon depletion of SETD1A, (**Fig. 6.10**). This finding suggests that SETD1A transcriptionally regulates EME1 expression levels on the chromatin.

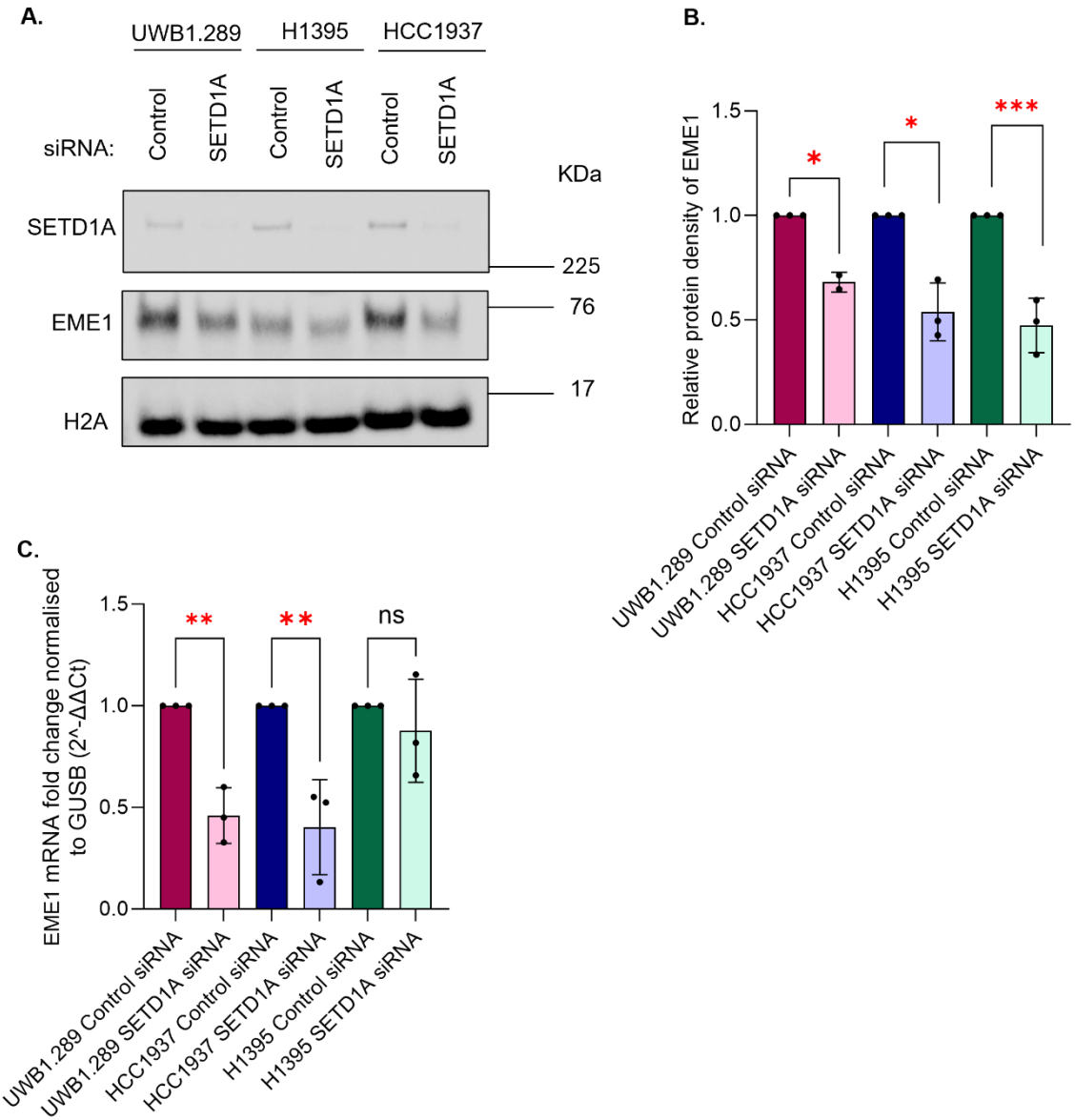

Figure 6.9- SETD1A regulates EME1 expression in HR-deficient cancer cell lines.

*UWB1.289, HCC1937 and H1395 cells were transfected with indicated siRNAs. (A.) Cells were harvested and whole cell extracts were immunoblotted using the indicated antibodies. (B.) Immunoblot quantification from (A.) using ImageJ. (C.) Cells were harvested, and RNA extracted. mRNA levels of EME1 transcripts were determined by qPCR. mRNA expression fold change normalised to GUSB was calculated using the 2^-ΔΔCt method. All plots represent the mean ± SD from three independent biological repeats. * = P <0.05, ** = P <0.01 *** = P <0.001 as determined by a one-way ANOVA with post-hoc Tukey's test for multiple comparisons.*

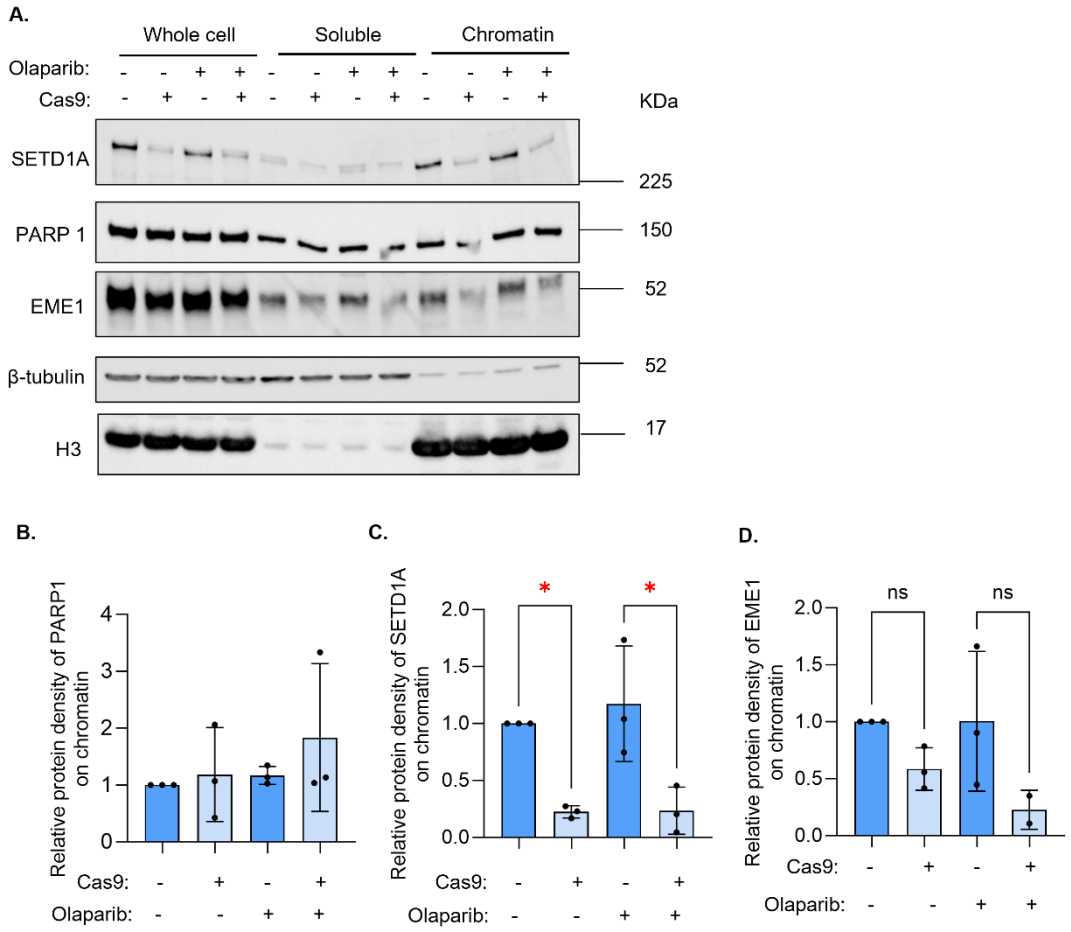

Figure 6.10- Cas9-mediated gene editing of SETD1A reduces recruitment of EME1 to chromatin.

*HeLa Kyoto iCas9 SETD1A gRNA #4 cells were treated with ± 1 µg/ml doxycycline for 48 hours to induce Cas9 expression. Following this the cells were treated with 10 µM olaparib for 24 hours after which cells were harvested and chromatin fractionation was performed. (A.) Western blot analysis of whole cell, nuclear soluble and chromatin bound fractions. Blots were probed with indicated antibodies. Histone H3 and β-tubulin were used as positive controls for the chromatin bound and nuclear soluble fractions, respectively. Quantification of (B.) PARP1, (C.) SETD1A and (D.) EME1 levels in the chromatin binding fraction relative to total protein expression in the whole cell lysate and normalised to the untreated control. Band signal intensity was quantified using ImageJ software. Data points represent mean ± SD from three independent biological repeats. ns= not statistically significant, * = P <0.05 as determined by a one-way ANOVA with post-hoc Tukey's test for multiple comparisons.*

6.6 Altered EME1 expression is associated with poor survival in BRCA1-deficient breast cancer

Reduced SETD1A expression is associated with decreased survival in some HR-deficient cancer types (**Fig 4.7**). Next, I examined whether SETD1A-mediated expression of *EME1* could also correlate with clinical outcomes of HR-deficient cancer patients. Using data obtained from cancer genomic databases I performed Kaplan-Meir survival analysis on ATM-, BRCA1-, or BRCA2-deficient lung, ovarian and breast cancer patients stratified by EME1 mRNA expression.

In most cases EME1 expression did not correlate with patient survival, except in the case of BRCA1-deficient breast cancer, where high EME1 expression associated with a poorer prognosis (**Fig. 6.11**). These findings suggest that EME1 correlates with survival in a specific subset of HR-deficient patients. Here we showed high EME1 expression is associated with poor survival, however, this differs to patients triaged by SETD1A expression, where low SETD1A expression was associated with poorer prognosis. Furthermore, we observed a significant difference in survival in *ATM*-deficient lung cancer patients triaged by SETD1A expression which we did not observed for *EME1,* suggesting EME1 and SETD1A expression have different effects for patient survival in HR-deficient tumours.

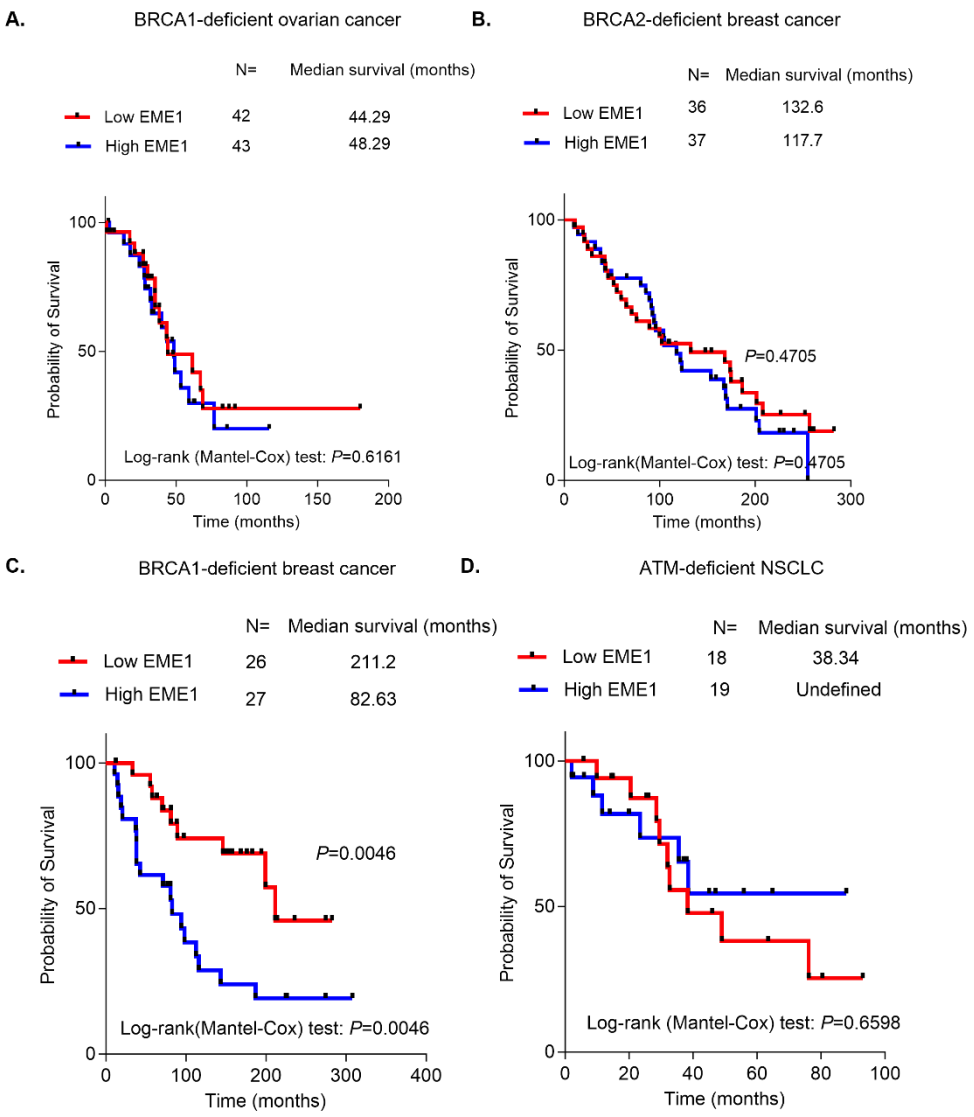

Figure 6.11- Higher EME1 expression is associated with poorer overall survival in BRCA1-deficient breast cancer.

Kaplan-Meir plots for overall survival of patients with HR-deficient cancer stratified by low versus high EME1 expression. (A.) BRCA1-deficient ovarian cancer from the TCGA database. (B.) BRCA2-deficient breast cancer from the METABRIC database. (C.) BRCA1-deficient breast cancer from the METABRIC database. (D.) ATM-deficient non-small cell lung cancer (NSCLC) from the TCGA database. HR gene-deficient patients were defined as homozygous deletion, mutation, or mRNA expression <=-2 SD below mean of the indicated HR-related genes. All data was obtained from the CBioPortal database https://www.cbioportal.org/. Patients in the 50% lower EME1 mRNA expression (red line) were compared to the 50% higher EME1 mRNA expression (blue line). Curve comparisons were performed using the Log-rank (mantel-Cox) test.

6.7 Loss of EME1 drives PARPi resistance in HR-deficient cells by restoring homologous recombination

Analysis of mRNA and protein expression through RNA-seq and qPCR and western blotting, respectively, show depletion of SETD1A is correlated with downregulation of EME1 expression. Given the known role of EME1 as the regulatory subunit of a structure specific cross-over endonuclease formed with MUS81, which cleaves branched DNA structures such as RFs, 3' DNA flaps and HJs (Wyatt *et al.*, 2013) (Wyatt *et al.*, 2017) (Sarbajna, Davies and West, 2014), we hypothesised SETD1A-mediated transcriptional regulation of EME1 could be the underlying mechanism for PARPi resistance in ATM- and BRCA1-deficient cells following loss of SETD1A.

To assess this, I depleted BRCA1, ATM and/or EME1 from HeLa cells and assessed response to olaparib using clonogenic survival assays (**Figs 6.12 A and 6.13 A**). In support of our hypothesis, EME1 loss phenotypically mirrored SETD1A depletion in both backgrounds, i.e. loss of EME1 compromised PARPi sensitivity (**Figs 6.12 and 6.13**). This was most evident in ATM-deficient cells, where depletion of EME1 significantly decreased Olaparib sensitivity (**Figs 6.12 C and D**).

Previously, we showed loss of SETD1A reduced PARPi sensitivity by restoring HR in ATM- and BRCA1-deficient cells, thus we next investigated whether decreased PARPi sensitivity upon loss of EME1 was also associated with increased HR. In keeping with SETD1A-depletion and PARPi sensitivity, loss of EME1 also increased RAD51 foci formation in both ATM- and BRCA1-deficient cells following exposure to PARPi (**Fig. 6.14**)**.** Together, these findings demonstrate that loss of SETD1A-dependent EME1 transcription drives PARPi resistance in HR-deficient cells by restoring HR.

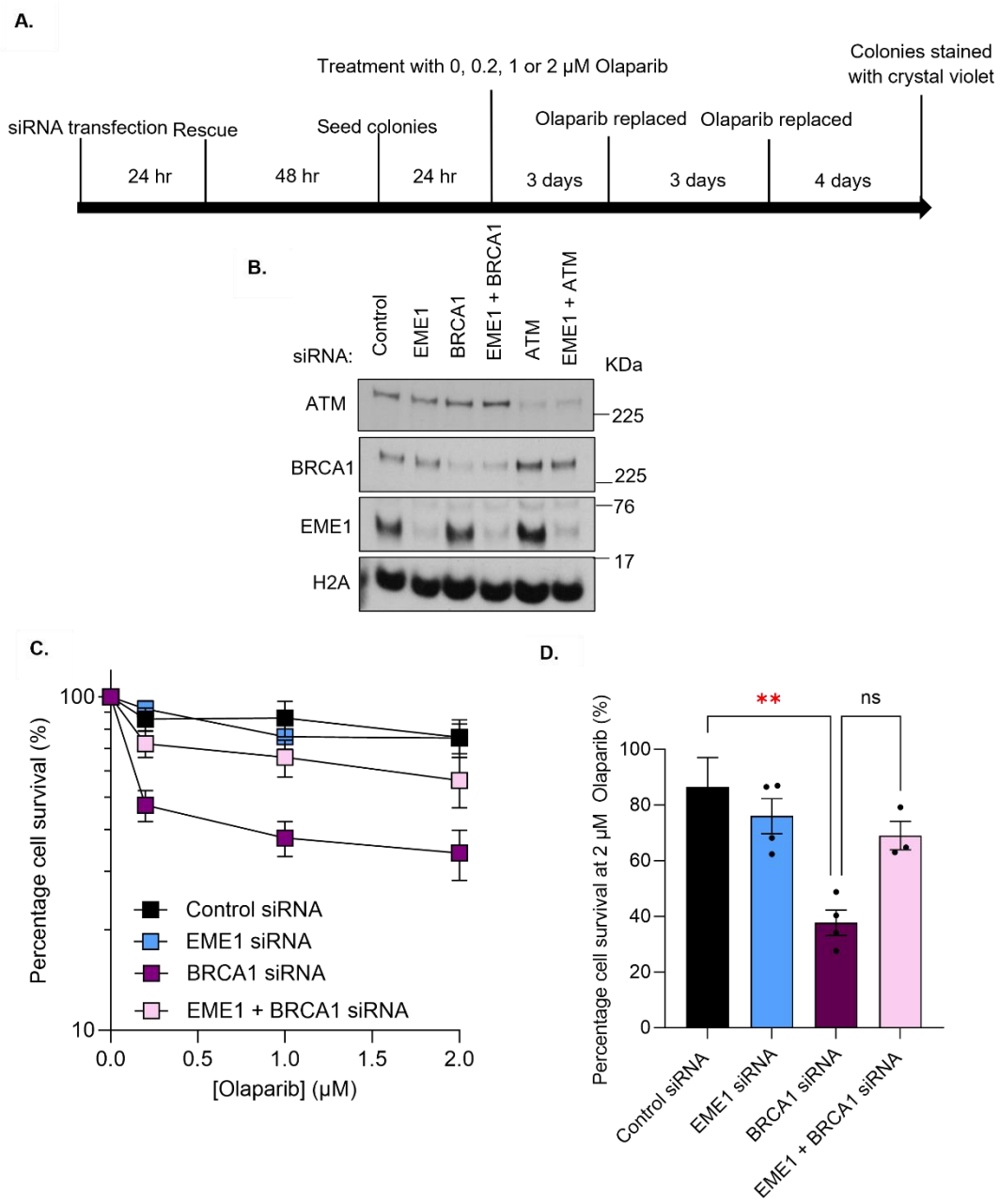

Figure 6.12- Loss of EME1 reduces sensitivity of BRCA1-deficient cells to olaparib treatment.

*(A.) Schematic of experimental time course. (B.) Whole cell extracts of HeLa cells treated with indicated siRNAs were immunoblotted with the indicated antibodies. (C.) Clonogenic survival curve for HeLa cells transfected with the indicated siRNAs. Transfected HeLa cells were exposed to the indicated doses of olaparib for 10 days before staining with crystal violet and colonies counted. (D.) Percentage cell survival from (C.) at 2 μM olaparib. Data points represent the mean ± SEM from three independent biological repeats. ns= not statistically significant, ** = P <0.01 as determined by a one-way ANOVA with Tukey's test for multiple comparisons.*

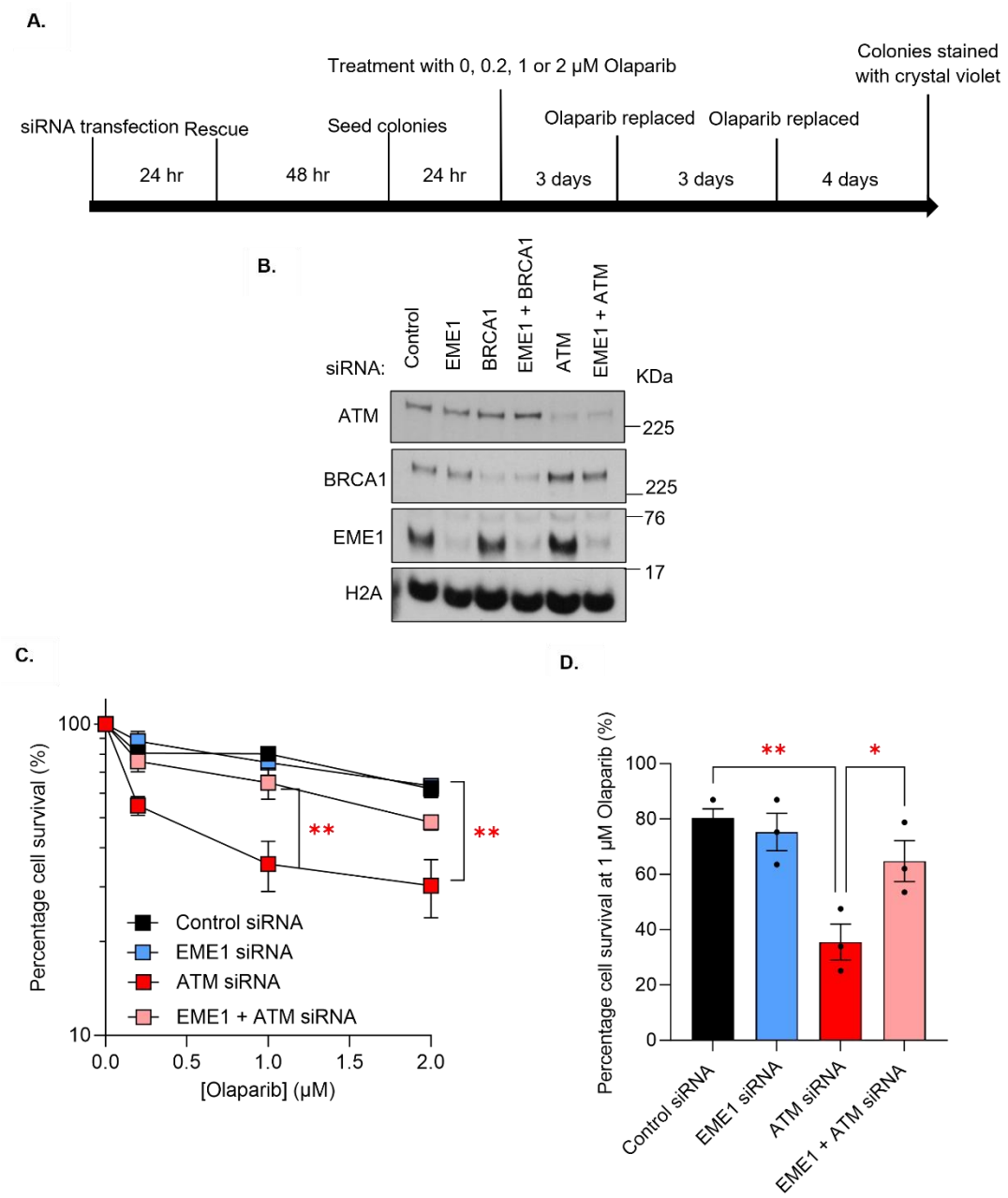

Figure 6.13- Loss of EME1 reduces sensitivity of ATM-deficient cells to olaparib treatment.

*(A.) Schematic of experimental time course. (B.) Whole cell extracts of HeLa cells treated with indicated siRNAs were immunoblotted with the indicated antibodies. (C.) Clonogenic survival curve for HeLa cells transfected with the indicated siRNAs. Transfected HeLa cells were exposed to the indicated doses of olaparib for 10 days before staining with crystal violet and colonies counted. (D.) Percentage cell survival from (C.) at 2 μM olaparib. Data points represent the mean ± SEM from three independent biological repeats. *= P <0.05, **= P <0.01 as determined by a two-way (C.) or one-way (D.) ANOVA with Tukey's test for multiple comparisons.*

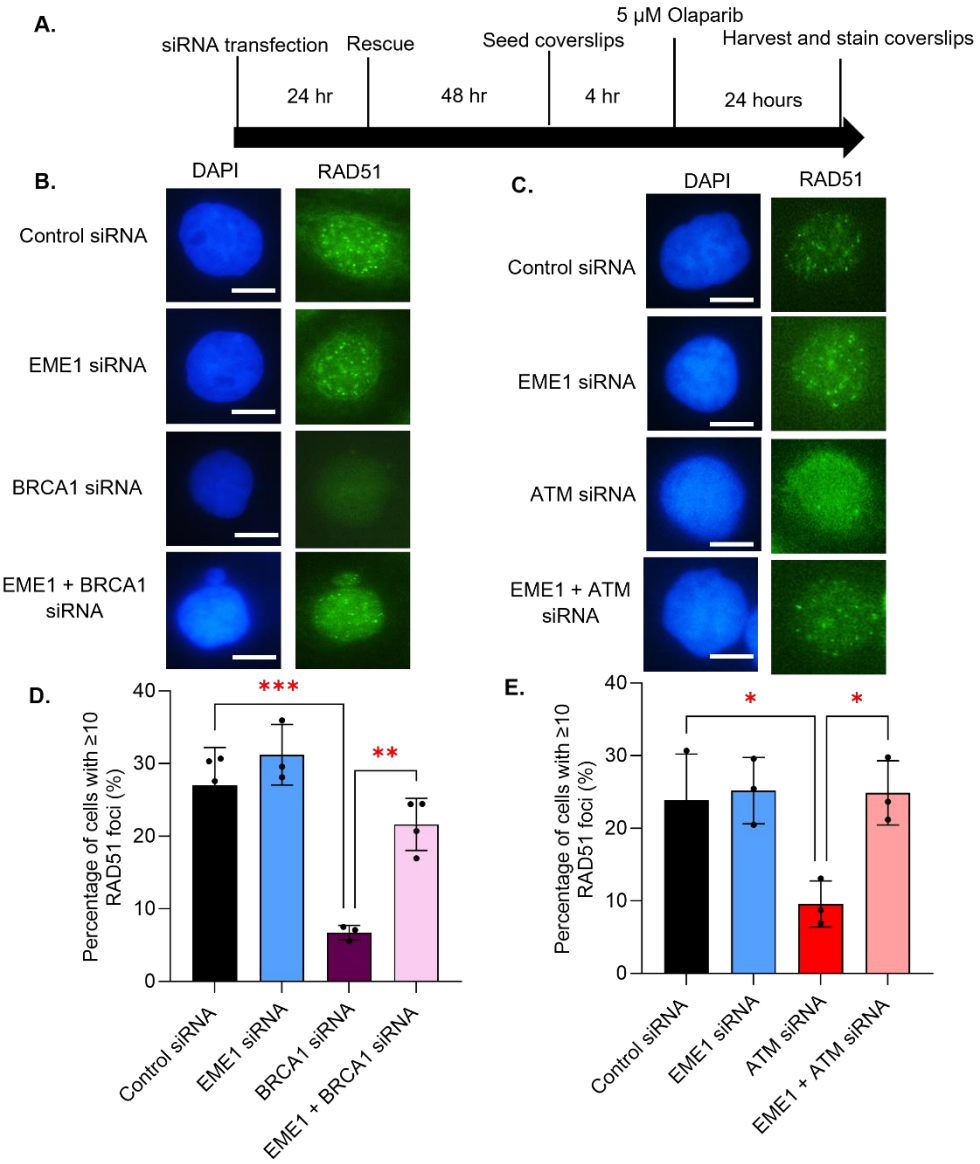

Figure 6.14- Loss of EME1 restores RAD51 foci formation in BRCA1- and ATM-deficient cells treated with olaparib.

*HeLa cells were transfected with indicated siRNAs and exposed to 5 μM olaparib for 24 hours. Cells were immunostained for RAD51 foci and nuclei counterstained with DAPI. Foci formation was enumerated by fluorescent microscopy (A.) Schematic of experimental time course. (B. and C.) Representative immunofluorescent images (scale bar 10 μm). (D. and E.) Graphical representation of the percentage of cells with ≥ 10 RAD51 foci 24 hours post olaparib treatment. At least 100 cells were counted per condition. Results represent the mean ± SD from three biologically independent experiments. * = P < 0.05, ** = P <0.01, ***= P <0.001 as determined by a one-way ANOVA with post-hoc Tukey's test for multiple comparisons.*

6.8 Loss of EME1 reduces RIF1 foci formation in G1 cells following ionising radiation

Restoration of HR following SETD1A depletion arises from defective H3K4me and reduced recruitment of RIF1 to DSBs (Bayley *et al.*, 2022). To our knowledge EME1 has not previously been identified to play a role in RIF1 recruitment at DSBs. To determine whether restored HR induced by EME1 loss, may be attributed to a novel role of EME1 in regulating RIF1 recruitment, I assessed RIF1 foci formation in SETD1A and/or EME1 depleted BRCA1-mutated HCC1937 breast cancer cells, following ionising radiation (**Fig. 6.15 A**).

In keeping with our findings that EME1 depletion restored HR in ATM- and BRCA1-deficient cells, depletion of EME1 resulted in a significant decrease in IR-induced RIF1 foci formation in G1 cells. This defect was to a similar extent as loss of SETD1A, and co-depletion of SETD1A and EME1 resulted in no further decrease in foci levels (**Figs 6.15 C and D**), suggesting these proteins act in the same pathway of RIF1 foci formation. Whilst loss of EME1 expression reduced RIF1 foci formation, there was no significant effect on RIF1 protein expression (**Fig. 6.15 E**), indicating that EME1 does not regulate RIF1 expression. These findings are unexpected and suggests a previously unidentified role for EME1 in RIF1 recruitment, contributing to the end-protection pathway, offering an exciting opportunity for future studies.

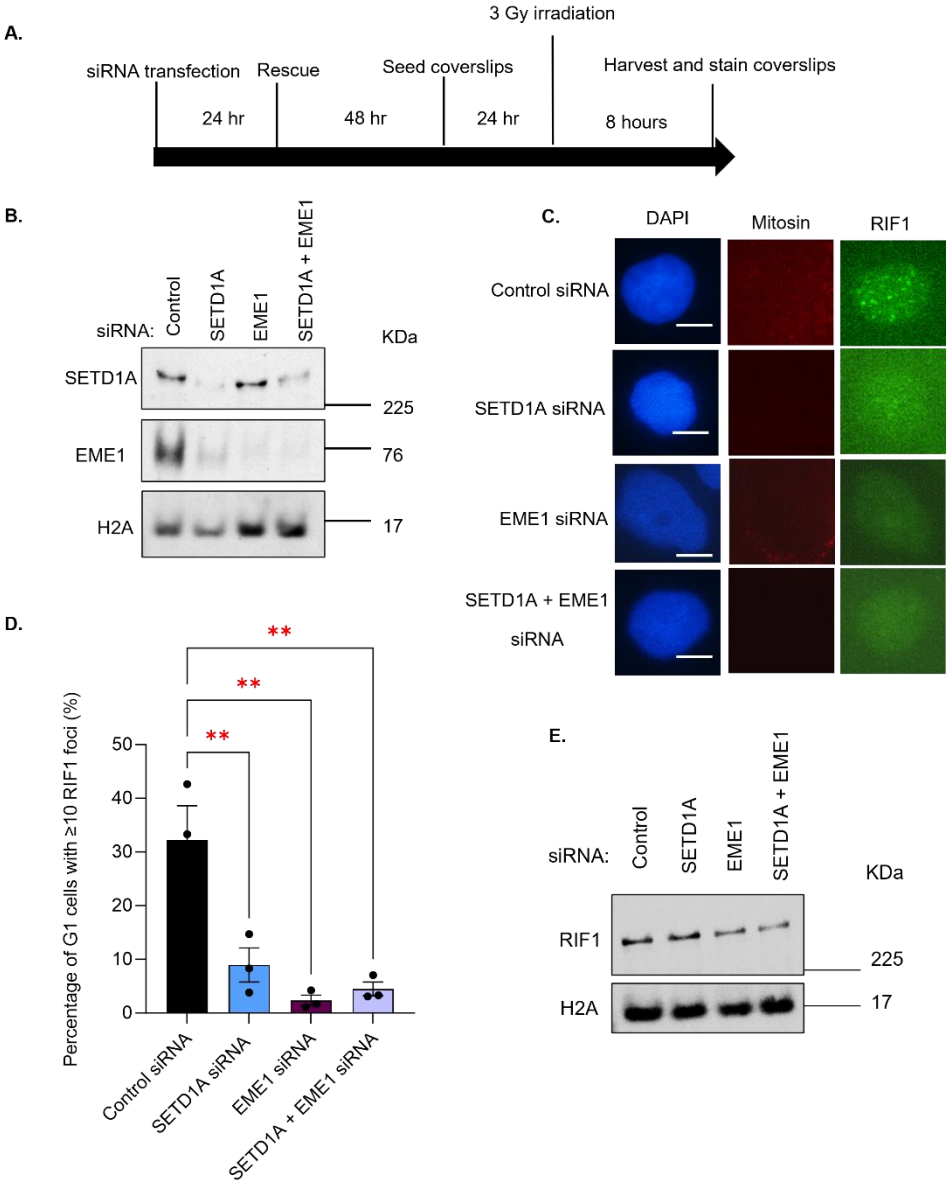

Figure 6.15- Loss of EME1 decreases RIF1 foci formation following ionising radiation in BRCA1-deficient cells.

*HCC1937 cells were transfected with indicated siRNA and seeded onto coverslips. Coverslips were harvested 8 hours post exposure to 3 Gy IR and immunostained for RIF1. G1 cells were identified as mitosin negative and nuclei counterstained with DAPI. (A.) Schematic of experimental time course. (C.) Representative immunofluorescent images (scale bar 10 μm). (D.) Quantification of the percentage of G1 cells with ≥10 RIF1 foci 8-hour post IR. At least 100 cells were counted per condition. (B.) and (E.) Whole cell extracts of cells treated with indicated siRNAs were immunoblotted with the indicated antibodies. Data points represent the mean ± SD from three independent biological repeats. ** = P <0.01 as determined by a one-way ANOVA with post-hoc Tukey's test for multiple comparisons.*

6.9 Discussion

6.9.1 SETD1A regulates the transcription of a small selection of gene targets in HeLa Kyoto iCas9 cells

SETD1A is considered a transcriptional regulator due to its role as a histone lysine methyltransferase, however, in this study only a small number of genes were differentially regulated following SETD1A deletion. This suggests SETD1A regulates a specific subset of genes in HeLa Kyoto iCas9 cells and has limited influence on global gene expression. This is consistent with our findings that SETD1A depletion does not change global H3K4me3 expression, as well as previous findings by Ishii *et al.* who found SETD1A regulated a comparable number of DEGs in a model of pancreatic ductal adenocarcinoma (Ishii *et al.*, 2023). Despite this, other studies have shown greater effects of SETD1A depletion on gene expression. For example, SETD1A deletion resulted in the downregulation of over 500 genes in a mouse model of leukaemia (Hoshii *et al.*, 2018). Together these studies highlight that SETD1A transcriptional regulation varies by cell type and SETD1A may play more important transcriptional roles in haematopoietic cells compared to other cell types.

As SETD1A acts as a transcriptional activator, it is not surprising that all but one of the DEGs (TM2 domain-containing protein 3 *(TM2D3*)) were downregulated upon SETD1A depletion. In this case, *TM2D3* transcription is likely an indirect target of SETD1A. TM2D3 is one of three highly conserved TM2 domain containing proteins encoded in the human genome (Jakobsdottir *et al.*, 2016). Previously, overexpression of TM2D3 led to activation of Notch signalling by increasing NOTCH1 cleavage and

cell surface expression (Masuda *et al.*, 2023), therefore it is possible that Notch signalling is also activated upon SETD1A depletion. Despite this, SETD1A has previously been shown to enhance Notch signalling by promoting the expression of Notch target genes in ovarian cancer development (Chai *et al.*, 2023). Therefore, upregulation of TM2D3 could enhance notch signalling in a negative feedback loop in response to loss of SETD1A. Notch signalling has previously been implicated in PARPi resistance, with increased NOTCH3 expression observed in olaparib resistant cells (Decker *et al.*, 2017). Thus, increased TM2D3 expression following SETD1A depletion could contribute to PARPi-resistance by increasing notch signalling. The role of SETD1A in Notch signalling offers a potential area for future investigation.

Four further genes were commonly downregulated upon loss of SETD1A regardless of genetic background and HR status, including *C19orf54*, which has since been renamed actin maturation protease *(ACTMAP)* due to its involvement in actin processing. To date SETD1A has not been implicated in this process but considering the known roles of actin maturation in the DDR (Huang, Zhang and Park, 2022; Torii *et al.*, 2023) and the important contribution of DDR and its rewiring in PARPi sensitivity, investigating the role of SETD1A in actin maturation is an interesting avenue for future investigation.

*TRMT1L (*tRNA methyltransferase 1 like*),* a tRNA methyltransferase (Jonkhout *et al.*, 2021), was also downregulated following loss of SETD1A. Several previous studies have also highlighted the role of SETD1A in regulating the expression of genes regulating tRNA related processes. (Hoshii *et al.*, 2018; Arndt *et al.*, 2018). Furthermore, the mouse ortholog of TRMT1L is implicated in motor coordination and cognitive functioning (Vauti *et al.*, 2007), which is in concordance with the key role of

SETD1A in neurodevelopment. Whilst there is no obvious link between TRMT1L expression and PARPi sensitivity, the expression of other tRNA modifying enzymes have previously been linked to cancer drug resistance (Añazco-Guenkova *et al.*, 2024), thus investigating the relationship between SETD1A, H3K4me3 and tRNA modifications is a potential area for future investigations.

SETD1A depletion also downregulated *C12orf66*, also known as KICSTOR subunit 2 (KICS2), a subunit of the KICSTOR protein complex, which negatively regulates mTORC1 signalling (Wolfson *et al.*, 2017). mTORC1 is a PI3K-related kinase which mediates cell growth and division through regulation of protein synthesis and turnover and lipid, nucleotide and glucose metabolism (Saxton and Sabatini, 2017). mTOR pathways have been shown to regulate DNA repair and clinical trials have shown a combination of PARP inhibition with mTOR inhibitors suppresses HR activity in breast cancer (Westin *et al.*, 2018; El Botty *et al.*, 2018). This provides a clear rationale for studying the relationship between SETD1A and mTOR signalling in relation to PARPi-resistance in the future.

We also confirmed the SETD1A-dependent regulation of EME1 on both the transcript and protein level. These findings are supported by previous studies which have also implicated SETD1A in regulating EME1 expression in HSCs (Arndt *et al.*, 2018). *EME1* (Essential meiotic structure-specific endonuclease 1) is a structure specific cross-over endonuclease that forms a heterodimeric endonuclease complex with the MUS81 structure-specific endonuclease subunit (MUS81). EME1 acts as the regulatory subunit of this complex and possesses no endonuclease activity alone. MUS81-EME1 subsequently forms part of the larger SMX trinuclease complex with SLX-4, SLX1, XPF and ERCC1 (Aprosoff *et al.*, 2023). Together the SMX complex

cleaves branched DNA structures such as RFs, 3’ DNA flaps and HJs (Wyatt *et al.*, 2013) (Wyatt *et al.*, 2017) (Sarbajna, Davies and West, 2014).

In addition to the genes discussed here, there were multiple other DEGs specific to SETD1A knockout on a BRCA1- or ATM-deficient background, including *ITGAM* and *CHAC1* or *DARS1* and *RECQL5*, respectively. The genes we have identified here offer additional future avenues for investigating new functionalities of SETD1A.

Further evidence supporting SETD1A-dependent transcriptional regulation of these DEGs came from analysis of murine ChIP-seq data, which identified SETD1A enrichment at the TSSs of genes identified in our RNA-sequencing analysis. This data suggests SETD1A binds to the promoter regions of these genes, where it is likely to catalyse H3K4me3 to drive transcriptional activation. In the future I would validate this ChIP-seq analysis in human cell lines, as well as assessing whether H3K4me3 is also enriched at these TSSs and how SETD1A knockout effects this enrichment. Initial evidence as to whether H3K4me3 may regulate the transcription of these genes was contradictory, as perturbation of H3K4me3 using the H3-K4A-GFP mutant cells downregulated EME1 expression in BRCA1-deficient cells, whilst increasing expression in control siRNA treated cells. These initial results suggest there could be additional mechanisms other than SETD1A-dependent H3K4me3 involved in the transcriptional regulation of EME1. For example, previous studies have shown that SETD1A can also regulate transcription via interaction between its non-catalytic FLOS domain and cyclin K (Hoshii *et al,* 2018).

Additional studies examining whether SETD1A overexpression subsequently restores expression of these DEGs would also help confirm the role for SETD1A in their transcriptional regulation.

6.9.2 Deregulated gene expression correlated with SETD1A expression in cancer patients

Many of the DEGs identified in the RNA-seq analysis were also deregulated in cancer patients with altered SETD1A expression. Furthermore, SETD1A knockdown resulted in a significant decrease in EME1 protein and mRNA expression in BRCA1-deficient cancer cell lines. These findings indicate that SETD1A-dependent transcriptional regulation of a subset of these DEGs has relevance in cancer cells and is conserved across multiple cancer types.

Increased EME1 expression was also associated with poor survival in BRCA1-deficient breast cancer patients. This is supported by previous studies showing high EME1 expression was also a risk factor for poor overall survival in kidney renal clear cell carcinoma (Li *et al.*, 2024). This is also supported by the high frequency of EME1 alterations in a variety of cancer types, indicating that EME1 expression is correlated with cancer patient survival. Whilst we observed that high EME1 levels correlated with poor survival, in fig 4.7 we showed poor survival was associated with low SETD1A expression, suggesting that EME1 and SETD1A expression levels have opposing effects on patient survival in BRCA1-deficient breast cancer patients. A key limitation of this survival analysis is the unavailability of clinic data relating to cancer treatment. Therefore, the differences in survival observed when patients are stratified by SETD1A vs. EME1 expression may be due to interactions with chemotherapeutics other than PARPi. Consequently, based on this data we cannot comment on how

SETD1A or EME1 expression levels may impact the survival of patients receiving PARPi therapy. Immunohistochemical staining for EME1 and SETD1A in tissue sections from cancer patients receiving PARPi therapy will help further confirm the relevance of SETD1A in the transcriptional regulation of EME1 and the impact on survival of patients undergoing PARPi treatment.

Interestingly, EME1 mRNA levels did not change in the *ATM*-mutated H1395 cell line following SETD1A depletion. Previously, we also showed that loss of SETD1A was unable to reduce PARPi sensitivity in the same cell line. This suggests that SETD1A is not the main regulator of EME1 mRNA expression in H1395 cells. We could also infer that loss of SETD1A is unable to confer PARPi sensitivity in this cell line due to their higher expression of EME1 mRNA.

6.9.3 SETD1A-dependent transcription of EME1 drives PARPi resistance in BRCA1- and ATM-deficient cells by restoring homologous recombination

Given the role of EME1 in the DDR through cleavage of branched DNA structures such as HJs, which form as intermediates of HR, we hypothesised SETD1A-mediated transcriptional regulation of EME1 could influence PARPi sensitivity in ATM- and BRCA1-deficient cells following loss of SETD1A. Confirming this, loss of EME1 phenocopied loss of SETD1A by reducing the sensitivity of ATM- and BRCA1-deficient cells to olaparib treatment. These findings are in agreement with findings from the D'Andrea lab who showed loss of the EME1 binding partner MUS81 renders BRCA2-deficient cells resistant to PARPi (Rondinelli *et al.*, 2017), further implicating the MUS81-EME1 complex in PARPi sensitivity in HR-deficient cells.

We also found that loss of EME1 restored HR in ATM- and BRCA1-deficient cells, suggesting similarly to loss of SETD1A, restoration of HR could also be the underlying mechanism of PARPi resistance in cells lacking EME1. This is an unexpected finding given that EME1 has previously been implicated in resolution of HJs, which occur during late-stages of HR (Castor *et al.*, 2013). Our results instead suggest a potential new anti-recombinogenic role for EME1. Despite this, other studies have called to question the role of EME1 in HR, for example, EME1 was not required for the resolution of DNA intermediates arising during HR-mediated gene targeting/conversion (Abraham *et al.*, 2003). Instead, this study implicated EME1 in maintaining genome stability by preventing aberrant chromosome structures forming following meiosis-induced DSB repair (Abraham *et al.*, 2003). To further confirm the HR status of cells lacking EME1, RAD51 foci results should be validated using the LMNA-CRISPR HR assay. Furthermore, the level of PARPi-induced genome instability following EME1 depletion should be assessed by measuring chromosomal radial formation in metaphase spreads.

Whilst EME1 contributes to the maintenance of genome stability in some contexts, it has also been shown to drive instability under certain conditions. For example, MUS81-EME1 cleavage products can contribute to chromosomal instability (CIN) in HR-defective CHK1-deficient cells (Calzetta, González Besteiro and Gottifredi, 2020). During S-phase, CHK1-deficient cells accumulate under-replicated DNA which subsequently enters mitosis. This triggers mitotic DNA synthesis (MiDAS), and the nascent DNA is subsequently cleaved by MUS81-EME1 to form DSBs, which drives CIN (Calzetta, González Besteiro and Gottifredi, 2020). PARPi treatment has also been shown to activate MiDAS in HR-deficient cells (Heijink *et al.*, 2022), due to the

accumulation of transcription-replication conflicts (TRCs) in early S-phase (Petropoulos *et al.*, 2024). Thus, HR-defective ATM- and BRCA1-deficient cells may also display increased CIN in response to PARPi treatment, due to MiDAS mediated repair of under-replicated DNA. Based on this information, I hypothesise loss of SETD1A-dependent EME1 expression may reduce PARPi sensitivity in these cells by reducing cleavage following MiDAS mediated repair and decreasing CIN. This theory is supported by earlier results demonstrating olaparib induced the accumulation of aberrant chromosomal structures such as radials in ATM- and BRCA1-deficient cells, which were subsequently reduced upon depletion of SETD1A. This potential mechanism for EME1 associated PARPi resistance provides an important area for future investigation, beginning with determining if EME1 depletion restores aberrant chromosome structures in HR-deficient cells in response to PARPi.

6.9.4 Loss of EME1 reduces recruitment of RIF1 to DSBs

Previously, it was shown that loss of SETD1A restores HR by reducing the recruitment of RIF1 to DSBs breaks (Bayley *et al.*, 2022). Unexpectedly, we also found that RIF1 foci formation was compromised following loss of EME1, and this was not due to significant differences in RIF1 protein expression. These findings suggest EME1 may work in the same pathway as SETD1A to facilitate RIF1-dependent NHEJ. To our knowledge this is the first study to identify a potential anti-recombinogenic role for EME1, offering an exciting opportunity for future research to investigate the precise mechanism in which EME1 contributes to RIF1 recruitment at DSBs. It remains to be determined whether this newly identified role for EME1 in regulating RIF1 foci formation is functionally linked to PARPi resistance or if loss of EME1 influences PARPi sensitivity through a distinct mechanism e.g. via control of

MiDAS mediated repair of PARPi-induced TRCs. We could begin to investigate this by determining if RIF1 depletion is epistatic with loss of EME1 in relation to PARPi-resistance in HR-deficient cells. Furthermore, to determine whether EME1 and SETD1A mediate PARPi-sensitivity through a shared mechanism, potentially involving the recruitment of RIF1 to restore HR, future studies combining SETD1A and EME1 depletion will help to determine whether SETD1A loss is epistatic with loss of EME1. In addition to this, we should investigate whether overexpression of EME1 can overcome the PARPi resistance induced by SETD1A loss.

As described above EME1 is a member of the structure-specific SMX trinuclease complex that plays a key role in resolving Holliday junctions. It will be important to uncover whether the role of EME1 as an endonuclease in association with this complex underpins PARPi resistance or whether EME1 plays a different distinct role independent of this complex in HR-deficient cells. Whilst we did not identify a role for SETD1A in the transcriptional regulation of any of these other SMX complex members in our analysis, it is possible that PARPi sensitivity could also be influenced by the expression of other complex members including MUS81, SLX-4, SLX or XPF. Future studies should assess the effect on SETD1A and EME1 depletion of the expression of these complex members and their role in PARPi sensitivity, HR and RIF1 recruitment should be investigated using clonogenic survival assays and DDR foci experiments.

MUS81 also forms a second structure-specific endonuclease with EME2, which shares homology with EME1. MUS81-EME2 has been shown to possess greater endonuclease activity and cleave a wider range of substrates compared to MUS81-EME1. Whilst both these complexes cleave 3’-flaps, RFs and HJs, MUS81-EME2

also cleaves D-loop recombination intermediates (Pepe and West, 2014). Additionally, in contrast to EME1, the accumulation of chromosome instability in CHK1-deficient cells does not rely on EME2 (Calzetta, González Besteiro and Gottifredi, 2020). Therefore, it would be interesting to investigate whether the induction of PARPi-resistance in HR-deficient cells is also specific to EME1 or whether this can be recapitulated through loss of EME2.

To summarise, in this chapter we identify the SETD1A-dependent transcription of EME1 as an additional potential mechanism underpinning PARPi resistance in HR-deficient cells lacking this KMT. Similarly to SETD1A, restoration of HR may also underpin PARPi resistance in cells lacking EME1. Furthermore, we identified a novel potential anti-recombinogenic role for EME1 in regulating the recruitment of RIF1 to DSBs. Determining the respective contributions of these two mechanisms of PARPi resistance and whether these SETD1A-dependent mechanisms are interlinked are important areas for future study.

7. CHAPTER 7: CONCLUSION

7.1 Summary and model

Previously, my lab identified a novel PARPi resistance mechanism in BRCA1-deficient cells, through loss of the lysine methyltransferase and pro-NHEJ factor, SETD1A. In this thesis I wanted to examine to applicability of SETD1A as a predictor of PARPi resistance across other DDR-deficient backgrounds, focusing on ATM.

7.1.1 SETD1A depletion reduces PARPi sensitivity by restoring homologous recombination in ATM- and BRCA1-deficient cells

In chapter three, I demonstrated that depletion of SETD1A or H3K4 methylation reduces PARPi sensitivity in ATM-deficient cells, by restoring HR and genomic instability arising from chromosomal fusions.

Previously, we attributed PARPi resistance in BRCA1-deficient cells lacking SETD1A to a failure to recruit RIF1, arising from defective H3K4 methylation and a subsequent loss of binding between H3K4me3 and RIF1 at damaged sites (Bayley *et al.*, 2022). In this thesis I identified the interaction between H3K4me3 and RIF1 was mediated by the N-terminal HEAT-repeat domains of RIF1. This data provides further details of the underlying mechanisms of the H3K4me3 dependent recruitment of RIF1 and further reinforces the notion that RIF1 reads the epigenetic status of chromatin to control DSB repair.

Together these findings build upon our previous work, providing further evidence that perturbation of pro-NHEJ pathways by loss of SETD1A drives PARPi resistance in multiple genetic contexts, supporting the key role for epigenetic regulators in mechanisms of PARPi resistance. Through analysis of cancer cell lines and cancer

genomic databases it is clear this mechanism of PARPi resistance in also relevant to multiple HR-deficient cancer types, increasing the patient population who could be potentially impacted by this mechanism of PARPi resistance.

Identification of a potential new PARPi resistance mechanism in ATM-deficient cells is a significant discovery contributing to improving our understanding of PARPi-resistance mechanisms applicable beyond contexts of BRCA1-defiency. To date this is one of a few identified mechanisms of PARPi resistance studied in ATM-deficient contexts, along with loss of 53BP1 (Hong *et al.*, 2016), upregulation of drug efflux pumps and acquisition of epithelial-to-mesenchymal transition (Gout *et al.*, 2021). Based on my findings, we could infer that PARPi sensitivity caused by the loss of ATM can be at least partially overcome by compromising other members of the 53BP1-RIF1-Shieldin pathway, further expanding our knowledge of PARP inhibitor resistance mechanisms relevant to this context.

Based on the findings that SETD1A reduces PARPi senstivity across ATM- and BRCA1-deficient cells it is possible this mechanism could be expanded to further HR gene deficiencies. For example, mutations in other HR-related genes such as *ARID1A*, *BRIP1*, *BARD1*, *RAD51* and *PALB2* could confer PARPi sensitivity *(Tsantikidi et al., 2023)*. Expanding this resistance mechanism to additional genetic contexts and cancer types will greatly increase the number of patients who may benefit from this improved understanding.

Despite evidence that this novel PARPi resistance could apply to multiple types of HR-deficiency, unpublished data has shown loss of SETD1A is unable to confer resistance in BRCA2-deficient cells (Sweatman *et al.*, 2024). Moreover, cancer

patients lacking functional BRCA2 could not be triaged by SETD1A expression. This is supported by studies showing loss of pro-NHEJ factors cannot drive PARPi resistance in BRCA2-deficient cells. Similarly, loss of 53BP1 is unable to restore the HR defect in PALB2-depleted cells (Belotserkovskaya *et al.*, 2020). Based on these findings, it is likely SETD1A-induced PARPi resistance will not be applicable to this HR-deficient context either, highlighting that SETD1A-induced PARPi resistance applies to some but not all HR-deficient contexts.

7.1.2 SETD1A-dependent transcription of EME1 drives PARPi resistance in ATM- and BRCA1-deficient cells

In chapter six we identified transcriptional regulation of EME1 may mediate reduced PARPi sensitivity following SETD1A depletion in HR-deficient cells. Accordingly, loss of EME1 expression reduced PARPi sensitivity and restored HR in both BRCA1- and ATM-deficient cells. Unexpectedly, loss of EME1 also reduced RIF1 recruitment to DSBs, presenting a potential novel anti-recombinogenic role for EME1 in partnership with SETD1A. To our knowledge this is the first time such a role for this protein has been demonstrated. It remains to be determined whether this newly identified role for EME1 in regulating RIF1 foci formation is functionally linked to PARPi resistance or if loss of EME1 influences PARPi sensitivity through a distinct mechanism e.g. via control of MiDAS mediated repair of PARPi-induced TRCs.

Combined with our previous findings in BRCA1-deficient cells (Bayley *et al.*, 2022), we propose a model by which loss of SETD1A or associated H3K4me3 reduces RIF1 recruitment to PARPi DSBs, compromising end-protection and increasing HR-mediated repair in both BRCA1- and ATM-deficient cells. Furthermore, we identified that loss of SETD1A may also confer PARPi-resistance by downregulating

expression of the crossover endonuclease EME1, further contributing to HR restoration through reduced recruitment of RIF1 (**Fig. 7.1**).

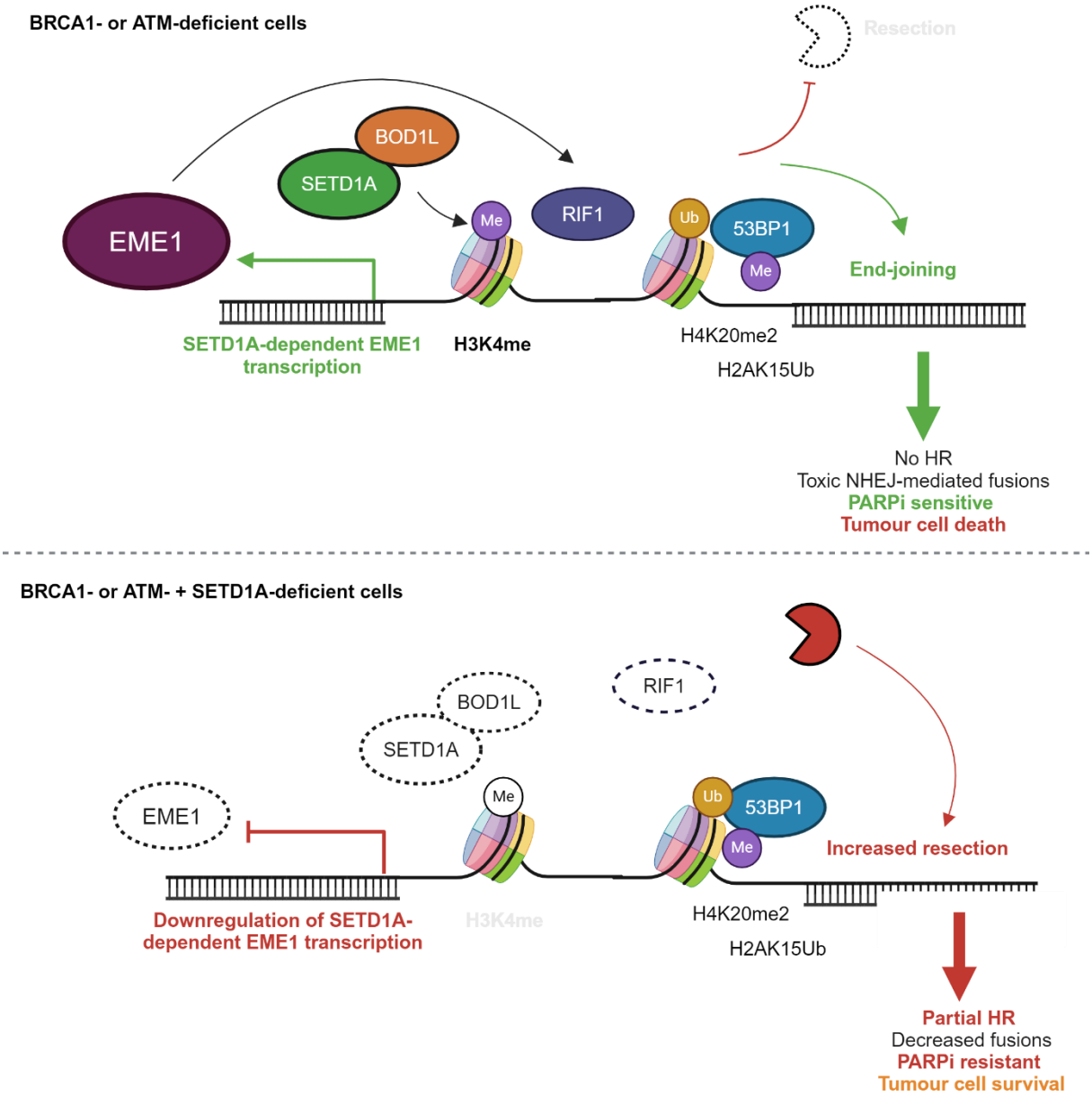

Figure 7.1- Loss of SETD1A-dependent EME1 transcription drives PARPi resistance in BRCA1- and ATM-deficient cells.

(Top) SETD1A methylates H3K4me3 to promote RIF1 localisation to DSBs, preventing DNA end-resection and promoting repair by NHEJ. SETD1A also drives the expression of the structure specific endonuclease EME1, which also regulates RIF1 recruitment. In BRCA1- or ATM-deficient cells, DNA end-resection and HR are inhibited, resulting in sensitivity to PARPi. (Bottom) Depletion of SETD1A or H3K4me3 results in downregulation of EME1 expression and decreased RIF1 localisation to DSBs. This restores HR to promote reduced PARPi sensitivity by increasing end-resection, enabling cells to survive PARPi induced DNA damage. Figure created with Biorender.

7.1.3 Phenotypic differences between SETD1A knockdown and Cas9-mediated gene editing

A further significant finding outlined in chapter five was that Cas9-mediated gene editing of SETD1A increased PARPi sensitivity of ATM-deficient cells. This strongly contrasted earlier findings observed following SETD1A knockdown, indicating the choice of method for genetic manipulation of SETD1A has significant impact on PARPi sensitivity. Investigation into the mechanism behind the phenotypic differences observed between methods of genetic manipulation revealed that complete depletion of SETD1A protein expression corresponds with the upregulation of p53 protein expression. This observation led me to predict a model in which loss of residual SETD1A protein expression increases p53 protein expression and activation of p53-mediated cell death via apoptosis, resulting in increased PARPi sensitivity in ATM-deficient cells (**Fig. 7.2**). As discussed in chapter 5, these experiments were performed in HeLa cells which have de-regulated p53 activity, due to the presence of HPV18 (Ajay, Meena and Bhat, 2012). Therefore, to further test this model in the future we would need to investigate the effect of SETD1A loss on PARPi-induced cell death and p53 expression comparing both p53 positive and p53 knockout cell lines.

This model could have implications for the use of SETD1A as a biomarker of patient response to PARPi, as it implies a threshold level of SETD1A expression is required for resistance to PARPi treatment. As low SETD1A mRNA expression is more common in cancer patients than deep deletion (**Fig. 7.3**), our results suggest siRNA-mediated SETD1A knockdown may be the preferred system to study PARPi resistance.

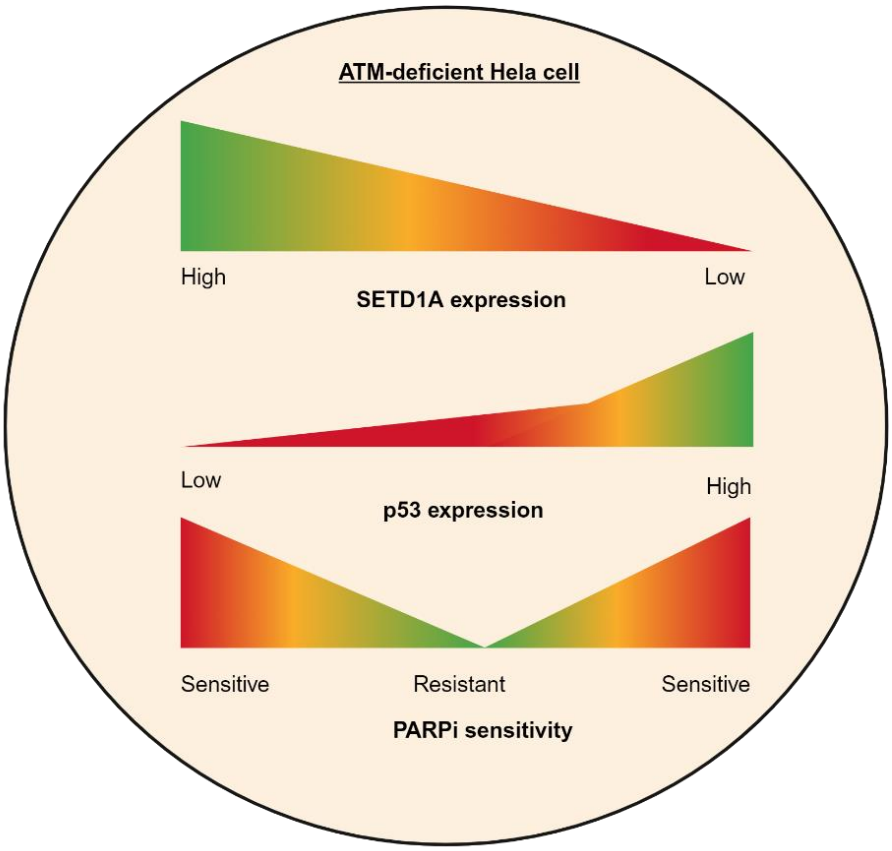

Figure 7.2- Model of how differential SETD1A levels influence PARPi sensitivity.

In the presence of SETD1A, ATM-deficient HeLa cells lack functional p53 transcription and display sensitivity to PARPi. Upon SETD1A knockdown, SETD1A protein expression decreases, along with PARPi sensitivity. However, when residual SETD1A expression is additionally depleted, p53 expression is activated to increase cell death via apoptosis and ATM-deficient cells regain PARPi sensitivity. Figure created with Biorender.

7.2 Therapeutic implications

7.2.1 Clinical relevance

It remains to be determined if loss of SETD1A is a bone fide pathological mechanism of PARPi resistance in patients with HR-deficient tumour types. Previous studies have shown patient derived lymphoblastoid cell lines with heterozygous loss-of-function SETD1A mutations have compromised RIF1 recruitment (Bayley *et al.*, 2022), indicating that these clinically relevant SETD1A mutations may also induce compromised NHEJ activity and thus could confer PARPi resistance.

Whilst this thesis focuses on the effects of decreased SETD1A expression, SETD1A is more commonly amplified in tumours, including hepatocellular carcinoma (Chen *et al.*, 2023), ovarian cancer (Chai *et al.*, 2023) and pancreatic cancer (Ishii *et al.*, 2023), where increased expression drives tumour progression and is correlated with poor outcomes. Pan cancer analysis of whole genomes using data from TCGA showed 6% of tumours possess SETD1A alterations. Of these ~50% were amplifications or increased mRNA expression, ~30% were deep deletions or low mRNA and ~20% were mutations of unknown significance (Gao *et al.*, 2013) (**Fig. 7.3**). This highlights that whilst upregulation of SETD1A expression is the most frequently observed SETD1A alteration in cancer patients, a significant percentage of patients display reduced SETD1A expression. Further analysis correlating SETD1A expression with HR-gene expression showed 4% of ovarian cancer patients with BRCA1-deficiency show low SETD1A expression (Gao *et al.*, 2013), highlighting that loss of SETD1A may occur in a significant number of patients eligible for PARPi treatment. However, this cancer genomics data does not include SETD1A protein expression levels, therefore, further analysis of protein expression through

immunohistochemical staining of tumour samples could result in the identification of an increased number of patients with reduced SETD1A expression.

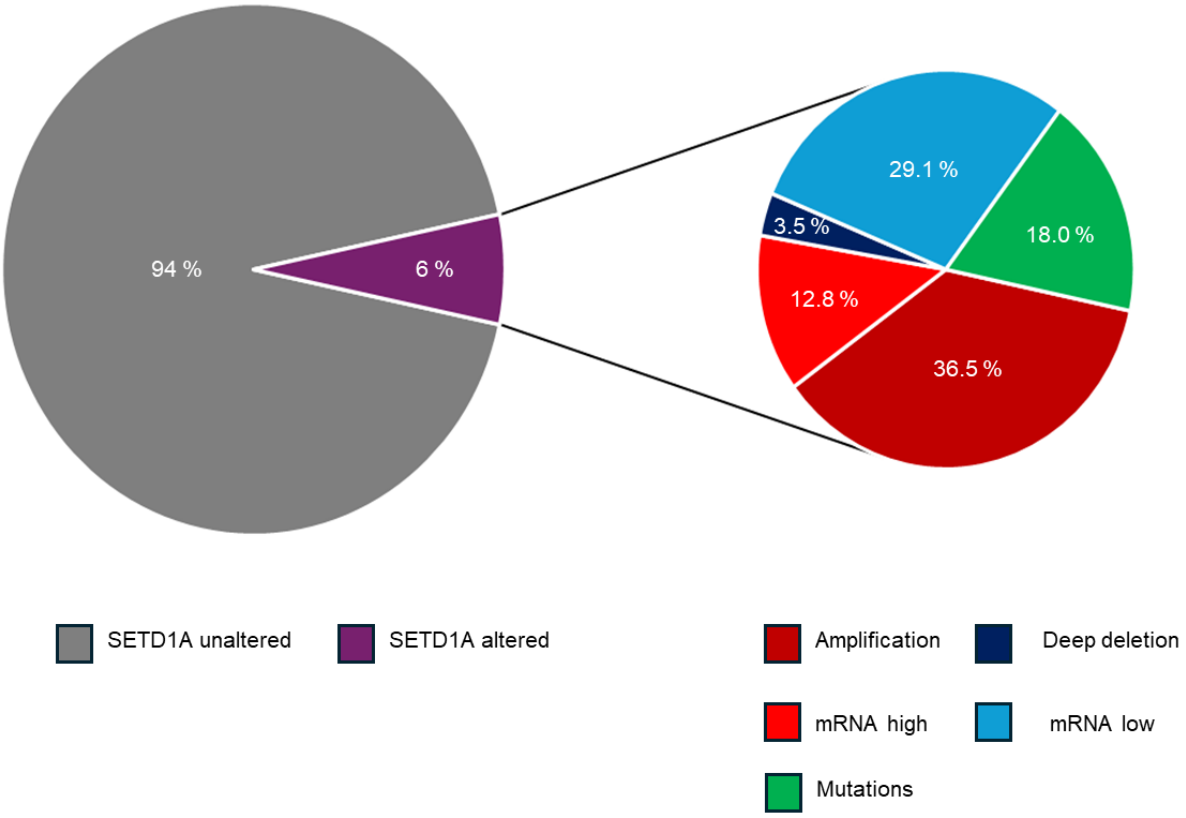

Figure 7.3- Pan-cancer analysis of SETD1A alterations.

Percentage of SETD1A alterations (amplifications, deep deletions, mutations, mRNA high and mRNA low) in a pan-cancer analysis of whole genomes from TCGA. All data was obtained from the CBioPortal database https://www.cbioportal.org/.

Monitoring SETD1A expression during the onset of PARPi resistance and linking *BRCA1* or *ATM* mutation status to SETD1A expression would be invaluable in evaluating its utility as a potential biomarker. Our findings suggest that SETD1A, H3K4me3, or EME1 activity/expression could be useful prognostic indicators for predicting which patients are more likely to develop PARPi resistance in the clinic. In the future we could conduct a retrospective trial measuring SETD1A, H3K4me3 or EME1 expression in archival tissue samples from BRCA1- and ATM-deficient patients who have received PARPi treatment. Based on our findings that residual SETD1A protein expression could influence PARPi sensitivity, performing immunohistochemistry to measure protein expression in formalin-fixed paraffin embedded tissues may be the most appropriate method of biomarker detection. However, this method is costly due to the requirement of specific antibodies. Alternatively, analysis of RNA expression has the advantages of being relatively low cost per gene, high throughput and requiring a small amount of tumour tissue sample.

7.2.2 Overcoming PARPi resistance

7.2.2.1 DDR inhibitors

Combination therapies are an effective way to sensitise cells to PARPi and overcome drug resistance. In this thesis I identify that loss of SETD1A induces PARPi resistance by restoring HR, therefore, preventing reactivation of this pathway could be a successful strategy for overcoming PARPi resistance in this context. Preclinical data suggests strategies combining PARPis with other DDR inhibitors can inhibit HR restoration and sensitise HR-proficient cells to PARPi (Smith *et al.*, 2024). A key example of this is ATR inhibition. ATR contributes to HR by promoting RAD51 loading

onto the DSB. As such, Kim *et al.* showed that combining ATR inhibition with PARPi synergised to decrease cell viability by reducing RAD51 foci formation and blocking HR in BRCA2 mutated PARPi resistant ovarian cancer cell lines (Kim *et al.*, 2020). This approach could be particularly effective for ATM-mutated tumours as ATR may be upregulated in these cells to compensate for lack of ATM function, providing a clear rationale for combining ATRi and PARPi in ATM-deficient contexts. Furthermore, a genome-wide CRISPR screen revealed loss of SETD1A sensitised three independent cell lines to the ATRi, AZD6738 (Wang *et al.*, 2019), providing further evidence that ATRi treatment could overcome PARPi resistance induced by loss of SETD1A.

Similar results have been observed using inhibitors of checkpoint kinase WEE1. Combining WEE1 inhibition (WEE1i) with olaparib in biliary tract cancer cell lines decreased CtIP and RAD51 expression to disrupt HR mediated repair, suggesting that this combination treatment can also induce synergistic anti-tumour effects by reinstating HR-deficiency (Seo *et al.*, 2022). Therefore, I hypothesise that combination treatment of ATM- or BRCA1-deficient cells with PARPi and WEE1i would counteract the restoration of HR induced by loss of SETD1A expression.

7.2.2.2 Epigenetic inhibitors

We hypothesise that SETD1A prevents HR through H3K4me3-mediated recruitment of RIF1 to DSBs, thereby PARPi resistance could be reversed by increasing H3K4me3 in the absence of SETD1A expression. Cells possess lysine demethylases that remove the methylation marks deposited by enzymes such as SETD1A. Over recent years selective demethylase inhibitors, such as KDM1A/LSD1 inhibitors (LSD1i), have been developed to directly counteract the actions of these histone

demethylases (Fang, Liao and Yu, 2019). Manipulating the balance between H3K4 methylation and demethylation to increase this epigenetic mark using demethylase inhibitors could offer a potential new method of combating SETD1A deficiency and thus PARPi resistance. Mukai *et al.* found that treatment of SETD1A-deficient neurons with LSD1i reduced axon branching deficits associated with SETD1A-deficiency (Mukai *et al.*, 2019), demonstrating that LSD1i are effective in counteracting SETD1A depletion. A recent study also provided initial evidence that LSD1i could overcome PARPi resistance. This study showed LSD1i sensitised ovarian cancer cells to PARPi by suppressing expression of genes involved in the HR pathway, converting HR-proficient tumours to HR-deficient tumours (Tao *et al.*, 2023). Together these findings suggest that the combination of PARPi and LSD1i could be used to overcome PARPi resistance caused by loss of SETD1A. An interesting avenue for future investigation would be to determine if suppression of LSD1 could reinstate EME1 transcription in SETD1A-deficient cells to reestablish PARPi sensitivity (**Fig. 7.4**).

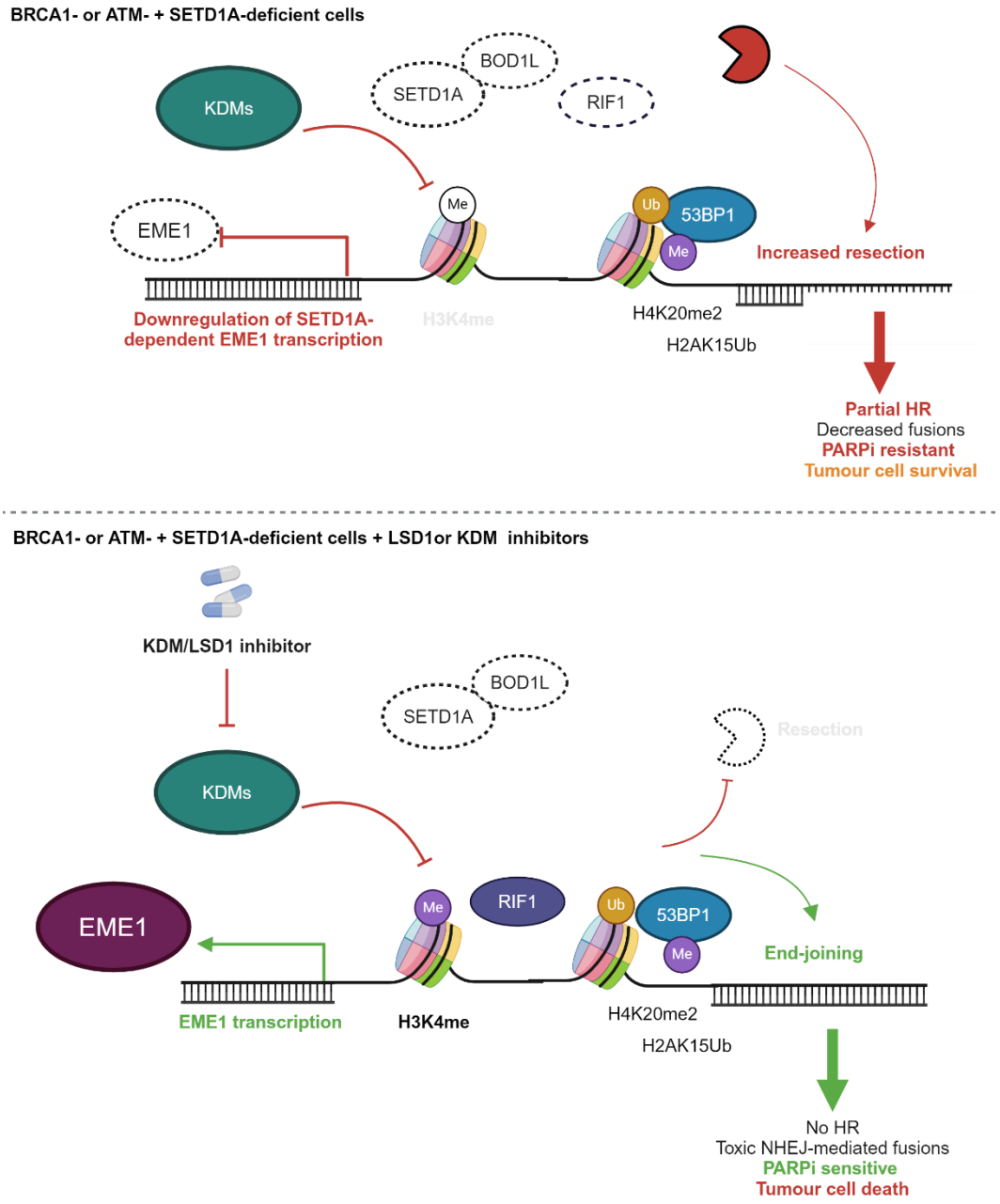

Figure 7.4- Restoring PARPi sensitivity in BRCA1- or ATM-deficient cells following loss of SETD1A using LSD1/KDM inhibitors.

Induction of PARPi resistance following loss of SETD1A or associated H3K4 methylation in ATM- or BRCA1-deficient cells could potentially be restored by inhibition of lysine demethylases (KDM) responsible for removing H3K4 methylation, such as KDM5A and LSD1. KDM inhibition will increase H3K4 methylation levels in the absence of SETD1A, reinstating EME1 transcription and RIF1 recruitment to DSBs. This will subsequently restore PARPi sensitivity by decreasing end-resection and perturbing homologous recombination (HR). Figure created with Biorender.

7.3 Extending the current study

The results in this thesis have raised additional questions that provide important areas for future investigations.

7.3.1 Further insights into the contribution of H3K4 methylation in PARPi resistance

To further characterise the nature of H3K4me3-dependent RIF1 recruitment to DSBs, I would aim to map the precise region responsible for the RIF1-H3K4me3 interaction. The first step would be to determine the minimal fragment required for this interaction by performing additional histone pulldown experiments using shorter fragments of RIF1 spanning the original 411 aa HEAT repeat fragment (**Fig. 3.17**). Following on from this, point mutations could be introduced in the RIF1 HEAT repeat domain to identify the key residues required for its interaction with H3K4me3.

To further confirm the contribution of H3K4 methylation in PARPi resistance in HR-deficient cells, the experiments detailed in (**Figs 3.8, 3.9 and 3.10**) should be repeated in cells expressing a variant of SETD1A lacking the catalytic SET domain (ΔSET) responsible for H3K4 methylation. In chapter three I also attempted to validate these findings by generating a KDM5A/RBBP2 lysine demethylase overexpression cell line, however I had difficulty optimising this process and due to time constraints, I decided to prioritise other avenues of investigation. However, in the future I would attempt to remove the FLAG tag on RBBP2 which may interfere with antibody detection of exogenous RBBP2 expression. Alternatively, I could utilise a lentiviral based system to create overexpression cells lines or introduce the plasmids by transient transfection. Previously our lab used this transient approach to

show that RBBP2 overexpression reduces H3K4 methylation levels independently of loss of SETD1A and effects the recruitment of RIF1 to DSBs in a similar manner to SETD1A depletion (Bayley *et al.*, 2022). Based on this and my previous findings, I hypothesise that RBBP2 expression would phenocopy SETD1A depletion to confer PARPi resistance in both BRCA1- and ATM-deficient cells.

7.3.2 Further insight into phenotypic differences between Cas9-mediated gene editing of SETD1A and siRNA-mediated knockdown

An unexpected finding of this thesis was that depletion of SETD1A by Cas9-mediated gene editing increased sensitivity to PARPi in ATM-deficient cells, opposing our earlier findings following SETD1A knockdown. In chapter five I hypothesised these differences in PARPi sensitivity were due to incomplete depletion of all SETD1A protein coding transcripts by the gRNAs used in CRISPR-Cas9 system. I would further extend this study by designing PCR primers specifically targeted to each individual transcript to further elucidate transcript abundance.

Furthermore, I observed that combining Cas9-mediated gene editing and SETD1A knockdown increased p53 protein expression. Therefore, the next step is to determine whether this is accompanied by an increase in p53 activity, leading to increased cell cycle arrest and apoptotic cell death. Levels of activated p53 could be measured by immunoblotting for p53 phosphorylation at serine 15. I could also measure p53 mediated cell death via apoptosis using the annexin V assay or detection of cleaved caspase 3 and PARP by western blotting.

7.3.3 Continued validation of RNA-sequencing hits.

Surprisingly, depletion of SETD1A causes only small changes in gene expression in HeLa Kyoto iCas9 cells, this could be due to compensation by other KMTs. In the future we could assess whether loss of SETD1A increases the expression of these other KMTs and if further depletion of these results in more significant changes in gene expression.

Nevertheless, we did identify some genes that were differentially expressed following loss of SETD1A. To further verify SETD1A-dependent regulation of these genes I would assess the impact of SETD1A overexpression on DEG expression using a lentiviral based system. To further verify the role of SETD1A-dependent H3K4me3 in the transcriptional regulation of these genes I would repeat ChIP-sequencing analysis in the HeLa Kyoto iCas9 cell lines and investigate the effect of SETD1A depletion on the enrichment of H3K4me3 at the promoter regions of the DEGs. To expand on this, I could also investigate the effect of a catalytically dead SETD1A mutant, deficient for histone methyltransferase activity, on DEG expression. I hypothesise that expression of the catalytically dead SETD1A mutant would lead to similar gene expression changes as SETD1A depletion.

7.3.4 Further insights into the contribution of EME1 in PARPi resistance

In chapter six, I observed that loss of EME1 reduced recruitment of RIF1 to DSBs induced by ionising radiation. This led me to hypothesise that EME1 could have a novel anti-recombinogenic role, facilitating RIF1-dependent NHEJ. Currently, we do not know whether EME1 mediates RIF1 recruitment by a direct interaction, to explore this further I would perform reciprocal co-immunoprecipitation experiments using

recombinant RIF1 and EME1 protein. As RIF1 forms part of the downstream 53BP1 effector pathway, I would also assess whether the recruitment of other 53BP1 factors such as REV7 and 53BP1 itself are also affected by EME1 depletion in response to DNA damage. If RIF1 recruitment is dependent on EME1 expression, it is possible that EME1 expression will also influence DSB repair via the NHEJ pathway. Our lab has previously used cells with conditional inactivation of the shelterin subunit TRF2 to investigate this pathway. Inactivation of TRF2 elicits telomere deprotection and the formation of NHEJ-mediated chromosome end-to-end fusions. Loss of pro-NHEJ factors such as RIF1 and SETD1A have been shown to reduce the formation of these fusions, therefore based on my hypothesis that EME1 also mediates NHEJ, I would predict that loss of EME1 will also reduce the formation of these fusions.

It would also be interesting to investigate whether some of the other known functions of MUS81-EME1, such as its role in cleaving nascent DNA during MiDAS in HR-deficient cells, are implicated in PARPi resistance. To assess whether olaparib induces MiDAS in BRCA1- and ATM-deficient cells, I would detect nascent DNA synthesis in metaphase cells with EdU labelling using the Click-I EdU assay. I would then assess the effect of EME1 depletion on cleavage of this newly synthesised DNA by measuring DAPI-negative gaps and breaks in DAPI-stained, EdU-incorporated metaphase spreads.

Since EME1 is part of the SMX trinuclease complex, it would be interesting to examine whether depleting other members of this complex, such as MUS81, SLX4 and SLX1 might also contribute to my observations. Furthermore, as the EME1 homologue, EME2 also forms an endonuclease complex with MUS81, it would be

interesting to examine whether depletion of EME2 expression could confer similar effects.

7.3.5 Extending findings to other PARP inhibitors

Clinically approved PARPi compounds primarily target PARP1, however, due to structural similarities in the NAD-binding domain, PARPi also inhibit other PARP enzymes, including PARP2 and PARP3 (Antolin *et al.*, 2020). Currently, PARP1 specific inhibitors, such as AZD5305, and PARP7 specific inhibitors, such as thioparib are in clinical development. Therefore, an interesting question would be to investigate whether SETD1A-induced PARPi resistance is specific to PARP1 inhibition, using these novel PARPi compounds.

7.4 Concluding remarks

In conclusion, I have demonstrated that loss of SETD1A and associated H3K4me3 offers a conserved mechanism of PARPi resistance in BRCA1- and ATM-deficient contexts via restoration of HR and/or transcriptional regulation of the crossover junction endonuclease EME1. As such, loss of SETD1A, H3K4me3 or EME1 expression may underlie PARPi resistance in the clinic and their expression or activity could offer potential new biomarkers to predict patient response. Consequently, these findings could improve the use of PARPi in the clinic by identifying patients likely to respond to therapy, ultimately improving patient outcomes.

8. REFERENCES

Abida, W., Patnaik, A., Campbell, D., Shapiro, J., Bryce, A. H., McDermott, R., Sautois, B., Vogelzang, N. J., Bambury, R. M., Voog, E., Zhang, J., Piulats, J. M., Ryan, C. J., Merseburger, A. S., Daugaard, G., Heidenreich, A., Fizazi, K., Higano, C. S., Krieger, L. E., Sternberg, C. N., Watkins, S. P., Despain, D., Simmons, A. D., Loehr, A., Dowson, M., Golsorkhi, T. and Chowdhury, S. (2020) 'Rucaparib in Men With Metastatic Castration-Resistant Prostate Cancer Harboring a BRCA1 or BRCA2 Gene Alteration', *J Clin Oncol,* 38(32), pp. 3763-3772.

Abplanalp, J., Leutert, M., Frugier, E., Nowak, K., Feurer, R., Kato, J., Kistemaker, H. V. A., Filippov, D. V., Moss, J., Caflisch, A. and Hottiger, M. O. (2017) 'Proteomic analyses identify ARH3 as a serine mono-ADP-ribosylhydrolase', *Nature Communications,* 8(1), pp. 2055.

Abraham, J., Lemmers, B., Hande, M. P., Moynahan, M. E., Chahwan, C., Ciccia, A., Essers, J., Hanada, K., Chahwan, R., Khaw, A. K., McPherson, P., Shehabeldin, A., Laister, R., Arrowsmith, C., Kanaar, R., West, S. C., Jasin, M. and Hakem, R. (2003) 'Eme1 is involved in DNA damage processing and maintenance of genomic stability in mammalian cells', *Embo j,* 22(22), pp. 6137-47.

Adams, K. E., Medhurst, A. L., Dart, D. A. and Lakin, N. D. (2006) 'Recruitment of ATR to sites of ionising radiation-induced DNA damage requires ATM and components of the MRN protein complex', *Oncogene,* 25(28), pp. 3894-3904.

Afgan, E., Baker, D., Batut, B., van den Beek, M., Bouvier, D., Čech, M., Chilton, J., Clements, D., Coraor, N., Grüning, B. A., Guerler, A., Hillman-Jackson, J., Hiltemann, S., Jalili, V., Rasche, H., Soranzo, N., Goecks, J., Taylor, J., Nekrutenko, A. and Blankenberg, D. (2018) 'The Galaxy platform for accessible, reproducible and collaborative biomedical analyses: 2018 update', *Nucleic Acids Research,* 46(W1), pp. W537-W544.

Aguilar-Quesada, R., Muñoz-Gámez, J. A., Martín-Oliva, D., Peralta, A., Valenzuela, M. T., Matínez-Romero, R., Quiles-Pérez, R., Murcia, J. M.-d., de Murcia, G., de Almodóvar, M. R. and Oliver, F. J. (2007) 'Interaction between ATM and PARP-1 in response to DNA damage and sensitization of ATM deficient cells through PARP inhibition', *BMC Molecular Biology,* 8(1), pp. 29.

Ajay, A. K., Meena, A. S. and Bhat, M. K. (2012) 'Human papillomavirus 18 E6 inhibits phosphorylation of p53 expressed in HeLa cells', *Cell & Bioscience,* 2(1), pp. 2.

Al-Minawi, A. Z., Saleh-Gohari, N. and Helleday, T. (2008) 'The ERCC1/XPF endonuclease is required for efficient single-strand annealing and gene conversion in mammalian cells', *Nucleic Acids Res,* 36(1), pp. 1-9.

Alberg, A. J., Kouzis, A., Genkinger, J. M., Gallicchio, L., Burke, A. E., Hoffman, S. C., Diener-West, M., Helzlsouer, K. J. and Comstock, G. W. (2007) 'A Prospective Cohort Study of Bladder Cancer Risk in Relation to Active Cigarette Smoking and Household

Exposure to Secondhand Cigarette Smoke', *American Journal of Epidemiology,* 165(6), pp. 660-666.

Alhmoud, J. F., Woolley, J. F., Al Moustafa, A. E. and Malki, M. I. (2020) 'DNA Damage/Repair Management in Cancers', *Cancers (Basel),* 12(4), pp. 1050.

Alsulami, M., Munawar, N., Dillon, E., Oliviero, G., Wynne, K., Alsolami, M., Moss, C., P, Ó. G., O'Meara, F., Cotter, D. and Cagney, G. (2019) 'SETD1A Methyltransferase Is Physically and Functionally Linked to the DNA Damage Repair Protein RAD18', *Mol Cell Proteomics,* 18(7), pp. 1428-1436.

Amé, J. C., Spenlehauer, C. and de Murcia, G. (2004) 'The PARP superfamily', *Bioessays,* 26(8), pp. 882-93.

Amin, H. M., Szabo, B., Abukhairan, R., Zeke, A., Kardos, J., Schad, E. and Tantos, A. (2023) 'In Vivo and In Vitro Characterization of the RNA Binding Capacity of SETD1A (KMT2F)', *Int J Mol Sci,* 24(22), pp. 16032.

Anand, R., Ranjha, L., Cannavo, E. and Cejka, P. (2016) 'Phosphorylated CtIP Functions as a Co-factor of the MRE11-RAD50-NBS1 Endonuclease in DNA End Resection', *Molecular Cell,* 64(5), pp. 940-950.

Añazco-Guenkova, A. M., Miguel-López, B., Monteagudo-García, Ó., García-Vílchez, R. and Blanco, S. (2024) 'The impact of tRNA modifications on translation in cancer: identifying novel therapeutic avenues', *NAR Cancer,* 6(1), pp. zcae012.

Antolin, A. A., Ameratunga, M., Banerji, U., Clarke, P. A., Workman, P. and Al-Lazikani, B. (2020) 'The kinase polypharmacology landscape of clinical PARP inhibitors', *Scientific Reports,* 10(1), pp. 2585.

Aprosoff, C. M., Dyakov, B. J. A., Cheung, V. H. W., Wong, C. J., Palandra, M., Gingras, A. C. and Wyatt, H. D. M. (2023) 'Comprehensive Interactome Mapping of the DNA Repair Scaffold SLX4 Using Proximity Labeling and Affinity Purification', *J Proteome Res,* 22(6), pp. 1660-1681.

Arndt, K., Kranz, A., Fohgrub, J., Jolly, A., Bledau, A. S., Di Virgilio, M., Lesche, M., Dahl, A., Höfer, T., Stewart, A. F. and Waskow, C. (2018) 'SETD1A protects HSCs from activation-induced functional decline in vivo', *Blood,* 131(12), pp. 1311-1324.

Asmamaw, M. and Zawdie, B. (2021) 'Mechanism and Applications of CRISPR/Cas-9-Mediated Genome Editing', *Biologics,* 15, pp. 353-361.

Awasthi, P., Foiani, M. and Kumar, A. (2015) 'ATM and ATR signaling at a glance', *J Cell Sci,* 128(23), pp. 4255-62.

Balmus, G., Pilger, D., Coates, J., Demir, M., Sczaniecka-Clift, M., Barros, A. C., Woods, M., Fu, B., Yang, F., Chen, E., Ostermaier, M., Stankovic, T., Ponstingl, H., Herzog, M., Yusa, K., Martinez, F. M., Durant, S. T., Galanty, Y., Beli, P., Adams, D. J., Bradley, A., Metzakopian, E., Forment, J. V. and Jackson, S. P. (2019) 'ATM

orchestrates the DNA-damage response to counter toxic non-homologous end-joining at broken replication forks', *Nat Commun,* 10(1), pp. 87.

Bayley, R., Borel, V., Moss, R. J., Sweatman, E., Ruis, P., Ormrod, A., Goula, A., Mottram, R. M. A., Stanage, T., Hewitt, G., Saponaro, M., Stewart, G. S., Boulton, S. J. and Higgs, M. R. (2022) 'H3K4 methylation by SETD1A/BOD1L facilitates RIF1-dependent NHEJ', *Molecular Cell*.

Bayley, R., Sweatman, E. and Higgs, M. R. (2023) 'New perspectives on epigenetic modifications and PARP inhibitor resistance in HR-deficient cancers', *Cancer Drug Resist,* 6(1), pp. 35-44.

Belotserkovskaya, R., Raga Gil, E., Lawrence, N., Butler, R., Clifford, G., Wilson, M. D. and Jackson, S. P. (2020) 'PALB2 chromatin recruitment restores homologous recombination in BRCA1-deficient cells depleted of 53BP1', *Nat Commun,* 11(1), pp. 819.

Bernstein, B. E., Kamal, M., Lindblad-Toh, K., Bekiranov, S., Bailey, D. K., Huebert, D. J., McMahon, S., Karlsson, E. K., Kulbokas, E. J., 3rd, Gingeras, T. R., Schreiber, S. L. and Lander, E. S. (2005) 'Genomic maps and comparative analysis of histone modifications in human and mouse', *Cell,* 120(2), pp. 169-81.

Berti, M., Ray Chaudhuri, A., Thangavel, S., Gomathinayagam, S., Kenig, S., Vujanovic, M., Odreman, F., Glatter, T., Graziano, S., Mendoza-Maldonado, R., Marino, F., Lucic, B., Biasin, V., Gstaiger, M., Aebersold, R., Sidorova, J. M., Monnat, R. J., Jr., Lopes, M. and Vindigni, A. (2013) 'Human RECQ1 promotes restart of replication forks reversed by DNA topoisomerase I inhibition', *Nat Struct Mol Biol,* 20(3), pp. 347-54.

Bhin, J., Paes Dias, M., Gogola, E., Rolfs, F., Piersma, S. R., de Bruijn, R., de Ruiter, J. R., van den Broek, B., Duarte, A. A., Sol, W., van der Heijden, I., Andronikou, C., Kaiponen, T. S., Bakker, L., Lieftink, C., Morris, B., Beijersbergen, R. L., van de Ven, M., Jimenez, C. R., Wessels, L. F. A., Rottenberg, S. and Jonkers, J. (2023) 'Multi-omics analysis reveals distinct non-reversion mechanisms of PARPi resistance in BRCA1- versus BRCA2-deficient mammary tumors', *Cell Rep,* 42(5), pp. 112538.

Biehs, R., Steinlage, M., Barton, O., Juhász, S., Künzel, J., Spies, J., Shibata, A., Jeggo, P. A. and Löbrich, M. (2017) 'DNA Double-Strand Break Resection Occurs during Non-homologous End Joining in G1 but Is Distinct from Resection during Homologous Recombination', *Molecular Cell,* 65(4), pp. 671-684.e5.

Bledau, A. S., Schmidt K Fau - Neumann, K., Neumann K Fau - Hill, U., Hill U Fau - Ciotta, G., Ciotta G Fau - Gupta, A., Gupta A Fau - Torres, D. C., Torres Dc Fau - Fu, J., Fu J Fau - Kranz, A., Kranz A Fau - Stewart, A. F., Stewart Af Fau - Anastassiadis, K. and Anastassiadis, K. (2014) 'The H3K4 methyltransferase Setd1a is first required at the epiblast stage, whereas Setd1b becomes essential after gastrulation', *Development,* 141(5), pp. 1022-35.

Bonfiglio, J. J., Fontana, P., Zhang, Q., Colby, T., Gibbs-Seymour, I., Atanassov, I., Bartlett, E., Zaja, R., Ahel, I. and Matic, I. (2017) 'Serine ADP-Ribosylation Depends on HPF1', *Molecular Cell,* 65(5), pp. 932-940.e6.

Bosnjak, M., Jesenko, T., Markelc, B., Janzic, L., Cemazar, M. and Sersa, G. (2021) 'PARP inhibitor olaparib has a potential to increase the effectiveness of electrochemotherapy in BRCA1 mutated breast cancer in mice', *Bioelectrochemistry,* 140, pp. 107832.

Bouwman, P., Aly, A., Escandell, J. M., Pieterse, M., Bartkova, J., van der Gulden, H., Hiddingh, S., Thanasoula, M., Kulkarni, A., Yang, Q., Haffty, B. G., Tommiska, J., Blomqvist, C., Drapkin, R., Adams, D. J., Nevanlinna, H., Bartek, J., Tarsounas, M., Ganesan, S. and Jonkers, J. (2010) '53BP1 loss rescues BRCA1 deficiency and is associated with triple-negative and BRCA-mutated breast cancers', *Nat Struct Mol Biol,* 17(6), pp. 688-95.

Bowen, N. and Kolodner, R. D. (2017) 'Reconstitution of Saccharomyces cerevisiae DNA polymerase ε-dependent mismatch repair with purified proteins', *Proceedings of the National Academy of Sciences,* 114(14), pp. 3607-3612.

Brouwer, I., Sitters, G., Candelli, A., Heerema, S. J., Heller, I., Melo de, A. J., Zhang, H., Normanno, D., Modesti, M., Peterman, E. J. G. and Wuite, G. J. L. (2016) 'Sliding sleeves of XRCC4–XLF bridge DNA and connect fragments of broken DNA', *Nature,* 535(7613), pp. 566-569.

Brown, D. A., Di Cerbo, V., Feldmann, A., Ahn, J., Ito, S., Blackledge, N. P., Nakayama, M., McClellan, M., Dimitrova, E., Turberfield, A. H., Long, H. K., King, H. W., Kriaucionis, S., Schermelleh, L., Kutateladze, T. G., Koseki, H. and Klose, R. J. (2017) 'The SET1 Complex Selects Actively Transcribed Target Genes via Multivalent Interaction with CpG Island Chromatin', *Cell Rep,* 20(10), pp. 2313-2327.

Brown, J. S., Lukashchuk, N., Sczaniecka-Clift, M., Britton, S., le Sage, C., Calsou, P., Beli, P., Galanty, Y. and Jackson, S. P. (2015) 'Neddylation promotes ubiquitylation and release of Ku from DNA-damage sites', *Cell Rep,* 11(5), pp. 704-14.

Bruin, M. A. C., Sonke, G. S., Beijnen, J. H. and Huitema, A. D. R. (2022) 'Pharmacokinetics and Pharmacodynamics of PARP Inhibitors in Oncology', *Clinical Pharmacokinetics,* 61(12), pp. 1649-1675.

Brustel, J., Muramoto, T., Fumimoto, K., Ellins, J., Pears, C. J. and Lakin, N. D. (2022) 'Linking DNA repair and cell cycle progression through serine ADP-ribosylation of histones', *Nature Communications,* 13(1), pp. 185.

Bryant, H. E. (2006) 'Inhibition of poly (ADP-ribose) polymerase activates ATM which is required for subsequent homologous recombination repair', *Nucleic Acids Research,* 34(6), pp. 1685-1691.

Bryant, H. E. and Helleday, T. (2006) 'Inhibition of poly (ADP-ribose) polymerase activates ATM which is required for subsequent homologous recombination repair', *Nucleic Acids Research,* 34(6), pp. 1685-1691.

Bryant, H. E., Petermann, E., Schultz, N., Jemth, A. S., Loseva, O., Issaeva, N., Johansson, F., Fernandez, S., McGlynn, P. and Helleday, T. (2009) 'PARP is activated at stalled forks to mediate Mre11-dependent replication restart and recombination', *The EMBO Journal,* 28(17), pp. 2601-2615-2615.

Bryant, H. E., Schultz, N., Thomas, H. D., Parker, K. M., Flower, D., Lopez, E., Kyle, S., Meuth, M., Curtin, N. J. and Helleday, T. (2005) 'Specific killing of BRCA2-deficient tumours with inhibitors of poly(ADP-ribose) polymerase', *Nature,* 434(7035), pp. 913-917.

Bunting, S. F., Callen, E., Wong, N., Chen, H. T., Polato, F., Gunn, A., Bothmer, A., Feldhahn, N., Fernandez-Capetillo, O., Cao, L., Xu, X., Deng, C. X., Finkel, T., Nussenzweig, M., Stark, J. M. and Nussenzweig, A. (2010) '53BP1 inhibits homologous recombination in Brca1-deficient cells by blocking resection of DNA breaks', *Cell,* 141(2), pp. 243-54.

Caldecott, K. W. (2020) 'Mammalian DNA base excision repair: Dancing in the moonlight', *DNA Repair,* 93, pp. 102921.

Calzetta, N. L., González Besteiro, M. A. and Gottifredi, V. (2020) 'Mus81-Eme1-dependent aberrant processing of DNA replication intermediates in mitosis impairs genome integrity', *Sci Adv,* 6(50), pp. eabc8257.

Cameron, D., Blake, Derek J., Bray, Nicholas J. and Hill, Matthew J. (2019) 'Transcriptional Changes following Cellular Knockdown of the Schizophrenia Risk Gene SETD1A Are Enriched for Common Variant Association with the Disorder', *Molecular Neuropsychiatry,* 5(2), pp. 109-114.

Campalans, A., Kortulewski, T., Amouroux, R., Menoni, H., Vermeulen, W. and Radicella, J. P. (2013) 'Distinct spatiotemporal patterns and PARP dependence of XRCC1 recruitment to single-strand break and base excision repair', *Nucleic acids research,* 41(5), pp. 3115-3129.

Caron, M.-C., Sharma, A. K., O'Sullivan, J., Myler, L. R., Ferreira, M. T., Rodrigue, A., Coulombe, Y., Ethier, C., Gagné, J.-P., Langelier, M.-F., Pascal, J. M., Finkelstein, I. J., Hendzel, M. J., Poirier, G. G. and Masson, J.-Y. (2019) 'Poly(ADP-ribose) polymerase-1 antagonizes DNA resection at double-strand breaks', *Nature Communications,* 10(1), pp. 2954.

Carreira, S., Porta, N., Arce-Gallego, S., Seed, G., Llop-Guevara, A., Bianchini, D., Rescigno, P., Paschalis, A., Bertan, C., Baker, C., Goodall, J., Miranda, S., Riisnaes, R., Figueiredo, I., Ferreira, A., Pereira, R., Crespo, M., Gurel, B., Nava Rodrigues, D., Pettitt, S. J., Yuan, W., Serra, V., Rekowski, J., Lord, C. J., Hall, E., Mateo, J. and de Bono, J. S. (2021) 'Biomarkers Associating with PARP Inhibitor Benefit in Prostate Cancer in the TOPARP-B Trial', *Cancer Discovery,* 11(11), pp. 2812-2827.

Castor, D., Nair, N., Déclais, A.-C., Lachaud, C., Toth, R., Macartney, Thomas J., Lilley, David M. J., Arthur, J. Simon C. and Rouse, J. (2013) 'Cooperative Control of Holliday Junction Resolution and DNA Repair by the SLX1 and MUS81-EME1 Nucleases', *Molecular Cell,* 52(2), pp. 221-233.

Cerami, E., Gao, J., Dogrusoz, U., Gross, B. E., Sumer, S. O., Aksoy, B. A., Jacobsen, A., Byrne, C. J., Heuer, M. L., Larsson, E., Antipin, Y., Reva, B., Goldberg, A. P., Sander, C. and Schultz, N. (2012) 'The cBio cancer genomics portal: an open platform for exploring multidimensional cancer genomics data', *Cancer Discov,* 2(5), pp. 401-4.

Chai, H., Pan, C., Zhang, M., Huo, H., Shan, H. and Wu, J. (2023) 'Histone methyltransferase SETD1A interacts with notch and promotes notch transactivation to augment ovarian cancer development', *BMC Cancer,* 23(1), pp. 96.

Chakraborty, U., Dinh, T. A. and Alani, E. (2018) 'Genomic Instability Promoted by Overexpression of Mismatch Repair Factors in Yeast: A Model for Understanding Cancer Progression', *Genetics,* 209(2), pp. 439-456.

Chao, C., Herr, D., Chun, J. and Xu, Y. (2006) 'Ser18 and 23 phosphorylation is required for p53-dependent apoptosis and tumor suppression', *Embo j,* 25(11), pp. 2615-22.

Chapman, J. R., Barral, P., Vannier, J. B., Borel, V., Steger, M., Tomas-Loba, A., Sartori, A. A., Adams, I. R., Batista, F. D. and Boulton, S. J. (2013) 'RIF1 is essential for 53BP1-dependent nonhomologous end joining and suppression of DNA double-strand break resection', *Mol Cell,* 49(5), pp. 858-71.

Chen, J., Xu, Z., Huang, H., Tang, Y., Shan, H. and Xiao, F. (2023) 'SETD1A drives stemness by reprogramming the epigenetic landscape in hepatocellular carcinoma stem cells', *JCI Insight,* 8(18), pp. e168375.

Christie, E. L., Pattnaik, S., Beach, J., Copeland, A., Rashoo, N., Fereday, S., Hendley, J., Alsop, K., Brady, S. L., Lamb, G., Pandey, A., deFazio, A., Thorne, H., Bild, A. and Bowtell, D. D. L. (2019) 'Multiple ABCB1 transcriptional fusions in drug resistant high-grade serous ovarian and breast cancer', *Nature Communications,* 10(1), pp. 1295.

Clarke, T. L., Sanchez-Bailon, M. P., Chiang, K., Reynolds, J. J., Herrero-Ruiz, J., Bandeiras, T. M., Matias, P. M., Maslen, S. L., Skehel, J. M., Stewart, G. S. and Davies, C. C. (2017) 'PRMT5-Dependent Methylation of the TIP60 Coactivator RUVBL1 Is a Key Regulator of Homologous Recombination', *Mol Cell,* 65(5), pp. 900-916.e7.

Cong, K., Peng, M., Kousholt, A. N., Lee, W. T. C., Lee, S., Nayak, S., Krais, J., VanderVere-Carozza, P. S., Pawelczak, K. S., Calvo, J., Panzarino, N. J., Turchi, J. J., Johnson, N., Jonkers, J., Rothenberg, E. and Cantor, S. B. (2021) 'Replication gaps are a key determinant of PARP inhibitor synthetic lethality with BRCA deficiency', *Mol Cell,* 81(15), pp. 3128-3144.e7.

Cruz, C., Castroviejo-Bermejo, M., Gutiérrez-Enríquez, S., Llop-Guevara, A., Ibrahim, Y. H., Gris-Oliver, A., Bonache, S., Morancho, B., Bruna, A., Rueda, O. M., Lai, Z., Polanska, U. M., Jones, G. N., Kristel, P., de Bustos, L., Guzman, M., Rodríguez, O., Grueso, J., Montalban, G., Caratú, G., Mancuso, F., Fasani, R., Jiménez, J., Howat, W. J., Dougherty, B., Vivancos, A., Nuciforo, P., Serres-Créixams, X., Rubio, I. T., Oaknin, A., Cadogan, E., Barrett, J. C., Caldas, C., Baselga, J., Saura, C., Cortés, J., Arribas, J., Jonkers, J., Díez, O., O'Connor, M. J., Balmaña, J. and Serra, V. (2018) 'RAD51 foci as a functional biomarker of homologous recombination repair and PARP inhibitor resistance in germline BRCA-mutated breast cancer', *Annals of Oncology,* 29(5), pp. 1203-1210.

Curtis, C., Shah, S. P., Chin, S. F., Turashvili, G., Rueda, O. M., Dunning, M. J., Speed, D., Lynch, A. G., Samarajiwa, S., Yuan, Y., Gräf, S., Ha, G., Haffari, G., Bashashati, A., Russell, R., McKinney, S., Langerød, A., Green, A., Provenzano, E., Wishart, G., Pinder, S., Watson, P., Markowetz, F., Murphy, L., Ellis, I., Purushotham, A., Børresen-Dale, A. L., Brenton, J. D., Tavaré, S., Caldas, C. and Aparicio, S. (2012) 'The genomic and transcriptomic architecture of 2,000 breast tumours reveals novel subgroups', *Nature,* 486(7403), pp. 346-52.

Davé, A., Cooley, C., Garg, M. and Bianchi, A. (2014) 'Protein Phosphatase 1 Recruitment by Rif1 Regulates DNA Replication Origin Firing by Counteracting DDK Activity', *Cell Reports,* 7(1), pp. 53-61.

Davies, H., Hunter, C., Smith, R., Stephens, P., Greenman, C., Bignell, G., Teague, J., Butler, A., Edkins, S., Stevens, C., Parker, A., O'Meara, S., Avis, T., Barthorpe, S., Brackenbury, L., Buck, G., Clements, J., Cole, J., Dicks, E., Edwards, K., Forbes, S., Gorton, M., Gray, K., Halliday, K., Harrison, R., Hills, K., Hinton, J., Jones, D., Kosmidou, V., Laman, R., Lugg, R., Menzies, A., Perry, J., Petty, R., Raine, K., Shepherd, R., Small, A., Solomon, H., Stephens, Y., Tofts, C., Varian, J., Webb, A., West, S., Widaa, S., Yates, A., Brasseur, F., Cooper, C. S., Flanagan, A. M., Green, A., Knowles, M., Leung, S. Y., Looijenga, L. H. J., Malkowicz, B., Pierotti, M. A., Teh, B. T., Yuen, S. T., Lakhani, S. R., Easton, D. F., Weber, B. L., Goldstraw, P., Nicholson, A. G., Wooster, R., Stratton, M. R. and Futreal, P. A. (2005) 'Somatic Mutations of the Protein Kinase Gene Family in Human Lung Cancer', *Cancer Research,* 65(17), pp. 7591-7595.

de Bono, J., Mateo, J., Fizazi, K., Saad, F., Shore, N., Sandhu, S., Chi, K. N., Sartor, O., Agarwal, N., Olmos, D., Thiery-Vuillemin, A., Twardowski, P., Mehra, N., Goessl, C., Kang, J., Burgents, J., Wu, W., Kohlmann, A., Adelman, C. A. and Hussain, M. (2020) 'Olaparib for Metastatic Castration-Resistant Prostate Cancer', *New England Journal of Medicine,* 382(22), pp. 2091-2102.

De Bont, R. and van Larebeke, N. (2004) 'Endogenous DNA damage in humans: a review of quantitative data', *Mutagenesis,* 19(3), pp. 169-185.

Debéthune, L., Kohlhagen, G., Grandas, A. and Pommier, Y. (2002) 'Processing of nucleopeptides mimicking the topoisomerase I–DNA covalent complex by tyrosyl-DNA phosphodiesterase', *Nucleic Acids Research,* 30(5), pp. 1198-1204.

Decker, J. T., Hobson, E. C., Zhang, Y., Shin, S., Thomas, A. L., Jeruss, J. S., Arnold, K. B. and Shea, L. D. (2017) 'Systems analysis of dynamic transcription factor activity identifies targets for treatment in Olaparib resistant cancer cells', *Biotechnol Bioeng,* 114(9), pp. 2085-2095.

Della-Maria, J., Zhou, Y., Tsai, M.-S., Kuhnlein, J., Carney, J. P., Paull, T. T. and Tomkinson, A. E. (2011) 'Human Mre11/Human Rad50/Nbs1 and DNA Ligase IIIα/XRCC1 Protein Complexes Act Together in an Alternative Nonhomologous End Joining Pathway*', *Journal of Biological Chemistry,* 286(39), pp. 33845-33853.

DelloRusso, C., Welcsh, P. L., Wang, W., Garcia, R. L., King, M.-C. and Swisher, E. M. (2007) 'Functional Characterization of a Novel BRCA1-Null Ovarian Cancer Cell Line in Response to Ionizing Radiation', *Molecular Cancer Research,* 5(1), pp. 35-45.

Deng, O., Dash, S., Nepomuceno, T. C., Fang, B., Yun, S. Y., Welsh, E. A., Lawrence, H. R., Marchion, D., Koomen, J. M., Monteiro, A. N. and Rix, U. (2022) 'Integrated proteomics identifies PARP inhibitor-induced prosurvival signaling changes as potential vulnerabilities in ovarian cancer', *Journal of Biological Chemistry,* 298(11), pp. 102550.

Dev, H., Chiang, T. W., Lescale, C., de Krijger, I., Martin, A. G., Pilger, D., Coates, J., Sczaniecka-Clift, M., Wei, W., Ostermaier, M., Herzog, M., Lam, J., Shea, A., Demir, M., Wu, Q., Yang, F., Fu, B., Lai, Z., Balmus, G., Belotserkovskaya, R., Serra, V., O'Connor, M. J., Bruna, A., Beli, P., Pellegrini, L., Caldas, C., Deriano, L., Jacobs, J. J. L., Galanty, Y. and Jackson, S. P. (2018) 'Shieldin complex promotes DNA end-joining and counters homologous recombination in BRCA1-null cells', *Nat Cell Biol,* 20(8), pp. 954-965.

Dianov, G. L. and Hübscher, U. (2013) 'Mammalian base excision repair: the forgotten archangel', *Nucleic Acids Res,* 41(6), pp. 3483-90.

Dickson, K.-A., Xie, T., Evenhuis, C., Ma, Y. and Marsh, D. J. (2021) 'PARP Inhibitors Display Differential Efficacy in Models of BRCA Mutant High-Grade Serous Ovarian Cancer', *International Journal of Molecular Sciences,* 22(16), pp. 8506.

Dieckman, L. (2021) 'Something’s gotta give: How PCNA alters its structure in response to mutations and the implications on cellular processes', *Progress in Biophysics and Molecular Biology,* 163, pp. 46-59.

Diéras, V., Han, H. S., Wildiers, H., Friedlander, M., Ayoub, J. P., Puhalla, S. L., Loirat, D., Ratajczak, C., Adamu, H., Girardi, V. and Arun, B. K. (2024) 'Veliparib with carboplatin and paclitaxel in BRCA-mutated advanced breast cancer (BROCADE3): Final overall survival results from a randomized phase 3 trial', *Eur J Cancer,* 200, pp. 113580.

Dobzhansky, T. (1946) 'Genetics of natural populations; recombination and variability in populations of Drosophila pseudoobscura', *Genetics,* 31(3), pp. 269-90.

Domchek, S. M. (2017) 'Reversion Mutations with Clinical Use of PARP Inhibitors: Many Genes, Many Versions', *Cancer Discov,* 7(9), pp. 937-939.

Dou, Y., Milne, T. A., Ruthenburg, A. J., Lee, S., Lee, J. W., Verdine, G. L., Allis, C. D. and Roeder, R. G. (2006) 'Regulation of MLL1 H3K4 methyltransferase activity by its core components', *Nature Structural & Molecular Biology,* 13(8), pp. 713-719.

Drew, Y., Mulligan, E. A., Vong, W.-T., Thomas, H. D., Kahn, S., Kyle, S., Mukhopadhyay, A., Los, G., Hostomsky, Z., Plummer, E. R., Edmondson, R. J. and Curtin, N. J. (2010) 'Therapeutic Potential of Poly(ADP-ribose) Polymerase Inhibitor AG014699 in Human Cancers With Mutated or Methylated BRCA1 or BRCA2', *JNCI: Journal of the National Cancer Institute,* 103(4), pp. 334-346.

Du, M., Gong, P., Zhang, Y., Liu, Y., Liu, X., Zhang, F. and Wang, X. (2021) 'Histone methyltransferase SETD1A participates in lung cancer progression', *Thorac Cancer,* 12(16), pp. 2247-2257.

Dungrawala, H., Bhat, K. P., Le Meur, R., Chazin, W. J., Ding, X., Sharan, S. K., Wessel, S. R., Sathe, A. A., Zhao, R. and Cortez, D. (2017) 'RADX promotes genome stability and modulates chemosensitivity by regulating RAD51 at replication forks', *Molecular cell,* 67(3), pp. 374-386. e5.

El-Brolosy, M. A. and Stainier, D. Y. R. (2017) 'Genetic compensation: A phenomenon in search of mechanisms', *PLoS Genet,* 13(7), pp. e1006780.

El Botty, R., Coussy, F., Hatem, R., Assayag, F., Chateau-Joubert, S., Servely, J. L., Leboucher, S., Fouillade, C., Vacher, S., Ouine, B., Cartier, A., de Koning, L., Cottu, P., Bièche, I. and Marangoni, E. (2018) 'Inhibition of mTOR downregulates expression of DNA repair proteins and is highly efficient against BRCA2-mutated breast cancer in combination to PARP inhibition', *Oncotarget,* 9(51), pp. 29587-29600.

Escribano-Díaz, C., Orthwein, A., Fradet-Turcotte, A., Xing, M., Young, Jordan T. F., Tkáč, J., Cook, Michael A., Rosebrock, Adam P., Munro, M., Canny, Marella D., Xu, D. and Durocher, D. (2013) 'A Cell Cycle-Dependent Regulatory Circuit Composed of 53BP1-RIF1 and BRCA1-CtIP Controls DNA Repair Pathway Choice', *Molecular Cell,* 49(5), pp. 872-883.

Eskelund, C. W., Dahl, C., Hansen, J. W., Westman, M., Kolstad, A., Pedersen, L. B., Montano-Almendras, C. P., Husby, S., Freiburghaus, C., Ek, S., Pedersen, A., Niemann, C., Räty, R., Brown, P., Geisler, C. H., Andersen, M. K., Guldberg, P., Jerkeman, M. and Grønbæk, K. (2017) 'TP53 mutations identify younger mantle cell lymphoma patients who do not benefit from intensive chemoimmunotherapy', *Blood,* 130(17), pp. 1903-1910.

Esteller, M., Silva, J. M., Dominguez, G., Bonilla, F., Matias-Guiu, X., Lerma, E., Bussaglia, E., Prat, J., Harkes, I. C., Repasky, E. A., Gabrielson, E., Schutte, M., Baylin, S. B. and Herman, J. G. (2000) 'Promoter Hypermethylation and BRCA1

Inactivation in Sporadic Breast and Ovarian Tumors', *JNCI: Journal of the National Cancer Institute,* 92(7), pp. 564-569.

Falck, J., Mailand, N., Syljuåsen, R. G., Bartek, J. and Lukas, J. (2001) 'The ATM-Chk2-Cdc25A checkpoint pathway guards against radioresistant DNA synthesis', *Nature,* 410(6830), pp. 842-7.

Falzon, M., Fewell, J. W. and Kuff, E. L. (1993) 'EBP-80, a transcription factor closely resembling the human autoantigen Ku, recognizes single- to double-strand transitions in DNA', *J Biol Chem,* 268(14), pp. 10546-52.

Fang, Y., Liao, G. and Yu, B. (2019) 'LSD1/KDM1A inhibitors in clinical trials: advances and prospects', *Journal of Hematology & Oncology,* 12(1), pp. 129.

Farmer, H., McCabe, N., Lord, C. J., Tutt, A. N. J., Johnson, D. A., Richardson, T. B., Santarosa, M., Dillon, K. J., Hickson, I., Knights, C., Martin, N. M. B., Jackson, S. P., Smith, G. C. M. and Ashworth, A. (2005) 'Targeting the DNA repair defect in BRCA mutant cells as a therapeutic strategy', *Nature,* 434(7035), pp. 917-921.

Faucher, D. and Wellinger, R. J. (2010) 'Methylated H3K4, a transcription-associated histone modification, is involved in the DNA damage response pathway', *PLoS Genet,* 6(8), pp. e1001082.

FDA (2023) *Oncology (Cancer)/Hematologic Malignancies Approval Notifications*. Available at: https://www.fda.gov/drugs/resources-information-approved-drugs/oncology-cancerhematologic-malignancies-approval-notifications (Accessed: 9th September 2024).

Finzel, A., Grybowski, A., Strasen, J., Cristiano, E. and Loewer, A. (2016) 'Hyperactivation of ATM upon DNA-PKcs inhibition modulates p53 dynamics and cell fate in response to DNA damage', *Mol Biol Cell,* 27(15), pp. 2360-7.

Fradet-Turcotte, A., Canny, M. D., Escribano-Díaz, C., Orthwein, A., Leung, C. C., Huang, H., Landry, M. C., Kitevski-LeBlanc, J., Noordermeer, S. M., Sicheri, F. and Durocher, D. (2013) '53BP1 is a reader of the DNA-damage-induced H2A Lys 15 ubiquitin mark', *Nature,* 499(7456), pp. 50-4.

Fujita, H., Ikeda, M., Ui, A., Ouchi, Y., Mikami, Y., Kanno, S. I., Yasui, A. and Tanaka, K. (2022) 'CHAMP1-POGZ counteracts the inhibitory effect of 53BP1 on homologous recombination and affects PARP inhibitor resistance', *Oncogene,* 41(19), pp. 2706-2718.

Gagné, J.-P., Isabelle, M., Lo, K. S., Bourassa, S., Hendzel, M. J., Dawson, V. L., Dawson, T. M. and Poirier, G. G. (2008) 'Proteome-wide identification of poly(ADP-ribose) binding proteins and poly(ADP-ribose)-associated protein complexes', *Nucleic Acids Research,* 36(22), pp. 6959-6976.

Galande, S. and Kohwi-Shigematsu, T. (1999) 'Poly(ADP-ribose) Polymerase and Ku Autoantigen Form a Complex and Synergistically Bind to Matrix Attachment Sequences *', *Journal of Biological Chemistry,* 274(29), pp. 20521-20528.

Gao, J., Aksoy, B. A., Dogrusoz, U., Dresdner, G., Gross, B., Sumer, S. O., Sun, Y., Jacobsen, A., Sinha, R., Larsson, E., Cerami, E., Sander, C. and Schultz, N. (2013) 'Integrative analysis of complex cancer genomics and clinical profiles using the cBioPortal', *Sci Signal,* 6(269), pp. pl1.

Garcia, V., Phelps, S. E., Gray, S. and Neale, M. J. (2011) 'Bidirectional resection of DNA double-strand breaks by Mre11 and Exo1', *Nature,* 479(7372), pp. 241-4.

Geng, L., Huntoon, C. J. and Karnitz, L. M. (2010) 'RAD18-mediated ubiquitination of PCNA activates the Fanconi anemia DNA repair network', *J Cell Biol,* 191(2), pp. 249-57.

Gesztes, W., Schafer, C., Young, D., Fox, J., Jiang, J., Chen, Y., Kuo, H.-C., Mwamukonda, K. B., Dobi, A., Burke, A. P., Moul, J. W., McLeod, D. G., Rosner, I. L., Petrovics, G., Tan, S.-H., Cullen, J., Srivastava, S. and Sesterhenn, I. A. (2022) 'Focal p53 protein expression and lymphovascular invasion in primary prostate tumors predict metastatic progression', *Scientific Reports,* 12(1), pp. 5404.

Gogola, E., Duarte, A. A., de Ruiter, J. R., Wiegant, W. W., Schmid, J. A., de Bruijn, R., James, D. I., Guerrero Llobet, S., Vis, D. J., Annunziato, S., van den Broek, B., Barazas, M., Kersbergen, A., van de Ven, M., Tarsounas, M., Ogilvie, D. J., van Vugt, M., Wessels, L. F. A., Bartkova, J., Gromova, I., Andújar-Sánchez, M., Bartek, J., Lopes, M., van Attikum, H., Borst, P., Jonkers, J. and Rottenberg, S. (2018) 'Selective Loss of PARG Restores PARylation and Counteracts PARP Inhibitor-Mediated Synthetic Lethality', *Cancer Cell,* 33(6), pp. 1078-1093.e12.

Gogola, E., Rottenberg, S. and Jonkers, J. (2019) 'Resistance to PARP Inhibitors: Lessons from Preclinical Models of BRCA-Associated Cancer', *Annual Review of Cancer Biology,* 3, pp. 235-254.

Golan, T., Hammel, P., Reni, M., Van Cutsem, E., Macarulla, T., Hall, M. J., Park, J. O., Hochhauser, D., Arnold, D., Oh, D. Y., Reinacher-Schick, A., Tortora, G., Algül, H., O'Reilly, E. M., McGuinness, D., Cui, K. Y., Schlienger, K., Locker, G. Y. and Kindler, H. L. (2019) 'Maintenance Olaparib for Germline BRCA-Mutated Metastatic Pancreatic Cancer', *N Engl J Med,* 381(4), pp. 317-327.

González-Bermúdez, L., Genescà, A., Terradas, M. and Martín, M. (2022) 'Role of H4K16 acetylation in 53BP1 recruitment to double-strand break sites in in vitro aged cells', *Biogerontology,* 23(4), pp. 499-514.

González-Martín, A., Pothuri, B., Vergote, I., DePont Christensen, R., Graybill, W., Mirza, M. R., McCormick, C., Lorusso, D., Hoskins, P., Freyer, G., Baumann, K., Jardon, K., Redondo, A., Moore, R. G., Vulsteke, C., O'Cearbhaill, R. E., Lund, B., Backes, F., Barretina-Ginesta, P., Haggerty, A. F., Rubio-Pérez, M. J., Shahin, M. S., Mangili, G., Bradley, W. H., Bruchim, I., Sun, K., Malinowska, I. A., Li, Y., Gupta, D. and Monk, B. J. (2019) 'Niraparib in Patients with Newly Diagnosed Advanced Ovarian Cancer', *N Engl J Med,* 381(25), pp. 2391-2402.

Goodarzi, A. A., Yu, Y., Riballo, E., Douglas, P., Walker, S. A., Ye, R., Härer, C., Marchetti, C., Morrice, N., Jeggo, P. A. and Lees-Miller, S. P. (2006) 'DNA-PK autophosphorylation facilitates Artemis endonuclease activity', *The EMBO Journal,* 25(16), pp. 3880-3889.

Gottipati, P., Vischioni, B., Schultz, N., Solomons, J., Bryant, H. E., Djureinovic, T., Issaeva, N., Sleeth, K., Sharma, R. A. and Helleday, T. (2010) 'Poly(ADP-Ribose) Polymerase Is Hyperactivated in Homologous Recombination–Defective Cells', *Cancer Research,* 70(13), pp. 5389-5398.

Gottlieb, T. M. and Jackson, S. P. (1993) 'The DNA-dependent protein kinase: Requirement for DNA ends and association with Ku antigen', *Cell,* 72(1), pp. 131-142.

Gout, J., Perkhofer, L., Morawe, M., Arnold, F., Ihle, M., Biber, S., Lange, S., Roger, E., Kraus, J. M., Stifter, K., Hahn, S. A., Zamperone, A., Engleitner, T., Müller, M., Walter, K., Rodriguez-Aznar, E., Sainz Jr, B., Hermann, P. C., Hessmann, E., Müller, S., Azoitei, N., Lechel, A., Liebau, S., Wagner, M., Simeone, D. M., Kestler, H. A., Seufferlein, T., Wiesmüller, L., Rad, R., Frappart, P.-O. and Kleger, A. (2021) 'Synergistic targeting and resistance to PARP inhibition in DNA damage repair-deficient pancreatic cancer', *Gut,* 70(4), pp. 743.

Grundy, G. J., Rulten, S. L., Zeng, Z., Arribas-Bosacoma, R., Iles, N., Manley, K., Oliver, A. and Caldecott, K. W. (2013) 'APLF promotes the assembly and activity of non-homologous end joining protein complexes', *The EMBO journal,* 32(1), pp. 112-125.

Gu, Y., Helenius, M., Väänänen, K., Bulanova, D., Saarela, J., Sokolenko, A., Martens, J., Imyanitov, E. and Kuznetsov, S. (2016) 'BRCA1-deficient breast cancer cell lines are resistant to MEK inhibitors and show distinct sensitivities to 6-thioguanine', *Scientific Reports,* 6(1), pp. 28217.

Guo, X., Bai, Y., Zhao, M., Zhou, M., Shen, Q., Yun, C.-H., Zhang, H., Zhu, W.-G. and Wang, J. (2017) 'Acetylation of 53BP1 dictates the DNA double strand break repair pathway', *Nucleic Acids Research,* 46(2), pp. 689-703.

Gutierrez, R. and O'Connor, T. R. (2021) 'DNA direct reversal repair and alkylating agent drug resistance', *Cancer Drug Resist,* 4(2), pp. 414-423.

Haince, J. F., McDonald, D., Rodrigue, A., Déry, U., Masson, J. Y., Hendzel, M. J. and Poirier, G. G. (2008) 'PARP1-dependent kinetics of recruitment of MRE11 and NBS1 proteins to multiple DNA damage sites', *J Biol Chem,* 283(2), pp. 1197-208.

Heeke, A. L., Pishvaian, M. J., Lynce, F., Xiu, J., Brody, J. R., Chen, W. J., Baker, T. M., Marshall, J. L. and Isaacs, C. (2018) 'Prevalence of Homologous Recombination-Related Gene Mutations Across Multiple Cancer Types', *JCO Precis Oncol,* 2, pp. 1-13.

Heijink, A. M., Stok, C., Porubsky, D., Manolika, E. M., de Kanter, J. K., Kok, Y. P., Everts, M., de Boer, H. R., Audrey, A., Bakker, F. J., Wierenga, E., Tijsterman, M., Guryev, V., Spierings, D. C. J., Knipscheer, P., van Boxtel, R., Ray Chaudhuri, A., Lansdorp, P. M. and van Vugt, M. A. T. M. (2022) 'Sister chromatid exchanges induced by perturbed replication can form independently of BRCA1, BRCA2 and RAD51', *Nature Communications,* 13(1), pp. 6722.

Heyer, W. D., Ehmsen, K. T. and Liu, J. (2010) 'Regulation of homologous recombination in eukaryotes', *Annu Rev Genet,* 44, pp. 113-39.

Hietanen, S., Lain, S., Krausz, E., Blattner, C. and Lane, D. P. (2000) 'Activation of p53 in cervical carcinoma cells by small molecules', *Proc Natl Acad Sci U S A,* 97(15), pp. 8501-6.

Higgs, Martin R., Reynolds, John J., Winczura, A., Blackford, Andrew N., Borel, V., Miller, Edward S., Zlatanou, A., Nieminuszczy, J., Ryan, Ellis L., Davies, Nicholas J., Stankovic, T., Boulton, Simon J., Niedzwiedz, W. and Stewart, Grant S. (2015) 'BOD1L Is Required to Suppress Deleterious Resection of Stressed Replication Forks', *Molecular Cell,* 59(3), pp. 462-477.

Higgs, M. R., Sato, K., Reynolds, J. J., Begum, S., Bayley, R., Goula, A., Vernet, A., Paquin, K. L., Skalnik, D. G., Kobayashi, W., Takata, M., Howlett, N. G., Kurumizaka, H., Kimura, H. and Stewart, G. S. (2018) 'Histone Methylation by SETD1A Protects Nascent DNA through the Nucleosome Chaperone Activity of FANCD2', *Mol Cell,* 71(1), pp. 25-41 e6.

Hoege, C., Pfander, B., Moldovan, G.-L., Pyrowolakis, G. and Jentsch, S. (2002) 'RAD6-dependent DNA repair is linked to modification of PCNA by ubiquitin and SUMO', *Nature,* 419(6903), pp. 135-141.

Hoeijmakers, J. H. (2001) 'Genome maintenance mechanisms for preventing cancer', *Nature,* 411(6835), pp. 366-74.

Hong, R., Ma, F., Zhang, W., Yu, X., Li, Q., Luo, Y., Zhu, C., Jiang, W. and Xu, B. (2016) '53BP1 depletion causes PARP inhibitor resistance in ATM-deficient breast cancer cells', *BMC Cancer,* 16(725).

Hoshii, T., Cifani, P., Feng, Z., Huang, C. H., Koche, R., Chen, C. W., Delaney, C. D., Lowe, S. W., Kentsis, A. and Armstrong, S. A. (2018) 'A Non-catalytic Function of SETD1A Regulates Cyclin K and the DNA Damage Response', *Cell,* 172(5), pp. 1007-1021.e17.

Hoshii, T., Perlee, S., Kikuchi, S., Rahmutulla, B., Fukuyo, M., Masuda, T., Ohtsuki, S., Soga, T., Nabet, B. and Kaneda, A. (2022) 'SETD1A regulates transcriptional pause release of heme biosynthesis genes in leukemia', *Cell Reports,* 41(9), pp. 111727.

Hsu, P. L., Shi, H., Leonen, C., Kang, J., Chatterjee, C. and Zheng, N. (2019) 'Structural Basis of H2B Ubiquitination-Dependent H3K4 Methylation by COMPASS', *Molecular Cell,* 76(5), pp. 712-723.e4.

Hu, Y., Petit, S. A., Ficarro, S. B., Toomire, K. J., Xie, A., Lim, E., Cao, S. A., Park, E., Eck, M. J., Scully, R., Brown, M., Marto, J. A. and Livingston, D. M. (2014) 'PARP1-driven poly-ADP-ribosylation regulates BRCA1 function in homologous recombination-mediated DNA repair', *Cancer Discov,* 4(12), pp. 1430-47.

Huang, Y., Zhang, S. and Park, J. I. (2022) 'Nuclear Actin Dynamics in Gene Expression, DNA Repair, and Cancer', *Results Probl Cell Differ,* 70, pp. 625-663.

Huertas, P. and Jackson, S. P. (2009) 'Human CtIP mediates cell cycle control of DNA end resection and double strand break repair', *J Biol Chem,* 284(14), pp. 9558-65.

Hurley, R. M., Wahner Hendrickson, A. E., Visscher, D. W., Ansell, P., Harrell, M. I., Wagner, J. M., Negron, V., Goergen, K. M., Maurer, M. J., Oberg, A. L., Meng, X. W., Flatten, K. S., De Jonge, M. J. A., Van Herpen, C. D., Gietema, J. A., Koornstra, R. H. T., Jager, A., den Hollander, M. W., Dudley, M., Shepherd, S. P., Swisher, E. M. and Kaufmann, S. H. (2019) '53BP1 as a potential predictor of response in PARP inhibitor-treated homologous recombination-deficient ovarian cancer', *Gynecol Oncol,* 153(1), pp. 127-134.

Hyllus, D., Stein, C., Schnabel, K., Schiltz, E., Imhof, A., Dou, Y., Hsieh, J. and Bauer, U. M. (2007) 'PRMT6-mediated methylation of R2 in histone H3 antagonizes H3 K4 trimethylation', *Genes Dev,* 21(24), pp. 3369-80.

Hyun, K., Jeon, J., Park, K. and Kim, J. (2017) 'Writing, erasing and reading histone lysine methylations', *Experimental & Molecular Medicine,* 49(4), pp. e324-e324.

Illuzzi, G., Staniszewska, A. D., Gill, S. J., Pike, A., McWilliams, L., Critchlow, S. E., Cronin, A., Fawell, S., Hawthorne, G., Jamal, K., Johannes, J., Leonard, E., Macdonald, R., Maglennon, G., Nikkilä, J., O'Connor, M. J., Smith, A., Southgate, H., Wilson, J., Yates, J., Cosulich, S. and Leo, E. (2022) 'Preclinical Characterization of AZD5305, A Next-Generation, Highly Selective PARP1 Inhibitor and Trapper', *Clin Cancer Res,* 28(21), pp. 4724-4736.

Ishiai, M., Kitao, H., Smogorzewska, A., Tomida, J., Kinomura, A., Uchida, E., Saberi, A., Kinoshita, E., Kinoshita-Kikuta, E., Koike, T., Tashiro, S., Elledge, S. J. and Takata, M. (2008) 'FANCI phosphorylation functions as a molecular switch to turn on the Fanconi anemia pathway', *Nature Structural & Molecular Biology,* 15(11), pp. 1138-1146.

Ishii, T., Akiyama, Y., Shimada, S., Kabashima, A., Asano, D., Watanabe, S., Ishikawa, Y., Ueda, H., Akahoshi, K., Ogawa, K., Ono, H., Kudo, A., Tanabe, M. and Tanaka, S. (2023) 'Identification of a novel target of SETD1A histone methyltransferase and the clinical significance in pancreatic cancer', *Cancer Science,* 114(2), pp. 463-476.

Isobe, S. Y., Hiraga, S. I., Nagao, K., Sasanuma, H., Donaldson, A. D. and Obuse, C. (2021) 'Protein phosphatase 1 acts as a RIF1 effector to suppress DSB resection prior to Shieldin action', *Cell Rep,* 36(2), pp. 109383.

Jackson, A. L., Burchard, J., Schelter, J., Chau, B. N., Cleary, M., Lim, L. and Linsley, P. S. (2006) 'Widespread siRNA "off-target" transcript silencing mediated by seed region sequence complementarity', *Rna,* 12(7), pp. 1179-87.

Jacobs, A. L. and Schär, P. (2012) 'DNA glycosylases: in DNA repair and beyond', *Chromosoma,* 121(1), pp. 1-20.

Jakobsdottir, J., van der Lee, S. J., Bis, J. C., Chouraki, V., Li-Kroeger, D., Yamamoto, S., Grove, M. L., Naj, A., Vronskaya, M., Salazar, J. L., DeStefano, A. L., Brody, J. A., Smith, A. V., Amin, N., Sims, R., Ibrahim-Verbaas, C. A., Choi, S.-H., Satizabal, C. L., Lopez, O. L., Beiser, A., Ikram, M. A., Garcia, M. E., Hayward, C., Varga, T. V., Ripatti, S., Franks, P. W., Hallmans, G., Rolandsson, O., Jansson, J.-H., Porteous, D. J., Salomaa, V., Eiriksdottir, G., Rice, K. M., Bellen, H. J., Levy, D., Uitterlinden, A. G., Emilsson, V., Rotter, J. I., Aspelund, T., Cohorts for, H., Aging Research in Genomic Epidemiology, c., Alzheimer's Disease Genetic, C., Genetic, Environmental Risk in Alzheimer's Disease, c., O'Donnell, C. J., Fitzpatrick, A. L., Launer, L. J., Hofman, A., Wang, L.-S., Williams, J., Schellenberg, G. D., Boerwinkle, E., Psaty, B. M., Seshadri, S., Shulman, J. M., Gudnason, V. and van Duijn, C. M. (2016) 'Rare Functional Variant in TM2D3 is Associated with Late-Onset Alzheimer's Disease', *PLOS Genetics,* 12(10), pp. e1006327.

Jaspers, J. E., Kersbergen, A., Boon, U., Sol, W., van Deemter, L., Zander, S. A., Drost, R., Wientjens, E., Ji, J., Aly, A., Doroshow, J. H., Cranston, A., Martin, N. M., Lau, A., O'Connor, M. J., Ganesan, S., Borst, P., Jonkers, J. and Rottenberg, S. (2013) 'Loss of 53BP1 causes PARP inhibitor resistance in Brca1-mutated mouse mammary tumors', *Cancer Discov,* 3(1), pp. 68-81.

Jiricny, J. (2013) 'Postreplicative mismatch repair', *Cold Spring Harb Perspect Biol,* 5(4), pp. a012633.

Jonkhout, N., Cruciani, S., Santos Vieira, H. G., Tran, J., Liu, H., Liu, G., Pickford, R., Kaczorowski, D., Franco, G. R., Vauti, F., Camacho, N., Abedini, S. S., Najmabadi, H., Ribas de Pouplana, L., Christ, D., Schonrock, N., Mattick, J. S. and Novoa, E. M. (2021) 'Subcellular relocalization and nuclear redistribution of the RNA methyltransferases TRMT1 and TRMT1L upon neuronal activation', *RNA Biol,* 18(11), pp. 1905-1919.

Jungmichel, S., Rosenthal, F., Altmeyer, M., Lukas, J., Hottiger, Michael O. and Nielsen, Michael L. (2013) 'Proteome-wide Identification of Poly(ADP-Ribosyl)ation Targets in Different Genotoxic Stress Responses', *Molecular Cell,* 52(2), pp. 272-285.

Kakarougkas, A. and Jeggo, P. A. (2014) 'DNA DSB repair pathway choice: an orchestrated handover mechanism', *The British journal of radiology,* 87(1035), pp. 20130685-20130685.

Kang, J.-Y., Park, J. W., Hwang, Y., Hahm, J. Y., Park, J., Park, K.-S. and Seo, S.-B. (2021a) 'The H3K4 methyltransferase SETD1A is required for proliferation of non-small cell lung cancer cells by promoting S-phase progression', *Biochemical and Biophysical Research Communications,* 561, pp. 120-127.

Kang, J. Y., Park, J. W., Hwang, Y., Hahm, J. Y., Park, J., Park, K. S. and Seo, S. B. (2021b) 'The H3K4 methyltransferase SETD1A is required for proliferation of non-small cell lung cancer cells by promoting S-phase progression', *Biochem Biophys Res Commun,* 561, pp. 120-127.

Karakas, B., Weeraratna, A. T., Abukhdeir, A. M., Konishi, H., Gustin, J. P., Vitolo, M. I., Bachman, K. E. and Park, B. H. (2007) 'P21 gene knock down does not identify genetic effectors seen with gene knock out', *Cancer Biol Ther,* 6(7), pp. 1025-30.

Keung, M. Y., Wu, Y., Badar, F. and Vadgama, J. V. (2020) 'Response of Breast Cancer Cells to PARP Inhibitors Is Independent of BRCA Status', *J Clin Med,* 9(4), pp. 940.

Khanna, K. K. and Jackson, S. P. (2001) 'DNA double-strand breaks: signaling, repair and the cancer connection', *Nat Genet,* 27(3), pp. 247-54.

Khatib, J. B., Nicolae, C. M. and Moldovan, G.-L. (2024) 'Role of Translesion DNA Synthesis in the Metabolism of Replication-associated Nascent Strand Gaps', *Journal of Molecular Biology,* 436(1), pp. 168275.

Kim, D. H., Tang, Z., Shimada, M., Fierz, B., Houck-Loomis, B., Bar-Dagen, M., Lee, S., Lee, S. K., Muir, T. W., Roeder, R. G. and Lee, J. W. (2013) 'Histone H3K27 trimethylation inhibits H3 binding and function of SET1-like H3K4 methyltransferase complexes', *Mol Cell Biol,* 33(24), pp. 4936-46.

Kim, G., Ison, G., McKee, A. E., Zhang, H., Tang, S., Gwise, T., Sridhara, R., Lee, E., Tzou, A., Philip, R., Chiu, H. J., Ricks, T. K., Palmby, T., Russell, A. M., Ladouceur, G., Pfuma, E., Li, H., Zhao, L., Liu, Q., Venugopal, R., Ibrahim, A. and Pazdur, R. (2015) 'FDA Approval Summary: Olaparib Monotherapy in Patients with Deleterious Germline BRCA-Mutated Advanced Ovarian Cancer Treated with Three or More Lines of Chemotherapy', *Clin Cancer Res,* 21(19), pp. 4257-61.

Kim, H. and D'Andrea, A. D. (2012) 'Regulation of DNA cross-link repair by the Fanconi anemia/BRCA pathway', *Genes Dev,* 26(13), pp. 1393-408.

Kim, H., Xu, H., George, E., Hallberg, D., Kumar, S., Jagannathan, V., Medvedev, S., Kinose, Y., Devins, K., Verma, P., Ly, K., Wang, Y., Greenberg, R. A., Schwartz, L., Johnson, N., Scharpf, R. B., Mills, G. B., Zhang, R., Velculescu, V. E., Brown, E. J. and Simpkins, F. (2020) 'Combining PARP with ATR inhibition overcomes PARP inhibitor and platinum resistance in ovarian cancer models', *Nature Communications,* 11(1).

Kim, M. and Kim, J. M. (2016) 'The role of USP1 autocleavage in DNA interstrand crosslink repair', *FEBS Letters,* 590(3), pp. 340-348.

King, A., Reichl, P. I., Metson, J. S., Parker, R., Munro, D., Oliveira, C., Sommerova, L., Becker, J. R., Biggs, D., Preece, C., Davies, B. and Chapman, J. R. (2024) 'Shieldin and CST co-orchestrate DNA polymerase-dependent tailed-end joining reactions independently of 53BP1-governed repair pathway choice', *Nature Structural & Molecular Biology*.

King, M.-C., Marks, J. H. and Mandell, J. B. (2003) 'Breast and ovarian cancer risks due to inherited mutations in BRCA1 and BRCA2', *Science,* 302(5645), pp. 643-6.

Klose, R. J., Yan, Q., Tothova, Z., Yamane, K., Erdjument-Bromage, H., Tempst, P., Gilliland, D. G., Zhang, Y. and Kaelin, W. G. (2007) 'The Retinoblastoma Binding Protein RBP2 Is an H3K4 Demethylase', *Cell,* 128(5), pp. 889-900.

Knijnenburg, T. A., Wang, L., Zimmermann, M. T., Chambwe, N., Gao, G. F., Cherniack, A. D., Fan, H., Shen, H., Way, G. P., Greene, C. S., Liu, Y., Akbani, R., Feng, B., Donehower, L. A., Miller, C., Shen, Y., Karimi, M., Chen, H., Kim, P., Jia, P., Shinbrot, E. and et, a. (2018) 'Genomic and Molecular Landscape of DNA Damage Repair Deficiency across The Cancer Genome Atlas', *Cell Reports,* 23(1), pp. 239-254.e6.

Kobayashi, S., Fukatsu, R., Kanoh, Y., Kakusho, N., Matsumoto, S., Chaen, S. and Masai, H. (2019) 'Both a Unique Motif at the C Terminus and an N-Terminal HEAT Repeat Contribute to G-Quadruplex Binding and Origin Regulation by the Rif1 Protein', *Mol Cell Biol,* 39(4), pp. e00364-18.

Kolb, A.-L., Gunn, A. R. and Lakin, N. D. (2017) 'Redundancy between nucleases required for homologous recombination promotes PARP inhibitor resistance in the eukaryotic model organism Dictyostelium', *Nucleic Acids Research,* 45(17), pp. 10056-10067.

Krokan, H. E. and Bjørås, M. (2013) 'Base excision repair', *Cold Spring Harb Perspect Biol,* 5(4), pp. a012583.

Kubota, E., Williamson, C. T., Ye, R., Elegbede, A., Peterson, L., Lees-Miller, S. P. and Bebb, D. G. (2014) 'Low ATM protein expression and depletion of p53 correlates with olaparib sensitivity in gastric cancer cell lines', *Cell Cycle,* 13(13), pp. 2129-37.

Kummeling, J., Stremmelaar, D. E., Raun, N., Reijnders, M. R. F., Willemsen, M. H., Ruiterkamp-Versteeg, M., Schepens, M., Man, C. C. O., Gilissen, C., Cho, M. T., McWalter, K., Sinnema, M., Wheless, J. W., Simon, M. E. H., Genetti, C. A., Casey, A. M., Terhal, P. A., van der Smagt, J. J., van Gassen, K. L. I., Joset, P., Bahr, A., Steindl, K., Rauch, A., Keller, E., Raas-Rothschild, A., Koolen, D. A., Agrawal, P. B., Hoffman, T. L., Powell-Hamilton, N. N., Thiffault, I., Engleman, K., Zhou, D., Bodamer, O., Hoefele, J., Riedhammer, K. M., Schwaibold, E. M. C., Tasic, V., Schubert, D., Top, D., Pfundt, R., Higgs, M. R., Kramer, J. M. and Kleefstra, T. (2020) 'Characterization of SETD1A haploinsufficiency in humans and Drosophila defines a novel neurodevelopmental syndrome', *Mol Psychiatry,* 26, pp. 2013–2024.

Kurosawa, A., Koyama, H., Takayama, S., Miki, K., Ayusawa, D., Fujii, M., Iiizumi, S. and Adachi, N. (2008) 'The requirement of Artemis in double-strand break repair depends on the type of DNA damage', *DNA Cell Biol,* 27(1), pp. 55-61.

Langelier, M.-F., Billur, R., Sverzhinsky, A., Black, B. E. and Pascal, J. M. (2021) 'HPF1 dynamically controls the PARP1/2 balance between initiating and elongating ADP-ribose modifications', *Nature Communications,* 12(1), pp. 6675.

Langelier, M.-F., Eisemann, T., Riccio, A. A. and Pascal, J. M. (2018) 'PARP family enzymes: regulation and catalysis of the poly(ADP-ribose) posttranslational modification', *Current opinion in structural biology,* 53, pp. 187-198.

Lanz, M. C., Dibitetto, D. and Smolka, M. B. (2019) 'DNA damage kinase signaling: checkpoint and repair at 30 years', *The EMBO Journal,* 38(18), pp. e101801.

Ledesma, F. C., El Khamisy, S. F., Zuma, M. C., Osborn, K. and Caldecott, K. W. (2009) 'A human 5′-tyrosyl DNA phosphodiesterase that repairs topoisomerase-mediated DNA damage', *Nature,* 461(7264), pp. 674-678.

Lee, C.-Y., Cheng, W.-F., Lin, P.-H., Chen, Y.-L., Huang, S.-H., Lei, K.-H., Chang, K.-Y., Ko, M.-Y. and Chi, P. (2023) 'An activity-based functional test for identifying homologous recombination deficiencies across cancer types in real time', *Cell Reports Medicine,* 4(11), pp. 101247.

Lee, J.-H. and Skalnik, D. G. (2005) 'CpG-binding Protein (CXXC Finger Protein 1) Is a Component of the Mammalian Set1 Histone H3-Lys4 Methyltransferase Complex, the Analogue of the Yeast Set1/COMPASS Complex*', *Journal of Biological Chemistry,* 280(50), pp. 41725-41731.

Lee, J.-H. and Skalnik, D. G. (2008) 'Wdr82 Is a C-Terminal Domain-Binding Protein That Recruits the Setd1A Histone H3-Lys4 Methyltransferase Complex to Transcription Start Sites of Transcribed Human Genes', *Molecular and Cellular Biology,* 28(2), pp. 609-618.

Lee, J.-H., Tate, C. M., You, J.-S. and Skalnik, D. G. (2007) 'Identification and Characterization of the Human Set1B Histone H3-Lys⁴ Methyltransferase Complex *', *Journal of Biological Chemistry,* 282(18), pp. 13419-13428.

Lehmann, B. D., Bauer, J. A., Chen, X., Sanders, M. E., Chakravarthy, A. B., Shyr, Y. and Pietenpol, J. A. (2011) 'Identification of human triple-negative breast cancer subtypes and preclinical models for selection of targeted therapies', *The Journal of Clinical Investigation,* 121(7), pp. 2750-2767.

Leidecker, O., Bonfiglio, J. J., Colby, T., Zhang, Q., Atanassov, I., Zaja, R., Palazzo, L., Stockum, A., Ahel, I. and Matic, I. (2016) 'Serine is a new target residue for endogenous ADP-ribosylation on histones', *Nature Chemical Biology,* 12(12), pp. 998-1000.

Lerdrup, M., Johansen, J. V., Agrawal-Singh, S. and Hansen, K. (2016) 'An interactive environment for agile analysis and visualization of ChIP-sequencing data', *Nature Structural & Molecular Biology,* 23(4), pp. 349-357.

Li, H. D., Ma, H. X., Ma, J. H., Kong, S. P., Zhao, S. T., Fan, S. Q., Qin, F. and Ma, J. G. (2024) 'A comprehensive analysis of essential meiotic endonuclease 1 to prognosis and immune infiltration in kidney renal clear cell carcinoma', *Eur Rev Med Pharmacol Sci,* 28(2), pp. 584-602.

Li, M. and Yu, X. (2013) 'Function of BRCA1 in the DNA Damage Response Is Mediated by ADP-Ribosylation', *Cancer Cell,* 23(5), pp. 693-704.

Li, Y., Schulz, V. P., Deng, C., Li, G., Shen, Y., Tusi, B. K., Ma, G., Stees, J., Qiu, Y., Steiner, L. A., Zhou, L., Zhao, K., Bungert, J., Gallagher, P. G. and Huang, S. (2016) 'Setd1a and NURF mediate chromatin dynamics and gene regulation during erythroid lineage commitment and differentiation', *Nucleic acids research,* 44(15), pp. 7173-7188.

Liang, C.-C., Greenhough, L. A., Masino, L., Maslen, S., Bajrami, I., Tuppi, M., Skehel, M., Taylor, I. A. and West, S. C. (2024) 'Mechanism of single-stranded DNA annealing by RAD52–RPA complex', *Nature,* 629(8012), pp. 697-703.

Lim, P. X., Zaman, M., Feng, W. and Jasin, M. (2024) 'BRCA2 promotes genomic integrity and therapy resistance primarily through its role in homology-directed repair', *Molecular Cell,* 84(3), pp. 447-462.e10.

Liu, L., Li, J., Ke, Y., Zeng, X., Gao, J., Ba, X. and Wang, R. (2022) 'The key players of parthanatos: opportunities for targeting multiple levels in the therapy of parthanatos-based pathogenesis', *Cell Mol Life Sci,* 79(1), pp. 60.

Lord, C. J. and Ashworth, A. (2012) 'The DNA damage response and cancer therapy', *Nature,* 481(7381), pp. 287-294.

Lu, H., Shamanna, R. A., de Freitas, J. K., Okur, M., Khadka, P., Kulikowicz, T., Holland, P. P., Tian, J., Croteau, D. L., Davis, A. J. and Bohr, V. A. (2017) 'Cell cycle-dependent phosphorylation regulates RECQL4 pathway choice and ubiquitination in DNA double-strand break repair', *Nature Communications,* 8(1), pp. 2039.

Lu, H., Zhang, Q., Laverty, D. J., Puncheon, A. C., Augustine, Mathew M., Williams, Gareth J., Nagel, Zachary D., Chen, Benjamin P. C. and Davis, Anthony J. (2023) 'ATM phosphorylates the FATC domain of DNA-PKcs at threonine 4102 to promote non-homologous end joining', *Nucleic Acids Research,* 51(13), pp. 6770-6783.

Luijsterburg, M. S., de Krijger, I., Wiegant, W. W., Shah, R. G., Smeenk, G., de Groot, A. J. L., Pines, A., Vertegaal, A. C. O., Jacobs, J. J. L., Shah, G. M. and van Attikum, H. (2016) 'PARP1 Links CHD2-Mediated Chromatin Expansion and H3.3 Deposition to DNA Repair by Non-homologous End-Joining', *Mol Cell,* 61(4), pp. 547-562.

Ma, C. J., Gibb, B., Kwon, Y., Sung, P. and Greene, E. C. (2017) 'Protein dynamics of human RPA and RAD51 on ssDNA during assembly and disassembly of the RAD51 filament', *Nucleic Acids Research,* 45(2), pp. 749–761.

Mamar, H., Fajka-Boja, R., Mórocz, M., Jurado, E. P., Zentout, S., Mihuţ, A., Kopasz, A. G., Mérey, M., Smith, R., Sharma, A. B., Lakin, N. D., Bowman, A. J., Haracska, L., Huet, S. and Timinszky, G. (2024) 'The loss of DNA polymerase epsilon accessory subunits POLE3-POLE4 leads to BRCA1-independent PARP inhibitor sensitivity', *Nucleic Acids Res,* 52(12), pp. 6994-7011.

Marei, H. E., Althani, A., Afifi, N., Hasan, A., Caceci, T., Pozzoli, G., Morrione, A., Giordano, A. and Cenciarelli, C. (2021) 'p53 signaling in cancer progression and therapy', *Cancer Cell International,* 21(1), pp. 703.

Marshall, C. H., Sokolova, A. O., McNatty, A. L., Cheng, H. H., Eisenberger, M. A., Bryce, A. H., Schweizer, M. T. and Antonarakis, E. S. (2019) 'Differential Response to Olaparib Treatment Among Men with Metastatic Castration-resistant Prostate Cancer Harboring BRCA1 or BRCA2 Versus ATM Mutations', *European Urology,* 76(4), pp. 452-458.

Martin, G. M., Smith, A. C., Ketterer, D. J., Ogburn, C. E. and Disteche, C. M. (1985) 'Increased chromosomal aberrations in first metaphases of cells isolated from the kidneys of aged mice', *Isr J Med Sci,* 21(3), pp. 296-301.

Masuda, W., Yamakawa, T., Ajima, R., Miyake, K., Umemiya, T., Azuma, K., Tamaru, J.-i., Kiso, M., Das, P., Saga, Y., Matsuno, K. and Kitagawa, M. (2023) 'TM2D3, a mammalian homologue of Drosophila neurogenic gene product Almondex, regulates surface presentation of Notch receptors', *Scientific Reports,* 13(1), pp. 20913.

Mateo, J., Carreira, S., Sandhu, S., Miranda, S., Mossop, H., Perez-Lopez, R., Nava Rodrigues, D., Robinson, D., Omlin, A., Tunariu, N., Boysen, G., Porta, N., Flohr, P., Gillman, A., Figueiredo, I., Paulding, C., Seed, G., Jain, S., Ralph, C., Protheroe, A., Hussain, S., Jones, R., Elliott, T., McGovern, U., Bianchini, D., Goodall, J., Zafeiriou, Z., Williamson, C. T., Ferraldeschi, R., Riisnaes, R., Ebbs, B., Fowler, G., Roda, D., Yuan, W., Wu, Y.-M., Cao, X., Brough, R., Pemberton, H., A'Hern, R., Swain, A., Kunju, L. P., Eeles, R., Attard, G., Lord, C. J., Ashworth, A., Rubin, M. A., Knudsen, K. E., Feng, F. Y., Chinnaiyan, A. M., Hall, E. and de Bono, J. S. (2015) 'DNA-Repair Defects and Olaparib in Metastatic Prostate Cancer', *New England Journal of Medicine,* 373(18), pp. 1697-1708.

Mateo, J., Porta, N., Bianchini, D., McGovern, U., Elliott, T., Jones, R., Syndikus, I., Ralph, C., Jain, S., Varughese, M., Parikh, O., Crabb, S., Robinson, A., McLaren, D., Birtle, A., Tanguay, J., Miranda, S., Figueiredo, I., Seed, G., Bertan, C., Flohr, P., Ebbs, B., Rescigno, P., Fowler, G., Ferreira, A., Riisnaes, R., Pereira, R., Curcean, A., Chandler, R., Clarke, M., Gurel, B., Crespo, M., Nava Rodrigues, D., Sandhu, S., Espinasse, A., Chatfield, P., Tunariu, N., Yuan, W., Hall, E., Carreira, S. and de Bono, J. S. (2020) 'Olaparib in patients with metastatic castration-resistant prostate cancer with DNA repair gene aberrations (TOPARP-B): a multicentre, open-label, randomised, phase 2 trial', *The Lancet Oncology,* 21(1), pp. 162-174.

Mateos-Gomez, P. A., Gong, F., Nair, N., Miller, K. M., Lazzerini-Denchi, E. and Sfeir, A. (2015) 'Mammalian polymerase θ promotes alternative NHEJ and suppresses recombination', *Nature,* 518(7538), pp. 254-257.

Matsuoka, S., Ballif, B. A., Smogorzewska, A., McDonald, E. R., Hurov, K. E., Luo, J., Bakalarski, C. E., Zhao, Z., Solimini, N., Lerenthal, Y., Shiloh, Y., Gygi, S. P. and Elledge, S. J. (2007) 'ATM and ATR Substrate Analysis Reveals Extensive Protein Networks Responsive to DNA Damage', *Science,* 316(5828), pp. 1160-1166.

Matsuoka, S., Rotman, G., Ogawa, A., Shiloh, Y., Tamai, K. and Elledge, S. J. (2000) 'Ataxia telangiectasia-mutated phosphorylates Chk2 in vivo and in vitro', *Proceedings of the National Academy of Sciences,* 97(19), pp. 10389-10394.

McCabe, N., Turner, N. C., Lord, C. J., Kluzek, K., Bialkowska, A., Swift, S., Giavara, S., O'Connor, M. J., Tutt, A. N., Zdzienicka, M. Z., Smith, G. C. and Ashworth, A. (2006) 'Deficiency in the repair of DNA damage by homologous recombination and sensitivity to poly(ADP-ribose) polymerase inhibition', *Cancer Res,* 66(16), pp. 8109-15.

McCormick, A., Donoghue, P., Dixon, M., O'Sullivan, R., O'Donnell, R. L., Murray, J., Kaufmann, A., Curtin, N. J. and Edmondson, R. J. (2017) 'Ovarian Cancers Harbor Defects in Nonhomologous End Joining Resulting in Resistance to Rucaparib', *Clinical Cancer Research,* 23(8), pp. 2050-2060.

Meijer, T. G., Martens, J. W. M., Prager-van der Smissen, W. J. C., Verkaik, N. S., Beaufort, C. M., van Herk, S., Robert-Finestra, T., Hoogenboezem, R. M., Ruigrok-Ritstier, K., Paul, M. W., Gribnau, J., Bindels, E. M. J., Kanaar, R., Jager, A., van Gent, D. C. and Hollestelle, A. (2024) 'Functional Homologous Recombination (HR) Screening Shows the Majority of BRCA1/2-Mutant Breast and Ovarian Cancer Cell Lines Are HR-Proficient', *Cancers (Basel),* 16(4).

Ménissier de Murcia, J., Ricoul, M., Tartier, L., Niedergang, C., Huber, A., Dantzer, F., Schreiber, V., Amé, J. C., Dierich, A., LeMeur, M., Sabatier, L., Chambon, P. and de Murcia, G. (2003) 'Functional interaction between PARP-1 and PARP-2 in chromosome stability and embryonic development in mouse', *Embo j,* 22(9), pp. 2255-63.

Milligan, J., Aguilera, J., Paglinawan, R. and Ward, J. (2000) 'DNA strand-break yields after post-irradiation incubation with base excision repair endonucleases implicate hydroxyl radical pairs in double-strand break formation', *International Journal of Radiation Biology,* 76(11), pp. 1475-1483.

Mirman, Z., Lottersberger, F., Takai, H., Kibe, T., Gong, Y., Takai, K., Bianchi, A., Zimmermann, M., Durocher, D. and de Lange, T. (2018) '53BP1–RIF1–shieldin counteracts DSB resection through CST- and Polα-dependent fill-in', *Nature,* 560(7716), pp. 112-116.

Mirman, Z., Sasi, N. K., King, A., Chapman, J. R. and de Lange, T. (2022) '53BP1–shieldin-dependent DSB processing in BRCA1-deficient cells requires CST–Polα–primase fill-in synthesis', *Nature Cell Biology,* 24(1), pp. 51-61.

Moore, K., Colombo, N., Scambia, G., Kim, B. G., Oaknin, A., Friedlander, M., Lisyanskaya, A., Floquet, A., Leary, A., Sonke, G. S., Gourley, C., Banerjee, S., Oza, A., González-Martín, A., Aghajanian, C., Bradley, W., Mathews, C., Liu, J., Lowe, E. S., Bloomfield, R. and DiSilvestro, P. (2018) 'Maintenance Olaparib in Patients with Newly Diagnosed Advanced Ovarian Cancer', *N Engl J Med,* 379(26), pp. 2495-2505.

Mukai, J., Cannavò, E., Crabtree, G. W., Sun, Z., Diamantopoulou, A., Thakur, P., Chang, C. Y., Cai, Y., Lomvardas, S., Takata, A., Xu, B. and Gogos, J. A. (2019) 'Recapitulation and Reversal of Schizophrenia-Related Phenotypes in Setd1a-Deficient Mice', *Neuron,* 104(3), pp. 471-487.e12.

Murai, J., Huang, S.-y. N., Das, B. B., Renaud, A., Zhang, Y., Doroshow, J. H., Ji, J., Takeda, S. and Pommier, Y. (2012) 'Trapping of PARP1 and PARP2 by Clinical PARP Inhibitors', *Cancer Research,* 72(21), pp. 5588.

Myers, J. S. and Cortez, D. (2006) 'Rapid Activation of ATR by Ionizing Radiation Requires ATM and Mre11', *Journal of Biological Chemistry,* 281(14), pp. 9346-9350.

Nacson, J., Krais, J. J., Bernhardy, A. J., Clausen, E., Feng, W., Wang, Y., Nicolas, E., Cai, K. Q., Tricarico, R., Hua, X., DiMarcantonio, D., Martinez, E., Zong, D., Handorf, E. A., Bellacosa, A., Testa, J. R., Nussenzweig, A., Gupta, G. P., Sykes, S. M. and Johnson, N. (2018) 'BRCA1 Mutation-Specific Responses to 53BP1 Loss-Induced Homologous Recombination and PARP Inhibitor Resistance', *Cell Rep,* 24(13), pp. 3513-3527.e7.

Nakamura, K., Saredi, G., Becker, J. R., Foster, B. M., Nguyen, N. V., Beyer, T. E., Cesa, L. C., Faull, P. A., Lukauskas, S., Frimurer, T., Chapman, J. R., Bartke, T. and Groth, A. (2019) 'H4K20me0 recognition by BRCA1–BARD1 directs homologous recombination to sister chromatids', *Nature Cell Biology,* 21(3), pp. 311-318.

Neeb, A., Herranz, N., Arce-Gallego, S., Miranda, S., Buroni, L., Yuan, W., Athie, A., Casals, T., Carmichael, J., Rodrigues, D. N., Gurel, B., Rescigno, P., Rekowski, J., Welti, J., Riisnaes, R., Gil, V., Ning, J., Wagner, V., Casanova-Salas, I., Cordoba, S., Castro, N., Fenor de la Maza, M. D., Seed, G., Chandran, K., Ferreira, A., Figueiredo, I., Bertan, C., Bianchini, D., Aversa, C., Paschalis, A., Gonzalez, M., Morales-Barrera, R., Suarez, C., Carles, J., Swain, A., Sharp, A., Gil, J., Serra, V., Lord, C., Carreira, S., Mateo, J. and de Bono, J. S. (2021) 'Advanced Prostate Cancer with ATM Loss: PARP and ATR Inhibitors', *European Urology,* 79(2), pp. 200-211.

Nguyen, L., W. M. Martens, J., Van Hoeck, A. and Cuppen, E. (2020) 'Pan-cancer landscape of homologous recombination deficiency', *Nature Communications,* 11(1), pp. 5584.

Nimonkar, A. V., Genschel, J., Kinoshita, E., Polaczek, P., Campbell, J. L., Wyman, C., Modrich, P. and Kowalczykowski, S. C. (2011) 'BLM-DNA2-RPA-MRN and EXO1-

BLM-RPA-MRN constitute two DNA end resection machineries for human DNA break repair', *Genes Dev,* 25(4), pp. 350-62.

Nishioka, K., Chuikov, S., Sarma, K., Erdjument-Bromage, H., Allis, C. D., Tempst, P. and Reinberg, D. (2002) 'Set9, a novel histone H3 methyltransferase that facilitates transcription by precluding histone tail modifications required for heterochromatin formation', *Genes Dev,* 16(4), pp. 479-89.

Noordermeer, S. M., Adam, S., Setiaputra, D., Barazas, M., Pettitt, S. J., Ling, A. K., Olivieri, M., Alvarez-Quilon, A., Moatti, N., Zimmermann, M., Annunziato, S., Krastev, D. B., Song, F., Brandsma, I., Frankum, J., Brough, R., Sherker, A., Landry, S., Szilard, R. K., Munro, M. M., McEwan, A., Goullet de Rugy, T., Lin, Z. Y., Hart, T., Moffat, J., Gingras, A. C., Martin, A., van Attikum, H., Jonkers, J., Lord, C. J., Rottenberg, S. and Durocher, D. (2018) 'The shieldin complex mediates 53BP1-dependent DNA repair', *Nature,* 560(7716), pp. 117-121.

O'Leary, M. N., Schreiber, K. H., Zhang, Y., Duc, A. C., Rao, S., Hale, J. S., Academia, E. C., Shah, S. R., Morton, J. F., Holstein, C. A., Martin, D. B., Kaeberlein, M., Ladiges, W. C., Fink, P. J., Mackay, V. L., Wiest, D. L. and Kennedy, B. K. (2013) 'The ribosomal protein Rpl22 controls ribosome composition by directly repressing expression of its own paralog, Rpl22l1', *PLoS Genet,* 9(8), pp. e1003708.

Ochi, T., Blackford, A. N., Coates, J., Jhujh, S., Mehmood, S., Tamura, N., Travers, J., Wu, Q., Draviam, V. M., Robinson, C. V., Blundell, T. L. and Jackson, S. P. (2015) 'PAXX, a paralog of XRCC4 and XLF, interacts with Ku to promote DNA double-strand break repair', *Science,* 347(6218), pp. 185-188.

Ogi, T., Limsirichaikul, S., Overmeer, R. M., Volker, M., Takenaka, K., Cloney, R., Nakazawa, Y., Niimi, A., Miki, Y., Jaspers, N. G., Mullenders, L. H., Yamashita, S., Fousteri, M. I. and Lehmann, A. R. (2010) 'Three DNA polymerases, recruited by different mechanisms, carry out NER repair synthesis in human cells', *Mol Cell,* 37(5), pp. 714-27.

Paes Dias, M., Tripathi, V., van der Heijden, I., Cong, K., Manolika, E. M., Bhin, J., Gogola, E., Galanos, P., Annunziato, S., Lieftink, C., Andújar-Sánchez, M., Chakrabarty, S., Smith, G. C. M., van de Ven, M., Beijersbergen, R. L., Bartkova, J., Rottenberg, S., Cantor, S., Bartek, J., Ray Chaudhuri, A. and Jonkers, J. (2021) 'Loss of nuclear DNA ligase III reverts PARP inhibitor resistance in BRCA1/53BP1 double-deficient cells by exposing ssDNA gaps', *Mol Cell,* 81(22), pp. 4692-4708.e9.

Panzarino, N. J., Krais, J. J., Cong, K., Peng, M., Mosqueda, M., Nayak, S. U., Bond, S. M., Calvo, J. A., Doshi, M. B., Bere, M., Ou, J., Deng, B., Zhu, L. J., Johnson, N. and Cantor, S. B. (2021) 'Replication Gaps Underlie BRCA Deficiency and Therapy Response', *Cancer Res,* 81(5), pp. 1388-1397.

Patel, A. G., Sarkaria, J. N. and Kaufmann, S. H. (2011) 'Nonhomologous end joining drives poly(ADP-ribose) polymerase (PARP) inhibitor lethality in homologous recombination-deficient cells', *Proceedings of the National Academy of Sciences,* 108(8), pp. 3406-3411.

Pepe, A. and West, S. C. (2014) 'Substrate specificity of the MUS81-EME2 structure selective endonuclease', *Nucleic Acids Res,* 42(6), pp. 3833-45.

Perkhofer, L., Schmitt, A., Romero Carrasco, M. C., Ihle, M., Hampp, S., Ruess, D. A., Hessmann, E., Russell, R., Lechel, A., Azoitei, N., Lin, Q., Liebau, S., Hohwieler, M., Bohnenberger, H., Lesina, M., Algül, H., Gieldon, L., Schröck, E., Gaedcke, J., Wagner, M., Wiesmüller, L., Sipos, B., Seufferlein, T., Reinhardt, H. C., Frappart, P. O. and Kleger, A. (2017) 'ATM Deficiency Generating Genomic Instability Sensitizes Pancreatic Ductal Adenocarcinoma Cells to Therapy-Induced DNA Damage', *Cancer Res,* 77(20), pp. 5576-5590.

Perrone, F., Mazzaschi, G., Minari, R., Verzè, M., Azzoni, C., Bottarelli, L., Nizzoli, R., Pluchino, M., Altimari, A., Gruppioni, E., Sperandi, F., Andrini, E., Guaitoli, G., Bertolini, F., Barbieri, F., Bettelli, S., Longo, L., Pagano, M., Bonelli, C., Tagliavini, E., Nicoli, D., Ubiali, A., Zangrandi, A., Trubini, S., Proietto, M., Gnetti, L. and Tiseo, M. (2022) 'Multicenter Observational Study on Metastatic Non-Small Cell Lung Cancer Harboring BRAF Mutations: Focus on Clinical Characteristics and Treatment Outcome of V600E and Non-V600E Subgroups', *Cancers (Basel),* 14(8).

Pesavento, J. J., Yang, H., Kelleher, N. L. and Mizzen, C. A. (2008) 'Certain and progressive methylation of histone H4 at lysine 20 during the cell cycle', *Mol Cell Biol,* 28(1), pp. 468-86.

Petropoulos, M., Karamichali, A., Rossetti, G. G., Freudenmann, A., Iacovino, L. G., Dionellis, V. S., Sotiriou, S. K. and Halazonetis, T. D. (2024) 'Transcription–replication conflicts underlie sensitivity to PARP inhibitors', *Nature,* 628(8007), pp. 433-441.

Pettitt, S. J., Krastev, D. B., Brandsma, I., Dréan, A., Song, F., Aleksandrov, R., Harrell, M. I., Menon, M., Brough, R., Campbell, J., Frankum, J., Ranes, M., Pemberton, H. N., Rafiq, R., Fenwick, K., Swain, A., Guettler, S., Lee, J.-M., Swisher, E. M., Stoynov, S., Yusa, K., Ashworth, A. and Lord, C. J. (2018) 'Genome-wide and high-density CRISPR-Cas9 screens identify point mutations in PARP1 causing PARP inhibitor resistance', *Nature Communications,* 9(1), pp. 1849.

Pierce, A., McGowan, P. M., Cotter, M., Mullooly, M., O'Donovan, N., Rani, S., O'Driscoll, L., Crown, J. and Duffy, M. J. (2013) 'Comparative antiproliferative effects of iniparib and olaparib on a panel of triple-negative and non-triple-negative breast cancer cell lines', *Cancer Biology & Therapy,* 14(6), pp. 537-545.

Pinder, J., Salsman, J. and Dellaire, G. (2015) 'Nuclear domain 'knock-in' screen for the evaluation and identification of small molecule enhancers of CRISPR-based genome editing', *Nucleic Acids Res,* 43(19), pp. 9379-92.

Pon, J. R. and Marra, M. A. (2015) 'Driver and passenger mutations in cancer', *Annu Rev Pathol,* 10, pp. 25-50.

Porter, I. M., Schleicher, K., Porter, M. and Swedlow, J. R. (2013) 'Bod1 regulates protein phosphatase 2A at mitotic kinetochores', *Nature Communications,* 4.

Prakash, S., Johnson, R. E. and Prakash, L. (2005) 'EUKARYOTIC TRANSLESION SYNTHESIS DNA POLYMERASES: Specificity of Structure and Function', *Annual Review of Biochemistry,* 74(Volume 74, 2005), pp. 317-353.

Rafiei, S., Fitzpatrick, K., Liu, D., Cai, M.-Y., Elmarakeby, H. A., Park, J., Ricker, C., Kochupurakkal, B. S., Choudhury, A. D., Hahn, W. C., Balk, S. P., Hwang, J. H., Van Allen, E. M. and Mouw, K. W. (2020) 'ATM Loss Confers Greater Sensitivity to ATR Inhibition Than PARP Inhibition in Prostate Cancer', *Cancer Research,* 80(11), pp. 2094-2100.

Rao, R. C. and Dou, Y. (2015) 'Hijacked in cancer: the KMT2 (MLL) family of methyltransferases', *Nature reviews. Cancer,* 15(6), pp. 334-346.

Ray Chaudhuri, A., Callen, E., Ding, X., Gogola, E., Duarte, A. A., Lee, J. E., Wong, N., Lafarga, V., Calvo, J. A., Panzarino, N. J., John, S., Day, A., Crespo, A. V., Shen, B., Starnes, L. M., de Ruiter, J. R., Daniel, J. A., Konstantinopoulos, P. A., Cortez, D., Cantor, S. B., Fernandez-Capetillo, O., Ge, K., Jonkers, J., Rottenberg, S., Sharan, S. K. and Nussenzweig, A. (2016) 'Replication fork stability confers chemoresistance in BRCA-deficient cells', *Nature,* 535(7612), pp. 382-7.

Reginato, G. and Cejka, P. (2020) 'The MRE11 complex: A versatile toolkit for the repair of broken DNA', *DNA Repair (Amst),* 91-92, pp. 102869.

Riches, L. C., Trinidad, A. G., Hughes, G., Jones, G. N., Hughes, A. M., Thomason, A. G., Gavine, P., Cui, A., Ling, S., Stott, J., Clark, R., Peel, S., Gill, P., Goodwin, L. M., Smith, A., Pike, K. G., Barlaam, B., Pass, M., O'Connor, M. J., Smith, G. and Cadogan, E. B. (2019) 'Pharmacology of the ATM inhibitor AZD0156: potentiation of irradiation and olaparib responses pre-clinically', *Molecular Cancer Therapeutics,* 19(1), pp. 13-25.

Robinson, D., Van Allen, E. M., Wu, Y. M., Schultz, N., Lonigro, R. J., Mosquera, J. M., Montgomery, B., Taplin, M. E., Pritchard, C. C., Attard, G., Beltran, H., Abida, W., Bradley, R. K., Vinson, J., Cao, X., Vats, P., Kunju, L. P., Hussain, M., Feng, F. Y., Tomlins, S. A., Cooney, K. A., Smith, D. C., Brennan, C., Siddiqui, J., Mehra, R., Chen, Y., Rathkopf, D. E., Morris, M. J., Solomon, S. B., Durack, J. C., Reuter, V. E., Gopalan, A., Gao, J., Loda, M., Lis, R. T., Bowden, M., Balk, S. P., Gaviola, G., Sougnez, C., Gupta, M., Yu, E. Y., Mostaghel, E. A., Cheng, H. H., Mulcahy, H., True, L. D., Plymate, S. R., Dvinge, H., Ferraldeschi, R., Flohr, P., Miranda, S., Zafeiriou, Z., Tunariu, N., Mateo, J., Perez-Lopez, R., Demichelis, F., Robinson, B. D., Schiffman, M., Nanus, D. M., Tagawa, S. T., Sigaras, A., Eng, K. W., Elemento, O., Sboner, A., Heath, E. I., Scher, H. I., Pienta, K. J., Kantoff, P., de Bono, J. S., Rubin, M. A., Nelson, P. S., Garraway, L. A., Sawyers, C. L. and Chinnaiyan, A. M. (2015) 'Integrative clinical genomics of advanced prostate cancer', *Cell,* 161(5), pp. 1215-1228.

Robinson, J. T., Thorvaldsdóttir, H., Winckler, W., Guttman, M., Lander, E. S., Getz, G. and Mesirov, J. P. (2011) 'Integrative genomics viewer', *Nature Biotechnology,* 29(1), pp. 24-26.

Robson, M., Im, S.-A., Senkus, E., Xu, B., Domchek, S. M., Masuda, N., Delaloge, S., Li, W., Tung, N., Armstrong, A., Wu, W., Goessl, C., Runswick, S. and Conte, P. (2017) 'Olaparib for Metastatic Breast Cancer in Patients with a Germline BRCA Mutation', *New England Journal of Medicine,* 377(6), pp. 523-533.

Rondinelli, B., Gogola, E., Yücel, H., Duarte, A. A., van de Ven, M., van der Sluijs, R., Konstantinopoulos, P. A., Jonkers, J., Ceccaldi, R., Rottenberg, S. and D'Andrea, A. D. (2017) 'EZH2 promotes degradation of stalled replication forks by recruiting MUS81 through histone H3 trimethylation', *Nature Cell Biology,* 19(11), pp. 1371-1378.

Ronson, G. E., Piberger, A. L., Higgs, M. R., Olsen, A. L., Stewart, G. S., McHugh, P. J., Petermann, E. and Lakin, N. D. (2018) 'PARP1 and PARP2 stabilise replication forks at base excision repair intermediates through Fbh1-dependent Rad51 regulation', *Nature Communications,* 9(1), pp. 746.

Rossi, A., Kontarakis, Z., Gerri, C., Nolte, H., Hölper, S., Krüger, M. and Stainier, D. Y. R. (2015) 'Genetic compensation induced by deleterious mutations but not gene knockdowns', *Nature,* 524(7564), pp. 230-233.

Rottenberg, S., Jaspers, J. E., Kersbergen, A., van der Burg, E., Nygren, A. O., Zander, S. A., Derksen, P. W., de Bruin, M., Zevenhoven, J., Lau, A., Boulter, R., Cranston, A., O'Connor, M. J., Martin, N. M., Borst, P. and Jonkers, J. (2008) 'High sensitivity of BRCA1-deficient mammary tumors to the PARP inhibitor AZD2281 alone and in combination with platinum drugs', *Proc Natl Acad Sci U S A,* 105(44), pp. 17079-84.

Ruiz, S., Mayor-Ruiz, C., Lafarga, V., Murga, M., Vega-Sendino, M., Ortega, S. and Fernandez-Capetillo, O. (2016) 'A Genome-wide CRISPR Screen Identifies CDC25A as a Determinant of Sensitivity to ATR Inhibitors', *Molecular Cell,* 62(2), pp. 307-313.

Rulten, S. L., Fisher, A. E. O., Robert, I., Zuma, M. C., Rouleau, M., Ju, L., Poirier, G., Reina-San-Martin, B. and Caldecott, K. W. (2011) 'PARP-3 and APLF Function Together to Accelerate Nonhomologous End-Joining', *Molecular Cell,* 41(1), pp. 33-45.

Ruscetti, T., Lehnert, B. E., Halbrook, J., Le Trong, H., Hoekstra, M. F., Chen, D. J. and Peterson, S. R. (1998) 'Stimulation of the DNA-dependent Protein Kinase by Poly(ADP-Ribose) Polymerase*', *Journal of Biological Chemistry,* 273(23), pp. 14461-14467.

Ruthenburg, A. J., Allis, C. D. and Wysocka, J. (2007) 'Methylation of lysine 4 on histone H3: intricacy of writing and reading a single epigenetic mark', *Mol Cell,* 25(1), pp. 15-30.

Sacho, E. J. and Maizels, N. (2011) 'DNA repair factor MRE11/RAD50 cleaves 3'-phosphotyrosyl bonds and resects DNA to repair damage caused by topoisomerase 1 poisons', *Journal of Biological Chemistry,* 286(52), pp. 44945-44951.

Saha, L. K., Murai, Y., Saha, S., Jo, U., Tsuda, M., Takeda, S. and Pommier, Y. (2021) 'Replication-dependent cytotoxicity and Spartan-mediated repair of trapped PARP1-DNA complexes', *Nucleic Acids Res,* 49(18), pp. 10493-10506.

Sakai, W., Swisher, E. M., Karlan, B. Y., Agarwal, M. K., Higgins, J., Friedman, C., Villegas, E., Jacquemont, C., Farrugia, D. J., Couch, F. J., Urban, N. and Taniguchi, T. (2008) 'Secondary mutations as a mechanism of cisplatin resistance in BRCA2-mutated cancers', *Nature,* 451(7182), pp. 1116-20.

Salz, T., Deng, C., Pampo, C., Siemann, D., Qiu, Y., Brown, K. and Huang, S. (2015) 'Histone Methyltransferase hSETD1A Is a Novel Regulator of Metastasis in Breast Cancer', *Mol Cancer Res,* 13(3), pp. 461-9.

Salz, T., Li, G., Kaye, F., Zhou, L., Qiu, Y. and Huang, S. (2014) 'hSETD1A Regulates Wnt Target Genes and Controls Tumor Growth of Colorectal Cancer Cells', *Cancer Research,* 74(3), pp. 775-786.

Sarbajna, S., Davies, D. and West, S. C. (2014) 'Roles of SLX1-SLX4, MUS81-EME1, and GEN1 in avoiding genome instability and mitotic catastrophe', *Genes Dev,* 28(10), pp. 1124-36.

Saredi, G., Huang, H., Hammond, C. M., Alabert, C., Bekker-Jensen, S., Forne, I., Reverón-Gómez, N., Foster, B. M., Mlejnkova, L., Bartke, T., Cejka, P., Mailand, N., Imhof, A., Patel, D. J. and Groth, A. (2016) 'H4K20me0 marks post-replicative chromatin and recruits the TONSL–MMS22L DNA repair complex', *Nature,* 534(7609), pp. 714-718.

Sato, K., Ishiai, M., Toda, K., Furukoshi, S., Osakabe, A., Tachiwana, H., Takizawa, Y., Kagawa, W., Kitao, H., Dohmae, N., Obuse, C., Kimura, H., Takata, M. and Kurumizaka, H. (2012) 'Histone chaperone activity of Fanconi anemia proteins, FANCD2 and FANCI, is required for DNA crosslink repair', *The EMBO Journal,* 31(17), pp. 3524-3536.

Saxton, R. A. and Sabatini, D. M. (2017) 'mTOR Signaling in Growth, Metabolism, and Disease', *Cell,* 168(6), pp. 960-976.

Schärer, O. D. (2013) 'Nucleotide excision repair in eukaryotes', *Cold Spring Harb Perspect Biol,* 5(10), pp. a012609.

Schmitt, A., Knittel, G., Welcker, D., Yang, T. P., George, J., Nowak, M., Leeser, U., Buttner, R., Perner, S., Peifer, M. and Reinhardt, H. C. (2017) 'ATM Deficiency Is Associated with Sensitivity to PARP1- and ATR Inhibitors in Lung Adenocarcinoma', *Cancer Res,* 77(11), pp. 3040-3056.

Schwarz, S. D., Xu, J., Gunasekera, K., Schürmann, D., Vågbø, C. B., Ferrari, E., Slupphaug, G., Hottiger, M. O., Schär, P. and Steinacher, R. (2024) 'Covalent PARylation of DNA base excision repair proteins regulates DNA demethylation', *Nature Communications,* 15(1), pp. 184.

Seo, H. R., Nam, A. R., Bang, J. H., Oh, K. S., Kim, J. M., Yoon, J., Kim, T. Y. and Oh, D. Y. (2022) 'Inhibition of WEE1 Potentiates Sensitivity to PARP Inhibitor in Biliary Tract Cancer', *Cancer Res Treat,* 54(2), pp. 541-553.

Setiaputra, D., Escribano-Díaz, C., Reinert, J. K., Sadana, P., Zong, D., Callen, E., Sifri, C., Seebacher, J., Nussenzweig, A., Thomä, N. H. and Durocher, D. (2022) 'RIF1 acts in DNA repair through phosphopeptide recognition of 53BP1', *Molecular Cell,* 82(7), pp. 1359-1371.e9.

Sharma Saha, S., Gentles, L., Bradbury, A., Brecht, D., Robinson, R., O'Donnell, R., Curtin, N. J. and Drew, Y. (2021) 'Genomic, Transcriptomic, and Functional Alterations in DNA Damage Response Pathways as Putative Biomarkers of Chemotherapy Response in Ovarian Cancer', *Cancers,* 13(6), pp. 1420.

Shen, Y., Rehman, F. L., Feng, Y., Boshuizen, J., Bajrami, I., Elliott, R., Wang, B., Lord, C. J., Post, L. E. and Ashworth, A. (2013) 'BMN 673, a Novel and Highly Potent PARP1/2 Inhibitor for the Treatment of Human Cancers with DNA Repair Deficiency', *Clinical Cancer Research,* 19(18), pp. 5003-5015.

Shi, H., Gao, L., Yin, H. and Jiang, M. (2024) 'BLM mutation is associated with increased tumor mutation burden and improved survival after immunotherapy across multiple cancers', *Cancer Med,* 13(1), pp. e6716.

Shi, Y., Venkataraman, S. L., Dodson, G. E., Mabb, A. M., LeBlanc, S. and Tibbetts, R. S. (2004) 'Direct regulation of CREB transcriptional activity by ATM in response to genotoxic stress', *Proc Natl Acad Sci U S A,* 101(16), pp. 5898-903.

Shigechi, T., Tomida, J., Sato, K., Kobayashi, M., Eykelenboom, J. K., Pessina, F., Zhang, Y., Uchida, E., Ishiai, M. and Lowndes, N. F. (2012) 'ATR–ATRIP kinase complex triggers activation of the Fanconi anemia DNA repair pathway', *Cancer research,* 72(5), pp. 1149-1156.

Sifri, C., Hoeg, L., Durocher, D. and Setiaputra, D. (2023) 'An AlphaFold2 map of the 53BP1 pathway identifies a direct SHLD3–RIF1 interaction critical for shieldin activity', *EMBO reports,* 24(8), pp. e56834.

Simoneau, A., Xiong, R. and Zou, L. (2021) 'The trans cell cycle effects of PARP inhibitors underlie their selectivity toward BRCA1/2-deficient cells', *Genes Dev,* 35(17-18), pp. 1271-1289.

Simonetta, M., de Krijger, I., Serrat, J., Moatti, N., Fortunato, D., Hoekman, L., Bleijerveld, O. B., Altelaar, A. F. M. and Jacobs, J. J. L. (2018) 'H4K20me2 distinguishes pre-replicative from post-replicative chromatin to appropriately direct DNA repair pathway choice by 53BP1-RIF1-MAD2L2', *Cell Cycle,* 17(1), pp. 124-136.

Simsek, D. and Jasin, M. (2010) 'Alternative end-joining is suppressed by the canonical NHEJ component Xrcc4-ligase IV during chromosomal translocation formation', *Nat Struct Mol Biol,* 17(4), pp. 410-6.

Singh, T., Kurki, M. I., Curtis, D., Purcell, S. M., Crooks, L., McRae, J., Suvisaari, J., Chheda, H., Blackwood, D., Breen, G., Pietiläinen, O., Gerety, S. S., Ayub, M., Blyth, M., Cole, T., Collier, D., Coomber, E. L., Craddock, N., Daly, M. J., Danesh, J., DiForti, M., Foster, A., Freimer, N. B., Geschwind, D., Johnstone, M., Joss, S., Kirov, G., Körkkö, J., Kuismin, O., Holmans, P., Hultman, C. M., Iyegbe, C., Lönnqvist, J., Männikkö, M., McCarroll, S. A., McGuffin, P., McIntosh, A. M., McQuillin, A., Moilanen, J. S., Moore, C., Murray, R. M., Newbury-Ecob, R., Ouwehand, W., Paunio, T., Prigmore, E., Rees, E., Roberts, D., Sambrook, J., Sklar, P., Clair, D. S., Veijola, J., Walters, J. T. R., Williams, H., Sullivan, P. F., Hurles, M. E., O'Donovan, M. C., Palotie, A., Owen, M. J., Barrett, J. C., Swedish Schizophrenia, S., Study, I., Study, D. D. D. and Consortium, U. K. (2016) 'Rare loss-of-function variants in SETD1A are associated with schizophrenia and developmental disorders', *Nat Neurosci,* 19, pp. 571-577.

Smeby, J., Kryeziu, K., Berg, K. C. G., Eilertsen, I. A., Eide, P. W., Johannessen, B., Guren, M. G., Nesbakken, A., Bruun, J., Lothe, R. A. and Sveen, A. (2020) 'Molecular correlates of sensitivity to PARP inhibition beyond homologous recombination deficiency in pre-clinical models of colorectal cancer point to wild-type TP53 activity', *eBioMedicine,* 59, pp. 102923.

Smith, G. C. and Jackson, S. P. (1999) 'The DNA-dependent protein kinase', *Genes Dev,* 13(8), pp. 916-34.

Smith, H. L., Willmore, E., Prendergast, L. and Curtin, N. J. (2024) 'ATR, CHK1 and WEE1 inhibitors cause homologous recombination repair deficiency to induce synthetic lethality with PARP inhibitors', *British Journal of Cancer,* 131(5), pp. 905-917.

Soria-Bretones, I., Cepeda-García, C., Checa-Rodriguez, C., Heyer, V., Reina-San-Martin, B., Soutoglou, E. and Huertas, P. (2017) 'DNA end resection requires constitutive sumoylation of CtIP by CBX4', *Nat Commun,* 8(1), pp. 113.

Sparks, Justin L., Chon, H., Cerritelli, Susana M., Kunkel, Thomas A., Johansson, E., Crouch, Robert J. and Burgers, Peter M. (2012) 'RNase H2-Initiated Ribonucleotide Excision Repair', *Molecular Cell,* 47(6), pp. 980-986.

Spellmon, N., Holcomb, J., Trescott, L., Sirinupong, N. and Yang, Z. (2015) 'Structure and Function of SET and MYND Domain-Containing Proteins', *International Journal of Molecular Sciences*, 16(1), pp. 1406-1428.

Spivak, G. (2015) 'Nucleotide excision repair in humans', *DNA Repair,* 36, pp. 13-18.

Steger, M., Murina, O., Hühn, D., Ferretti, L. P., Walser, R., Hänggi, K., Lafranchi, L., Neugebauer, C., Paliwal, S., Janscak, P., Gerrits, B., Del Sal, G., Zerbe, O. and Sartori, A. A. (2013) 'Prolyl isomerase PIN1 regulates DNA double-strand break repair by counteracting DNA end resection', *Mol Cell,* 50(3), pp. 333-43.

Stiff, T., O'Driscoll, M., Rief, N., Iwabuchi, K., Löbrich, M. and Jeggo, P. A. (2004) 'ATM and DNA-PK function redundantly to phosphorylate H2AX after exposure to ionizing radiation', *Cancer Res,* 64(7), pp. 2390-6.

Stingele, J., Schwarz, Michael S., Bloemeke, N., Wolf, Peter G. and Jentsch, S. (2014) 'A DNA-Dependent Protease Involved in DNA-Protein Crosslink Repair', *Cell,* 158(2), pp. 327-338.

Ström, C. E., Johansson, F., Uhlén, M., Szigyarto, C. A.-K., Erixon, K. and Helleday, T. (2011) 'Poly (ADP-ribose) polymerase (PARP) is not involved in base excision repair but PARP inhibition traps a single-strand intermediate', *Nucleic Acids Research,* 39(8), pp. 3166-3175.

Sun, W., Zhao, X., Lu, Z. and Guo, Q. (2018) 'P53 introduction enhances chemotherapy-induced apoptosis in Hela cells', *Translational Cancer Research,* 7(4), pp. 1103-1111.

Susvirkar, V. and Faesen, A. C. (2023) 'Shieldin complex assembly kinetics and DNA binding by SHLD3', *Communications Biology,* 6(1), pp. 384.

Sweatman, E., Bayley, R., Selemane, R. and Higgs, M. R. 2024. SETD1A-dependent EME1 transcription drives PARPi sensitivity in HR deficient tumour cells. bioRxiv.

Taglialatela, A., Alvarez, S., Leuzzi, G., Sannino, V., Ranjha, L., Huang, J. W., Madubata, C., Anand, R., Levy, B., Rabadan, R., Cejka, P., Costanzo, V. and Ciccia, A. (2017) 'Restoration of Replication Fork Stability in BRCA1- and BRCA2-Deficient Cells by Inactivation of SNF2-Family Fork Remodelers', *Mol Cell,* 68(2), pp. 414-430.e8.

Tajima, K., Matsuda, S., Yae, T., Drapkin, B. J., Morris, R., Boukhali, M., Niederhoffer, K., Comaills, V., Dubash, T., Nieman, L., Guo, H., Magnus, N. K. C., Dyson, N., Shioda, T., Haas, W., Haber, D. A. and Maheswaran, S. (2019) 'SETD1A protects from senescence through regulation of the mitotic gene expression program', *Nature Communications,* 10(1), pp. 2854.

Tajima, K., Yae, T., Javaid, S., Tam, O., Comaills, V., Morris, R., Wittner, B. S., Liu, M., Engstrom, A., Takahashi, F., Black, J. C., Ramaswamy, S., Shioda, T., Hammell, M., Haber, D. A., Whetstine, J. R. and Maheswaran, S. (2015) 'SETD1A modulates cell cycle progression through a miRNA network that regulates p53 target genes', *Nat Commun,* 6, pp. 8257.

Takamatsu, S., Murakami, K. and Matsumura, N. (2024) 'Homologous Recombination Deficiency Unrelated to Platinum and PARP Inhibitor Response in Cell Line Libraries', *Scientific Data,* 11(1), pp. 171.

Tang, J., Cho, N. W., Cui, G., Manion, E. M., Shanbhag, N. M., Botuyan, M. V., Mer, G. and Greenberg, R. A. (2013) 'Acetylation limits 53BP1 association with damaged chromatin to promote homologous recombination', *Nat Struct Mol Biol,* 20(3), pp. 317-25.

Tao, L., Zhou, Y., Pan, X., Luo, Y., Qiu, J., Zhou, X., Chen, Z., Li, Y., Xu, L., Zhou, Y., Zuo, Z., Liu, C., Wang, L., Liu, X., Tian, X., Su, N., Yang, Z., Zhang, Y., Gou, K., Sang, N., Liu, H., Zou, J., Xiao, Y., Zhong, X., Xu, J., Yang, X., Xiao, K., Liu, Y., Yang, S., Peng, Y., Han, J., Cen, X. and Zhao, Y. (2023) 'Repression of LSD1 potentiates homologous recombination-proficient ovarian cancer to PARP inhibitors through down-regulation of BRCA1/2 and RAD51', *Nature Communications,* 14(1), pp. 7430.

Taylor, A. M. R., Lam, Z., Last, J. I. and Byrd, P. J. (2015) 'Ataxia telangiectasia: more variation at clinical and cellular levels', *Clinical Genetics,* 87(3), pp. 199-208.

ter Brugge, P., Kristel, P., van der Burg, E., Boon, U., de Maaker, M., Lips, E., Mulder, L., de Ruiter, J., Moutinho, C., Gevensleben, H., Marangoni, E., Majewski, I., Jóźwiak, K., Kloosterman, W., van Roosmalen, M., Duran, K., Hogervorst, F., Turner, N., Esteller, M., Cuppen, E., Wesseling, J. and Jonkers, J. (2016) 'Mechanisms of Therapy Resistance in Patient-Derived Xenograft Models of BRCA1-Deficient Breast Cancer', *JNCI: Journal of the National Cancer Institute,* 108(11), pp. djw148.

Thompson, D., Duedal, S., Kirner, J., McGuffog, L., Last, J., Reiman, A., Byrd, P., Taylor, M. and Easton, D. F. (2005) 'Cancer risks and mortality in heterozygous ATM mutation carriers', *J Natl Cancer Inst,* 97(11), pp. 813-22.

Tirman, S., Quinet, A., Wood, M., Meroni, A., Cybulla, E., Jackson, J., Pegoraro, S., Simoneau, A., Zou, L. and Vindigni, A. (2021) 'Temporally distinct post-replicative repair mechanisms fill PRIMPOL-dependent ssDNA gaps in human cells', *Mol Cell,* 81(19), pp. 4026-4040.e8.

Tomimatsu, N., Mukherjee, B., Catherine Hardebeck, M., Ilcheva, M., Vanessa Camacho, C., Louise Harris, J., Porteus, M., Llorente, B., Khanna, K. K. and Burma, S. (2014) 'Phosphorylation of EXO1 by CDKs 1 and 2 regulates DNA end resection and repair pathway choice', *Nature Communications,* 5(1), pp. 3561.

Tomlinson, G. E., Chen, T. T., Stastny, V. A., Virmani, A. K., Spillman, M. A., Tonk, V., Blum, J. L., Schneider, N. R., Wistuba, II, Shay, J. W., Minna, J. D. and Gazdar, A. F. (1998) 'Characterization of a breast cancer cell line derived from a germ-line BRCA1 mutation carrier', *Cancer Res,* 58(15), pp. 3237-42.

Torii, T., Sugimoto, W., Itoh, K., Kinoshita, N., Gessho, M., Goto, T., Uehara, I., Nakajima, W., Budirahardja, Y., Miyoshi, D., Nishikata, T., Tanaka, N., Hirata, H. and Kawauchi, K. (2023) 'Loss of p53 function promotes DNA damage-induced formation of nuclear actin filaments', *Cell Death & Disease,* 14(11), pp. 766.

Toss, A., Tenedini, E., Piombino, C., Venturelli, M., Marchi, I., Gasparini, E., Barbieri, E., Razzaboni, E., Domati, F., Caggia, F., Grandi, G., Combi, F., Tazzioli, G., Dominici, M., Tagliafico, E. and Cortesi, L. (2021) 'Clinicopathologic Profile of Breast Cancer in Germline ATM and CHEK2 Mutation Carriers', *Genes (Basel),* 12(5).

Tsantikidi, A., Papadopoulou, E., Metaxa-Mariatou, V., Kapetsis, G., Tsaousis, G., Meintani, A., Florou-Chatzigiannidou, C., Gazouli, M., Papadimitriou, C., Timotheadou, E., Kotsakis, A., Boutis, A., Boukovinas, I., Kampletsas, E., Kontovinis,

L., Fountzilas, E., Andreadis, C., Karanikiotis, C., Filippou, D., Theodoropoulos, G., Özdoğan, M. and Nasioulas, G. (2023) 'The Utility of NGS Analysis in Homologous Recombination Deficiency Tracking', *Diagnostics (Basel),* 13(18).

Tsherniak, A., Vazquez, F., Montgomery, P. G., Weir, B. A., Kryukov, G., Cowley, G. S., Gill, S., Harrington, W. F., Pantel, S., Krill-Burger, J. M., Meyers, R. M., Ali, L., Goodale, A., Lee, Y., Jiang, G., Hsiao, J., Gerath, W. F. J., Howell, S., Merkel, E., Ghandi, M., Garraway, L. A., Root, D. E., Golub, T. R., Boehm, J. S. and Hahn, W. C. (2017) 'Defining a Cancer Dependency Map', *Cell,* 170(3), pp. 564-576.e16.

Tung, N. M., Robson, M. E., Ventz, S., Santa-Maria, C. A., Nanda, R., Marcom, P. K., Shah, P. D., Ballinger, T. J., Yang, E. S., Vinayak, S., Melisko, M., Brufsky, A., DeMeo, M., Jenkins, C., Domchek, S., D'Andrea, A., Lin, N. U., Hughes, M. E., Carey, L. A., Wagle, N., Wulf, G. M., Krop, I. E., Wolff, A. C., Winer, E. P. and Garber, J. E. (2020) 'TBCRC 048: Phase II Study of Olaparib for Metastatic Breast Cancer and Mutations in Homologous Recombination-Related Genes', *Journal of Clinical Oncology,* 38(36), pp. 4274-4282.

Turner, N. C., Lord, C. J., Iorns, E., Brough, R., Swift, S., Elliott, R., Rayter, S., Tutt, A. N. and Ashworth, A. (2008) 'A synthetic lethal siRNA screen identifying genes mediating sensitivity to a PARP inhibitor', *Embo j,* 27(9), pp. 1368-77.

Tusi, B. K., Deng, C., Salz, T., Zeumer, L., Li, Y., So, C. W. E., Morel, L. M., Qiu, Y. and Huang, S. (2015) 'Setd1a regulates progenitor B-cell-to-precursor B-cell development through histone H3 lysine 4 trimethylation and Ig heavy-chain rearrangement', *FASEB journal : official publication of the Federation of American Societies for Experimental Biology,* 29(4), pp. 1505-1515.

Ueno, S., Sudo, T. and Hirasawa, A. (2022) 'ATM: Functions of ATM Kinase and Its Relevance to Hereditary Tumors', *International Journal of Molecular Sciences,* 23(1), pp. 523.

Valabrega, G., Scotto, G., Tuninetti, V., Pani, A. and Scaglione, F. (2021) 'Differences in PARP Inhibitors for the Treatment of Ovarian Cancer: Mechanisms of Action, Pharmacology, Safety, and Efficacy', *Int J Mol Sci,* 22(8).

Vauti, F., Goller, T., Beine, R., Becker, L., Klopstock, T., Hölter, S. M., Wurst, W., Fuchs, H., Gailus-Durner, V., de Angelis, M. H. and Arnold, H.-H. (2007) 'The mouse Trm1-like gene is expressed in neural tissues and plays a role in motor coordination and exploratory behaviour', *Gene,* 389(2), pp. 174-185.

Veeck, J., Ropero, S., Setien, F., Gonzalez-Suarez, E., Osorio, A., Benitez, J., Herman, J. G. and Esteller, M. (2010) 'BRCA1 CpG island hypermethylation predicts sensitivity to poly(adenosine diphosphate)-ribose polymerase inhibitors', *J Clin Oncol,* 28(29), pp. e563-4; author reply e565-6.

Waks, A. G., Cohen, O., Kochupurakkal, B., Kim, D., Dunn, C. E., Buendia Buendia, J., Wander, S., Helvie, K., Lloyd, M. R., Marini, L., Hughes, M. E., Freeman, S. S., Ivy, S. P., Geradts, J., Isakoff, S., LoRusso, P., Adalsteinsson, V. A., Tolaney, S. M.,

Matulonis, U., Krop, I. E., D'Andrea, A. D., Winer, E. P., Lin, N. U., Shapiro, G. I. and Wagle, N. (2020) 'Reversion and non-reversion mechanisms of resistance to PARP inhibitor or platinum chemotherapy in BRCA1/2-mutant metastatic breast cancer', *Ann Oncol,* 31(5), pp. 590-598.

Wang, C., Jette, N., Moussienko, D., Bebb, D. G. and Lees-Miller, S. P. (2017a) 'ATM-Deficient Colorectal Cancer Cells Are Sensitive to the PARP Inhibitor Olaparib', *Transl Oncol,* 10(2), pp. 190-196.

Wang, C., Wang, G., Feng, X., Shepherd, P., Zhang, J., Tang, M., Chen, Z., Srivastava, M., McLaughlin, M. E., Navone, N. M., Hart, G. T. and Chen, J. (2019) 'Genome-wide CRISPR screens reveal synthetic lethality of RNASEH2 deficiency and ATR inhibition', *Oncogene,* 38(14), pp. 2451-2463.

Wang, L., Collings, C. K., Zhao, Z., Cozzolino, K. A., Ma, Q., Liang, K., Marshall, S. A., Sze, C. C., Hashizume, R., Savas, J. N. and Shilatifard, A. (2017b) 'A cytoplasmic COMPASS is necessary for cell survival and triple-negative breast cancer pathogenesis by regulating metabolism', *Genes Dev,* 31(20), pp. 2056-2066.

Wang, L. M., Wang, P., Chen, X. M., Yang, H., Song, S. S., Song, Z., Jia, L., Chen, H. D., Bao, X. B., Guo, N., Huan, X. J., Xi, Y., Shen, Y. Y., Yang, X. Y., Su, Y., Sun, Y. M., Gao, Y. L., Chen, Y., Ding, J., Lang, J. Y., Miao, Z. H., Zhang, A. and He, J. X. (2023) 'Thioparib inhibits homologous recombination repair, activates the type I IFN response, and overcomes olaparib resistance', *EMBO Mol Med,* 15(3), pp. e16235.

Wang, R., Liu, J., Li, K., Yang, G., Chen, S., Wu, J., Xie, X., Ren, H. and Pang, Y. (2021) 'An SETD1A/Wnt/β-catenin feedback loop promotes NSCLC development', *J Exp Clin Cancer Res,* 40(1), pp. 318.

Watson, Z. L., Yamamoto, T. M., McMellen, A., Kim, H., Hughes, C. J., Wheeler, L. J., Post, M. D., Behbakht, K. and Bitler, B. G. (2019) 'Histone methyltransferases EHMT1 and EHMT2 (GLP/G9A) maintain PARP inhibitor resistance in high-grade serous ovarian carcinoma', *Clinical Epigenetics,* 11(1), pp. 165.

Weerts, M. J. A., Lanko, K., Guzmán-Vega, F. J., Jackson, A., Ramakrishnan, R., Cardona-Londoño, K. J., Peña-Guerra, K. A., van Bever, Y., van Paassen, B. W., Kievit, A., van Slegtenhorst, M., Allen, N. M., Kehoe, C. M., Robinson, H. K., Pang, L., Banu, S. H., Zaman, M., Efthymiou, S., Houlden, H., Järvelä, I., Lauronen, L., Määttä, T., Schrauwen, I., Leal, S. M., Ruivenkamp, C. A. L., Barge-Schaapveld, D., Peeters-Scholte, C., Galehdari, H., Mazaheri, N., Sisodiya, S. M., Harrison, V., Sun, A., Thies, J., Pedroza, L. A., Lara-Taranchenko, Y., Chinn, I. K., Lupski, J. R., Garza-Flores, A., McGlothlin, J., Yang, L., Huang, S., Wang, X., Jewett, T., Rosso, G., Lin, X., Mohammed, S., Merritt, J. L., 2nd, Mirzaa, G. M., Timms, A. E., Scheck, J., Elting, M. W., Polstra, A. M., Schenck, L., Ruzhnikov, M. R. Z., Vetro, A., Montomoli, M., Guerrini, R., Koboldt, D. C., Mosher, T. M., Pastore, M. T., McBride, K. L., Peng, J., Pan, Z., Willemsen, M., Koning, S., Turnpenny, P. D., de Vries, B. B. A., Gilissen, C., Pfundt, R., Lees, M., Braddock, S. R., Klemp, K. C., Vansenne, F., van Gijn, M. E., Quindipan, C., Deardorff, M. A., Hamm, J. A., Putnam, A. M., Baud, R., Walsh, L., Lynch, S. A., Baptista, J., Person, R. E., Monaghan, K. G., Crunk, A., Keller-Ramey,

J., Reich, A., Elloumi, H. Z., Alders, M., Kerkhof, J., McConkey, H., Haghshenas, S., Maroofian, R., Sadikovic, B., Banka, S., Arold, S. T. and Barakat, T. S. (2021) 'Delineating the molecular and phenotypic spectrum of the SETD1B-related syndrome', *Genet Med,* 23(11), pp. 2122-2137.

Wei, H. and Yu, X. (2016) 'Functions of PARylation in DNA Damage Repair Pathways', *Genomics, Proteomics & Bioinformatics,* 14(3), pp. 131-139.

Wei, S., Li, C., Yin, Z., Wen, J., Meng, H., Xue, L. and Wang, J. (2018) 'Histone methylation in DNA repair and clinical practice: new findings during the past 5-years', *Journal of Cancer,* 9(12), pp. 2072-2081.

Westin, S. N., Litton, J. K., Williams, R. A., Shepherd, C. J., Brugger, W., Pease, E. J., Soliman, P. T., Frumovitz, M. M., Levenback, C. F., Sood, A., Meyer, L., Moulder, S. L., Valero, V., Saleem, S., Rodriguez, A. M., Cyriac, A., Engerman, L., Samuel, C., Mills, G. B. and Coleman, R. L. (2018) 'Phase I trial of olaparib (PARP inhibitor) and vistusertib (mTORC1/2 inhibitor) in recurrent endometrial, ovarian and triple negative breast cancer', *Journal of Clinical Oncology,* 36(15_suppl), pp. 5504-5504.

Weston, V. J., Oldreive, C. E., Skowronska, A., Oscier, D. G., Pratt, G., Dyer, M. J., Smith, G., Powell, J. E., Rudzki, Z., Kearns, P., Moss, P. A., Taylor, A. M. and Stankovic, T. (2010) 'The PARP inhibitor olaparib induces significant killing of ATM-deficient lymphoid tumor cells in vitro and in vivo', *Blood,* 116(22), pp. 4578-87.

White, D., Rafalska-Metcalf, I. U., Ivanov, A. V., Corsinotti, A., Peng, H., Lee, S. C., Trono, D., Janicki, S. M. and Rauscher, F. J., 3rd (2012) 'The ATM substrate KAP1 controls DNA repair in heterochromatin: regulation by HP1 proteins and serine 473/824 phosphorylation', *Mol Cancer Res,* 10(3), pp. 401-14.

Williamson, C. T., Muzik, H., Turhan, A. G., Zamò, A., O'Connor, M. J., Bebb, D. G. and Lees-Miller, S. P. (2010) 'ATM deficiency sensitizes mantle cell lymphoma cells to poly(ADP-ribose) polymerase-1 inhibitors', *Mol Cancer Ther,* 9(2), pp. 347-57.

Wolfson, R. L., Chantranupong, L., Wyant, G. A., Gu, X., Orozco, J. M., Shen, K., Condon, K. J., Petri, S., Kedir, J., Scaria, S. M., Abu-Remaileh, M., Frankel, W. N. and Sabatini, D. M. (2017) 'KICSTOR recruits GATOR1 to the lysosome and is necessary for nutrients to regulate mTORC1', *Nature,* 543(7645), pp. 438-442.

Woodhouse, B. C., Dianova, I. I., Parsons, J. L. and Dianov, G. L. (2008) 'Poly(ADP-ribose) polymerase-1 modulates DNA repair capacity and prevents formation of DNA double strand breaks', *DNA Repair,* 7(6), pp. 932-940.

Wu, J., Chai, H., Shan, H., Pan, C., Xu, X., Dong, W., Yu, J. and Gu, Y. (2021) 'Histone Methyltransferase SETD1A Induces Epithelial-Mesenchymal Transition to Promote Invasion and Metastasis Through Epigenetic Reprogramming of Snail in Gastric Cancer', *Front Cell Dev Biol,* 9, pp. 657888.

Wu, J., Chai, H., Xu, X., Yu, J. and Gu, Y. (2020) 'Histone methyltransferase SETD1A interacts with HIF1α to enhance glycolysis and promote cancer progression in gastric cancer', *Mol Oncol,* 14(6), pp. 1397-1409.

Wyatt, H. D. M., Laister, R. C., Martin, S. R., Arrowsmith, C. H. and West, S. C. (2017) 'The SMX DNA Repair Tri-nuclease', *Molecular Cell,* 65(5), pp. 848-860.e11.

Wyatt, Haley D. M., Sarbajna, S., Matos, J. and West, Stephen C. (2013) 'Coordinated Actions of SLX1-SLX4 and MUS81-EME1 for Holliday Junction Resolution in Human Cells', *Molecular Cell,* 52(2), pp. 234-247.

Wysocka, J., Swigut, T., Xiao, H., Milne, T. A., Kwon, S. Y., Landry, J., Kauer, M., Tackett, A. J., Chait, B. T., Badenhorst, P., Wu, C. and Allis, C. D. (2006) 'A PHD finger of NURF couples histone H3 lysine 4 trimethylation with chromatin remodelling', *Nature,* 442(7098), pp. 86-90.

Xiong, Y., Guo, Y., Liu, Y., Wang, H., Gong, W., Liu, Y., Wang, X., Gao, Y., Yu, F., Su, D., Wang, F., Zhu, Y., Zhao, Y., Wu, Y., Qin, Z., Sun, X., Ren, B., Jiang, B., Jin, W., Shen, Z., Tang, Z., Song, X., Wang, L., Liu, X., Zhou, C. and Jiang, B. (2020) 'Pamiparib is a potent and selective PARP inhibitor with unique potential for the treatment of brain tumor', *Neoplasia,* 22(9), pp. 431-440.

Xu, G., Chapman, J. R., Brandsma, I., Yuan, J., Mistrik, M., Bouwman, P., Bartkova, J., Gogola, E., Warmerdam, D., Barazas, M., Jaspers, J. E., Watanabe, K., Pieterse, M., Kersbergen, A., Sol, W., Celie, P. H. N., Schouten, P. C., van den Broek, B., Salman, A., Nieuwland, M., de Rink, I., de Ronde, J., Jalink, K., Boulton, S. J., Chen, J., van Gent, D. C., Bartek, J., Jonkers, J., Borst, P. and Rottenberg, S. (2015) 'REV7 counteracts DNA double-strand break resection and affects PARP inhibition', *Nature,* 521(7553), pp. 541-544.

Yang, G., Chen, Y., Wu, J., Chen, S.-H., Liu, X., Singh, A. K. and Yu, X. (2020a) 'Poly(ADP-ribosyl)ation mediates early phase histone eviction at DNA lesions', *Nucleic Acids Research,* 48(6), pp. 3001-3013.

Yang, G., Liu, C., Chen, S.-H., Kassab, M. A., Hoff, J. D., Walter, N. G. and Yu, X. (2018) 'Super-resolution imaging identifies PARP1 and the Ku complex acting as DNA double-strand break sensors', *Nucleic Acids Research,* 46(7), pp. 3446-3457.

Yang, L., Jin, M., Park, S. J., Seo, S. Y. and Jeong, K. W. (2020b) 'SETD1A Promotes Proliferation of Castration-Resistant Prostate Cancer Cells via FOXM1 Transcription', *Cancers (Basel),* 12(7).

Yang, Y.-G., Cortes, U., Patnaik, S., Jasin, M. and Wang, Z.-Q. (2004) 'Ablation of PARP-1 does not interfere with the repair of DNA double-strand breaks, but compromises the reactivation of stalled replication forks', *Oncogene,* 23(21), pp. 3872-3882.

Yap, T., Im, S.-A., Schram, A., Sharp, A., Balmana, J., Baird, R., Brown, J., Schwaederle, M., Pilling, E., Moorthy, G., Linardopoulos, S., Dowson, A., Pound, C.,

Lukacs, E., Cosulich, S. and Luen, S. (2022) 'Abstract CT007: PETRA: First in class, first in human trial of the next generation PARP1-selective inhibitor AZD5305 in patients (pts) with BRCA1/2, PALB2 or RAD51C/D mutations', *Cancer Research,* 82, pp. CT007-CT007.

Yi, C. and He, C. (2013) 'DNA repair by reversal of DNA damage', *Cold Spring Harb Perspect Biol,* 5(1), pp. a012575.

Yuen, K. C., Slaughter, B. D. and Gerton, J. L. (2017) 'Condensin II is anchored by TFIIIC and H3K4me3 in the mammalian genome and supports the expression of active dense gene clusters', *Science advances,* 3(6), pp. e1700191-e1700191.

Zhang, F., Ma, J., Wu, J., Ye, L., Cai, H., Xia, B. and Yu, X. (2009) 'PALB2 links BRCA1 and BRCA2 in the DNA-damage response', *Curr Biol,* 19(6), pp. 524-9.

Zhang, J., Chen, L., Zhang, J. and Wang, Y. (2019) 'Drug Inducible CRISPR/Cas Systems', *Comput Struct Biotechnol J,* 17, pp. 1171-1177.

Zhao, W., Steinfeld, J. B., Liang, F., Chen, X., Maranon, D. G., Jian Ma, C., Kwon, Y., Rao, T., Wang, W., Sheng, C., Song, X., Deng, Y., Jimenez-Sainz, J., Lu, L., Jensen, R. B., Xiong, Y., Kupfer, G. M., Wiese, C., Greene, E. C. and Sung, P. (2017) 'BRCA1-BARD1 promotes RAD51-mediated homologous DNA pairing', *Nature,* 550(7676), pp. 360-365.

Zhou, Y. and Paull, T. T. (2013) 'DNA-dependent protein kinase regulates DNA end resection in concert with Mre11-Rad50-Nbs1 (MRN) and ataxia telangiectasia-mutated (ATM)', *Journal of Biological Chemistry,* 288(52), pp. 37112-37125.

Zhuang, X., Yao, J., Li, X., Jiang, Y., Zhong, M., Tan, J., Zhou, H., Li, G., Zha, J. and Xu, B. (2024) 'Anlotinib suppresses the DNA damage response by disrupting SETD1A and inducing p53-dependent apoptosis in Transformed Follicular Lymphoma', *Int J Med Sci,* 21(1), pp. 70-79.

Zimmermann, M., Lottersberger, F., Buonomo, S. B., Sfeir, A. and de Lange, T. (2013) '53BP1 regulates DSB repair using Rif1 to control 5' end resection', *Science,* 339(6120), pp. 700-4.